Chromium dust deposition on plant leaves in Sekhukhuneland, South Africa, and the importance of leaf traits

S Adhikari

orcid.org/0000-0003-0924-5349

Thesis accepted in fulfilment of the requirements for the degree *Doctor of Philosophy in Science with Botany* at the North-West University

Promoter:	Prof SJ Siebert
Co-promoter:	Dr A Jordaan
Co-promoter:	Dr JM Silva

Graduation November 2021
30717582

Acknowledgements

I am grateful to the Universal good energy that is guiding me.

I am deeply indebted to Prof R Nikolova for her initiatives regarding my PhD study and for keeping faith in me.

The National Research Foundation of South Africa (NRF) is thanked for the financial support.

I would like to express my sincere gratitude to Prof SJ Siebert, for the patient guidance, continuous support, encouragement and expert advice he has provided throughout my study duration. Dr Jordaan, Dr JM Silva and Prof F Siebert are thanked for their valuable guidance all along.

I would like to extend my gratitude to Prof JP Beukes (Chemistry Department, NWU) for his guidance, and for financing some of the analyses and for constructing the overlay back trajectory maps. Many thanks to Yolindi Coetzee and Ralph Glastonbury (Chemistry Department, NWU) for assisting me with the lab work.

I gratefully thank Mr Ricart Boneschans (Geology Department, NWU) for his guidance and help with the XRF analysis. Thanks to Prof Suria Ellis (Statistical Consultation Services, NWU) for her assistance in statistical analysis. Kenneth Tshinavhe (Potlake Nature Reserve, Sekhukhuneland) and Musa Mkhwanazi (South African Weather Service) are thanked for providing the meteorological data. Thanks to Eco Analytica Laboratory (NWU) for analysing the samples.

Special thanks to Dennis Komape for identifying the plant species and assisting with fieldwork and sample preparation. Marlize Muller is thanked for her help in many ways. Thanks to the members of the Herbarium (NWU, Potchefstroom Campus). Wynand Muller and Shaunelle Pretorius (UESM, NWU) are thanked for creating the study area maps.

I would like to offer my gratitude to Marina Du Plessis, who accommodated me in her peaceful guesthouse for the past two years even during those challenging times and made me feel at home. Refentse and Murendeni, thank you so much for your friendship, support and love.

Lastly, my husband, Dr A Goswami, is thanked for proofreading this thesis. The completion of my thesis would not have been possible without your constant loving support.

Dedicated to my mother and sister.

Declaration

I, Sutapa Adhikari, declare that this thesis is an original report of my research, and has not been submitted for any other degree/examination at any other university. All collaborative contributions have been indicated clearly and acknowledged. Due references have been provided in full on all supporting literature and resources. This PhD thesis is being submitted for the Doctor of Philosophy degree at the North-West University, Potchefstroom Campus, South Africa.

Sutapa Adhikari (PhD candidate)

Prof SJ Siebert (Promoter)

Dr A Jordaan (Assistant Promoter)

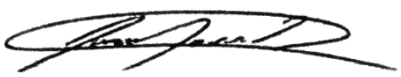

Dr JM Silva (Co-promoter)

Abstract

Chromium (Cr) is a hazardous heavy metal and its highest oxidized state, hexavalent Cr (Cr(VI)), can be carcinogenic. The ultramafic outcrops of Sekhukhuneland, South Africa, which belong to the Rustenburg Layered Suite, are mined heavily for Cr, yet Cr contamination of the local vegetation is understudied. The present study aims to understand if Cr pollution in a mining environment is adsorbed or accumulated by plant leaves with a primary focus on commonly used food and medicinal plant species in Sekhukhuneland. The following techniques were applied to attain the main research objectives: (i) to comprehend the global trend on environmental Cr pollution and Cr accumulation by useful plants, a systematic review was conducted, (ii) to investigate the presence of Cr dust on leaf surfaces, Energy dispersive x-ray spectroscopy (EDS) based elemental analysis of leaf surfaces was performed, (iii) plant morphology, leaf macromorphology and Scanning electron microscope (SEM) imaged leaf micromorphology were studied to assess their influence on foliar Cr dust deposition, (iv) combination of bi- and multivariate statistical techniques were applied to identify Cr sources on leaf surfaces and assess the interaction between plant morphology and Cr pollution, (v) to evaluate the contribution of dust to foliar Cr content and human health risk, total Cr and Cr(VI) was quantified in selected useful plant leaves, and finally (vi) to evaluate the phytoremediation potential of dominant local species, foliar metal bioaccumulation factors were determined. The systematic review suggested a global occurrence of Cr accumulation above the international permissible limits by useful plants, especially in polluted areas. Findings from the present study confirmed human activity sourced Cr dust deposition on the useful plant leaf surfaces. It was found that larger leaves and taller plants could be susceptible to foliar Cr dust deposition. Plant morphological traits, i.e. leaf area, epicuticular wax, stomata size and plant height, and Cr pollution in terms of proximity and number of polluters, however, collectively determine foliar Cr dust deposition. Cr content in leaves of food and medicinal plants exceeded international safe limits by several folds suggesting Cr contamination. Deposited dust contributed significantly towards the total Cr content of leaves (p<0.001). Lifelong carcinogenic health risk was estimated for total Cr and Cr(VI) content of leafy vegetables. Accumulation of several metals in leaves by the local metallophytes especially the indigenous species indicated the prospect of phytoremediation. Tailing soils are major Cr sources including dust borne Cr to local vegetation. Results confirmed Cr enrichment of plant leaves due to Cr dust deposition and Cr accumulation in leaf tissue. Cr pollution and associated human health risk should be of priority concern in Sekhukhuneland. At the same time, extended research on local metallophytes may suggest sustainable techniques to limit further dispersion of hazardous elements from polluted sites.

Keywords: Accumulation, carcinogenic risk, energy dispersive x-ray spectroscopy, hexavalent chromium, leaf area, plant height, scanning electron microscope, serpentine, tailings

Table of content

List of tables

List of figures

Chapter 1

Introduction

1.1 Background

The rise in worldwide industrial demand for chromium (Cr) has increased the mining and metal processing thereof, with consequent generation of hazardous waste including dust (Kimbrough *et al*., 1999; Shahid *et al*., 2017). Globally, Cr mining, ferrochrome smelting, and associated waste dumping are primarily investigated for soil pollution and plant contamination via root exposure to liquid or solid waste (Dhal *et al*., 2010a, 2010b; Kien *et al*., 2010; Mohanty *et al*., 2012). Foliar exposure of Cr dust remains less explored despite being a major metal contamination route for cultivated crops (Bi *et al*., 2009; Liu *et al.*, 2019; Wang *et al.*, 2019).

Dust deposition on plant leaves is mainly a function of two factors - plant morphology and pollution source (Castanheiro *et al.*, 2020). Plant morphological traits, namely plant height, foliar macro- (i.e. leaf blade size) and micromorphology (i.e. epicuticular wax, stomata, trichomes or hairs), enhance exposure and available area and create interactive leaf surfaces for particle deposition (Neinhuis & Barthlott, 1998; Mo *et al*., 2015; Leonard *et al.*, 2016; Chen *et al.*, 2017; Castanheiro *et al.*, 2020). Local pollution factors (e.g. proximity to source(s)) affects particle concentration, whereas source type determines the chemical composition and size of dust particles (Csavina *et al*., 2012; Entwistle *et al.*, 2019). Estimating the combined influence of the above-mentioned factors is therefore critical to comprehend the leaf-dust interaction process.

The biological toxicity of Cr depends on its oxidation state, which determines its solubility and bioavailability (Kimbrough *et al*., 1999). Tri- (Cr(III)) and hexavalent (Cr(VI)) are the most stable Cr forms in the environment (Kimbrough *et al*., 1999). The presence of Cr(VI) compounds in any environmental matrix is a risk, as this chemical species is extremely reactive, soluble and hence leach rapidly to become bioavailable (Kimbrough *et al*., 1999; Oze *et al*., 2004; Dhal *et al.*, 2010b). Moreover, the carcinogenicity of Cr has been confirmed for only Cr(VI) (the United States Environmental Protection Agency, Integrated Risk Information System, 1986; International Agency for Research on Cancer, 1990), and hence, chemical speciation is the fundamental basis to categorise Cr toxicity and estimate the human health risks (Yaman, 2020). There is, however, frequent interspecies conversion between Cr(III) and Cr(VI) depending on multiple reaction parameters (e.g. pH, Eh, temperature, and presence of oxidizer and reducer), which makes it challenging to determine Cr(VI) concentrations in a given matrix (Kimbrough *et al*., 1999). This is reflected by a scarcity of literature regarding Cr(VI) determination in plant tissue.

Cr mines and waste dumps are generous sources of anthropogenic Cr and other metals in soil (Dhal *et al.*, 2010a, 2010b; Kien *et al.*, 2010), while ultramafic and serpentine soils are naturally enriched with such elements (Proctor, 2003; Siebert *et al.*, 2002; Oze *et al*., 2004). Areas influenced by both anthropogenic (mining-related activities) and geogenic (ultramafic soils) metal sources may present complex edaphic environments (Gaspar *et al.*, 2020) where factors such as land use and topography affect elemental compositions of soils and plants (Rosemary *et al.*, 2014; Gaspar *et al.*, 2020).

1.2 Motivation

Sekhukhuneland in South Africa was selected as an ideal region to study plant leaf-Cr dust interaction since the region presents habitats characterised by Cr-enriched chromitite outcrops, ultramafic soils and multiple active mines and operating ferrochrome smelters (Siebert *et al.*, 2002; Tshehla & Djolov, 2018; Scoon & Viljoen, 2019). While the floristic diversity (Van Wyk & Van Wyk, 1997; Siebert *et al.*, 2002, 2003) and food and medicinal use-value of the local vegetation (Semenya *&* Potgieter, 2014; Mogale *et al.*, 2019) are well studied, no scientific literature is available on Cr dust contamination and metal accumulation or adsorption by local vegetation. Under the prevailing high atmospheric dust pollution (Tshehla & Djolov, 2018), people inhabiting these mining areas could be unknowingly subjected to regular exposure to Cr via ingestion of dust contaminated useful plants. Likewise, although global reports confirmed the influence of natural (topography) and anthropogenic (land use) factors on the spatial distribution of heavy metals in topsoil and plants (Rosemary *et al*., 2014; Gasper *et al*., 2020), such association is still to be explored for Sekhukhuneland. Besides its geological importance as a metalliferous site (mineral-rich outcrops and mines, Baker *et al.*, 2010) the region is also understudied in terms of metallophytes.

1.3 Study aim and objectives

The study aims to understand if Cr pollution in a mining environment is adsorbed or accumulated by plant leaves. More specifically, the thesis considers the contribution of dust towards Cr accumulation in and adsorption to plant leaves, the potential human health risk associated with leaf consumption, and the accumulation of metals in the soils and the metallophytes (leaves) under the influence of topography and land use.

Hypotheses and objectives

Globally, Cr has attracted much attention as a transition element specifically due to the distinctly different chemistry of Cr(III) and Cr(VI) (Kimbrough *et al*., 1999; Dhal *et al*., 2010a, 2010b; Shahid *et al*., 2017). Cr reaction mechanisms in the environment, toxicity potential, environmental remediation techniques and phytotoxicity have been investigated sufficiently (Kimbrough *et al*.,

1999; Gomes *et al*., 2017; Shahid *et al*., 2017). It was therefore hypothesised that (1) interlinking and integrating prominent Cr research areas would help to understand the global trend regarding Cr pollution and Cr-plant (food and medicinal plants) interaction. Chapter 2 presents a systematic review that tests this hypothesis.

Objective 1: To assess Cr chemistry, toxicity and describe known chemical reaction mechanisms in the environment.
Objective 2: To evaluate phytotoxicity in useful plants and describe known plant-Cr interactions.

Recent investigations confirmed the presence of Cr-rich particulate matter of varied size and elemental composition in the regional air mass over Sekhukhuneland (Tshehla & Djolov, 2018; Tshehla & Wright, 2019) and past reports stating variation in plant morphology to affect dust accumulation by plant leaves (Neinhuis & Barthlott, 1998; Mo *et al*., 2015; Leonard *et al.*, 2016; Chen *et al*., 2017; Castanheiro *et al.*, 2020), it was hypothesized that (2) atmospheric Cr pollution in the region would result in deposition of such particles on the leaf surfaces, with the influence of species specific morphological traits. The hypothesis was tested in Chapter 3.

Objective 3: To attest to the presence of Cr dust on plant leaf surfaces.
Objective 4: To assess the size and shape of Cr dust to understand the morphology of the particles.
Objective 5: To describe the plant morphological traits that are related to the deposition of Cr dust on leaf surfaces.

Since the study region is polluted by different types of Cr emitters, namely mines, ferrochrome smelters and ore transport routes (Tshehla & Djolov, 2018; Tshehla & Wright, 2019), it was postulated that (3) multifaceted anthropogenic Cr exposure would alter the elemental composition of the local soils and plant leaves and that plant morphology and pollution source factors (proximity to and number) would be responsible for differential Cr particle deposition on either side of the leaf. Chapter 4 was focused on testing this hypothesis.

Objective 6: To identify possible sources of Cr in soils and on plant leaf surfaces based on their elemental composition.
Objective 7: To determine the leaf surface-Cr dust interaction by assessing the contribution from plant morphological (e.g. plant height, leaf area, epicuticular wax, stomata and trichome size and density) and pollution source (proximity to and the number of mines, road) variables on this interaction process.

Elevated levels of Cr in soil and vegetation in areas around Cr mines, ferrochrome smelters and waste sites were reported (Pöykiö *et al*., 2005; Dhal *et al*., 2010a, 2010b; Kien *et al*., 2010; Sokol *et al.*, 2010). The hazard impact of such polluters could be increased by the release of Cr(VI) in the environment (Dhal *et al*., 2010a; Coetzee *et al*., 2018) and emission of dust that contains multiple toxic elements (Pöykiö *et al*., 2005; Sokol *et al.*, 2010). Therefore, it was hypothesized that (4) the aggregation of various Cr polluters in Sekhukhuneland could be related to the Cr dust deposition on leaves, and that Cr(VI) would be detected in leaves. Also, (5) hazardous dust deposition would be responsible for substantial human health risk associated with multiple elements. The hypotheses were tested in Chapter 5.

Objective 8: To determine the contribution of deposited Cr particles to Cr accumulation in and on leaves of useful plants.
Objective 9: To quantify the Cr(VI) content of the leaves.
Objective 10: To assess the effects of variables (growth form, pollution, soil) on Cr contamination of plant leaves.
Objective 11: To estimate the human health risk associated with the consumption of dust contaminated plant leaves.

Topography (hilly terrain) and land use (such as mining) could be critical determinant of metal distribution in soil and plants. Plants differ in metal accumulation potential depending on the growth form (Visoottiviseth *et al.*, 2002). Furthermore, serpentine and mining areas are reported to harbour metallophytes that survive on toxic concentrations of metals in soils by accumulating and/or excluding metals (Baker, 1981). It was postulated that (6) topography, land use and growth forms would drive the concentration of metals in soils and plants along a catena in Sekhukhuneland. In addition, (7) the dominant plant species of the region could be categorized as metallophytes. Chapter 6 tests these hypotheses.

Objective 12: To evaluate the influence of topography, land use (for soils and plant) and growth forms (plant) on metal accumulation in soils and plant leaf tissue.
Objective 13: To determine the foliar metal bioaccumulation factors for the dominant plant species.

1.4 Outline of the thesis

Chapter 2 presents a systematic evaluation of global interdisciplinary research on Cr, e.g. toxicity mechanism, environmental sources, phytotoxicity, exposure pathways to plants, accumulation by food and medicinal plants and human health effects. Results highlighted the influence of anthropogenic Cr sources and especially Cr dust deposition on and accumulation by plant leaves.

Findings revealed gaps that are addressed in the present study. The Chapter will be submitted to the *South African Journal of Botany*, Title: Chromium pollution of food and medicinal plants: A review with emphasis on the role of anthropogenic activities.

Chapter 3 identifies Cr dust on the leaves of food and medicinal plant species sampled from randomly selected home gardens and communal lands (rangelands). Results indicated plant morphological traits that enhanced foliar Cr dust contamination. An effect of proximity to active Cr source(s) was highlighted. Part of the chapter is published in *Acta Horticulturae*, Adhikari *et al*., 2021, Title: Chromium dust deposition on *Moringa oleifera* leaves harvested by local communities in Sekhukhuneland, South Africa (Appendix G). The complete chapter is submitted to the *South African Journal of Botany*, Title: Evidence of chromium dust pollution on the leaves of food and medicinal plants from mining areas of Sekhukhuneland, South Africa.

Chapter 4 considers the sources of Cr on leaf surfaces and in soil resulting from anthropogenic pollution. A comprehensive statistical analysis approach (including bi- and multivariate techniques) determined the relation between plant morphology and pollution sources concerning Cr dust deposition. Overlay back trajectory maps indicated the effect of wind movement on dust deposition in sampling sites. The chapter will be submitted to *Environmental Management*, Title: Plant morphology and pollution source collectively determine the level of chromium dust contamination of plant leaves in Sekhukhuneland, South Africa.

Chapter 5 reports on the contribution of Cr dust deposition on Cr accumulation by plant leaves based on a comparative analysis of unwashed and washed leaves. Cr(VI) accumulation was also reported. A comparative analytical approach (washed/unwashed leaves) extended the understanding of lifelong health risks (i.e. non-carcinogenic and carcinogenic) associated with plant leaves exposed to dust containing several toxic elements including Cr. The chapter will be submitted to *Chemosphere,* Title: Accumulation of chromium and other hazardous elements by useful plant leaves and potential health risk to consumers in a dust-polluted mining-smelting region of South Africa.

Chapter 6 examines metal distribution patterns in soil and plant leaves as a consequence of topography and land use. Metal accumulation in plants was also evaluated for different growth forms. Findings presented foliar metal bioaccumulation potential of the dominant species of Sekhukhuneland catena. The chapter will be submitted to *Science of the Total Environment*, Title: Metallophytes in a centre of endemism: Distribution and bioaccumulation of metals in soils and plants.

Chapter 7 summarises conclusions deduced from the findings of each chapter. They were aligned with the study aim and objectives. Derived conclusions provided some perspective on the susceptibility of plant leaves to atmospheric dust contamination in Cr mining and ferrochrome smelters affected areas, health risks associated with the ingestion of dust contaminated plant leaves, the importance of thorough washing of leaves before use and the possibility of the use of metallophytes to mitigate metal enrichment in catena soils in Sekhukhuneland. Study limitations were presented. A final synthesis revealed scientific gaps to be addressed.

References

Baker, A.J.M. 1981. Accumulators and excluders – strategies in the response of plants to heavy metals. *Journal of Plant Nutrition,* 3:643–654.

Baker, A.J.M., Ernst, W.H.O., van der Ent, A., Malaisse, F. & Ginocchio, R. 2010. Metallophytes: the unique biological resource, its ecology and conservational status in Europe, central Africa and Latin America. In: Batty, L.C. & Hallberg, K.B., eds. *Ecology of industrial pollution*, Cambridge: Cambridge University Press. pp. 7–40.

Bi, X., Feng, X., Yang, Y., Li, X., Shin, G.P.Y., Li, F., … Fu, Z. 2009. Allocation and source attribution of lead and cadmium in maize (*Zea mays* L.) impacted by smelting emissions. *Environmental Pollution,* 157(3):834–839.

Castanheiro, A., Hofman, J., Nuyts, G., Joosen, S., Spassov, S., Blust, R., … Samson, R. 2020. Leaf accumulation of atmospheric dust: biomagnetic, morphological and elemental evaluation using SEM, ED-XRF and HR-ICP-MS. *Atmospheric Environment*, 221, art. 117082. https://doi:10.1016/j.atmosenv.2019.117082

Chen, L., Liu, C., Zhang, L., Zou, R. & Zhang, Z. 2017. Variation in tree species ability to capture and retain airborne fine particulate matter ($PM_{2.5}$). *Scientific Report*, 7(1):1–11.

Coetzee, J.J., Bansal, N. & Chirwa, E.M.N. 2018. Chromium in environment, Its toxic effect from chromite-mining and ferrochrome industries, and its possible bioremediation. *Exposure and Health,* 12:51–62.

Csavina, J., Field, J., Taylor, M.P., Gao, S., Landázuri, A., Betterton, E.A. & Eduardo Sáez, A. 2012. A review on the importance of metals and metalloids in atmospheric dust and aerosol from mining operations. *Science of The Total Environment,* 433:58–73.

Dhal, B., Thatoi, H.N., Das, N.N. & Pandey, B.D. 2010a. Reduction of hexavalent chromium by *Bacillus* sp. isolated from chromite mine soils and characterization of reduced product. *Journal of Chemical Technology & Biotechnology,* 85(11):1471–1479.

Dhal, B., Das, N.N., Pandey, B.D. & Thatoi, H.N. 2010b. Environmental Quality of the Boula-Nuasahi chromite mine area in India. *Mine Water and the Environment,* 30(3):191–196.

Entwistle, J.A., Hursthouse, A.S., Marinho Reis, P.A. & Stewart, A.G. 2019. Metalliferous mine dust: human health impacts and the potential determinants of disease in mining communities. *Current Pollution Reports,* 5:67–83.

Gaspar, L., Lizaga, I. & Navas, A. 2020. Elemental mobilisation by sheet erosion affected by soil organic carbon and water fluxes along a radiotraced soil catena with two contrasting parent materials. *Geomorphology,* 370(1), art. 107387. https://doi.org/10.1016/j.geomorph.2020.107387

Gomes, M.A. da C., Hauser-Davis, R.A., Suzuki, M.S. & Vitória, A.P. 2017. Plant chromium uptake and transport, physiological effects and recent advances in molecular investigations. *Ecotoxicology and Environmental Safety*, 140:55–64.

Kien, C.N., Noi, N.V., Son, L.T., Ngoc, H., Tanaka, S., Nishina, T. & Iwasak, K. 2010. Heavy metal contamination of agricultural soils around a chromite mine in Vietnam. *Soil Science and Plant Nutrition*, 56:344–356.

Kimbrough, D.E., Cohen, Y., Winer, A.M., Creelman, L. & Mabuni, C. 1999. A critical assessment of chromium in the environment. *Critical Reviews in Environmental Science and Technology*, 29(1):1–46.

Leonard, R.J., McArthur, C. & Hochuli, D.F. 2016. Particulate matter deposition on roadside plants and the importance of leaf trait combinations. *Urban Forestry & Urban Greening,* 20:249–253.

Liu, H-L., Zhou, J., Li, M., Hu, Y., Liu, X. & Zhou, J. 2019. Study of the bioavailability of heavy metals from atmospheric deposition on the soil-pakchoi (*Brassica chinensis* L.) system. *Journal of Hazardous Materials*, 362:9–16.

Mo, L., Ma, Z., Xu, Y., Sun, F., Lun, X., Liu, X., Chen, J. & Yu, X. 2015. Assessing the capacity of plant species to accumulate particulate matter in Beijing, China. *Plos One,* 10(10), e0140664. https://doi.org/10.1371/journal.pone.0140664

Mogale, M.M.P., Raimondo, D.C. & Van Wyk, B-E. 2019. The ethnobotany of central Sekhukhuneland, South Africa. *South African Journal of Botany,* 122:90–119.

Mohanty, M., Pattnaik, M.M., Mishra, A.K. & Patra, H.K. 2012. Bio-concentration of chromium – an *in situ* phytoremediation study at south Kaliapani chromite mining area of Orissa, India. *Environmental Monitoring and Assessment*, 184(2):1015–1024.

Neinhuis, C. & Barthlott. W. 1998. Seasonal changes of leaf surface contamination in beech, oak, and ginkgo in relation to leaf micromorphology and wettability. *New Phytologist*, 138:91–98.

Oze, C., Fendorf, S., Bird, D.K. & Coleman, R.G. 2004. Chromium geochemistry of serpentine soils. *International Geology Review*, 46(2):97–126.

Pöykiö, R., Mäenpä, A., Perämäki, P., Niemelä, M. & Välimäki, I. 2005. Heavy metals (Cr, Zn, Ni, V, Pb, Cd) in lingonberries (*Vaccinium vitis-idaea* L.) and assessment of human exposure in two industrial areas in the Kemi-Tornio region, northern Finland. *Archives of Environmental Contamination and Toxicology*, 48:338–343.

Proctor, J. 2003. Vegetation and soil and plant chemistry on ultramafic rocks in the tropical Far East. *Perspectives in Plant Ecology, Evolution and Systematics,* 6(1,2):105–124.

Rosemary, F., Vitharana, U.W.A., Indraratne, S.P. & Weerasooriya, S.V.R. 2014. Concentrations of trace metals in selected land uses of a dry zone soil catena of Sri Lanka. *Tropical Agricultural Research*, 25:512–522.

Scoon, R.N. & Viljoen, M.J. 2019. Geoheritage of the eastern limb of the Bushveld Igneous Complex, South Africa: a uniquely exposed layered igneous intrusion. *Geoheritage,* 11:1723–1748.

Semenya, S.S. & Potgieter, M.J. 2014. Medicinal plants cultivated in Bapedi traditional healers homegardens, Limpopo Province, South Africa. *African Journal of Traditional, Complementary and Alternative Medicines*, 11(5):126–132.

Shahid, M., Shamshad, S., Rafiq, M., Khalid, S., Bibi, I., Niazi, N.K., … Rashid, M.I. 2017. Chromium speciation, bioavailability, uptake, toxicity and detoxification in soil-plant system: a review. *Chemosphere*, 178:513–533.

Siebert, S.J., Van Wyk, A.E. & Bredenkamp, G.J. 2002. The physical environment and major vegetation types of Sekhukhuneland, South Africa. *South African Journal of Botany,* 68(2):127–142.

Siebert, S.J., Matthee, M. & Van Wyk, A.E. 2003. Semi-arid savanna of the Potlake Nature Reserve and surrounding areas in Sekhukhuneland, South Africa. *Koedoe*, 46(1):29–52.

Sokol, E.V., Nigmatulina, E.N. & Nokhrin, D.Y. 2010. Dust emission of chromium from chromite ore processing residue disposal areas in the vicinity of Krasnogorskii village in Chelyabinsk Oblast. *Contemporary Problems of Ecology*, 3(6):621–630.

Tshehla, C. & Djolov, G. 2018. Source profiling, source apportionment and cluster transport analysis to identify the sources of PM and the origin of air masses to an industrialised rural area in Limpopo. *Clean Air Journal*, 28(2):54–66.

Tshehla, C. & Wright, C.Y. 2019. Spatial variability of PM_{10}, $PM_{2.5}$ and PM chemical components in an industrialised rural area within a mountainous terrain. *South African Journal of Science,* 115(9/10), art. 6174. https://doi.org/10.17159/ sajs.2019/6174

Van Wyk, B. & Van Wyk, P. 1997. *Field Guide to Trees of Southern Africa*. Cape Town: Struik.

Visoottiviseth, P., Francesconi, K. & Sridokchan, W. 2002. The potential of Thai indigenous plant species for the phytoremediation of arsenic contaminated land. *Environmental Pollution*, 118(3):453–461.

Yaman, B. 2020. Health effects of chromium and its concentrations in cereal food together with sulfur. *Exposure and Health*, 12:153–161.

Chapter 2

Chromium pollution of useful plants – global trends

2.1 Introduction

Chromium (Cr) is, respectively, the 7th and 21st most abundant transition element on the Earth's crust and in crystalline rocks (Cervantes *et al*., 2001; Babula *et al*., 2008; Ertani *et al*., 2017; Gomes *et al*., 2017). The industrial feasibility of multiple physical and chemical properties of this heavy metal has resulted in the global popularity of Cr with metallurgical units being the largest (95%) collective Cr users (Dhal *et al*., 2013; Shahid *et al*., 2017). As a result, discarded Cr materials in the environment are increasing continuously (Shahid *et al*., 2017). Cr complexes are persistent, toxic and mobile, and may interfere with biogeochemical cycles, interrupt ecosystem processes and biosphere functioning (Maharia *et al*., 2010; Unver *et al*., 2015; Gomes *et al*., 2017).

Environmental Cr concentrations are a combined contribution from geogenic (rocks and minerals) and anthropogenic sources (Kimbrough *et al*., 1999; Shanker *et al*., 2005; Meena *et al*., 2010; Nagajyoti *et al*., 2010; Unver *et al*., 2015; Gomes *et al*., 2017). Increasing bioavailability and biomobility of Cr in different environmental matrices is, however, a direct consequence of human-activity associated disposal (Dhal *et al*., 2013; Shahid *et al*., 2017). As a consequence, higher Cr concentrations are noted in all the major cultivation segments, i.e. agricultural and farmlands and urban gardens, as well as in rangelands (Awodele *et al*., 2013; Dhal *et al*., 2013; Owolabi *et al*., 2016; Kim *et al*., 2015, 2017; Vaikosen & Alade, 2017; Milićević *et al*., 2018). This raises health concerns related to ingestion of food and medicinal plants harvested from such sites due to Cr being a carcinogenic element (Kimbrough *et al*., 1999; Cervantes *et al*., 2001; Barouchas *et al*., 2014; Ertani *et al*., 2017; Shahid *et al*., 2017).

Most studies focus on Cr pollution effects in major city centres (Säumel *et al*., 2012; Ishaq *et al*., 2013; Mahmood *et al*., 2013; Li *et al*., 2015; Unver *et al*., 2015; Pennisi *et al*., 2017), while other high-risk pollution zones such as mines and smelters, and surrounding areas inhabited mostly by underprivileged communities, are often overlooked. Metal mining is noteworthy as it continuously contaminates the surroundings leading to metal accumulation in biota (Nagajyoti *et al*., 2010; Shahid *et al*., 2016). In South Africa, prolonged health consequences among rural people as a result of exposure to soil polluted with multiple toxic heavy metals released from a gold mine was reported (Kamunda *et al.*, 2016). Heavy metal contamination of food (China, Cheng *et al*., 2017; Zhang *et al*., 2019) and medicinal plants (India, Maharia *et al*., 2010) from mining sites were reported also. These studies highlighted the health hazards associated with the ingestion of useful plants exposed to mine wastes. In addition to solid and liquid waste, mining emits large volumes

of atmospheric particulate matter (PM) (Kimbrough *et al*., 1999; Nagajyoti *et al*., 2010) that may disperse over large distances. Elevated concentrations of foliar heavy metals in vegetation surrounding mining and urbanised regions are well documented (Voutsa *et al*., 1996; Säumel *et al*., 2012; Shahid *et al*., 2016). Contamination of food and medicinal plants may undermine food security and threaten the supply of affordable and sustainable produce to communities in urban and peri-urban crop production settings (Säumel *et al*., 2012; Aziz *et al*., 2016).

This review aims to gather information on preselected research themes dealing with Cr pollution in the environment (Kimbrough *et al*., 1999; Nagajyoti *et al*., 2010; Dhal *et al*., 2013; Ertani *et al*., 2017) and Cr-plant interactions (Cervantes *et al*., 2001; Shanker *et al*., 2005; Babula *et al*., 2008; Aziz *et al*., 2016; Gomes *et al*., 2017; Shahid *et al*., 2016, 2017). The objective of the former was to assess Cr chemistry, toxicity and describe known chemical reaction mechanisms in the environment. The objective of the latter was to evaluate phytotoxicity in useful plants and describe known plant-Cr interactions. This comprehensive account was required to interlink and integrate prominent and correlated research areas to understand Cr pollution and Cr-plant (food and medicinal plants) interaction patterns in a global context. The review sets out to explore Cr toxicity [Cr(III) and Cr(VI)] in plants, its environmental sources, accumulation pathways, and health impacts on humans. Effects of anthropogenic emissions were given special attention to indicate Cr pollution as a prime contamination source especially within urban establishments.

2.2 Methodology of literature selection

2.2.1 Selection of literature

Independent SCOPUS searches were conducted on 7 and 8 October 2018 to develop search strings (Table A1, Appendix A) to retrieve articles on three search categories, i.e. “Cr toxicity in food plants”, “Cr toxicity in medicinal plants” and “Cr toxicity in food/medicinal plants” (under the most cited category in SCOPUS). For the ‘food plants’ category, the main words included in the search process were chromium, food, plants, pollution, toxicity, crops, vegetables, accumulation and deposition. The literature search process for the ‘medicinal plant’ category included keywords: chromium, medicinal, plants, pollution and contamination. Research areas specifically excluded from the systematic search were wastewater, sewage and sludge. The third search was conducted to obtain the ‘most cited’ articles regarding environment-Cr-plant research. For this search, chromium, pollution, toxicity, plants, food, medicinal and heavy metal were the main keywords. SCOPUS database on the following subject areas, Agricultural and Biological Sciences, Environmental Sciences, Pharmacology and Earth and Planetary Sciences was primarily targeted while Medicine, Biochemistry, Biotechnology and Engineering were excluded. The search process was limited to the ‘English’ language.

SCOPUS search results generated a preliminary database of 240 articles. From there, the final list of literature was drawn based on the available abstracts and keywords that fell within one or more of the inclusion criteria, (i) Cr chemistry, its environmental interactions and toxicity, (ii) origins of Cr in nature (geogenic/anthropogenic), and (iii) Cr-plant interaction/phytotoxicity mechanisms. Research primarily aimed at other heavy metal(s), wastewater irrigation, soil amendment and phytoremediation were omitted as outside the scope of this research. A total of 39 articles were selected (Fig. 2.1). An additional set of 24 articles that met the inclusion criteria and were considered highly relevant were include despite not being picked up by systematic searches in SCOPUS. The complete literature database, therefore, comprised of 63 research papers (Table A2, Appendix A). The study may have unintentionally excluded other relevant articles as a result of the search engine oriented article selection process.

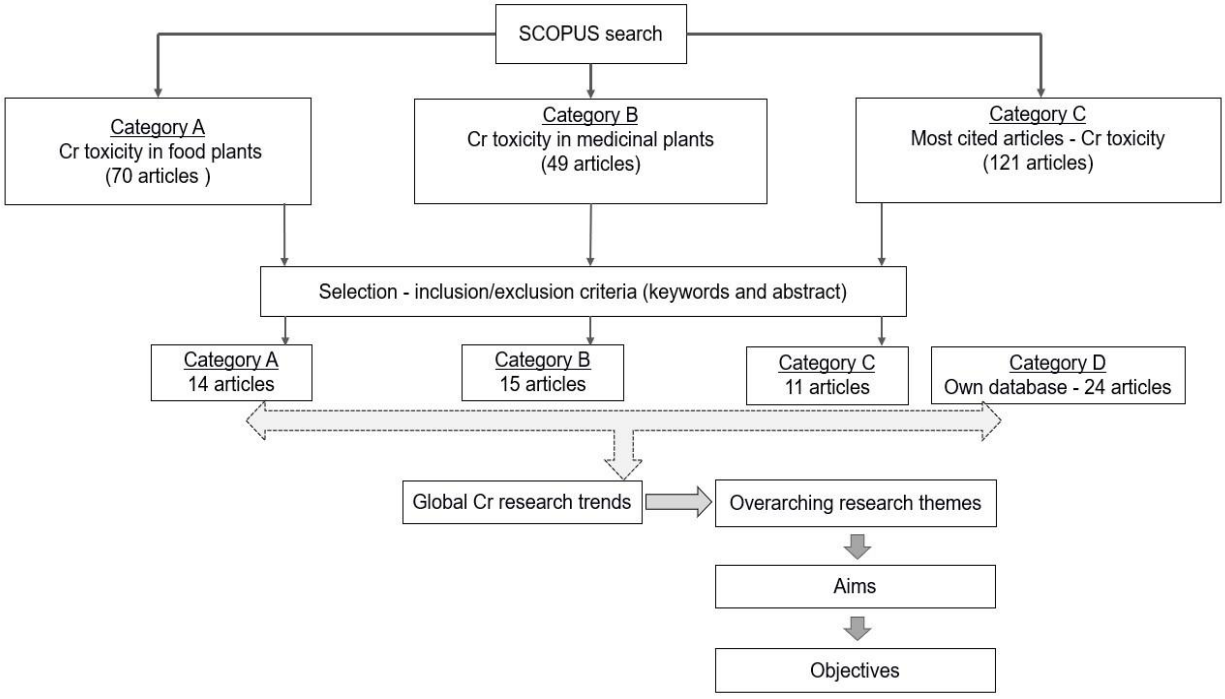

Figure 2.1. Systematic search and article selection process.

2.2.2 Research themes

From the selected literature, it was evident that global research on environmental Cr pollution was mainly focused on its chemistry and toxicity, reaction mechanisms, remediation methods, phytotoxicity and Cr accumulation by useful plants. A further study of the selected literature revealed interconnectedness among these study fields with regards to environment-Cr-plant interaction process. The present investigation hence conducted and concluded on the following seven overarching Cr research themes: (1) toxicity, (2) environmental sources, (3) accumulation pathways by plants, (4) phytotoxicity, (5) accumulation by food and (6) medicinal plants, and (7)

toxicity impact on human health. The research themes and sub-themes summarised outcomes reported in the reviewed literature to explore environmental Cr pollution and Cr-plant interaction (Fig. 2.2).

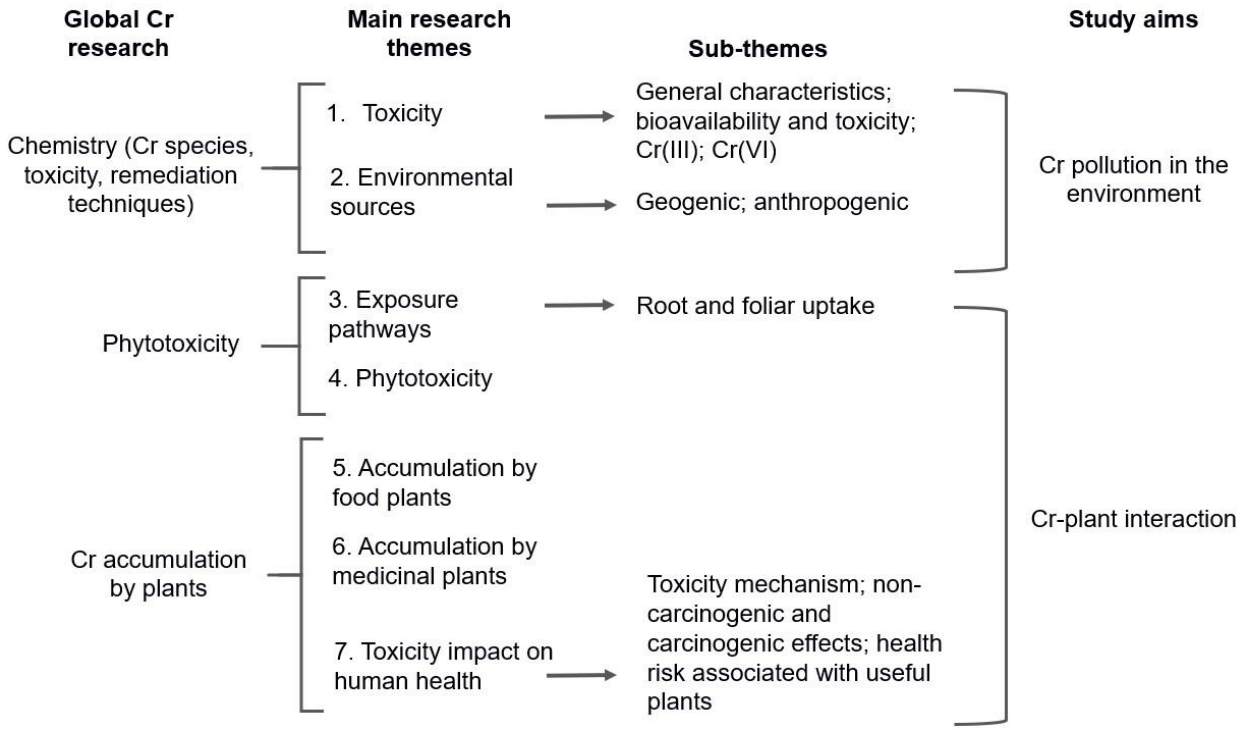

Figure 2.2. Research themes and aims of the review.

Based on the primary research focus of the retrieved articles they were grouped under one or more research themes to analyse further (Table A3, Appendix A). During the study, knowledge gaps have been identified that limit the complete understanding of these intricately connected and complex study fields, and at the same time may indicate future research courses.

2.3 Results and discussion

2.3.1 Toxicity

2.3.1.1 General characteristics

Cr is one of the top 129 environmental pollutants, and hexavalent forms are recognised as one of the 14 most hazardous substances to living organisms (Ertani *et al*., 2017). Cr is the sixth most abundant transition element that may exist in varied oxidation states, Cr^{2-} to Cr^{6+} (Zayed *et al*., 1998; Barouchas *et al*., 2014; Gomes *et al*., 2017; Shahid *et al.*, 2017). Under natural conditions, tri- (Cr(III)) and hexavalent (Cr(VI)) forms are the most stable ones associated with biological toxicity impacts (Shanker *et al*., 2005; Dhal *et al*., 2013; Barouchas *et al*., 2014; Ertani *et al*., 2017; Gomes *et al*., 2017; Shahid *et al*., 2017). Other oxidation states are unstable transition forms

primarily generated during interspecies conversion reactions (i.e. Cr(III)⇌Cr(VI)) (Oze *et al*., 2004; Shanker *et al*., 2005; Shahid *et al*., 2017).

Cr bioavailability, mobility and toxicity are interrelated depending on the mix of total Cr, concentrations of oxidation states and the conversion dynamics of oxidation states (Kimbrough *et al*., 1999; Sungur *et al*., 2013). Unlike other heavy metals with multiple oxidation states, e.g. Al, Cd, Hg and Pb, Cr has attracted less attention from plant and environmental scientists (Sungur *et al*., 2013) due to its complex electronic chemistry, frequent conversion between oxidation states, and differential electrical charge, physicochemical and biochemical reactivity, bioavailability, solubility, mobility and hazard potential of Cr oxidation states (Kimbrough *et al*., 1999; Panichev *et al*., 2005; Shanker *et al*., 2005; Sungur *et al*., 2013; Barouchas *et al*., 2014). In this regard, the global inadequacy of available literature on Cr species determination in plant systems is well-acknowledged (Zayed *et al*., 1998).

2.3.1.2 Bioavailability and toxicity

In soil, excess Cr is primarily added as industrial solid and liquid waste as chromate by-products, ferrochromium slag and chromium plating baths which contains combinations of Cr(III) and Cr(VI) compounds (Kimbrough *et al*., 1999). Once in the soil environment, these complexes are subjected to prevalent reactions, i.e. oxidation-reduction, sorption-desorption and precipitation-dissolution (Kimbrough *et al*., 1999; Dhal *et al*., 2013; Barouchas *et al*., 2014; Gomes *et al*., 2017; Shahid *et al.*, 2017). Hence, both these chemical species may coexist and generate at the same time depending on their respective concentrations and interconversion rate at a given time (Dhal *et al*., 2013). In addition, soil parameters, e.g. pH, electrothermal potential of reaction, cation exchange capacity, temperature, light, presence of sorbents, reducing and oxidising agents, organic carbon, clay content, and microbial and other biological composition may further interfere with the interconversion mechanism (Kimbrough *et al*., 1999; Ding *et al*., 2014; Shahid *et al*., 2017). It is, however, difficult to conclude the independent significance of each parameter on Cr bioavailability, mobility and toxicity as these are intertwined under natural conditions (Ding *et al*., 2014).

Under most soil conditions, oxidation of Cr(III) to Cr(VI) is an atypical process due to the limited presence of natural oxidising agents, mainly manganese (Mn) oxides, i.e. (III)/(IV), and hydrogen peroxide (H_2O_2) (Kimbrough *et al*., 1999; Dhal *et al*., 2013; Gomes *et al*., 2017). Chemical form and concentration of Cr(III), and presence of low molecular weight organic matter that can chelate Cr(III) to retard its oxidation rate may also affect such reactions (Kimbrough *et al*., 1999; Dhal *et al*., 2013). On the other hand, reduction of Cr(VI) to Cr(III) can be a frequent reaction in soil (Kimbrough *et al*., 1999; Shanker *et al*., 2005) under acidic pH, high levels of humic and organic

substances, and in presence of common reducers, e.g. vanadium, sulphides or Fe(II) compounds (Cervantes *et al*., 2001; Dhal *et al*., 2013).

2.3.1.3 Trivalent Cr

Cr(III) is thermodynamically the most stable and abundant chemical form of the element found in nature (unpolluted conditions) (Kimbrough *et al*., 1999; Pandey *&* Sharma*,* 2003; Barouchas *et al*., 2014; Ertani *et al*., 2017). Cr(III) as chromite ($FeCr_2O_4$) is the principal ore and most Cr(III) compounds in nature are formed as a result of natural weathering of minerals (Oze *et al*., 2004; Kazakis *et al*., 2018). After its formation, Cr(III) rapidly precipitates as chromium hydroxides or iron-chromium hydroxides or adsorbed on mineral beds or soil organic colloids to present low hazard potential (Cervantes *et al*., 2001; Barouchas *et al*., 2014; Kazakis *et al*., 2018). These complexes have low solubility and reactivity and under reducing environments with pH > 4, Cr(III) complexes are stable (Cervantes *et al*., 2001; Oze *et al*., 2004; Kazakis *et al*., 2018). An acidic environment may release it from such fixed forms to become bioavailable (Oze *et al*., 2004; Kazakis *et al*., 2018).

2.3.1.4 Hexavalent Cr

Thermodynamically, Cr(VI) is the second most stable form and, unlike Cr(III), is mostly generated by human activities and seldom by natural processes (Kimbrough *et al*., 1999; Dhal *et al*., 2013). Approximately 35% of the total human released Cr is accounted for as Cr(VI) upon release (Kimbrough *et al*., 1999; Dhal *et al*., 2013). Cr(VI) often reacts with oxygen to form oxyanion forming complexes, chromate (CrO_4^{2-}) at pH value > 6.4, and bi-chromate ($HCrO^{4-}$) and di-chromate ($Cr_2O_7^{2-}$) at pH < 6.4 (Oze *et al*., 2004; Dhal *et al*., 2013). Chromate is the most abundant form of Cr(VI) found in discarded solid and liquid waste (Dhal *et al*., 2013; Ertani *et al*., 2017). Such complexes are carcinogenic and corrosive with high mobility, bioavailability and oxidising potential (Oze *et al*., 2004; Panichev *et al*., 2005; Dhal *et al*., 2013; Kazakis *et al*., 2018). With such properties, Cr(VI) complexes, therefore, act as persistent environmental pollutants under oxidising conditions and at alkaline pH with low organic content otherwise depleting available reducing agents (Kimbrough *et al*., 1999; Cervantes *et al*., 2001; Dhal *et al*., 2013; Ding *et al*., 2014; Kazakis *et al*., 2018). Water solubility at a wide range of pH (acidic to alkaline) (Dhal *et al*., 2013) and ability to form unstable and highly reactive complexes in weathering solutions capacitates Cr(VI) to induce harmful reactions in living organisms (refer to section 2.3.7) (Zayed *et al*., 1998; Kimbrough *et al*., 1999; Tiwari *et al*., 2009; Sungur *et al*., 2013).

2.3.2 Environmental sources

2.3.2.1 Geogenic

Cr is a natural component of rocks and soils (Shahid *et al*., 2017) and the mean Cr concentration on earth's crust is around 100 µg g^{-1} while it stays within the 10–200 µg g^{-1} range in soil and sediments (Kazakis *et al*., 2018). Cr levels are primarily determined by the chemical composition of the bedrock, environmental conditions and natural processes (Dube *et al*., 2004; Maharia *et al*., 2010; Nagajyoti *et al*., 2010). Among natural processes, weathering of rocks and minerals, and soil erosion are the noteworthy contributors of geogenic Cr (~ 80%) (Maharia *et al*., 2010; Nagajyoti *et al*., 2010; Kozak *et al*., 2015). Cr concentrations in rocks however differ greatly (Kimbrough *et al*., 1999). Chromite is abundant in mafic (170–200 µg g^{-1}) and ultramafic igneous rocks (1600–3400 µg g^{-1}) (Shahid *et al*., 2017). In other igneous and sedimentary rocks, e.g. basalt, granite and shales, Cr levels range between 2–1000 µg g^{-1} (Nagajyoti *et al*., 2010; Ertani *et al*., 2017; Shahid *et al.*, 2017). Shale contains the highest concentrations of metals including Cr among sedimentary rocks followed by lime and sandstones (Nagajyoti *et al*., 2010; Shahid *et al.*, 2017).

Compared to other soil types, serpentinite-derived (metamorphosed igneous rock) soils host higher Cr concentrations (> 200 µg g^{-1} to 6 wt%) (Oze *et al*., 2004; Ertani *et al*., 2017; Kazakis *et al*., 2018). Serpentine soils are characterized by unfavourable conditions for plant growth, such as low water retention capacity, wide pH range (acidic to alkaline, 5.5–9.5), higher levels of heavy metals (e.g. Co, Cr and Ni), and low amounts of essential nutrients (e.g. Ca, K and P) with high Mg to Ca ratios (Oze *et al*., 2004; Zlatić *et al*., 2017). In general, plants growing in such soils are reported to accumulate elevated levels of available heavy metals, although Cr toxicity impact on plants cultivated in geogenic Cr rich soils is poorly investigated and understood (Oze *et al*., 2004).

Other noteworthy natural sources of Cr are volcanic eruption, forest wildfires, floods, tsunamis and accumulation of forest litter (Maharia *et al*., 2010; Nagajyoti *et al*., 2010; Kozak *et al*., 2015). Wind and marine aerosols play a critical role in the dispersion of heavy metals that can alter concentrations (Nagajyoti *et al*., 2010; Kim *et al*., 2015).

2.3.2.2 Anthropogenic

Cr has manifold applications in numerous industries (Cervantes *et al*., 2001; Rai *et al*., 2005; Shanker *et al*., 2005; Nagajyoti *et al*., 2010; Dhal *et al*., 2013; Ertani *et al*., 2017; Shahid *et al.*, 2017). Cr(VI) is mainly used in chrome alloy, metal finishing and chrome-plating, oxidiser in chemical industry, production of chemicals and pigment, leather tanning, corrosion inhibition, and cooling tower water treatment (Kimbrough *et al*., 1999; Shanker *et al*., 2005; Babula *et al*., 2008; Dhal *et al*., 2013). The majority of its release is ascribed to Cr mining, chrome-plating, leather

tanning, chemical industry and fugitive emissions from cooling towers (Dhal *et al*., 2013). Cr(III) is well-utilised as a tinting agent and employed in fewer industries, namely ceramics, glass, photography and textile (Dhal *et al*., 2013). Primary emitters of Cr(III) are industrial cooling towers and traffic (Babula *et al*., 2008; Shahid *et al.*, 2017).

In developing countries, Cr release is a major environmental issue due to the fast expansion of industries accompanied by a lack of functional environmental management systems (Abbasi *et al*., 2013; Cheng *et al*., 2017). Cr contaminants may reach soils through direct waste disposal from industries in solid or liquid form, leaching from dumpsites and landfills, urban effluent discharge, and precipitation of atmospheric PM from industries, and incineration of solid waste and refuse (Kimbrough *et al*., 1999; Rai *et al*., 2005; Yang *et al*., 2007; Maharia *et al*., 2010; Nagajyoti *et al*., 2010; Vaikosen & Alade, 2017). Consequently, geogenic Cr amounts in the environment could be increased by human released waste (Cervantes *et al*., 2001; Kim *et al*., 2015, 2017; Kazakis *et al*., 2018).

Among others, mining is concluded as one of the noteworthy Cr polluters (Dhal *et al*., 2013). Furthermore, ores exposed by mining operations pollute the environment at an expedited rate than natural weathering processes (Nagajyoti *et al*., 2010). Cr mining may add significant levels of Cr with elevated concentrations of toxic Cr(VI) in soil (Dhal *et al*., 2013). In general, mine tailings and dumpsites are hence recognised as major points of heavy metal pollution (Dhal *et al*., 2013; Kamunda *et al*., 2016; Dobbins *et al*., 2021). The severity of pollution and degradation of the habitat often correlates with proximity to mining activities (Nagajyoti *et al*., 2010; Dhal *et al*., 2013; Shahid *et al.*, 2016).

Overuse of inorganic (e.g. chemical fertilisers, fungicides and pesticides containing Cr, Cd, Cu, Ni, Pb and Zn) and/or organic agro-products (e.g. phosphorus fertilizers and biosolids containing Cr) in modern farming practice may further increase Cr quantities in agricultural soils (Yang *et al*., 2007; Nagajyoti *et al*., 2010; Shahid *et al.*, 2016, 2017; Milićević *et al*., 2018). Thereby, changing soil physicochemical parameters that lead to unfavourable mineral composition and altered microbial activity (Tiwari *et al*., 2009; Li *et al*., 2014; Unver *et al*., 2015; Vaikosen & Alade, 2017).

In urban regions, atmospheric PM bearing Cr from mines, smelters, industries, fugitive emissions from industrial cooling towers, waste incinerators, fuel combustion and traffic exhaust are prime Cr emitters (Voutsa *et al*., 1996; Babula *et al*., 2008; Nagajyoti *et al*., 2010; Feng *et al*., 2011; Säumel *et al*., 2012; Kim *et al*., 2015, 2017; Li *et al*., 2015; Shahid *et al.*, 2016, 2017; Kazakis *et al*., 2018). Cr containing PM may remain in the air for seven to ten days, and the atmospheric half-life of Cr(VI) is 16 hours to 4.8 days (Kimbrough *et al.*, 1999; Venter *et al*., 2016). Once

released such particles can disperse or re-suspended from the soil by prevailing wind currents redistributing Cr (Kimbrough *et al*., 1999; Venter *et al*., 2016).

In short, global Cr demand, therefore, resulted in increased mining activities (Shahid *et al.*, 2017) and subsequent influx of Cr from multiple release points into the environment (Awodele *et al*., 2013; Unver *et al*., 2015). As a result, higher soil Cr levels were noted globally (Ertani *et al*., 2017) and in some soils in China, it reached up to 1.1% as a consequence of extensive industrial usage (Shahid *et al.*, 2017).

2.3.3 Accumulation pathways by plants

Plants can be exposed to heavy metals via soils to root systems and from the atmosphere to foliage (Feng *et al*., 2011; Wahsha *et al*., 2014; Shahid *et al.*, 2016; Vaikosen & Alade, 2017; Pajević *et al*., 2018). Hence, to comprehend metal contamination of plants both these exposure pathways need to be accounted for. The foliar exposure pathway becomes important in areas affected by hazardous dust emitters such as mines, smelters, industries, traffic or in urban agglomerations that are polluted by multiple emission points (Voutsa *et al*., 1996; Feng *et al*., 2011; Säumel *et al*., 2012; Unver *et al*., 2015; Shahid *et al.*, 2016).

2.3.3.1 Root uptake

Soil acts as a primary heavy metal sink that can readily make toxic substances available to the plant root system (Arsenov *et al*., 2016). Metals produce water-soluble ions that can be taken up easily by plant roots at elevated concentrations (Arsenov *et al*., 2016; Pajević *et al*., 2018). In a polluted soil environment, however, root-metal interactions depend on multiple variables such as the metal (concentration, distribution and size of particles, chemical speciation, synergistic/antagonistic relationship with co-existing elements); soil parameters (redox potential, pH, temperature, aeration, moisture, organic matter content, and mineral and microbial composition); plant features (species, phenological stage, water relation, accumulation traits, accumulating organs); and soil and atmospheric pollution levels in that area (pollution source and chemical variability of pollutants) (Voutsa *et al*., 1996; Mandiwana *et al*., 2007; Wahsha *et al*., 2014; Arsenov *et al*., 2016; Anjum *et al*., 2017; Gomes *et al*., 2017; Sun *et al*., 2018). Dry (atmospheric particles settling on soil) and wet (via air moisture, dew, fog rain and snow) deposition of aerial particulate matter can increase metal concentrations in soil (Voutsa *et al*., 1996; Kimbrough *et al*., 1999). Wind dispersion and deposition rate of dust, irrigation measures and edaphic factors (e.g. texture and organic matter) can influence dust origin and deposition further (Voutsa *et al*., 1996). For Cr, carbonate ions (CO_3^{2-}) and low molecular weight organic acids (e.g. oxalic, citric, succinic, tartaric, malic and salicylic acid) are noted to influence solubility and phytoavailability of Cr(VI) and Cr(III), respectively (Panichev *et al*., 2005; Mandiwana *et al*.,

2007; Ertani *et al*., 2017). While, the availability of geogenic Cr(VI) is mainly determined by the solubility of soil minerals (Panichev *et al*., 2005).

2.3.3.2 Foliar uptake

United States Environmental Protection Agency (USEPA) described Cr as one of 18 core hazardous air pollutants and one of 33 urban air pollutants (Shahid *et al.*, 2017). Deposition of atmospheric pollutants is one of the important metal contamination pathways besides polluted soil and wastewater (Säumel *et al*., 2012; Shahid *et al.*, 2016). Investigations indicating higher than expected levels of toxic elements in plant tissues when cultivated in unpolluted soils are often concluded to be a result of aerial pollution (Larsen *et al*., 1992; Voutsa *et al*., 1996; Feng *et al*., 2011; Säumel *et al*., 2012). Airborne Cr contamination and foliar Cr uptake, however, remains an under-investigated field of research compared to other heavy metals (Shahid *et al.*, 2016). Nevertheless, safety concerns regarding food and medicinal crops from urban gardens (Säumel *et al*., 2012; Kim *et al*., 2015; Pennisi *et al*., 2017), farmlands (Li *et al*., 2015; Kim *et al*., 2017) and wild plants harvested from sites impacted by atmospheric emissions (Ishaq *et al*., 2013; Unver *et al*., 2014), have been raised globally. Apart from pollution during cultivation, crops can be exposed to dust deposition during post-harvest stages such as transportation, marketing and sale (Säumel *et al*., 2012; Arsenov *et al*., 2016; Kumar *et al*., 2018). Foliar dust contamination may differ based on plant species, variations in emission rates and meteorological conditions mainly wind speed and direction and precipitation (Voutsa *et al*., 1996; Pajević *et al*., 2018).

2.3.4 Phytotoxicity

As a non-essential element to plants, excess Cr can exert negative effects on plants (Shanker *et al*., 2005). Cr uptake, translocation and accumulation are however greatly affected by the presence and bioavailability of dominant chemical species (i.e. Cr(III) and Cr(VI)) in the ambient environment (Panichev *et al*., 2005; Shanker *et al*., 2005; Ertani *et al*., 2017; Gomes *et al*., 2017). Under intracellular conditions, both Cr(VI) and Cr(III) can cause oxidative damage by generating reactive oxygen species (ROS) upon reduction (Panichev *et al*., 2005; Shanker *et al*., 2005; Mandiwana *et al*., 2007; Anjum *et al*., 2017; Ertani *et al*., 2017; Gomes *et al*., 2017). Uptake rate and phytotoxic impact of Cr(VI) is however far greater than Cr(III) (Zayed *et al.*, 1998; Cervantes *et al*., 2001; Barouchas *et al*., 2014). Cr stress generally alters metabolic processes by modification of pigment structure and production (chlorophyll, anthocyanin, carotenoids); elevated production of metabolites (glutathione, ascorbic acid); and increased generation of new metabolites (phytochelatins, histidine) as part of toxicity tolerance and resistance mechanisms (Shanker *et al*., 2005; Nagajyoti *et al*., 2010; Ertani *et al*., 2017; Gomes *et al*., 2017). Major plant processes affected by Cr stress is depicted in Table 2.1.

Table 2.1. Prominent plant processes affected by Cr exposure. NR, not reported in the reviewed literature.

Process	Plant species (reference)	
	Food plants	Medicinal plants
Antioxidative defence mechanisms, physiological and biochemical processes	*Brassica oleracea* (Pandey & Sharma, 2003); *Pisum sativum* (Tiwari *et al*., 2009); *Raphanus sativus* (Dube *et al*., 2004; Tiwari *et al*., 2013); *Zea mays* (Anjum *et al*., 2017)	*Ocimum tenuiflorum* (Rai *et al*., 2004)
Growth and development	*Brassica oleracea* (Pandey & Sharma, 2003); *Lactuca sativa* (Li *et al*., 2014); *Pisum sativum* (Tiwari *et al*., 2009); *Raphanus sativus* (Dube *et al*., 2004; Tiwari *et al*., 2013); *Zea mays* (Anjum *et al*., 2017)	NR
Nutrient uptake	*Pisum sativum* (Tiwari *et al*., 2009); *Raphanus sativus* (Dube *et al*., 2004; Tiwari *et al*., 2013)	*Cynara scolymus, Ocimum basilicum*, *Rosmarinus officinalis* (Boechat *et al*., 2016)
Yield and biomass	*Brassica oleracea* (Pandey & Sharma, 2003); *Daucus carota* (Ding *et al*., 2014); *Pisum sativum* (Tiwari *et al*., 2009); *Raphanus sativus* (Dube *et al*., 2004)	*Ocimum tenuiflorum* (Rai *et al*., 2004); *Cynara scolymus, Ocimum basilicum*, *Rosmarinus officinalis* (Boechat *et al*., 2016)

As an external stressor, Cr has no dedicated uptake route in plants (Shanker *et al*., 2005). Therefore, it competes with essential nutrients (e.g. Fe, P, S) for a carrier binding site and interferes with normal nutrient uptake (Shanker *et al*., 2005; Ertani *et al*., 2017). Plants normally initiate an antioxidative defense mechanism to combat metal stress (Nagajyoti *et al*., 2010; Anjum *et al*., 2017), although under high Cr concentrations this system may fail to overcome multiple phytotoxic effects (Anjum *et al*., 2017). The 'root barrier' mechanism may convert highly toxic Cr(VI) to Cr(III) by means of enzymatic and non-enzymatic reactions (Cervantes *et al*., 2001; Ertani *et al*., 2017; Shahid *et al.*, 2017). Translocation of Cr(III) to above-ground parts is thereby restricted (Babula *et al*., 2008; Tiwari *et al*., 2009; Wahsha *et al*., 2014). Furthermore, Cr(III), being unable to cross cell membranes, tend to form complexes with available organic molecules (e.g. glutathione, NAD(P)H, $FADH_2$, pentoses, organic acids) and are stored in cell walls or vacuoles

in the root zone (Shanker *et al*., 2005; Ertani *et al*., 2017). It further explains the lower hazard potency linked to Cr(III) in plants (Shanker *et al*., 2005). Such processes (e.g. root barrier and Cr(III) sequestration in root cells), therefore, indicates a greater environmental significance (Ertani *et al*., 2017) considering the role of plants as a daily nutritional source in the human diet.

2.3.5 Accumulation by food plants

Heavy metals are regarded as one of the major pollution agents of food crops (Luginina & Egoshina, 2013). Increased Cr levels can create a competitive/synergistic soil environment that may change absorption dynamics of essential elements to affect the food value of plant species (Tiwari *et al*., 2013; Wahsha *et al*., 2014). The chemical make-up of the growth media as well as the ability of the plant species to accumulate toxic elements, therefore, determine the chemical composition of the plant (Pajević *et al*., 2018). Soil Cr limits (Table 2.2) are therefore critical prerequisites to maintain acceptable cultivation practices. Chemical species specific Cr limits are however not mentioned in the reviewed literature.

Cr generally has low phytoavailability, primarily because it exists mostly as the least reactive Cr(III) forms in nature, but also due to frequent conversion of available hazardous Cr(VI) to Cr(III) (Ye *et al*., 2015). Plants grown on Cr polluted soils are however reported to accumulate toxic levels of Cr despite low root to shoot mobility as recorded for this heavy metal (Pandey & Sharma, 2003; Gomes *et al*., 2017; Dobbins *et al*., 2021). No clear correlation exists between soil and plant accumulated Cr levels, as this is a complex interaction depending on metal availability, plant growth stage and response to metal stress (species and genotype-specific traits, and Cr uptake and translocation rates (species determined traits) (Voutsa *et al*., 1996; Säumel *et al*., 2012; Anjum *et al*., 2017). Globally, Cr limits in food plants are determined (Table 2.3) to ensure food safety, but for South Africa (Department of Health, 2016) such limits are yet to be set. Like soil, Cr species based limits for plants are not reported in sourced articles.

Table 2.2. Total Cr concentration limits in soil set by countries and regulatory bodies.

Soil Cr concentration (μg g^{-1})	Organisation/country	Reference
50	Australia	Kamunda *et al*., 2016
100	Austria	Ding *et al*., 2014; Shahid *et al.*, 2017
65	Bulgaria	Kamunda *et al*., 2016
64	Canada	Ding *et al*., 2014; Shahid *et al.*, 2017
200	China	Kamunda *et al*., 2016
200	Czech Republic	Ding *et al*., 2014; Shahid *et al.*, 2017
150	European Union	Kamunda *et al*., 2016
100	FAO/WHO	Kamunda *et al*., 2016
60	Germany	Kamunda *et al*., 2016
150	Poland	Ding *et al*., 2014; Shahid *et al.*, 2017
100	Serbia	Ding *et al*., 2014; Shahid *et al.*, 2017
6.5	South Africa	Kamunda *et al*., 2016
250	Taiwan	Kamunda *et al*., 2016
100	Tanzania	Kamunda *et al*., 2016
130	United Kingdom	Kamunda *et al*., 2016

FAO, Food and Agriculture Organization; WHO, World Health Organisation.

Table 2.3. Cr limits set for food plants.

Cr concentration (μg g^{-1})	Organisation/country	Reference
0.5 (fresh wt. of vegetables)	China	Yang *et al*., 2007; Ding *et al*., 2014; Cheng *et al*., 2017
2.3 (dry wt. of vegetables)	FAO/WHO	Arsenov *et al*., 2016; Pajević *et al*., 2018
0.005 and 0.02 in vegetable and foodstuff	Turkey	Unver *et al*., 2015

FAO, Food and Agriculture Organization; WHO, World Health Organisation.

All plant species with the highest Cr concentrations in different accumulating parts, i.e. lettuce leaves (Li *et al*., 2015), maize roots and wheat stems (Wahsha *et al*., 2014), and soybean grains (Zhang *et al*., 2019) were either impacted by human induced Cr pollution or combined effects of geogenic and human emissions (Table A4, Appendix A). Around 73% of all plant species with the highest reported Cr excluding laboratory set up as in these cases Cr concentrations were simulated, exceeded the WHO/FAO Cr permissible limit (2.3 μg g^{-1} dry wt.) for food plants. Cr species differentiation in food plants can be perceived as a potential shortfall in the available literature. Zayed *et al.* (1998) detected only Cr(III) in plant parts using x-ray absorption

spectroscopy irrespective of the application of Cr(III) or Cr(VI). The authors concluded a possible conversion of Cr(VI) to Cr(III) in plant root system before transportation. Nevertheless, increased Cr accumulation and higher root to shoot transfer rate were detected for Cr(VI) application. This supports the greater hazard potential of Cr(VI) when present in plant growth media compared to Cr(III).

Investigated species sourced from farmlands, wild, markets and experimental setup varied in accumulated Cr amounts. The highest Cr concentrations were, farmland produce (125.52 µg g^{-1}, Li *et al*., 2015) > wild collected (14.75 µg g^{-1}, Abbasi *et al*., 2013) > market products (3.67 µg g^{-1}, Pajević *et al.*, 2018) > 'other condition' (1 species, experimental plot, 0.3 µg g^{-1}, Larsen *et al*., 1992). This suggests the importance of evaluation of plant origin to understand variations in exposure types, e.g. growth media, fertilisers and pesticides, irrigation water, as well as local atmospheric dust levels. Anthropogenic Cr pollution effects were suggested for a higher number of species (twelve) than geogenic Cr (three, Wahsha *et al*., 2014; Milićević *et al*., 2018). This implies a higher contamination potential of anthropogenic Cr polluters.

Seasonal variation recorded for potato (Arsenov *et al*., 2016) and spinach (Pajević *et al*., 2018) further indicates the significance of growth environments, especially when affected by fluctuations in anthropogenic Cr emissions. In addition, reported differences in Cr concentrations between unwashed and washed samples suggested the importance of dust deposited Cr (Unver *et al*., 2015; Kim *et al*., 2017). Higher Cr concentrations in aerial parts than roots in washed lettuce (soil > aerial parts > roots) was also concluded as a result of atmospheric Cr (Li *et al*., 2015). Proximity to PM emission sources was identified as a crucial parameter and leafy vegetables could be particularly vulnerable when grown or harvested from such sites (Larsen *et al*., 1992; Li *et al*., 2015; Kim *et al*., 2017). Thorough washing of raw vegetables was hence suggested as a precautionary measure (Kim *et al*., 2015).

Variations in accumulation trends were observed for different species (i.e. root > leaf > stem (cabbage) (Pandey & Sharma, 2003); leaf > pulp > seed > skin (grape) (Milićević *et al*., 2018), aerial parts > root (lettuce) (Li *et al*., 2015); root > leaf > stem > grain (maize, for both farm produced and laboratory tested samples) (Wahsha *et al*., 2014; Anjum *et al*., 2017); root > stem > leaf > seed (pea) (Tiwari *et al*., 2009); root > stem > leaf (radish) (Dube *et al*., 2004; Tiwari *et al*., 2013); and root > stem > grain (wheat) (Wahsha *et al*., 2014). Such findings substantiate plant trait controlled metal accumulation patterns.

2.3.6 Accumulation by medicinal plants

Herbal medicine based knowledge systems have been a key component of human civilisation and are well preserved over time by indigenous communities (Mahmood *et al*., 2013; Boechat *et al*., 2016; Owolabi *et al*., 2016; Kumar *et al*., 2018). Modern medicinal pharmacopoeia includes around 25% of drugs with plant-derived constituents and many others based on the chemical analogues of such substances (Vaikosen & Alade, 2017). About 80% of populations in developing countries, and around 70 to 80% of the total world population relies on medicinal plant-based remedies within the domain of alternative medicine (Panichev *et al*., 2005; Rai *et al*., 2005; Awodele *et al*., 2013; Mahmood *et al*., 2013; Sungur *et al*., 2014; Owolabi *et al*., 2016; Kumar *et al*., 2018). The global popularity of herbal medicine is based on its highly acclaimed and accepted curative properties with easy availability, negligible reported side-effects, affordability, multi-functionality use (e.g. antiviral, antibacterial and antifungal agents), and growing recognition from the fast-evolving scientific communities (Rai *et al*., 2005; Ishaq *et al*., 2013). Therefore, a global surge in demand for plant-based medication is noticed in recent times (Shah *et al*., 2016).

Medicinal plants, therefore, provide another means of heavy metal exposure to humans (Barouchas *et al*., 2014; Kozak *et al*., 2015; Vaikosen & Alade, 2017; Kumar *et al*., 2018). Accumulation of heavy metals in medicinal plants has been reported globally, e.g. China (Dong *et al*., 2017); India (Maharia *et al*., 2010; Kozak *et al*., 2015; Kumar *et al*., 2018); Nigeria (Awodele *et al*., 2013; Vaikosen & Alade, 2017); Pakistan (Shah *et al*., 2016); South Africa (Owolabi *et al*., 2016); Thailand (Kozak *et al*., 2015) and Turkey (Unver *et al*., 2015). Reports suggest various environmental Cr exposure, such as parent rock (Zlatić *et al*., 2017), natural calamities (Kozak *et al*., 2015), atmospheric pollution (Ishaq *et al*., 2013; Unver *et al*., 2015; Kumar *et al*., 2018), industrial emission (Rai *et al*., 2005; Mahmood *et al*., 2013), mining (Maharia *et al*., 2010), metal smelting operations (Owolabi *et al*., 2016), intensive use of metal-rich pesticides (Awodele *et al*., 2013; Vaikosen & Alade, 2017), and unhealthy post-harvest preservation (Kumar *et al*., 2018). Contamination of medicinal plants can be visualised as an interactive process among geography, geology and climate of the area, air and soil pollution, concentration and exposure time of the pollutant, plant species, cultivation practice, harvesting time, and processing and preservation of materials (Ishaq *et al*., 2013; Dong *et al*., 2017; Kumar *et al*., 2018). Continuous evaluation of medicinal plants reaching markets along with awareness to prohibit any collection of raw materials from polluted sites should be encouraged (Kumar *et al*., 2018).

Both curative and toxicity properties of medicinal plants depend on their chemical composition (Ishaq *et al*., 2013). Good agriculture and collection practice, good manufacturing practice and good laboratory practice are, hence, recommended to ensure the effectiveness and acceptable quality of raw medicinal plants and their derivatives to guarantee consumer safety (Kumar *et al*.,

2018). WHO (2007) suggested mandatory heavy metal analysis of herbal drugs before the sale (Rai *et al*., 2005; Shah *et al*., 2016; Kumar *et al*., 2018). Globally, primary health care and the ethnobotany sectors extract phytochemicals from around 35,000 to 50,000 plant species (Mahmood *et al*., 2013; Vaikosen & Alade, 2017). Despite such popularity, according to WHO (2004), traditional medicines may present considerable human health risk due to uncontrolled marketing and sale of plant materials without proper quality regulation assessments (Awodele *et al*., 2013; Boechat *et al*., 2016). Therefore, Cr concentration limits in medicinal plants and herbal products are governed (Table 2.4).

Table 2.4. Chromium safety limits in medicinal plants.

Safety limit	Country/organisation	Reference
2 µg g^{-1}	Maximum residual level (MRL) in raw medicinal plants (WHO, 2005)	Vaikosen & Alade, 2017 Kumar *et al*., 2018
20 µg day^{-1}	National limit for finished herbal products, Canada	Dong *et al*., 2017
2 µg g^{-1} dry weight	National permissible limit in raw plant material, Canada	Dong *et al*., 2017

The majority of the species that accumulated the highest amounts of Cr as reported in the reviewed literature, precisely seventeen out of twenty-seven (63%), exceeded WHO permissible limit (2 µg g^{-1}) recommended for medicinal plants (Table A5, Appendix A). Like the food plants, investigated medicinal species in reviewed literature were sourced from farms, markets and wild, but some were unspecified (Table A5, Appendix A). The highest Cr concentration per plant origin groups varied, i.e. farmed (368 µg g^{-1}, Owolabi *et al.*, 2016) > wild-collected (177.4 µg g^{-1}, Zlatić *et al.*, 2017) > market products (74.2 µg g^{-1}, Shah *et al.*, 2016) > 'not specified' (27 µg g^{-1}, Rai *et al*., 2005). This also points out the importance of possible Cr exposures during cultivation and post-harvest stages as suggested by Kumar *et al.* (2018). Considerable Cr concentrations determined in wild medicinal plants could be perceived as an immediate health threat to its local consumers.

Among different plant tissues, the highest Cr concentrations were recorded in flowers (tsunami-affected area, Kozak *et al*., 2015), followed by root (city emissions, Mahmood *et al*., 2013), shoot (tsunami-affected area, Kozak *et al*., 2015) and leaves (city emissions, Mahmood *et al*., 2013). Results, therefore, suggest both geogenic sources and anthropogenic activities induce elevated Cr accumulation by medicinal plants in various parts.

In *Albizia lebbeck* (Fabaceae, Ishaq *et al*., 2013) from Turkey, higher Cr levels in unwashed plant materials compared to the washed ones advocates the contribution of aerial dust deposition in city/urban regions. High dust contamination of aerial parts from traffic polluted areas (leaves > shoot > seeds > root) support the greater influence of such pollution in urban settings. Increased root accumulation (followed by shoot > leaves > seeds) in industrial areas corroborates solid and/or liquid industrial waste as a major soil contamination source (Kimbrough *et al*., 1999) resulting in elevated root uptake. For residential and non-residential areas, the trend is shoot > root > leaves > seeds and leaves > root > shoot > seeds, respectively. This could be predicted as a combined effect of various Cr release points and wind dispersed dust, respectively. The findings by the authors hence highlight alteration of Cr storage organs depending on pollution type and dominant exposure pathways. Furthermore, in total, six wild collected, two cultivated, one from the 'not specified' group and two laboratory-tested species were reported to accumulate Cr from polluted soils in different plant organs that indicated species specific traits regarding variations in accumulating tissue.

For laboratory tested species, chemical speciation (Cr(III) or Cr(VI)), applied Cr concentrations and exposure duration had critical effects on accumulation. Cr species specific analysis revealed higher Cr(III) accumulation than Cr(VI). Results varied with the applied Cr analysis methods (Barouchas *et al*., 2014). Two farm cultivated species (*Capsicum annuum* and *Nepeta cataria*) from Cr and vanadium smelter polluted sites were noted to accumulate Cr(VI) in various plant parts (Owolabi *et al*., 2016). Findings suggest a scarcity of Cr(VI) determination in plants collected from natural habitat compared to laboratory based investigations.

2.3.7 Toxicity impact on human health

2.3.7.1 Toxicity mechanism

In general, Cr concentrations in plants stay within 1 µg g^{-1} and ranges between 0.02–0.2 µg g^{-1} and seldom goes above 5 µg g^{-1} when grown in normal or unpolluted soils (Barouchas *et al*., 2014). However, as detailed in the previous sections (2.3.5 and 2.3.6), plants are reported to accumulate higher concentration of Cr than the above mentioned values. Ingestion is hence one of the major Cr exposure pathways to humans other than inhalation of atmospheric particles and dermal contact of Cr containing dust, soil, liquid and manufactured commodities (Dhal *et al*., 2013; Barouchas *et al*., 2014; Wahsha *et al*., 2014; Ertani *et al*., 2017). Cr health hazard effects depend on the exposure concentration and time, and type of chemical species (Kimbrough *et al*., 1999; Dhal *et al*., 2013; Ertani *et al*., 2017; Shahid *et al*., 2017). In general, excess heavy metals in human systems could result in altered biochemical processes and accumulation in vital organs to induce severe health conditions (Li *et al*., 2015; Arsenov *et al*., 2016).

Cr(III) is considered an essential trace nutrient for human health (WHO, 2000) (Zayed *et al*., 1998; Ding *et al*., 2014; Kamunda *et al*., 2016; Cheng *et al*., 2017; Ertani *et al*., 2017). However, at an elevated exposure, Cr(III) could act as a mutagenic substance (an agent to increase mutation frequency) and react with the phosphate group of DNA leading to impaired replication and transcription, induce structural and functional damage to DNA polymerase and other enzymes to disrupt cellular functioning (Cervantes *et al*., 2001).

Cr(VI) compounds pose greater hazard potential than Cr(III) based on their ability to diffuse through prokaryotic and eukaryotic cell membranes (Kimbrough *et al*., 1999; Babula *et al*., 2008; Dhal *et al*., 2013; Sungur *et al*., 2013; Barouchas *et al*., 2014; Shahid *et al.*, 2017). Under intra-cellular conditions, various biological molecules (NAD(P)H, $FADH_2$, different pentoses, glutathione, vitamin C, Vitamin B_{12}, cytochrome P-450, and mitochondrial respiratory chain) may reduce Cr(VI) to produce higher amounts of ROS than Cr(III) due to high redox potential and production of unstable intermediates such as Cr(V) that can initiate detrimental effects (Cervantes *et al*., 2001; Babula *et al*., 2008; Dhal *et al*., 2013; Sungur *et al*., 2013; Barouchas *et al*., 2014; Shahid *et al.*, 2017). Cr(VI) could be up to 100 times more toxic to living organisms than Cr(III) (Dhal *et al*., 2013; Shahid *et al.*, 2017).

2.3.7.2 Non-carcinogenic effects

Exposure to high levels of Cr(III) may cause health ailments such as respiratory illness, gastrointestinal tract problems and dermal disorders in humans (Sun *et al*., 2018). Cr(VI) is a mutagenic and teratogenic (deformation in a fetus) substance with greater abilities to trigger a diverse array of acute and chronic non-carcinogenic disorders (Table 2.5) (Dhal *et al*., 2013; Kamunda *et al*., 2016; Ertani *et al*., 2017; Shahid *et al.*, 2017).

Table 2.5. Non-carcinogenic health effects of Cr(VI).

Exposure pathway	Health impacts	Reference
Dermal contact	Corrosiveness, irritation, ulcers, allergic sensitisation (allergic contact dermatitis, ACD), dermatosis	Kimbrough *et al*., 1999 Rai *et al*., 2005 Ertani *et al*., 2017
Inhalation	Ulceration, perforation of the nasal septum, irritation of pharynx and larynx, bronchitis, bronchospasm, coughing, asthma, itching of nose, and damage of kidney and liver due to Cr excretion	Kimbrough *et al*., 1999 Rai *et al*., 2005 Ertani *et al*., 2017
Ingestion	Prolonged ingestion causes skin rash, gastric disorders, ulcer, stomach upset, kidney and hepatic damage, large quantities may result in death (humans and animals)	Zayed *et al*., 1998 Kimbrough *et al*., 1999 Awodele *et al*., 2013 Kamunda *et al*., 2016

2.3.7.3 Carcinogenic effects

Cr is recognised as a human carcinogen by the International Agency for Research on Cancer, USEPA and WHO (Kimbrough *et al*., 1999; Dhal *et al*., 2013; Shahid *et al.*, 2017; Zhang *et al*., 2019). Cr(VI) is rated as a Class 1 human carcinogen (Zayed *et al*., 1998; Panichev *et al*., 2005; Mandiwana *et al*., 2007; Babula *et al*., 2008; Ding *et al*., 2014; Li *et al*., 2015; Kazakis *et al*., 2018). However, Cr(VI) has been reported as carcinogen by inhalation and may cause cancer in lungs and other upper respiratory and gastrointestinal tract organs (e.g. oesophagus, trachea, larynx, and stomach) (Kimbrough *et al*., 1999). On the contrary, carcinogenicity of Cr(III) is not established yet.

2.3.7.4 Health risk associated with useful plants

Green plants convert inorganic elemental forms into organically bound nutritional complexes (Panichev *et al*., 2005; Ye *et al*., 2015; Arsenov *et al*., 2016; Pajević *et al*., 2018). Under normal conditions, plants absorb and accumulate negligible amounts of toxic metals along with essential elements (Unver *et al*., 2015; Arsenov *et al*., 2016), but elevated concentrations of hazardous elements in the environment may result in excess accumulation that can diminish the use value of useful plants (Voutsa *et al*., 1996; Säumel *et al*., 2012; Unver *et al*., 2015; Ye *et al*., 2015; Milićević *et al*., 2018). Health hazard incidents from polluted food crops are reported from both developed and developing countries (Säumel *et al*., 2012). Table 2.6 summarises the health risks estimated by the authors.

Table 2.6. Health risk potential associated with ingestion of Cr contaminated food plants (chemical species not described).

Food plant	Human health risk potential	Cr source(s)	Reference
Grapevine (*Vitis* spp.)	Non-carcinogenic and carcinogenic health risk within the safe limits	Possible effect of parent material, traffic and industry	Milićević *et al*., 2018
Edible lily (*Lilium davidii* var. *unicolor*)	Carcinogenic (adults > children) and non-carcinogenic health risk for multiple metals including Cr	Not specified	Sun *et al*., 2018
Leafy, fruit and leguminous vegetables	Non-carcinogenic risk along with meat and fish consumption	Coal mine	Cheng *et al*., 2017
Leafy vegetables	Considerable non-carcinogenic and carcinogenic risk	Several industries	Abbasi *et al*., 2013
Soybean grains (*Glycine max*)	Least possible non-carcinogenic and carcinogenic risk	Multiple metal mining	Zhang *et al*., 2019

None of the reviewed literature reported human health risks associated with investigated medicinal plants. A study by Olwolabi *et al.* (2016) estimated the quantity of Cr(VI) in prepared tea from various parts of medicinal plants harvested from a ferrochrome smelter affected farm. The authors suggested negligible health risks related to consumption of medicinal tea. Inadequacy of literature in this regard reflect a scientific knowledge gap. Boechat *et al.* (2016) reported certain medicinal plants to tolerate elevated levels of heavy metals in soils and accumulate higher concentrations in tissues without any visible symptoms that may lead to unknowing ingestion and undesirable health consequences.

2.3.8 Synthesis and gap analysis

From the sourced literature, Cr phytotoxicity seems to be more of a chemical species dependent phenomenon in terms of higher absorption, translocation and accumulation rate of Cr(VI) than Cr(III). The bioavailability of Cr species is therefore highly relevant and vital in this regard. Cr species oriented assessments must be a prime focus to understand the toxicity mechanisms better, but complex interspecies conversion dynamics makes toxicity evaluation difficult in any

biological system. Hence, only a limited number of studies looked into species specific Cr accumulation in food and medicinal plants (Fig. A1, Appendix A).

Both Cr(III) (mostly present as chemically inert forms with low mobility, solubility and toxicity in unpolluted environments), and Cr(VI) (generally human activity produced, highly toxic with greater mobility, solubility and reactivity) with contrasting properties may induce harmful effects in a living system. Anthropogenic Cr-waste materials containing a single or combination of Cr species may increase the bioavailability of the element. Findings from literature indicated the potential of various human activity based Cr pollution (e.g. traffic, industries, waste incineration, cumulative city emissions) to contaminate food and medicinal plants via root and foliar uptake from polluted growth media and atmosphere, respectively. Globally, urban settlements with multiple Cr emitters presented far higher Cr contamination potential of useful plants. In addition, Cr accumulation in plant part(s) depends on the dominant exposure pathways to the plant.

Cultivation practice and the ambient environment under which farms operate may present considerable pollution threats as farm produce had the highest Cr levels for both categories of useful plants. However, detection of high Cr levels in plant species from different sources (wild, farms and markets) may signify the need for regularity in the assessment of heavy metals in useful crops reaching consumers. For food plants, most studies focused on farm produce or market products with insufficiency in reports on home garden and wild harvested crops. Often poor people living in, and around polluted urban zones rely on such sources to meet their daily needs. This indicates a gap to be addressed in future. For medicinal plants, a reverse situation is seen with maximum species analysed were wild collected, followed by market product and farm produce. This could be based on the high use value of locally grown and wild harvested species that are readily available and frequently tested to ensure consumer safety. A high percentage of investigated food (73%) and medicinal (63%) plants reported in literature accumulated Cr above the limits set by WHO/FAO. This is an important finding considering the frequency of use and consumer value attached to food and medicinal plants globally.

Cr contamination of useful plants can be concluded as a complex and interlinked process involving multiple variables, (1) plant traits (e.g. ability to absorb, translocate and store Cr in different organs and Cr-stress response mechanism), (2) pollution sources (e.g. traffic, city-generated, industrial, mining), distance from the source and pollution levels, (3) geology (parent rock) and climate (e.g. seasonal variations, weather phenomena like tsunami, meteorological factors such as wind direction and speed) of the region, (4) cultivation practice (e.g. use of agricultural products and irrigation water) and collection process such as farmed, marketed or

wild harvested, and (5) concentrations of available Cr species (i.e. Cr(III) and/or Cr(VI) that determine interspecies conversion rate and consequent plant uptake and toxicity potential).

Based on the reviewed articles, the present study identified research areas that require further attention (Fig. A1, Appendix A). Contrasting the significance of dust borne Cr deposition, this exposure pathway is under investigated globally for useful plant leaves. With respect to Cr pollution sources, mining areas should be targeted more often for potential Cr pollution of food- and medicinal plants. Similarly, geogenic contributions of Cr towards contamination of crops require further attention. Distinctly low efforts towards human health assessments associated with medicinal plants (5%) were indicated compared to food plant based studies (30%) which can underestimate the health hazard potential associated with frequent and repeated use of medicinal plants by local people. Home garden grown medicinal plants and wild harvested food crops were not evaluated adequately compared to farm and market products for both categories of useful plants. On a global scale, geographic distribution based unequal availability in studies was indicated.

Summary

The review attempted to analyse prominent investigations on Cr as a toxic heavy metal and its adverse effects on useful plants, emphasizing the impact of human activity sourced Cr. The process has led to the following conclusions. Cr toxicity potential relies on dominant chemical species and rather complicated interspecies conversion dynamics. However, generation and conversion between Cr(III) and Cr(VI) in the environment is primarily associated with the chemical composition of the geogenic substrate and disposed waste materials under the influence of ambient soil parameters and reactions.

Cr, mostly as Cr(III) oxidation state, is a less mobile component of rocks and soil, that generally remains unavailable to plants due to low solubility and reactivity. On the contrary, human disposed Cr chemicals containing Cr(VI) are persistent environmental pollutants with higher hazard potential towards living things based on increased solubility, mobility, availability and reactivity. Therefore, greater Cr bioavailability in the environment is primarily associated with varied anthropogenic emissions.

Regarding Cr exposure pathways to plants, both root and foliar uptake are recognised as viable routes. To a greater extent, foliar uptake of airborne particulate matter is noted as more effective in areas with elevated atmospheric pollution. Determination of dust deposition on the above-ground plant parts especially on leafy vegetables therefore may reveal vital information related to

Cr accumulation under such environments. Thorough washing of raw vegetables before consumption is well recommended, therefore.

As an external stressor, Cr may induce severe phytotoxic effects on vital plant processes. Activation of different enzymatic and non-enzymatic responses may combat the stress up to a certain extent. Further compartmentalisation of Cr in the root zone may restrict its translocation to aerial parts and limit its hazard impact. Plant species, however, differ with regards to Cr tolerance, response and visual toxicity symptoms.

Cr accumulation is reported in different types of food plants such as leafy, fruit, stem and root vegetables, and grain crops. Cr contamination in terms of deposition and accumulation in plants can be visualised as a complex functioning of multiple variables associated with plant species, Cr oxidation state, cultivation/collection procedure and ambient environment. Evaluation of anthropogenic Cr pollution may become critical to improve the understanding of contamination levels and predicting necessary management steps, especially in urban and expanding peri-urban areas.

The review deduces that medicinal plants that withstand elevated metal concentrations may provide key species to study toxicity response. Cr accumulation by medicinal plants is a global concern based on the worldwide popularity of ethnomedicinal knowledge systems and the high use value of such species to indigenous people. Natural processes and anthropogenic pollution can influence Cr accumulation by medicinal plants in conjunction with elemental factors and plant traits.

Both Cr(III) and Cr(VI) are hazardous to humans. The latter is specifically identified as a human carcinogen. The hazard potency of Cr depends on the exposure concentration and time with available chemical species. Inside a cell, Cr(VI) is more potent to generate higher amounts of ROS compared to Cr(III) to interfere with biological molecules and functions. Ingestion of Cr-polluted food and medicinal plants was reported to present a diverse array of health ailments to humans.

This review as an effort towards interlinking multiple research fields on Cr toxicity and Cr-useful plant (food and medicinal plants) interaction may provide a global perspective to understand Cr hazard potential. The greater influence of anthropogenic Cr in this regard is highlighted which is relevant and reasonable to the rapidly urbanising world. Indicated knowledge gaps could stimulate future scientific interest and induce necessary environmental management initiatives to

assess and limit Cr impact on food and medicinal plants and spread awareness to reduce Cr transfer to humans.

References

Abbasi, A.M., Iqbal, J., Khan, M.A. & Shah, M.H. 2013. Health risk assessment and multivariate apportionment of trace metals in wild leafy vegetables from lesser Himalayas, Pakistan. *Ecotoxicology and Environmental Safety,* 92:237–244.

Anjum, S.A., Ashraf, U., Khan, I., Tanveer, M., Shahid, M., Shakoor, A. & Wang, L. 2017. Phyto-toxicity of chromium in maize: oxidative damage, osmolyte accumulation, anti-oxidative defense and chromium uptake. *Pedosphere*, 27(2):262–273.

Arsenov, D.D., Nikolić, N.P., Borišev, M.K., Župunski, M.D. & Pajević, S.P. 2016. Heavy metal contamination of vegetables from green markets in Novi Sad. *Matica Srpska Journal of Natural Sciences*, 131:99–108.

Awodele, O., Popoola, T.D., Amadi, K.C., Coker, H.A.B. & Akintonwa, A. 2013. Traditional medicinal plants in Nigeria - remedies or risks. *Journal of Ethnopharmacology,* 150:614–618.

Aziz, M.A., Adnan, M., Begum, S., Azizullah, A., Nazir, R. & Iram, S. 2016. A review on the elemental contents of Pakistani medicinal plants: implications for folk medicines. *Journal of Ethnopharmacology,* 188:177–192.

Babula, P., Adam, V., Opatrilova, R., Zehnalek, J., Havel, L. & Kizek, R. 2008. Uncommon heavy metals, metalloids and their plant toxicity: a review. *Environmental Chemistry Letters*, 6:189–213.

Barouchas, P., Moustakas, N., Liopa-Tsakalidi, A. & Akoumianaki-Ioannidou, A. 2014. Effect of trivalent and hexavalent chromium (Cr) on the total Cr concentration in the vegetative plant parts of spearmint (*Mentha spicata* L.), lemon verbena (*Lippia citriodora* L.) and peppermint (*Mentha piperita* L.). *Australian Journal of Crop Science*, 8(3):363–368.

Boechat, C.L., Carlos, F.S., Gianello, C. & de Oliveira Camargo, F.A. 2016. Heavy metals and nutrients uptake by medicinal plants cultivated on multi-metal contaminated soil samples from an abandoned gold ore processing site. *Water Air Soil Pollution*, 227, art. 392. https://doi.org/10.1007/s11270-016-3096-4

Cervantes, C., Campos-García, J., Devars, S., Gutiérrez-Corona, F., Loza-Tavera, H., Torres-Guzmán, J.C. & Moreno-Sánchez, R. 2001. Interactions of chromium with microorganisms and plants. *Federation of European Microbiological Societies Microbiology Reviews,* 25:335–347.

Cheng, J., Zhang, X., Tang, Z., Yang, Y., Nie, Z. & Huang, Q. 2017. Concentrations and human health implications of heavy metals in market foods from a Chinese coal-mining city. *Environmental Toxicology and Pharmacology*, 50:37–44.

Department of Health (South Africa). 2016. Foodstuffs, cosmetics and disinfectants Act 1972 (Act number 54 of 1972): regulations relating maximum levels of metals in foodstuff. *Government Gazette*, 15954: 16 September.

Dhal, B., Thatoi, H.N., Das, N.N. & Pandey, B.D. 2013. Chemical and microbial remediation of hexavalent chromium from contaminated soil and mining/metallurgical solid waste: a review. *Journal of Hazardous Materials*, 250/251:272–291.

Ding, C., Li, X., Zhang, T., Ma, Y. & Wang, X. 2014. Phytotoxicity and accumulation of chromium in carrot plants and the derivation of soil thresholds for Chinese soils. *Ecotoxicology and Environmental Safety*, 108:179–186.

Dobbins, D.C., Marcelo-Silva, J. & Siebert, S.J. 2021. Screening the phytoextractability of trace metals by *Aloe cryptopoda* Baker and *Aloe vera* (L.) Burm.f. cultivated on mine tailings. *South African Journal of Botany*, 140:110–113.

Dong, X.L., Zhang, J., Zhao, Y.L., Zuo, Z.T., Wang, Y.Z. & Zhang, Z.Y. 2017. Multivariate analyses of major and trace elements in 19 species of herbs consumed in Yunnan, China. *International Journal of Food Properties,* 20(7):1666–1676.

Dube, B.K., Sinha, P., Gopal, R. & Chatterjee, C. 2004. Chromium phytotoxicity alters metabolism in radish. *Journal of Vegetable Crop Production*, 10(2):61–71.

Ertani, A., Mietto, A., Borin, M. & Nardi, S. 2017. Chromium in agricultural soils and crops: a review. *Water Air Soil Pollution*, 228:190. https://doi.org/10.1007/s11270-017-3356-y

Feng, J., Wang, Y., Zhao, J., Zhu, L., Bian, X. & Zhang, W. 2011. Source attributions of heavy metals in rice plant along highway in eastern China. *Journal of Environmental Sciences*, 23(7):1158–1164.

Gomes, M.A. da C., Hauser-Davis, R.A., Suzuki, M.S. & Vitória, A.P. 2017. Plant chromium uptake and transport, physiological effects and recent advances in molecular investigations. *Ecotoxicology and Environmental Safety*, 140:55–64.

Ishaq, M., Rehman, A., Adnan, M., Ullah, N., Ahmad, I. & Aamir, M. 2013. Comparative study of heavy metals in *Albizia lebbeck,* collected from different environmental sites. *International Journal of Pharmaceutical Sciences Reviews and Research*, 20(2):5–9.

Kamunda, C., Mathuthu, M. & Madhuku, M. 2016. Health risk assessment of heavy metals in soils from Witwatersrand gold mining basin, South Africa. *International Journal of Environmental Research and Public Health*, 13, art. 663. https://doi.org/10.3390/ijerph13070663

Kazakis, N., Kantiranis, N., Kalaitzidou, K., Kaprara, E., Mitrakas, M., Frei, R., … Filippidis, A. 2018. Environmentally available hexavalent chromium in soils and sediments impacted by dispersed fly ash in Sarigkiol basin (northern Greece). *Environmental Pollution,* 235:632–641.

Kim, H.-S., Kim, K.-R., Lim, G.-H., Kim, J.-W. & Kim, K.-H. 2015. Influence of airborne dust on the metal concentrations in crop plants cultivated in a rooftop garden in Seoul. *Soil Science and Plant Nutrition*, 61:88–97.

Kim, H.S., Kim, K.-R., Kim, W.-I., Owens, G. & Kim, K.-H. 2017. Influence of road proximity on the concentrations of heavy metals in Korean urban agricultural soils and crops. *Archives of Environmental Contamination and Toxicology*, 72:260–268.

Kimbrough, D.E., Cohen, Y., Winer, A.M., Creelman, L. & Mabuni, C. 1999. A critical assessment of chromium in the environment. *Critical Reviews in Environmental Science and Technology*, 29(1):1–46.

Kozak, L., Kokocinski, M., Niedzielski, P. & Lorenc, S. 2015. Bioaccumulation of metals and metalloids in medicinal plant *Ipomoea pes-caprae* from areas affected by tsunami. *Environmental Toxicology and Chemistry*, 34(2):252–257.

Kumar, N., Kulsoom, M., Shukla, V., Kumar, D., Priyanka, Kumar, S., … Dwivedi, N. 2018. Profiling of heavy metal and pesticide residues in medicinal plants. *Environmental Science and Pollution Research*, 25:29505–29510.

Larsen, E.H., Moseholm, L. & Nielsen, M.M. 1992. Atmospheric deposition of trace elements around point sources and human health risk assessment. II: Uptake of arsenic and chromium by vegetables grown near a wood preservation factory. *The Science of the Total Environment*, 126:263–275.

Li, B., Yali, Y., Guo, W. & Chen, Q. 2014. Study on the migration of heavy metals pollution from soil to lettuce. *Conference proceedings*. Annual International Meeting (American Society of Agricultural and Biological Engineers ASABE – CSBE/SCGAB, 2014), Montreal, Canada. Quebec: ASABE. https://elibrary.asabe.org/abstract.asp?aid=44905 Date of access: 11 Jan. 2019.

Li, N., Kang, Y., Pan, W., Zeng, L., Zhang, Q. & Luo, J. 2015. Concentration and transportation of heavy metals in vegetables and risk assessment of human exposure to bioaccessible heavy metals in soil near a waste-incinerator site, South China. *Science of the Total Environment*, 521–522:144–151.

Luginina, E.A. & Egoshina, T.L. 2013. The peculiarities of heavy metals accumulation by wild medicinal and fruit plants. *Annals of Warsaw University of Life Sciences*, 61:97–103.

Maharia, R.S., Dutta, R.K., Acharya, R. & Reddy, A.V.R. 2010. Heavy metal bioaccumulation in selected medicinal plants collected from Khetri copper mines and comparison with those collected from fertile soil in Haridwar, India. *Journal of Environmental Science and Health*, 45(2):174–181.

Mahmood, A., Rashid, S. & Malik, R.N. 2013. Determination of toxic heavy metals in indigenous medicinal plants used in Rawalpindi and Islamabad cities, Pakistan. *Journal of Ethnopharmacology*, 148:158–164.

Mandiwana, K.L., Panichev, N., Kataeva, M. & Siebert, S.J. 2007. The solubility of Cr(III) and Cr(VI) compounds in soil and their availability to plants. *Journal of Hazardous Materials*, 147(2):540–545.

Meena, A.K., Bansal, P., Kumar, S., Rao, M.M. & Garg, V.K. 2010. Estimation of heavy metals in commonly used medicinal plants: a market basket survey. *Environmental Monitoring and Assessment*, 170:657–660.

Milićević, T., Urošević, M.A., Relić, D., Vuković, G., Škrivanj, S. & Popović, A. 2018. Bioavailability of potentially toxic elements in soil-grapevine (leaf, skin, pulp and seed) system and environmental and health risk assessment. *Science of the Total Environment*, 626:528–545.

Nagajyoti, P.C., Lee, K.D. & Sreekanth, T.V.M. 2010. Heavy metals, occurrence and toxicity for plants: a review. *Environmental Chemistry Letters,* 8:199–216.

Owolabi, I.A., Mandiwana, K.L. & Panichev, N. 2016. Speciation of chromium and vanadium in medicinal plants. *South African Journal of Chemistry,* 69:67–71.

Oze, C., Fendorf, S., Bird, D.K. & Coleman, R.G. 2004. Chromium geochemistry of serpentine soils. *International Geology Review*, 46(2):97–126.

Pajević, S., Arsenov, D., Nikolić, N., Borišev, M., Orčić, D., Župunski, M. & Mimica-Dukić, N. 2018. Heavy metal accumulation in vegetable species and health risk assessment in Serbia. *Environmental Monitoring and Assessment*, 190(8), art. 459. https://doi.org/10.1007/s10661-018-6743-y

Pandey, N. & Sharma C.P. 2003. Chromium interference in iron nutrition and water relations of cabbage. *Environmental and Experimental Botany*, 49:195–200.

Panichev, N., Mandiwana, K.L., Kataeva, M. & Siebert, S.J. 2005. Determination of Cr(VI) in plants by electrothermal atomic absorption spectrometry after leaching with sodium carbonate. *Spectrochimica Acta Part B: Atomic Spectroscopy,* 60(5):699–703.

Pennisi, G., Gasperi, D., Mancarella, S., Antisari, V.L., Vianello, G., Orsini, F. & Gianquinto, G. 2017. Soilless cultivation in urban gardens for reduced potentially toxic elements (PTEs) contamination risk. *Acta Horticulturae*, art. 1189. https://doi.org/10.17660/ActaHortic.2017.1189.72

Rai, V., Vajpayee, P., Singh, S.N. & Mehrotra, S. 2004. Effect of chromium accumulation on photosynthetic pigments, oxidative stress defense system, nitrate reduction, proline level and eugenol content of *Ocimum tenuiflorum* L. *Plant Science*, 167:1159–1169.

Rai, V., Agnihotri, A.K., Khatoon, S., Rawat, A.K.S. & Mehrotra, S. 2005. Chromium in some herbal drugs. *Bulletin of Environmental Contamination and Toxicology*, 74:464–469.

Säumel, I., Kotsyuk, I., Hölscher, M., Lenkereit, C., Weber, F. & Kowarik, I. 2012. How healthy is urban horticulture in high traffic areas? Trace metal concentrations in vegetable crops from plantings within inner city neighbourhoods in Berlin, Germany. *Environmental Pollution*, 165:124–132.

Shah, W.A., Zakiullah, Khuda, F., Khan, F. & Saeed, M. 2016. Comparison of toxic heavy metals concentration in medicinal plants and their respective branded herbal formulations commonly available in Khyber Pakhtunkhwa. *Pakistan Journal of Pharmaceutical Sciences,* 29(4):1251–1256.

Shahid, M., Dumat, C., Khalid, S., Schreck, E., Xiong, T. & Niazi, N.K. 2016. Foliar heavy metal uptake, toxicity and detoxification in plants: a comparison of foliar and root metal uptake. *Journal of Hazardous Materials*, 325:36–58.

Shahid, M., Shamshad, S., Rafiq, M., Khalid, S., Bibi, I., Niazi, N.K., … Rashid, M.I. 2017. Chromium speciation, bioavailability, uptake, toxicity and detoxification in soil-plant system: a review. *Chemosphere*, 178:513–533.

Shanker, A.K., Cervantes, C., Loza-Tavera, H. & Avudainayagam, S. 2005. Chromium toxicity in plants. *Environment International,* 31:739–753.

Sun, H., Cheng, H., Lin, L., Deng, K. & Cui, X. 2018. Bioaccumulation and sources of metal(loid)s in lilies and their potential health risks. *Ecotoxicology and Environmental Safety,* 151:228–235.

Sungur, S., Kılboz, Y. & Atan, M.M. 2013. Determination of chromium species in various medicinal plants consumed in Hatay region in Turkey. *International Journal of Food Properties*, 16:1711–1716.

Tiwari, K.K., Dwivedi, S., Singh, N.K., Rai, U.N. & Tripathi, R.D. 2009. Chromium (VI) induced phytotoxicity and oxidative stress in pea (*Pisum sativum* L.): biochemical changes and translocation of essential nutrients. *Journal of Environmental Biology*, 30(3):389–394.

Tiwari, K.K., Singh, N.K. & Rai, U.N. 2013. Chromium phytotoxicity in radish (*Raphanus sativus*): effects on metabolism and nutrient uptake. *Bulletin of Environmental Contamination and Toxicology,* 91(3):339–344.

Unver, M.C., Ugulu, I., Durkan, N., Baslar, S. & Dogan, Y. 2015. Heavy metal contents of *Malva sylvestris* sold as edible greens in the local markets of Izmir. *Ekoloji*, 24(96):13–25.

Vaikosen, E.N. & Alade, G.O. 2017. Determination of heavy metals in medicinal plants from the wild and cultivated garden in Wilberforce Island, Niger Delta region, Nigeria. *Journal of Pharmacy & Pharmacognosy Research*, 5(2):129–143.

Venter, A.D., Beukes, J.P., van Zyl, G.P., Josipovic, M., Jaars, K. & Vakkari, V. 2016. Regional Cr(VI) pollution from the Bushveld Complex, South Africa. *Atmospheric Pollution Research,* 7(5):762–767.

Voutsa, D., Grimanis, A. & Samara, C. 1996. Trace elements in vegetables grown in an industrial area in relation to soil and air particulate matter. *Environmental Pollution,* 94(3):325–335.

Wahsha, M., Fontana, S., Nadimi-Goki, M. & Bini, C. 2014. Potentially toxic elements in food crops (*Triticum aestivum* L., *Zea mays* L.) grown on contaminated soils. *Journal of Geochemical Exploration*, 147:189–199.

Yang, Q., Li, H. & Long, F. 2007. Heavy metals of vegetables and soils of vegetable bases in Chongqing, southwest China. *Environmental Monitoring and Assessment,* 130(1-3):271–279.

Ye, X., Xiao, W., Zhang, Y., Zhao, S., Wang, G., Zhang, Q. & Wang, Q. 2015. Assessment of heavy metal pollution in vegetables and relationships with soil heavy metal distribution in Zhejiang province, China. *Environmental Monitoring and Assessment*, 187(6), https://doi.org/10.1007/s10661-015-4604-5

Zayed, A., Lytle, C.M., Qian, J.H. & Terry, N. 1998. Chromium accumulation, translocation and chemical speciation in vegetable crops. *Planta*, 206:293–299.

Zhang, T., Xu, W., Lin, X., Yan, H., Ma, M. & He, Z. 2019. Assessment of heavy metals pollution of soybean grains in North Anhui of China. *Science of the Total Environment,* 646:914–922.

Zlatić, N.M., Stanković, M.S. & Simić, Z.S. 2017. Secondary metabolites and metal content dynamics in *Teucrium montanum* L. and *Teucrium chamaedrys* L. from habitats with serpentine and calcareous substrate. *Environmental Monitoring and Assessment*, 189, art. 110, https://doi.org/10.1007/s10661-017-5831-8

Chapter 3

Plant morphological traits related to foliar chromium dust deposition

3.1 Introduction

Atmospheric pollution in urban and peri-urban areas is characterised by notable concentrations of airborne dust particulate matter (PM) of anthropogenic origin (Sæbø *et al*., 2012; Weber *et al*., 2014; Perini *et al*., 2017). Globally, airborne PM is known to induce severe health conditions with concerning mortality rates (Popek *et al*., 2015; Sgrigna *et al*., 2015; Perini *et al*., 2017; Weerakkody *et al*., 2018). PM is defined as particles with a diameter of 0.001–100 µm (Popek *et al*., 2015; Sgrigna *et al*., 2015) and diverse in origin, mrophology, size, and physical and chemical properties (Grantz *et al*., 2003; Chen *et al*., 2015). Major PM size categories have been set as fine ($PM_{2.5}$, 0.1–2.5 µm), coarse (PM_{10}, 2.5–10 µm) and large (PM > 10 µm) (Dzierżanowski *et al*., 2011; Popek *et al*., 2015). The size determines whether particles remain as aerosols (~ 0.1 µm), are wind-transported (1–10 µm) before being deposited, or quickly deposited by gravity (> 10 µm) close to the source (Kimbrough *et al*., 1999; Janhäll, 2015; Popek *et al*., 2015). Chemically, PM could contain harmful substances (Csavina *et al*., 2012; Shahid *et al*., 2016). Heavy metals in fine particles (Ram *et al*., 2012) are disseminated by wind over long distances, up to 10,000 km, depending on climate and topography (Grantz *et al*., 2003; Csavina *et al*., 2012). Air currents, therefore, have a far greater spatial-temporal dispersion range of pollutants than water, soil or biological systems (Csavina *et al*., 2012).

Airborne heavy metals with high bioaccumulation and hazard potential are, therefore, regarded as atmospheric contaminants of local and global scale (Grantz *et al*., 2003). Mines are one of the major PM emitters of assorted sizes carrying Cr and other toxic metals, e.g. arsenic, mercury and lead (Csavina *et al*., 2012; Shahid *et al*., 2016). The metal smelting and slag dump frequently disperse PM of ≤ 2–2.5 µm, whereas ore crushing and grinding produce ≥ 2.5 µm particles (Csavina *et al*., 2012; Entwistle *et al*., 2019). Therefore, elevated levels of heavy metals on plant foliage near smelters and mines are reported frequently (Grantz *et al*., 2003; Shahid *et al*., 2016). Foliar uptake and further translocation of hazardous heavy metals within the plant system generates considerable health risk concern if consumed by humans or livestock (Schreck *et al*., 2012; Xiong *et al*., 2019), still, this toxicity pathway is underestimated compared to soil-root transfer (Shahid *et al*., 2016).

Plants are noted to mitigate PM-linked heavy metal polluted air in urban regions (Tomasević *et al*., 2005; Janhäll, 2015; Chen *et al*., 2017). Dust mitigation by plants is affected by plant height as this trait determines foliar dust exposure associated with both air interception as well as wind

and rain-induced particles from soil (Dreicer *et al*., 1984; Nowak *et al*., 2006; Sæbø *et al*., 2012). Trees ranked highest in this regard (Nguyen *et al*., 2015; Chen *et al*., 2017) as they have advantageous height, and dense dust capturing canopies (Beckett *et al*., 2000; Ram *et al*., 2012). Tree canopy shape affects air interception and foliar dust deposition thereafter (Tallis *et al*., 2011; Wang *et al*., 2015). In contrast, dust trapping properties of herbaceous plants are not exploited fully, despite forming the most common ground covers in urban environments (Weber *et al*., 2014).

Large surface area per unit volume of leafy canopies acts as receptors and sinks of air transported heavy metals (Ram *et al.*, 2012). Diverse leaf macro- (arrangement and orientation, leaf blade size, firmness, folding of margin, surface flatness) and micro- (roughness, epicuticular wax, stomata, and pubescence) morphological traits have frequently been linked to dust collection by plants (Naidoo & Naidoo, 2005; Dzierżanowski *et al.*, 2011; El-Khatib *et al*., 2011; Weber *et al*., 2014; Mo *et al*., 2015; Chen *et al*., 2017; Perini *et al*., 2017; Castanheiro *et al*., 2020). In addition, deciduousness determines atmospheric dust exposure period (Sæbø *et al*., 2012; Watanabe, 2015). Aerial particle mitigation potential of evergreen leaves, especially during winter, is known to be beneficial for atmospheric dust removal (Beckett *et al*., 2000; Popek *et al*., 2015; Zha *et al*., 2019). Identifying plant morphological traits that increase dust deposition and adhesion, therefore, provides valuable information to comprehend the susceptibility of vegetation to dust in a polluted environment. Other factors that influence dust adhesion on vegetation are particle shape, size and chemistry, proximity and source type as well as meteorological parameters (e.g. humidity, rainfall, temperature, and wind speed and direction) (Grantz *et al*., 2003; Liu *et al*., 2012; Castanheiro *et al*., 2020).

Extensive industrial use of Cr creates a continuous influx of Cr waste in the environment (Sokol *et al*., 2010; Coetzee *et al*., 2018). This may be concerning considering the potential of this element, together with five other environmental pollutants (arsenic, mercury, lead, pesticides and radionuclides), to present the highest degree of health threats to humans (Csavina *et al*., 2012). Environmental pollution by Cr mining, smelting, slag dumps, ore transport, ore processing residue and contaminated soils is well documented (Pöykiö *et al*., 2005; Sokol *et al*., 2010; Coetzee *et al*., 2018). Human settlements, farmlands as well as natural vegetation surrounding such areas are, hence, exposed (Kimbrough *et al*., 1999; Pöykiö *et al*., 2005; Sokol *et al*., 2010).

As a mineral-rich country, South Africa does address mine pollution, especially dust dispersion and mitigation (Grange, 1973; Utembe *et al*., 2015). Ingestion along with inhalation and dermal contact are primary Cr exposure pathways to humans (Coetzee *et al*., 2018). Yet, compared to the rest of the world, literature on Cr contamination of useful plants from South African mining

areas is negligible. The Rustenburg Layered Suite of Sekhukhuneland region in South Africa is exploited heavily for Cr and platinum (Pt) deposits (Scoon & Viljoen, 2019), but has scant available scientific data on Cr contamination of vegetation, especially related to dust pollution.

The chapter is aimed to provide evidence of Cr dust deposition on the leaf surfaces of food and medicinal plants used by the inhabitants of the Sekhukhuneland mining and smelting region and profile plant and especially leaf morphological features that enhance the process. In addition, total dust amount on plant leaves was estimated to understand the cumulative dust accumulation potential of individual species. A combination of Scanning electron microscopy (SEM) and Energy dispersive x-ray spectroscopy (EDS) was applied to achieve the aim. It was hypothesized that atmospheric Cr particles in the study region (Tshehla & Djolov, 2018) would be deposited on foliar surfaces of the local vegetation. To test this, EDS elemental analysis was conducted on adaxial and abaxial leaf surfaces to (1) attest to the presence of Cr dust on foliar surfaces from the overall elemental composition spectra of leaf surfaces and by identifying particles that contain Cr, and (2) to assess the size distribution and shape of Cr dust to understand the morphology of the particles from SEM images. Next, based on the global reports on how varied plant morphology influences foliar dust deposition (Mo *et al*., 2015; Chen *et al*., 2017), it was postulated that variation in such characteristics of sampled tree and forb species (six each) will have differential dust collection abilities. To investigate this, firstly, plant morphology (growth form, plant height, tree canopy shape), leaf macromorphological details (inclination, compound or simple, leaf area, firmness, folding of margin and surface flatness), and secondly, SEM captured images of leaf surface micromorphology (epidermal cell outlines, veins, epicuticular wax, stomata and trichomes) were used to describe the traits concerning foliar (1) adhesion of Cr particles, and (2) total dust density. An abaxial/adaxial surface-oriented analytical approach was considered to assess if leaf sides differ in terms of dust contamination as frequently reported in past investigations (Ottelé *et al.*, 2010; Ram *et al*., 2012; Mo *et al*., 2015). EDS analysis was applied as a reliable and easily reproducible technique that can be used for rapid identification of dust borne hazardous elements on aerial plant parts in air-polluted areas of South Africa.

3.2 Materials and method

3.2.1 Study area

The study area is located in a region extending from 24°15′ S and 29°50′ E to 24°54′ S and 30°08′ E in Fetakgomo-Tubatse municipality of the Sekhukhune District in Limpopo Province, South Africa (Fig. 3.1). The distinct physiography dominated by the mountainous terrain and broad valleys is the result of the complex local geology (Siebert *et al*., 2002; Tshehla & Wright, 2019). The Olifants and Steelpoort rivers and their tributaries mainly shaped the regional terrain (Siebert *et al*., 2002; Bamisaiye *et al*., 2014; Scoon & Viljoen, 2019). Underlying igneous rock belts of the

Rustenburg Layered Suite (RLS) of the eastern Bushveld Igneous Complex (BIC) hold world-renowned deposits of Cr and Pt (Naldrett *et al*., 2012; Scoon & Viljoen, 2019). The region is characterised by chromitite outcrops and ultramafic soils (Siebert *et al.*, 2002). Study localities had an elevation range of 759–985 m above sea level. Most of the mines and associated development, agriculture and human settlements located in the valleys. The mountainous topography of the region influences the temperature gradient between highlands and deep valleys that affect wind movement and the spatial distribution of dust in Sekhukhuneland (Tshehla & Wright, 2019).

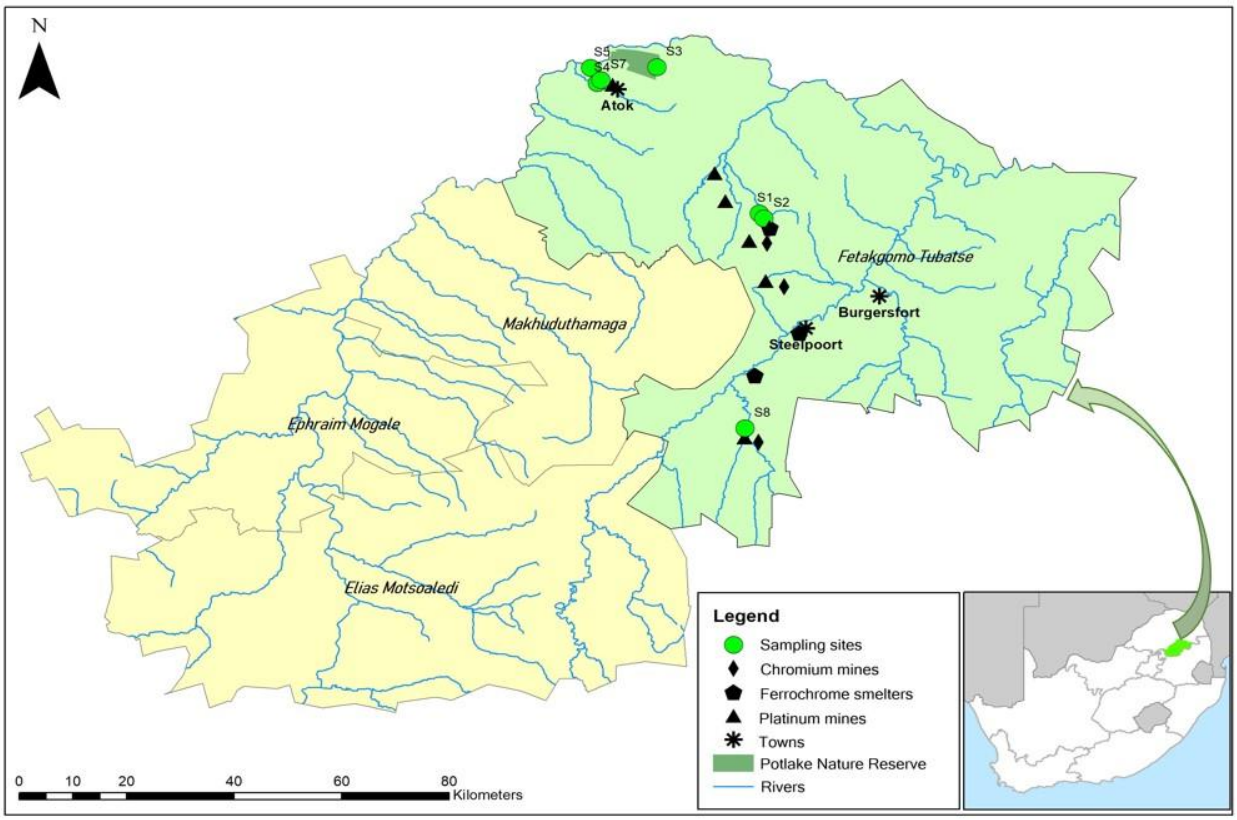

Figure 3.1. Sampling sites, Cr-Pt mines, and ferrochrome smelters in Sekhukhune District (green region on map insert), and in neighbouring areas. The Weather station is located in the Potlake Nature Reserve (PNR).

Sampling was completed at the end of the seasonal dry spell during early summer (November) before the peak seasonal rainfall (December to February), to enhance aerial retention and transportation of dry dust on new growth. November was considered suitable to capture the aerial dust fall-out effect during spring (August to October) as reported by Dudu *et al.* (2018) for a gold mining area in South Africa. During November, the mean daily temperature and humidity were 7–39 °C and 11–29%, respectively, with 39.5 mm total rainfall for the month (Table B1, Appendix B). Weather data was obtained from Potlake Nature Reserve (PNR) (24°16′25″ S; 29°55′24″ E) (Fig. 3.1).

Dust removal by rainfall was avoided by completing sample collection two weeks after the first non-significant rainfall event (Perini *et al*., 2017) of the season, which was below 15 mm, the lower limit of rainfall that washes off foliar dust and thereby starting a new deposition cycle (Liu *et al*., 2012). Low relative humidity during the sampling period posed a limited effect as high humidity influences PM size, its retention and deposition (Csavina *et al*., 2012; Nguyen *et al*., 2015; Chen *et al.*, 2017).

Local geology (Chapter 5, section 5.2.1 and Chapter 6, section 6.2.1), dust sources (e.g. mines, smelters, dumps, and roads) (Chapter 4, sections 4.2.1 and Chapter 5, section 5.2.1) and wind movements (Chapter 4, sections 4.2.2) are detailed in successive chapters to link such features with the specific aims and objectives of the chapters.

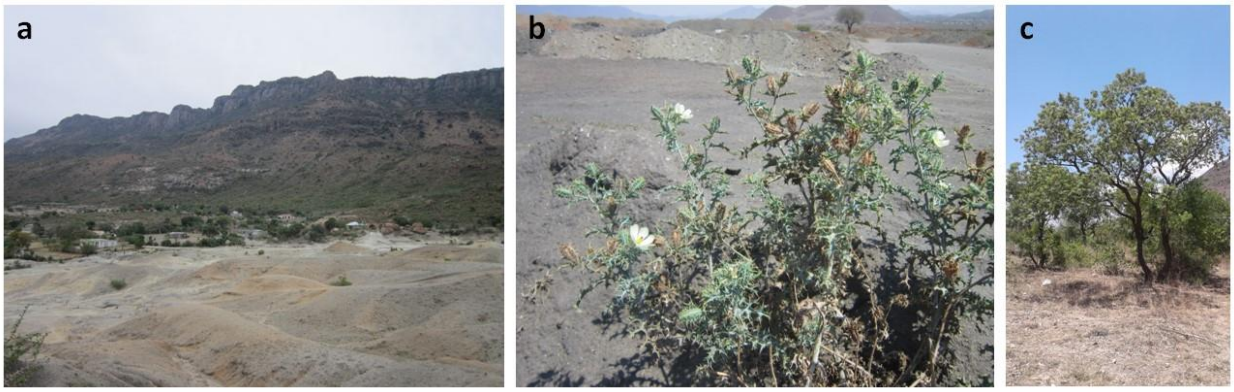

Figure 3.2. Disturbed and comparatively less disturbed localities in the study region. a. Typical mine tailing; b. *Argemone ochroleuca* growing on a tailing; c. *Ozoroa paniculosa* sampled from the natural chromitite outcrops in the less disturbed mountains. Photographs by Mr Dennis Komape.

Seven sampling sites were selected near prominent Cr-dust emitters, namely mines, tailings, informal Cr excavation sites, and natural Cr-enriched chromitite outcrops (Fig. 3.2). Plants (Fig. 3.2b) collected from highly disturbed localities such as tailings (Fig. 3.2a) looked extremely dusty compared to species sampled from natural habitats such as the chromitite outcrops in the mountains (Fig. 3.2c). A stratified sampling strategy with an increase in distance from 2 to 20 km from the nearest mine was followed. Selected distance zones were < 3 (site 2 and 7), 3–5 (site 1, 4 and 8), 5–15 (site 5) and 15–20 km (site 3). Site 1 and 2 were less than 4.5 km and site 8 was around 12 km from the nearest ferrochrome smelter. All the sampling sites were located near one of two main roads (R37 and R555) in the region.

3.2.2 Sample collection

On first arrival at a study site, care was taken to identify deposition of blackish Cr dust on the vegetation. This mining region is primarily inhabited by the Bapedi who use both garden grown

and wild harvested plants as immediate and affordable food or medicinal sources (Semenya & Potgieter, 2014; Mogale *et al*., 2019), hence, such species were targeted for this study. All useful plant species identified at each site were sampled. Overall, twelve species were sampled, six forbs and six trees, and six of these were sampled from home gardens and others from rangelands (Table 3.1).

Leaves of full-grown food and medicinal plants recorded on the biocultural plant-use list for Sekhukhuneland (Mogale *et al*., 2019) were sampled randomly. Tree leaves were collected from the outer canopy and at a constant height of 1–2 m from the ground level to ensure homogeneity (Liang *et al*., 2016). Leaves from multiple branches of full-grown forbs were sampled (Speak *et al.*, 2012). Mature leaves per species were collected, as full-grown leaves are known to hold maximum particles (Nguyen *et al*., 2015; Popek *et al*., 2015). Species specific composite samples were formed. Sampling and handling thereafter were done with utmost care and according to accepted procedures to prevent dust loss from leaves (Chen *et al*., 2017; Liu *et al*., 2018). Voucher specimens were deposited in A. P. Goossens Herbarium, North-West University, South Africa.

Freshly collected unwashed leaves were preserved in two ways. One half was air-dried thoroughly and stored in marked brown paper bags while the rest was immediately fixed in 70% ethanol after collection. Both dried and fixed samples were stored at room temperature until the analysis. Preparation procedures of leaves for SEM-EDS analysis were adopted from past studies (Pathan *et al*., 2009; Ram *et al*., 2012). For EDS analysis, 0.01 weight percentage (wt%) was determined as the lowest element detection limit (Ottelé *et al*., 2010; Perini *et al*., 2017). Elemental wt% is defined as the elemental mass fraction quantified by the EDS recorded x-ray peaks and corresponding intensity generated from an element (Newbury & Ritchie, 2013; Goldstein *et al*., 2017). A schematic diagram of leaf preparation and SEM-EDS analysis is presented in Figure 3.3.

Table 3.1. Twelve plant species studied with biocultural use (trees first, followed by forbs). Plant height (mean, m). *Exotic and [cv]cultivated species. Collection site: HG, home garden; RL, rangeland.

Sampling site	Plant species	Family	Specimen number	Life form	Plant height (m)	Leaf use
S2 (HG) 24°31′58.9″ S 30°08′07.1″ E	*Carica papaya* L.*[cv]	Caricaceae	PUC0014908	Small tree (evergreen)	6.87	Treatment of tuberculosis, sexually transmitted disease and skin ailments
S3 (HG) 24°15′39.7″ S 29°57′20.8″ E	*Citrus limon* (L.) Osbeck*[cv]	Rutaceae	PUC0014913	Small tree (evergreen)	0.99	Tuberculosis treatment
S7 (HG) 24°17′03.8″ S 29°51′44.3″ E	*Moringa oleifera* Lam.*[cv]	Moringaceae	PUC0014923	Small tree (deciduous)	4.93	Energy tea, treat diabetes mellitus
S8 (RL) 24°54′40.2″ S 30°06′12.6″ E	*Ozoroa paniculosa* (Sond.) R.Fern. & A.Fern.	Anacardiaceae	PUC0014925	Medium tree (evergreen)	11.76	Mountain tea for general well-being
S4 (RL) 24°17′21.6″ S 29°51′22.9″ E	*Peltophorum africanum* Sond.	Fabaceae	PUC0014917	Medium tree (deciduous)	8.82	Treat white spots on the face (topical use)
S2 (HG)	*Psidium guajava* L.*[cv]	Myrtaceae	PUC0014909	Small tree (evergreen)	4.39	Treat poisoned patients

S1 (RL) 24°31′26.7″ S 30°07′37.4″ E	*Argemone ochroleuca* L.*	Papaveraceae	PUC0014906	Forb (annual)	0.76	Treat dermal growth (topical use)
S2 (RL)	*Catharanthus roseus* (L.) G. Don*	Apocynaceae	PUC0014910	Forb (perennial)	0.53	Leaf use not noted.
S1 (RL)	*Gomphocarpus fruticosus* (L.) W.T.Aiton	Apocynaceae	PUC0014907	Forb (perennial)	1.45	Leafy vegetable, treat kidney problems, headache
S3 (HG)	*Ipomoea batatas* (L.) Lam.*[cv]	Convolvulaceae	PUC0014914	Forb (annual)	0.19	Leafy vegetable
S2 (RL)	*Senna italica* Mill.	Fabaceae	PUC0014911	Forb (perennial)	0.17	Leaf use not noted.
S5 (RL) 24°15′43.9″ S 29°50′42.1″ E	*Tribulus terrestris* L.	Zygophyllaceae	PUC0014919	Forb (annual)	0.07	Leafy vegetable

3.2.3 SEM-EDS analysis

3.2.3.1 Elemental Cr detection

Elemental composition analysis of leaf surfaces was conducted to indicate foliar Cr dust contamination and obtain the overall wt% of elemental Cr present. For each species, four air-dried leaves were randomly selected and from each leaf, a few small strips were cut from the middle section under a Nikon stereomicroscope. Leaf strips representing either the adaxial or abaxial leaf surfaces were mounted on aluminium (Al) specimen stubs with double-sided carbon tape. Stubs were then coated with gold/palladium (Au/Pd) (Eiko IB2 ion sputter coater) to analyse at 15 kV and 10 mm working distance with an Oxford X-map 20 EDS detector and INCA software integrated into an FEI Quanta 250 FEG SEM.

3.2.3.2 Cr particle identification

To identify individual Cr particle on leaf surfaces, leaves fixed in 70% ethanol were used. Ethanol based fixatives are safer compared to other hazardous conventional chemicals (Chieco *et al*., 2013). Leaves initially fixed in 70% ethanol were further dehydrated up to 100% ethanol and thereafter leaf strips were cut following the air-dried leaf procedure. Leaf strips were then critical point dried using CO_2 as the transition fluid and then mounted, coated, and analysed with EDS as for air-dried leaves. EDS elemental spectrums of randomly chosen particles on adaxial and abaxial leaf surfaces were recorded to identify Cr containing ones.

3.2.3.3 Cr particle morphology

Specimen stubs prepared for Cr particle identification (section 3.2.3.2) were further coated with carbon (C) (Emscope TB500 C-coater) to improve conductivity for imaging the identified Cr particles with the FEI Quanta 250 FEG SEM at 5 kV and a working distance of 10 mm. Micrographs were used to determine the size, size distribution and shape of deposited Cr particles.

3.2.3.4 Total dust density

The same stubs described in section 3.2.3.2 were used to capture images of deposited dust particles with SEM. Dust accumulation was determined by counting particles on five randomly chosen areas of 200 μm^2 on SEM micrographs per leaf surfaces per species and calculating the mean and standard deviation (Weerakkody *et al.*, 2018).

3.2.3.5 Leaf surface micromorphology

To evaluate the influence of leaf micromorphological features on total dust and Cr particle adhesion, SEM images of prepared ethanol fixed leaf (section 3.2.3.2) were studied further in

conjunction with the dust analysis results. Epicuticular wax morphology and wax crystalloid aggregation patterns were identified from micrographs following the classification by Barthlott *et al.* (1998).

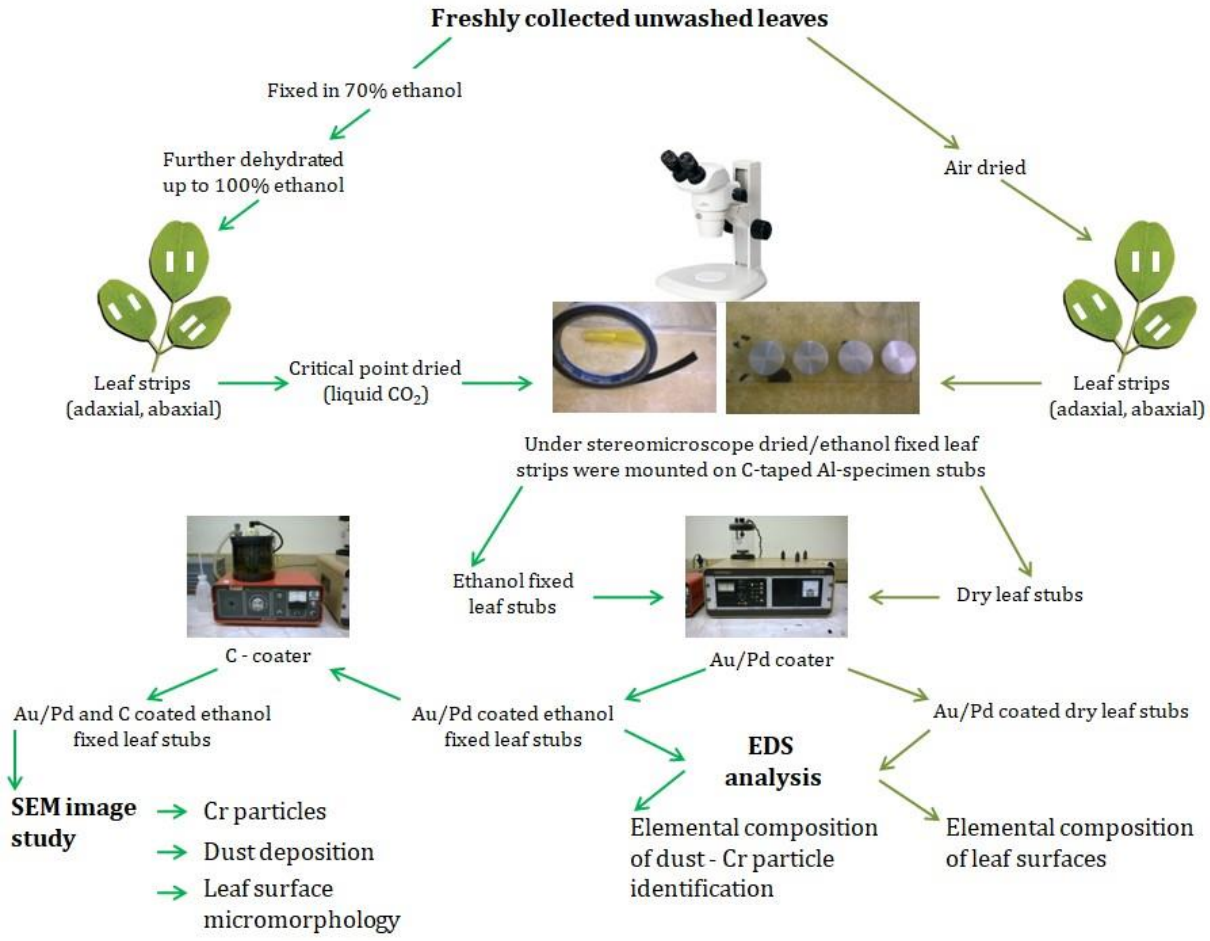

Figure 3.3. The schematic diagram of sample preparation and SEM-EDS analysis.

3.2.3.6 Counts

ImageJ software (Java image processing program) was used to count and measure (lengths) stomata and trichomes on five randomly chosen areas (200 µm^2) on micrographs per leaf surface per species following methods described by Ottelé *et al.* (2010). All counts were standardised to per mm^2, and corresponding means and standard deviations were determined. Cr particles were measured following the same procedure. The three PM size fractions quantified in this study were fine ($PM_{2.5}$), coarse (PM_{10}) and large (PM > 10 µm).

3.2.4 Plant morphology

Plant species were categorised based on growth form (i.e. trees and forbs) and canopy shape (i.e. oval, round, spreading and umbrella) to study their influence on foliar dust deposition. Plant

heights were measures for three individuals per species and corresponding means were calculated.

3.2.5 Leaf macromorphology

For each plant species, leaf macromorphological details were studied to assess the effect of such characteristics on the total dust and Cr particle deposition on leaf surfaces. Accordingly, leaf inclination, deciduousness, compound/simple, leaf blade firmness, folding of margin and surface flatness was categorised. Species wise leaf blade size (area) was determined by the standard formula, LA = GN x GA, where LA is the leaf area (size), GN is the number of grid and GA is the area of a grid (Li *et al*., 2008). The method was repeated for several leaves sampled from more than three individuals and corresponding means and standard deviations were calculated per species.

3.2.6 Data analysis

To assess the relationship between the highest Cr wt% and corresponding particle size, Pearson correlation coefficient analysis (*r*) was performed per leaf side. This was aimed to find out if the highest Cr amounts are correlated to any specific particle size fraction. Measured plant (plant height), leaf macro- (leaf size) and micro- (stomata and trichome size and density) morphological traits were analysed using Pearson correlation coefficient to determine their relations with total dust density, PM size distribution (fine, coarse, and large), leaf surface Cr wt% and Cr particle sizes. To evaluate the effects of non-quantifiable morphological traits, i.e. growth forms (tree and forbs) and leaf type (simple and complex) on PM size distribution, leaf surface Cr wt% and Cr particle sizes, a non-parametric Kruskal-Wallis test was conducted on such categories. Hierarchical Cluster Analysis was performed to group species based on total dust accumulation potential (Sæbø *et al*., 2012). The analysis was aimed to reveal the shared characteristics (Lu *et al*., 2010) of species that may explain total dust accumulation potential per group. A dendrogram using the Ward linkage method in conjunction with Euclidean distance was created to visualise the cluster analysis result (Lu *et al*., 2010). Formed clusters are presented with the letter ‘C’ and corresponding cluster number in the figure of this study. An ANOVA followed by the post hoc multiple comparison test (Tukey’s Honestly Significant Difference, HSD) was conducted on the formed groups based on the hierarchical cluster analysis outcomes to see if groups differ significantly regarding total dust counts. Finally, the Kruskal-Wallis test was performed to test if the two leaf sides differed significantly regarding total dust density, PM size fractions, Cr wt% and Cr particle size. Data was standardised when the input contained variables in different units and tested for homogeneity. Throughout the result interpretation, statistical significance was considered at $p<0.05$. Statistica version 7 was used for Pearson correlation analysis and IBM SPSS version 27 was used for ANOVA, Hierarchical cluster analysis and Kruskal-Wallis test.

3.3 Results

3.3.1 Foliar Cr detection

EDS analysis of air-dried leaves indicated Cr in foliar dust for eight out of twelve plant species. Other frequently detected elements (i.e. Al, Calcium (Ca), Iron (Fe), Magnesium (Mg), Potassium (K), Silicon (Si) and Sulphur (S)) are listed in Table 3.2. Detected Cr ranged between 0.07–1.56 and 0.09–0.28 wt% on the adaxial (Ad) and abaxial (Ab) surfaces, respectively. The highest Cr wt% per species were recorded in the following descending order: *C. papaya* (1.56 wt%, Ad) > *P. africanum* (0.28, Ab) > *A. ochroleuca* (0.21, Ad) > *G. fruticosus* (0.17, Ab) > *M. oleifera* (0.16, Ab) > *P. guajava* (0.15, Ab) > *C. roseus* (0.14, Ad) > *O. paniculosa* (0.13, Ad). *C. papaya* had the highest elemental values for multiple elements (Si > Fe > Cr > Al) on the adaxial surface. A similar group of elements (Si > Fe > Al) had the highest wt% values on the abaxial leaf surface of *I. batatas*. The highest wt% of Ca, Mg and S on both leaf surfaces were determined in *T. terrestris*, *P. guajava* and *A. ochroleuca*, respectively, while the highest K wt% vales were observed for *G. fruticosus* (Ad) and *I. batatas* (Ab).

Table 3.2. Major elements detected on air-dried leaf surfaces (wt%, trees first, followed by forbs). Highest values per element per leaf surface are in bold. Ad, adaxial; Ab, abaxial; nd, not detected (below the EDS detection limit, 0.01 wt%).

Elements		Cr	Fe	Al	Si	Ca	Mg	K	S
C. limon	Ad	nd	0.19	0.1	0.39	0.47	0.29	0.79	0.14
	Ab	nd	nd	nd	0.23	0.41	0.3	0.68	nd
C. papaya	Ad	**1.56**	**2.12**	**0.41**	**2.82**	0.55	3.21	1.82	0.54
	Ab	nd	nd	nd	0.31	1.5	1.84	2.11	0.49
M. oleifera	Ad	nd	nd	nd	0.21	1.43	4.47	0.8	0.19
	Ab	0.16	0.22	0.14	0.38	1.07	3.37	0.81	0.19
O. paniculosa	Ad	0.13	nd	nd	0.18	nd	2.71	0.1	nd
	Ab	nd	nd	nd	0.13	nd	nd	0.4	0.11
P. africanum	Ad	0.11	0.3	0.21	0.56	0.86	0.49	0.14	0.15
	Ab	**0.28**	0.4	0.3	0.8	0.89	2.03	0.25	nd
P. guajava	Ad	0.07	0.19	0.09	0.28	0.1	**6.86**	nd	nd
	Ab	0.15	0.3	0.18	0.62	0.28	**6.4**	0.35	0.08
A. ochroleuca	Ad	0.21	0.37	0.26	0.75	0.21	4.68	1.36	**1.25**
	Ab	0.09	0.17	0.13	0.42	0.12	4.01	1.47	**0.94**
G. fruticosus	Ad	0.11	0.35	0.14	0.42	0.41	4.46	**2.57**	0.14
	Ab	0.17	0.27	nd	0.41	0.59	2.45	1.85	0.15
C. roseus	Ad	0.14	0.36	0.17	0.58	0.6	4.09	0.24	nd
	Ab	0.12	0.32	0.12	0.31	0.44	3.98	0.47	nd
I. batatas	Ad	nd	0.47	0.27	1.58	0.19	1.75	2.03	0.15

	Ab	nd	**0.78**	**0.32**	**1.98**	nd	1.54	**2.3**	0.12
S. italica	Ad	nd	nd	nd	0.14	0.61	0.67	1.58	0.16
	Ab	nd	nd	nd	0.23	0.72	0.68	1.37	0.09
T. terrestris	Ad	nd	nd	0.08	0.24	**2.69**	1.51	1.15	0.38
	Ab	nd	nd	nd	0.11	**3.31**	0.88	1.23	0.46

3.3.2 Cr particles

3.3.2.1 Cr particle identification

EDS elemental analysis of randomly chosen dust on ethanol fixed leaf surfaces identified Cr containing particles and recorded their most abundant accompanying elements (Table 3.3). Cr amounts in particles ranged between 0.2 to 23.17 wt%. Cr particles with the highest Cr wt% were detected in *C. roseus* (Ad, 23.17; Ab, 13.72), *M. oleifera* (Ab, 23.07) and *A. ochroleuca* (Ad, 20.8; Ab, 18.87). The highest wt% values of the other elements were Fe (21.86) > Si (15.42) > Mg (6.86) > Ca (5.67) > Al (4.83) > K (2.13) > Ti (0.88). Fe, Si, Al and Ca were detected in all Cr particles, while Mg and K in > 50% and Ti in < 50% of identified Cr particles.

Some of the largest Cr-containing particles were detected on *C. papaya*, *M. oleifera* and *P. guajava*, and the smallest on *C. roseus* and *G. fruticosus* (Table 3.3). Cr values in the largest (81.16 µm) and smallest (1.87 µm) particle were 13.46 and 13.73 wt%, respectively (Table 3). Pearson correlation coefficient analysis did not yield any significant relationship between Cr wt% and the corresponding size of Cr-containing particles for adaxial or abaxial surfaces.

Table 3.3. EDS elemental composition of Cr-containing particles (with highest detected Cr wt%) and corresponding particle sizes. Highest values per leaf surface per species are in bold. Ad, adaxial; Ab, abaxial; nd, not detected (below the EDS detection limit, 0.01 wt%).

Elements		Cr	Fe	Al	Si	Ti	Ca	Mg	K	Largest particle (µm)
C. papaya	Ad	13.46	10.13	3.84	3.46	0.19	0.7	3.21	0.27	**81.16**
	Ab	0.21	11.41	0.9	**15.42**	nd	nd	1.84	**2.13**	**30.89**
M. oleifera	Ad	0.49	5.4	2.49	**9.11**	0.36	**2.19**	4.47	0.49	25.85
	Ab	**23.03**	**16.03**	4.28	0.96	**0.31**	0.2	3.37	0.57	15.37
P. guajava	Ad	0.4	10.39	3.12	7.08	**0.88**	0.1	**6.86**	0.29	8.64
	Ab	1.78	2.29	2.1	5.66	nd	**5.67**	**6.4**	0.6	20.89
O. paniculosa	Ad	0.2	2.96	1.11	4.56	nd	3.21	2.71	**0.57**	6.02
	Ab	0.75	1.53	0.77	1.09	0.12	0.17	nd	0.23	14.77
C. roseus	Ad	**23.17**	15.68	**4.83**	1.35	0.32	1.04	4.09	nd	12.39
	Ab	13.72	10.04	**4.3**	0.45	nd	0.28	3.98	nd	1.87
A. ochroleuca	Ad	20.8	13.21	3.93	3.96	nd	0.87	4.68	nd	6.79
	Ab	18.87	11.37	3.45	1.39	nd	1.29	4.01	0.28	7.53
P. africanum	Ad	5.39	**21.86**	0.79	2.6	nd	0.96	0.49	0.38	4.29
	Ab	14.9	10.39	2.97	1.12	nd	1.36	2.03	0.2	6.58
G. fruticosus	Ad	1.47	3.39	0.81	6.04	nd	2.06	4.46	0.44	3.8
	Ab	9.52	6.39	2.18	1.48	0.18	1.91	2.45	0.36	1.89

3.3.2.2 Morphology of Cr particles

Cr particles varied in shape and were generally angular and irregular (Fig. 3.4). Such particles were seen deposited singly and as an agglomeration (agglomeration is the collection of small diameter solid particles into larger ones), for example, in *C. roseus* (photo not provided). Identified Cr particles were observed on various leaf surface micromorphological structures such as epicuticular wax (*C. papaya,* Fig. 3.4a, *M. oleifera, P. africanum, P. guajava*), prominent leaf veins (*O. paniculosa*, Fig. 3.4b), stomata especially on the stoma aperture of *C. roseus* and guard cells in *A. ochroleuca* (Fig. 3.4c), and on the furrows and ridges created by the convex epidermal cell outlines (*C. papaya, G. fruticosus*, Fig. 3.4d*, M. oleifera, P. africanum*). In many species, Cr particles smaller than stoma aperture were observed (*A. ochroleuca,* Fig. 3.4c, *C. roseus*).

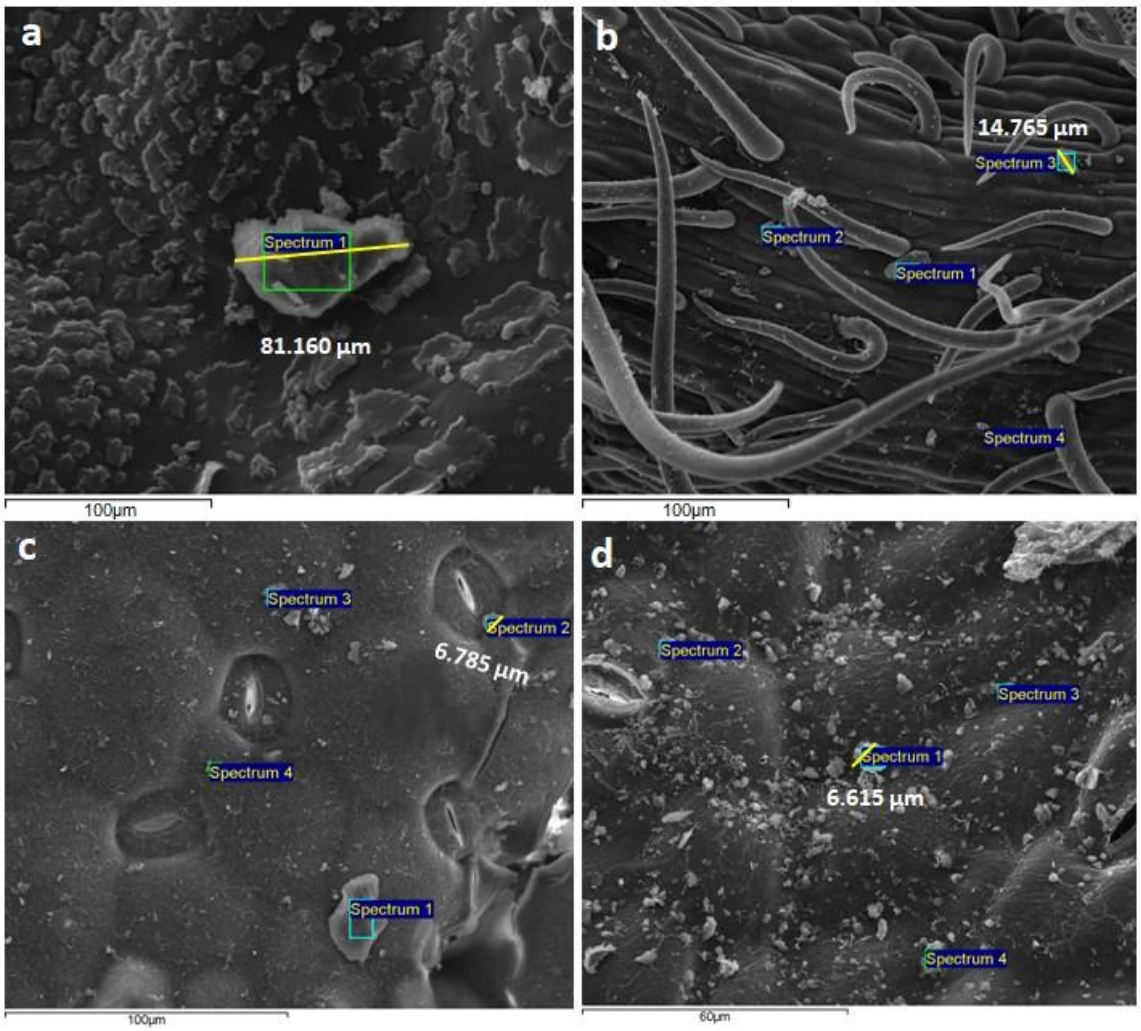

Figure 3.4. Selected micrographs of identified Cr particles on plant leaf surfaces (trees first followed by forbs). a. Large irregular and angular shaped particle on dense adaxial wax platelets of *Carica papaya*; b. particle on the abaxial vein of *Ozoroa paniculosa*; c. particle lodged on guard cell on the adaxial surface of *Argemone ochroleuca*; d. deposited particle on the rough adaxial leaf surface created by the convex epidermal cell outlines of *Gomphocarpus fruticosus*. 'Spectrum' indicates particles randomly selected for EDS elemental analysis to identify Cr-containing particles.

Measured Cr particles ranged between 1.87 (in *C. roseus*) to 81.16 µm (in *C. papaya*) (Table 3.3) belonging to all three PM size fractions. Cr was found on 40 and 43% of randomly analysed particles on adaxial and abaxial surfaces, respectively. Identified Cr particle on the adaxial and abaxial surfaces of all the species showed an abundance of PM_{10} (53%) and > 10 µm particles (38%).

3.3.3 Total dust accumulation

All three PM size fractions were encountered on leaf surfaces. Particles larger than 10 µm were the least encountered on both leaf surfaces, whereas $PM_{2.5}$ and PM_{10} accounted for 93% of the total deposition with almost equal contributions. Dust density ranged between 226–4470 particles mm^{-2}. Plant species showed variation regarding total dust density (Table 3.4). Cluster analysis classified dust density into three species clusters (Fig. 3.5a): low (200–900 particles mm^{-2}), moderate (901–3000 particles mm^{-2}) and high (3001–5000 particles mm^{-2}) (Fig. 3.5b). A follow-up ANOVA analysis (Table B2, Appendix B) on the three groups of species (low, moderate and high total dust density) created after cluster analysis, indicated a significant difference in means between group 1 and 2 ($p<0.001$), 1 and 3 ($p<0.001$) and 2 and 3 ($p<0.05$) (Fig. 3.5c).

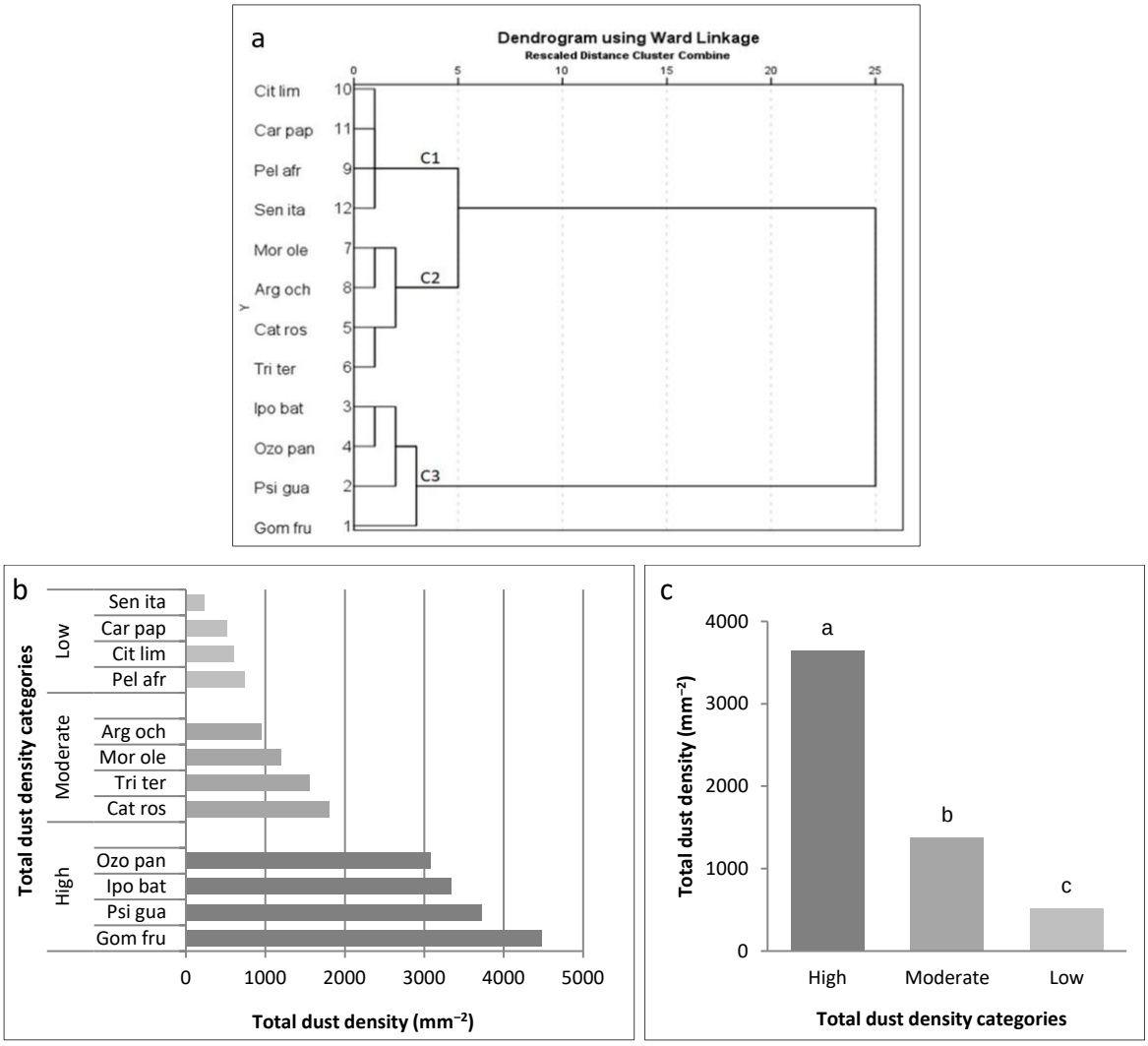

Figure 3.5. Total dust accumulation by plant species. a. Cluster dendrogram featuring three leaf dust density clusters; C1, low: 200–900 particles mm^{-2}; C2, moderate: 901–3000 particles mm^{-2}; C3, high: 3001–5000 particles mm^{-2}; b. plant species within each dust density cluster (mean counts); c. significant difference in mean values among the three dust density clusters (low, moderate and high total dust counts); different letters indicate significant difference (p<0.05). Arg och = *Argemone ochroleuca*, Car pap = *Carica papaya*; Cat ros = *Catharanthus roseus*, Cit lim = *Citrus limon*, Gom fru = *Gomphocarpus fruticosus*, Ipo bat = *Ipomoea batatas*, Mor ole = *Moringa oleifera*, Ozo pan = *Ozoroa paniculosa*, Pel afr = *Peltophorum africanum*, Psi gua = *Psidium guajava*, Sen ita = *Senna italica*, Tri ter = *Tribulus terrestris*.

3.3.4 Plant morphology

3.3.4.1 Plant height and habit

Considerable height variations within the tree (0.99–11.8 m) and forb (0.07–0.76 m) categories were noted (Table 3.1). Pearson correlation produced significant relation between plant height

and size of Cr particles detected on the abaxial surface (p<0.05). This indicated larger Cr particles on the abaxial leaf surfaces of taller species than shorter plants. Kruskal-Wallis test between the two growth forms also presented similar results with significantly larger Cr particles (p<0.05) on the abaxial leaf surfaces of trees (2–12 m) than that of forbs (< 2 m) (Fig. 3.6) (Table B3, Appendix B). Trees had some of the highest (*P. guajava* > *O. paniculosa*) and lowest (*C. papaya* < *C. limon*) total dust counts. Except for *S. italica* which had the lowest total dust density, all forbs had moderate to high total dust densities.

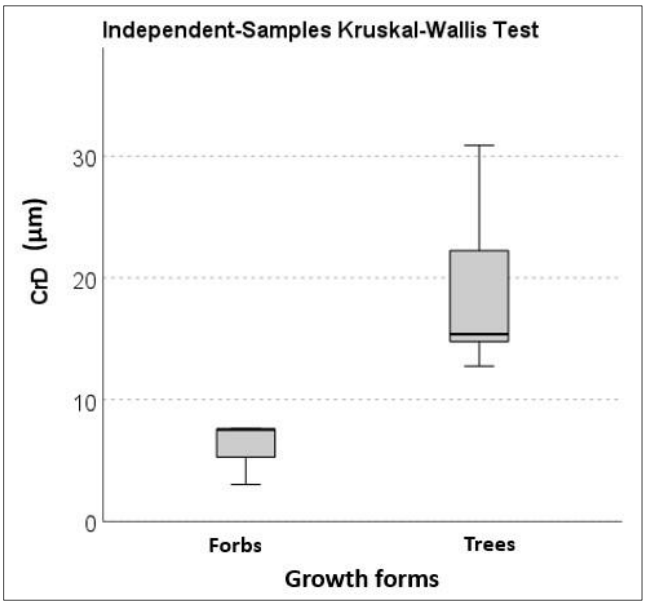

Figure 3.6. Significant difference in Cr particle size on the abaxial leaf surface between the growth forms. Whiskers represent the largest and smallest sizes. Significant difference at p<0.05. CrD, Cr particle size (µm).

Four evergreen and two deciduous tree species (Table 3.1) were sampled to account for the effect of protracted and short exposure period on dust deposition. Both evergreen (*P. guajava* and *O. paniculosa*) and deciduous (*M. oleifera*) species had some of the highest total dust counts (Table 3.4). Likewise, the highest Cr wt% values were observed for both evergreen (*C. papaya*), and deciduous (*P. africanum*) species (Table 3.2).

3.3.4.2 Tree canopy

Four types of tree canopy shapes, i.e. oval, round, spreading and umbrella were observed for the six species (Fig. 3.7) based on the categorisation described in literature (Jiménez *et al*., 2014; Joshi & Joshi, 2014; Othman *et al*., 2015). An oval canopy shape created by almost vertical branches was observed for *M. oleifera* that had moderate values for both total dust counts and Cr wt%. A round canopy shape was noted for *C. limon* and *P. africanum* with compact branching and dense leaves that had comparatively low total dust counts and below detection limit Cr wt% on *C. limon* but the highest abaxial Cr wt% on the latter. High total dust densities and moderate

Cr wt% values were determined for *O. paniculosa* and *P. guajava* that had spreading canopy shapes formed by mostly horizontal branches. A distinct umbrella-like tree shape with few branches and leaves was seen for *C. papaya* that had second-lowest total dust counts but the highest adaxial Cr wt%.

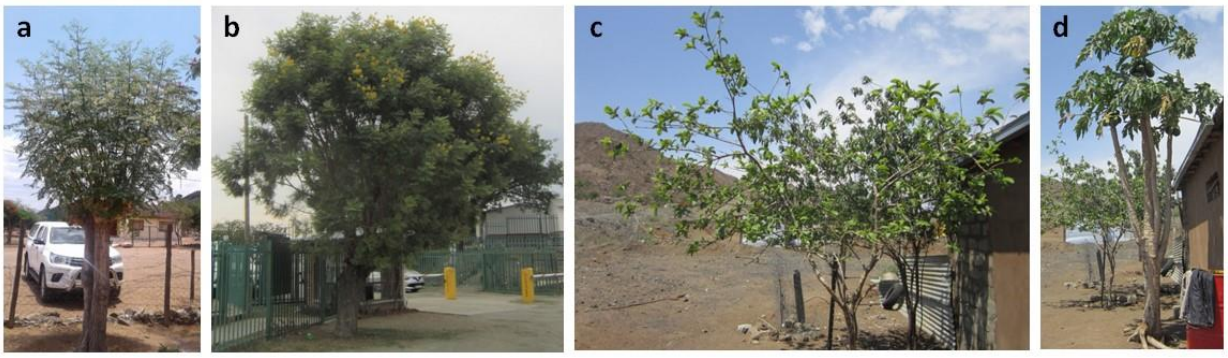

Figure 3.7. Tree canopy shapes observed for sampled species. a. Oval (*Moringa oleifera*); b. round (*Citrus limon*; *Peltophorum africanum* – in the photo); c. spreading (*Ozoroa paniculosa*; *Psidium guajava* – in the photo); d. umbrella (*C. papaya*). Photographs by Mr Dennis Komape.

3.3.5 Foliar morphology

3.3.5.1 Macromorphology

Leaves showed variation in macromorphology (Table 3.4). Leaf area ranged from 3.5 to 669.7 cm^2 and the pinnae of compound leaves were 0.1–1.07 cm^2. Pearson correlation coefficient analysis detected significant positive relation between leaf area to Cr wt% (r = 0.987, p<0.001), Cr particle size (r = 0.8691, p<0.001) and coarse PM size fraction (r = 0.6256, p<0.05) for the adaxial leaf side (Table 3.5). For the abaxial surface, leaf area was positively correlated to Cr particle size (r = 0.6837, p<0.05). Kruskal-Wallis test performed for simple/compound leaf categories for each leaf surface (Table B4, Appendix B) and between the adaxial and abaxial leaf surface (Table B5, Appendix B) did not produce any significant difference in terms of foliar Cr wt%, Cr particle size, total dust or PM size fractions.

In general, leaf inclination less than right angles (< 90°) was frequently noted and had higher total dust density than the drooping mature leaves (> 90°) as seen for *C. papaya* and almost vertically aligned leaves of *S. italica*. Concave leaf blades (arced to the inside) were a common feature that showed greater dust accumulation than the flat leaves of *S. italica*. Lamina firmness and texture varied among species (Table 3.4). Thick leaves of *A. ochroleuca, C. limon, C. papaya* and *S. italica* had moderate to low total dust densities. Species with upward folded margins had moderate (*A. ochroleuca*) to high (*P. guajava*) dust density. Other than *C. limon, C. roseus*, *G. fruticosus, I. batatas* and *M. oleifera* that had almost uniform dust coverage, accumulation of dust was mainly

visible on distinct roughness features such as veins and epidermal grooves and furrows on both leaf surfaces of most species (Table 3.4).

Table 3.4. Leaf macromorphology and observed dust deposition patterns. Leaf size, cm^2, mean ± SD; total dust density, mean (particle number combining the two surfaces, per mm^2).

Leaf type	Plant species	Leaf size (cm^2)	Total dust density (mm^{-2})	Inclination, leaf blade	Field observations on foliar dust deposition
Simple	*A. ochroleuca*	9.17±6.8	952	≤ 90°, concave, narrowly lanceolate, margin lobbed and folded upward, prickles on margin and veins, tough, firm, thick	Dust accumulated in the middle of the cup-shaped blade and on prominent veins
	C. limon	11.31±2.3	598	≤ 90°, concave, oblong to elliptic-ovate, smooth, firm, thick	Leaves without much visible dust deposition and mostly as uniform layers
	C. papaya	669.68±184.7	520	~ 90°, concave, palmate, rough, firm, thick	Distinct dust deposition on the epidermal grooves and deep veins
	C. roseus	4.91±2.2	1796	≤ 90°, concave, elliptical to obovate, smooth, firm	Uniform dust layers that sometimes concentrate on the veins
	G. fruticosus	3.47±1.2	4470	≤ 45°, concave, narrowly linear to elliptical, sticky, moderately firm	Sticky leaves were almost uniformly covered with dust
	I. batatas	3.32±1.8	3334	~ 90°, concave, palmate, rough, firm	Almost uniformly dusty
	O. paniculosa	4.08±1	3080	≤ 90°, concave, elliptic to elliptic-oblong, margin wavy, rough, firm	Dusty with more deposition on the veins and wavy margin

	P. guajava	23.9±16.5	3716	≤ 90°, concave, elliptical to oblong, margins folded upwards, rough, firm	Dusty with more accumulation on deep veins
Compound	*M. oleifera*	0.81±0.3	1196	≤ 45°, concave to flat, tripinnate, elliptical to obovate, slightly rough, moderately firm	Almost uniformly dusty
	P. africanum	0.2±0.2	734	≤ 90°, slightly concave, paripinnate, oblong or linear-oblong, rough, firm	Dust on veins, margins, and hairy underside
	S. italica	1.07±0.3	226	Almost vertical, flat, bipinnate, leaflets oblong-obovate, firm, thick	Vertically aligned leaves looked slightly dusty
	T. terrestris	0.1±0.02	1552	~ 90°, concave, paripinnate, ovate to elliptic-oblong, rough, moderately firm	Dust deposition on veins, hairy underside and margins

Table 3.5. Pearson correlation coefficient values for plant morphology (plant height), leaf macro- (leaf area) and micromorphological (stomata and trichome size and density) traits. Significant values are in bold. Ad, adaxial; Ab, abaxial. Significance, * = p<0.05; ** = p<0.01; *** = p<0.001.

Variable	Cr wt%		Cr particle size		Total dust density		$PM_{2.5}$ (fine)		PM_{10} (coarse)		PM > 10 µm (large)	
	Ad	Ab	Ad	Ab	Ad	Ab	Ad	Ab	Ad	Ab	Ad	Ab
Plant height	0.3103	0.2271	0.3646	**0.6937***	0.2260	–0.190	–0.0470	0.4305	–0.0410	–0.4431	0.3291	–0.0580
Leaf area	**0.987****	–0.2717	**0.8691****	**0.6837***	–0.2386	–0.2835	–0.5618	–0.1661	**0.6256***	0.377	–0.2396	–0.2994
Stomata size	–0.2404	0.5373	–0.4042	–0.1471	0.0969	0.2583	0.1386	**–0.6696***	0.1314	0.5153	0.0034	0.3617
Stomata density	–0.2808	0.1008	–0.4634	0.4075	–0.1425	0.037	0.0001	0.0011	–0.2088	–0.058	0.1078	0.0886
Trichome size	–0.2971	0.0206	–0.1172	–0.1929	**0.5865***	–0.0562	0.2283	–0.1101	–0.3438	–0.115	0.4324	0.3716
Trichome density	–0.3155	–0.239	0.0595	0.1736	0.0751	–0.0567	–0.1358	–0.5295	0.0603	–0.5055	0.2824	–0.133

3.3.5.2 Micromorphology

SEM micrographs captured diverse micro-morphological details of adaxial (Fig. 3.8) and abaxial (Fig. 3.9) leaf surfaces as summarized in Table 3.6 and 3.7. Convex epidermal cell outlines were observed frequently that created prominent surface roughness with formed furrows and grooves. Such foliar surface roughness was particularly prominent on both leaf surfaces of *A. ochroleuca, C. papaya*, *M. oleifera, S. italica* and abaxial surface of *P. africanum* (Figs. 3.8 and 3.9). *O. paniculosa* had tabular epidermal cell outlines on the adaxial surface with distinct edges that created roughness (Fig. 3.8d). Protruding veins were noted on both leaf surfaces of several species (Table 3.6). SEM images captured high concentrations of accumulated dust on or near the abaxial veins in *C. limon*, *C. papaya* (Fig. 3.9a) and *C. roseus* (Fig. 3.9h) and on the adaxial veins of *P. guajava* (Fig. 3.8f). Dust deposition was observed on the epidermal glands on both surfaces of *I. batatas* (Figs. 3.8j and 3.9j).

Stomata size (length) ranged between 5.39 (*S. italica*, Ad) to 22.54 µm (*A. ochroleuca*, Ab). Stomata density range was much greater on the abaxial (6–146 mm^{-2}) than the adaxial (5–47 mm^{-2}) leaf side. *G. fruticosus* had the lowest (adaxial surface) and *P. guajava* the highest stomata density (abaxial surface). Stomata remained obscured on *O. paniculosa* due to wax and a thick layer of trichomes on the adaxial and abaxial leaf surfaces, respectively. Dust deposition on stoma aperture (*C. roseus*, Figs. 3.8h and 3.9h; *I .batatas*, Fig. 3.8j), around and on the guard cells (*A. ochroleuca*, 3.8g; *I .batatas*, Fig. 3.8j*; G. fruticosus*, Fig. 3.9i), on the cuticular ledge around the stomata (*C. limon*; *C. roseus*; *P. guajava*, Fig. 3.9f), near the sunken stomata (*M. oleifera*, Fig. 3.9c; *P. africanum*), and dust blocked stomata (Figs. 3.8l and 3.9b) were observed. Of the identified Cr particles, 88% were within the stomata size range (6.61–22.54 µm) of the eight species with detected Cr. Pearson correlation coefficient analysis indicated a significant negative relation between stomata size and fine PM number ($p<0.05$) (Table 3.5).

Most species had non-glandular trichomes. Both glandular and non-glandular trichomes were observed on adaxial and abaxial leaf surfaces of *O. paniculosa* (Figs. 3.8d and 3.9d) while *G. fruticosus* had only glandular trichomes on both leaf surfaces (Fig. 3.8i). The length and density of trichomes occurred in the range 60.24–708.69 µm and 2.6–484 mm^{-2}, respectively. Like stomata, the highest trichome length and density values were determined for the abaxial leaf surfaces. Glandular and non-glandular trichomes were imaged with accumulated dust at their bases (for example, *P. guajava*, Fig. 3.9f) and on surfaces such as for *M. oleifera* (Fig. 3.8c), *P. africanum* (Fig. 3.9e), *P. guajava* (Fig. 3.9f) and *T. terrestris* (Fig. 3.9l). Smaller particles were observed on trichome surfaces. Trichome size had a significant positive correlation with the adaxial total dust density ($p<0.05$) (Table 3.5).

Epicuticular wax layers with various wax crystalloid morphologies and aggregation patterns were observed (Table 3.6). Among the different wax structures, smooth wax films (*C. roseus, I. batatas*) or wax films with plates (*C. limon, G. fruticosus, O. paniculosa*) and granules (*P. guajava*) were common among the species. Densely packed wax plates (*P. africanum, S. italica*), platelets (*C. papaya, M. oleifera*) and threads (*A. ochroleuca*) were also observed. Degraded wax structures were visible on SEM images of leaves of *C. papaya, M. oleifera, P. africanum* and *S. italica*. *T. terrestris* showed no distinct morphological wax structures but it had prominent cuticular folds on epidermal cells as similarly seen on *C. roseus* and *I. batatas*. Epicuticular wax structures were observed with dust particles of various sizes (Figs. 3.8 and 3.9). Dust accumulation was observed on cuticular folds near stomata (*G. fruticosus; I. batatas,* Fig. 3.8j; *T. terrestris*) and cuticular ledge around stomata (*C. limon*, *C. roseus*, *P. guajava*). On *P. africanum*, wax-covered stomata were observed on the abaxial surface.

Table 3.6. Structural details of epicuticular wax and prominent leaf surface micromorphology in the following order: epidermal cell shape, veins, cuticle, epiedermal glands, stomata and trichomes. Ad, adaxial; Ab, abaxial; NOB, not observed.

Plant species	Epicuticular wax crystalloid morphology and aggregation patterns		Prominent micromorphological features
	Ad	Ab	
C. limon	Wax films with parallel plates	Wax films with parallel plates	Convex (Ad, Ab), deep veins (Ad, Ab), stomata with a cuticular ledge (Ab)
C. papaya	Very dense non-entire platelets	Very dense rosette of platelets	Convex forming distinct epidermal ridges and grooves (Ad, Ab), deep veins (Ad, Ab)
M. oleifera	Very dense rosette of platelets	Very dense rosette of platelets	Convex with deep epidermal ridges and grooves, sunken stomata (Ab), sparsely hairy (Ad)
O. paniculosa	Wax films with plates	Wax films	Tabular or flat with distinct edges (Ad) and convex (Ab) forming ridges and grooves, prominent veins (Ad, Ab), sparsely hairy (Ad), puberulous (Ab)
P. africanum	Plates	Plates	Convex forming epidermal ridges and grooves, sunken stomata (Ad, Ab), sparsely (Ad) and moderately (Ab) hairy
P. guajava	Wax films with granules	Wax films with dense granules	Convex with prominent grooves and ridges (Ad, Ab), deep veins (Ad, Ab); cuticular ledge around stomata (Ab), sparsely (Ad) and moderately (Ab) hairy
A. ochroleuca	Very dense threads	Very dense threads	Convex with deep epidermal ridges and grooves, prominent veins (Ad, Ab)
C. roseus	Wax films	Wax films	Convex, distinct epidermal ridged and grooves, deep veins (Ad, Ab), prominent cuticular folds, stomata with a cuticular ledge (Ad, Ab)
G. fruticosus	Wax films with plates	Wax films with dense plates	Convex creating ridges and grooves (Ad, Ab), cuticular folds around stomata (Ad), sparsely hairy (Ad, Ab)

I. batatas	Wax films	Wax films	Convex forming deep grooves and ridges, distinct cuticular folds, epidermal glands (Ad, Ab)
S. italica	Very dense plates	Very dense rosette of platelets	Convex, deep epidermal ridged and grooves, sparsely (Ad) and moderately hairy (Ab)
T. terrestris	NOB	NOB	Convex creating deep grooves and ridges, cuticular folds around stomata and on epidermal cells (Ad, Ab), sparsely hairy (Ad), very long hairs (Ab)

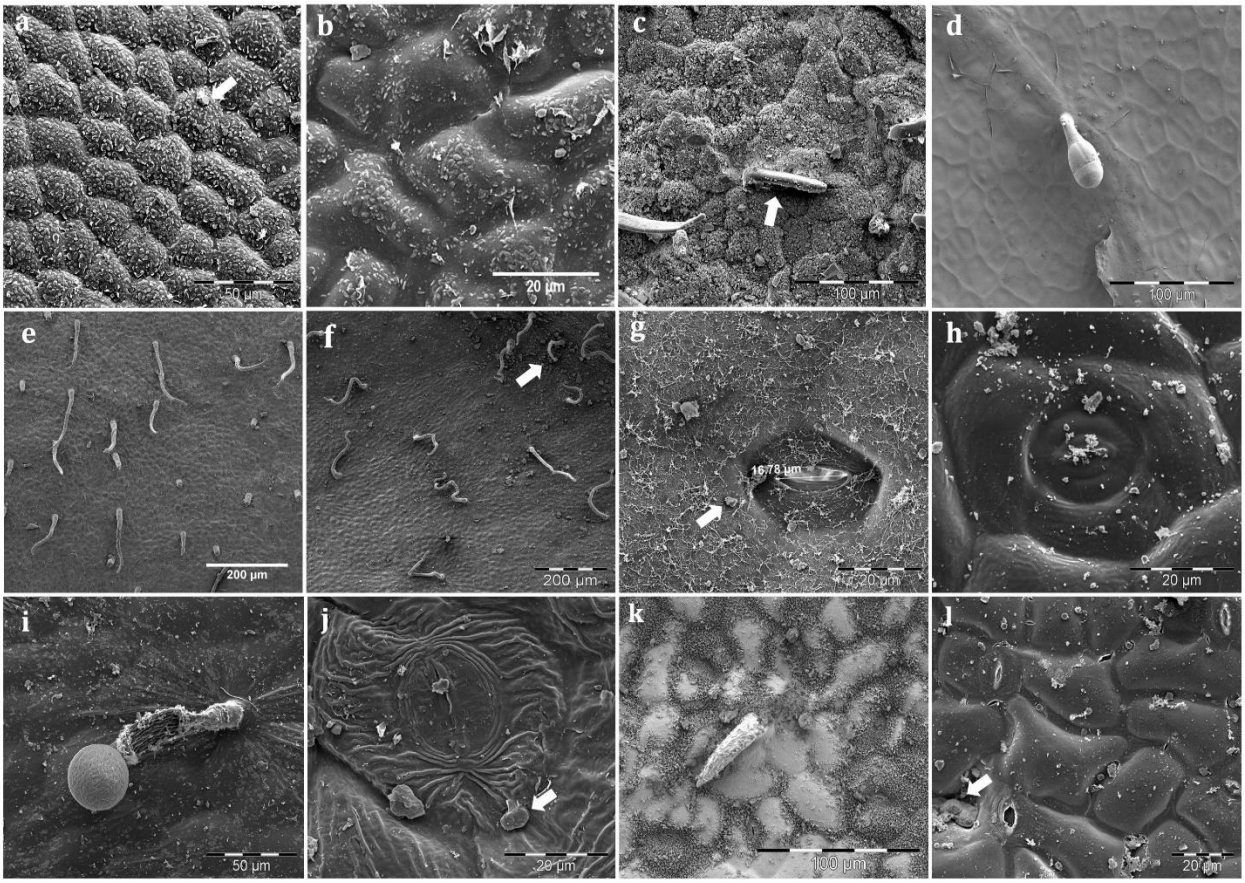

Figure 3.8. SEM images of adaxial leaf surface micromorphology with deposited dust. Trees first followed by forbs. a. *Carica papaya*, dust (arrowed) on the convex epidermal cells with dense wax platelets; b. *Citrus limon*, convex epidermal cells with wax plates and deposited dust; c. *Moringa oleifera*, dense epicuticular wax on the convex epidermal cells, dust on trichome (arrowed); d. *Ozoroa paniculosa,* tabular epidermal cells, glandular trichome; e. *Peltophorum africanum*, convex epidermal cells, trichomes; f. *Psidium guajava,* distinct vein (arrowed) and trichome bases collecting dust; g. *Argemone ochroleuca,* dust deposition on epicuticular wax threads and around the stoma (arrowed); h. *Catharanthus roseus,* deposited particles on convex epidermal cells, stoma and guard cells; i. *Gomphocarpus fruticosus*, glandular trichome and deposited dust; j. *Ipomoea batatas,* prominent cuticular folds with dust (arrowed), dust on stoma aperture; k. *Senna italica*, convex epidermal cells, dense wax plates and trichome; l. *Tribulus terrestris*, convex epidermal cells with deposited dust and formed particle agglomeration on stoma (arrowed).

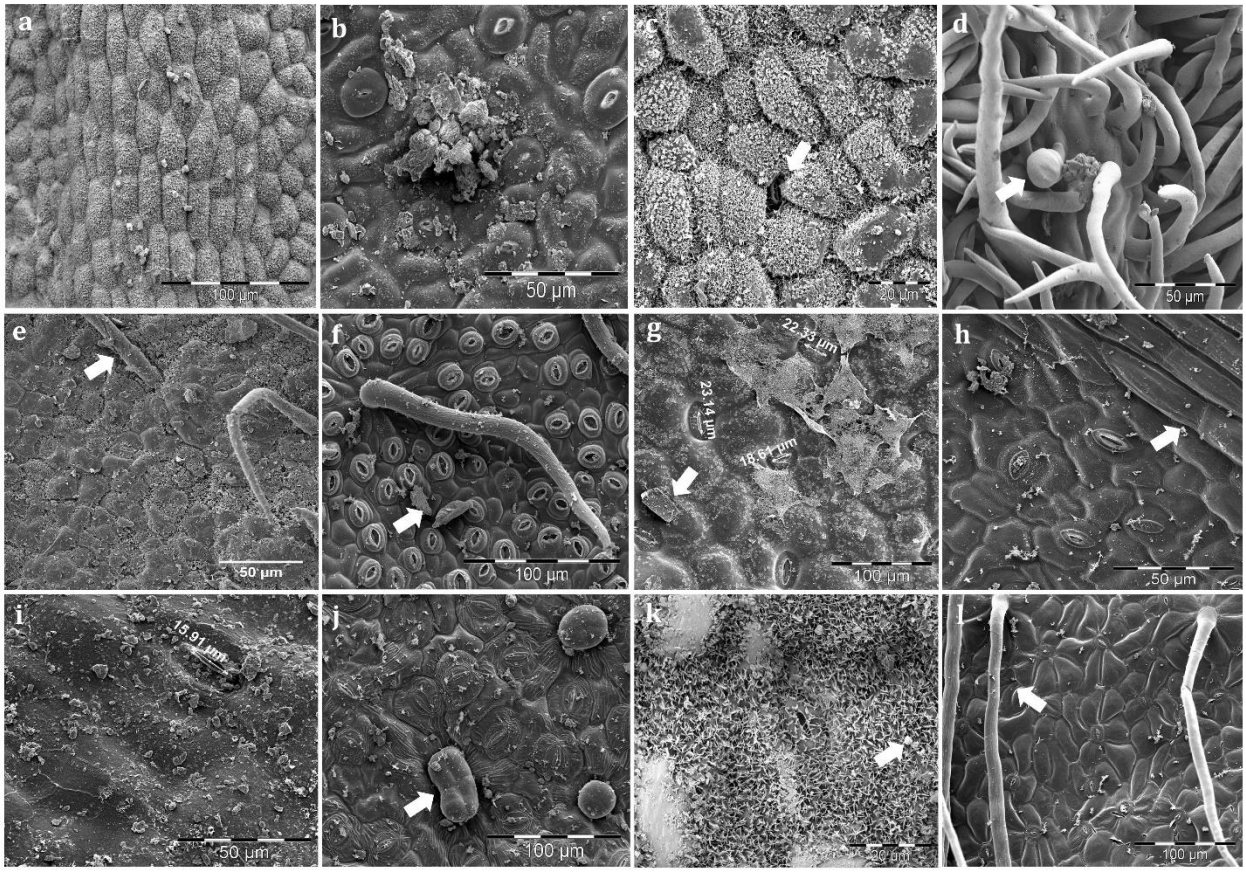

Figure 3.9. SEM micrographs of abaxial leaf surface micromorphology with deposited dust. Trees first followed by forbs. a. *Carica papaya*, surface roughness due to epidermal cell convexity, dust on vein; b. *Citrus limon*, a cuticular ledge around stomata and particle agglomeration; c. *Moringa oleifera*, sunken stoma (arrowed), epidermal cell convexity created deep ridges and grooves with dust; d. *Ozoroa paniculosa*, puberulous surface with dust on vein; glandular (arrowed) and non-glandular trichomes; e. *Peltophorum africanum*, dense wax on convex epidermal cells, trichomes with dust; f. *Psidium guajava,* cuticular ledge around stomata, deposited dust (arrowed), dust on trichome; g. *Argemone ochroleuca*, epicuticular wax threads, stomata, deposited dust particles (arrowed); h. *Catharanthus roseus*, distinct vein with dust (arrowed), and cuticular ledge around stomata; i. *Gomphocarpus fruticosus*, accumulation of particles on the guard cells, dust on epidermal cells; j. *Ipomoea batatas*, dust deposition on prominent cuticular wax folds and epidermal glands (arrowed); k. *Senna italica*, stoma, dense epicuticular wax plates, dust (arrowed). l. *Tribulus terrestris*, dust on convex epidermal cell outlines, trichomes with dust (arrowed).

Table 3.7. Stoma and trichome features. Size (length, µm), mean ± SD; density (per mm^2), mean ± SD. a, Confirmed as absent; ×not observed due to wax; ××not detected due to puberulous surface. Ad, adaxial; Ab, abaxial.

Plant Species	Stomata				Trichome			
	Size (µm)		Density (mm^{-2})		Size (µm)		Density (mm^{-2})	
	Ad	Ab	Ad	Ab	Ad	Ab	Ad	Ab
C. limon	a	4.63±0.8	a	81±20.1	a	a	a	a
C. papaya	a	6.61±1.46	a	68±14.8	a	a	a	a
M. oleifera	a	7.29±3.3	a	32±8.4	81.51±17.7	a	13±5.7	a
O. paniculosa	×	××	×	××	218.9±72.7	118.96±14.5	2.6±0.5	484±77.9
P. africanum	14.06± 1.7	12.9±2.7	9±6.5	26±11.4	152.6±19.9	316.87±67.7	9±4.2	33±2.7
P. guajava	a	8.05±2.1	a	146±37.2	171.75±31.7	188.41±28.8	8±4.5	18±5.7
G. fruticosus	18.59±1.7	14.98±2.3	5±3.5	6±2.2	72.13±47.3	101.93±31.6	8±2.7	4±2.2
A. ochroleuca	15.45±0.7	22.54±2.9	15±5	15±6.1	a	a	a	a
C. roseus	8.95±1.7	8.35±1.5	14±8.9	103±9.7	a	a	a	a
I. batatas	13.39±2.7	15.06±1.6	22±7.6	45±7.9	a	a	a	a
S. italica	5.39± 1.2	6.38±1.8	16±5.5	11±8.9	60,24±13,7	45.54±14.9	7±2.7	12±2.7
T. terrestris	6.12±0.5	5.79±1.3	47±16.4	13±2.7	116.85±40.1	708.69±210.5	4±2.2	12±2.7
Range	5.39–18.59	4.63–22.54	5–47	6–146	60.24–218.9	45.54–708.69	2.6–13	4–484

3.4 Discussion

3.4.1 Foliar dust deposition

Around 43% of randomly analysed particles on all species contained Cr in this study, which was an important finding considering the frequency of the metal in dust particles of mining-smelting areas in Sekhukhuneland. Species specific variation in leaf elemental composition as observed in this study corroborated results reported on traffic exposed plant leaves (Tomasević *et al.*, 2005; Castanheiro *et al*., 2020). The abundance of Fe, Al, Si and Mg in Cr particles resembles chromite mineralogy and the elemental composition of ferrochrome smelter dust (Tshehla & Djolov, 2018). As the elemental composition of dust particles found on plants, especially leaves, indicates air pollution (Perini *et al*., 2017; Castanheiro *et al*., 2020), findings from the present study, showing similarity in the chemical composition of leaf surfaces and deposited PM, signify atmospheric Cr particle contamination of plant leaves. Further source identification of Cr particles deposited on leaf surfaces may point out polluters that contribute the most.

Olowoyo *et al.* (2010) reported variation in deposited traffic dust sizes on *Jacaranda mimosifolia* leaves from polluted areas in South Africa. In the present study, Cr particle size varies as noted by Castanheiro *et al.* (2020) for deposited traffic emitted particles on different plant leaves. Variation in Cr particle shape and agglomeration of such particles matched such occurrence reported for traffic dust (Ottelé *et al*., 2010; Sternberg *et al*., 2010; Castanheiro *et al*., 2020).

In the present study, fine, coarse, and large Cr particles were observed with 91% contribution from $PM_{2.5}$ (fine) and PM_{10} (coarse) ($PM_{10} > PM_{2.5}$) fractions. A higher number of foliar PM_{10} could be explained by the abundance of this PM size fraction that exceeded WHO annual guidelines of 20 µg m^{-3} in the regional air mass in Sekhukhuneland (Tshehla & Djolov, 2018). A simulated rain experiment by Perini *et al.* (2017) suggested that precipitation is unlikely to wash away PM_{10} from waxy leaves. In this regard, the effect of the domestic washing procedure of plant leaves practiced in the region could be investigated to find out the effectiveness of washing with water.

A weak correlation between Cr wt% and corresponding particle size in the present study suggested possible hazard potential linked to all Cr PM size fractions from mining and smelting areas. The hazard potential of PM predominantly depends on its size that generally affects its chemistry (Csavina *et al*., 2012; Sæbø *et al*., 2012). For example, in the air mass over the BIC in South Africa, the most hazardous Cr(VI) (hexavalent Cr, the highest oxidation form of Cr) is frequently found in $PM_{2.5}$ but also PM_{10} (Venter *et al*., 2016). Detection of Cr in both $PM_{2.5}$ and PM_{10} in the present study, therefore, requires elaborate investigation in terms of the presence of Cr(VI).

Total dust counts on investigated leaves had a similar size distribution with PM < 10 µm as the most abundant dust size where $PM_{2.5}$ counts exceeded PM_{10}. These two PM size fractions are regarded as more hazardous to human health than PM > 10 µm (Zha *et al*., 2019). Similar observations were frequently reported in previous studies with higher concentrations of the above-mentioned PM size fractions on plant leaves from polluted environments (Ottelé *et al*., 2010; Zha *et al*., 2019). A low number of > 10 µm PM on leaf surfaces of the studied species could be due to easy removal of these particles by meteorological influences, e.g. wind and rain (Dzierżanowski *et al*., 2011; Perini *et al*., 2017). As $PM_{2.5}$ are mostly emitted by human activities (Ottlé *et al*., 2010; Sternberg *et al*., 2010), determination of ~ 47% of the total dust particles from this size fraction in this study might indicate substantial anthropogenic contributions towards dust pollution of useful plant leaves in Sekhukhuneland.

3.4.2 Influence of plant traits

Plant species showed variation in detected foliar Cr wt%, Cr particle size and total dust density based on plant morphology. Plant height enhanced deposition of larger Cr dust on the abaxial surface that can be explained by the fact that plant tallness creates air turbulence (Tallis *et al*., 2011) that may lead to greater impaction linked aerial PM deposition of varied sizes on the abaxial leaf surface (Ram *et al*., 2012). This further explains the presence of larger particles on the abaxial leaf surfaces of trees due to advantageous height.

Lower dust counts for dense rounded canopies of *C. limon* and *P. africanum* can be ascribed to thick foliage that hinders air passage and dust deposition thereafter (Wu *et al*., 2018). This further explains a higher dust deposition on spreading tree shapes of *O. paniculosa* and *P. guajava* as a result of easy airflow through such canopy structure. The oval canopy of *M. oleifera* with near-vertical branches could have restricted wind movement as similarly noted for conical tree shape in city traffic polluted area (Ram *et al*., 2012). The umbrella-like simple construction of *C. papaya* (Jiménez *et al*., 2014) without branch complexity and a low number of leaves may have limited available canopy area for dust particle deposition (Nguyen *et al*., 2015).

Among macromorphological traits, simple and compound leaves had comparable dust accumulation capacity in terms of Cr particles and total dust. Past reports noted dust collection efficiency by simple (El-Khatib *et al*., 2011) and compound leaved species (Olowoyo *et al*., 2010). In the present study, larger leaves showed a greater probability of Cr particle deposition that conformed with past reports suggesting broad leaves as suitable dust particle collectors (Mo *et al*., 2015; Nguyen *et al*., 2015; Shi *et al*., 2016). For the trees with the highest Cr wt%, the evergreen leaves of *C. papaya* exposed to atmospheric dust throughout the year and compound leaves of *P. africanum* and *M. oleifera* with large cumulative leaf surfaces may have improved Cr

dust accumulation. Various evergreen (Perini *et al*., 2017) and compound leaved tree species (Olowoyo *et al*., 2010) were reported as suitable urban dust accumulators. The evergreen leaves of *P. guajava* and *O. paniculosa* might have a similar effect with regards to high total dust counts. Bigger leaves also presented larger surfaces for increased PM_{10} deposition in the present study. In contrast, Weerakkody *et al.* (2018) reported small leaves (1.7 cm^2) to accumulate significantly high quantities of PM_{10} than medium (28.9 cm^2) and large (59.6 cm^2) leaves due to a higher edge effect (accumulation of more dust on leaf edges and tip) than bigger leaves. Future research may focus on this subject to conclude better.

Among other commonly detected leaf macromorphological features, leaf inclination towards the axis and concave and firm leaf blades as observed for *A. ochroleuca*, *P. africanum* and *M. oleifera* that had some of the highest Cr wt% values, suggest these traits to favour Cr dust deposition. Findings are supported by El-Khatib *et al*. (2011) that provided a detailed account of several species highlighting such features to increase foliar dust capture potential. For the two highest total dust collecting forbs, *G. fruticosus* and *I. batatas*, such leaf traits may have a positive influence. The palmate leaf shape of *C. papaya* and *I. batatas* might have enhanced Cr dust deposition and total dust accumulation, respectively, as this complex leaf shape increases foliar dust deposition possibility (Weerakkody *et al*., 2018). Upward folded leaf margins as seen for *A. ochroleuca* and *P. guajava* could have improved their Cr particle and total dust holding capacity further.

In the present study, none of the investigated micromorphological traits showed any significant relation to foliar Cr wt% or Cr particle size. However, as revealed by the SEM images such features could influence dust accumulation by individual species as discussed below. The highest Cr wt% on *C. papaya* and *A. ochroleuca* on the adaxial and *P. africanum* and *M. oleifera* on the abaxial surfaces could be a combined influence of prominent epicuticular wax structures and epidermal cell outlines creating grooves and ridges. Grooves were frequently reported to increase foliar dust deposition in various species (Wang *et al*., 2015; Liang *et al*., 2016; Chen *et al*., 2017; Zha *et al*., 2019; Castanheiro *et al.*, 2020). Protruding veins on *C. papaya* and *A. ochroleuca* could be an important trait to hold dust as reported for different plant species by Chen *et al.* (2017).

On these species, dense epicuticular wax structural details and sticky wax surfaces could have favoured dust deposition, retention and particle adsorption based on the lipophilic/hydrophilic nature of deposited dust particles (Dzierżanowski *et al*., 2011; Schreck *et al*., 2012; Nguyen *et al*., 2015; Perini *et al.*, 2017; Liu *et al*., 2018; Weerakkody *et al*., 2018). Waxy leaves were frequently reported to have high dust quantities in literature (Sæbø *et al*., 2012; Perini *et al.*, 2017; Liu *et al*., 2018; Weerakkody *et al*., 2018).

Sunken stomata in *P. africanum* and *M. oleifera*, and large stomata size for *A. ochroleuca* may contribute to surface roughness that may aid Cr dust adhesion (El-Khatib *et al*., 2011). Most identified Cr particles (88%) in the present study are within the stomata size range that may indicate the possibility of Cr particle internalization by stomata. Contradictory reports on dust uptake by stomata were presented. Chen *et al.* (2017) suggested dust uptake through stomata as an intermittent phenomenon, but Schreck *et al.* (2012) and Xiong *et al.* (2019) suggested such occurrence as a major foliar uptake pathway for PM bound heavy metals.

For *G. fruticosus*, *O. paniculosa*, *P. guajava* and *C. roseus* that had comparatively low EDS detected Cr amounts, the following leaf micromorphological traits could have been critical. All the species had wax films on leaves that could have favoured Cr contamination as Wang *et al.* (2015) suggested this type of wax as dust enhancing trait. Glandular trichomes on *G. fruticosus* and *O. paniculosa* might have created sticky surfaces for greater dust adhesion as suggested by Weerakkody *et al.* (2018) and Zha *et al.* (2019) for leaves with such features. Cuticular folds near stomata on *G. fruticosus* and cuticular ledges around stomata in *C. roseus* and *P. guajava* could have increased dust adhesion further as discussed by El-Khatib *et al*. (2011) for various species. Presence of trichomes in all except *C. roseus*, is expected to hold more dust on leaf surfaces (Sæbø *et al*., 2012; Chen *et al*., 2017; Weerakkody *et al*., 2018).

Regarding total dust density, the ‘high’ dust density group was primarily represented by species with more desirable micromorphological traits concerning foliar dust adhesion as suggested in literature (Mo *et al*., 2015; Chen *et al*., 2017; Weerakkody *et al*., 2018; Zha *et al*., 2019): trichomes on both surfaces of all the species except *I. batatas*, roughness created by epicuticular cell outlines (*G. fruticosus, P. guajava, I. batatas*), deep veins (*P. guajava*, *O. paniculosa*) and presence of stomata and wax on leaves. In addition to this, species specific characteristics as discussed in previous sections could have further increased the total dust number. This group therefore primarily indicates trichomes and wax features to promote dust deposition. As indicated in the present study, longer trichomes on the adaxial leaf surfaces could have increased total dust collection as well. Similarly, Chiam *et al.* (2019) indicated adaxial trichomes to be responsible for around 60% of deposited dust.

Stomata on both leaf surfaces except *M. oleifera* that had stomata on the abaxial surface only, together with trichomes, wax, epidermal ridges and furrows could have favoured foliar dust adhesion (Ram *et al*., 2012; Wang *et al*., 2015; Chen *et al*., 2017) for species under the ‘moderate’ dust density group. For this group, the main dust improving traits could be stomata and wax. The ‘low’ total dust accumulators were primarily characterized by dust adhesion limiting traits such as thick leaves of *C. limon*, *C. papaya* and *S. italica*, smooth leaf surface of *C. limon* and deciduous

leaves of *P. africanum* that had dust exposure for a limited time. In literature, all these traits are noted to result in lower dust amounts (Liu *et al*., 2012; Nguyen *et al*., 2015). In the present study, larger stomata restricting $PM_{2.5}$ deposition on the abaxial leaf surfaces contradicted past reports (Liang *et al*., 2016; Zha *et al*., 2019). The study by Chen *et al.* (2017) on a variety of tree species, reported no definite correlation between stomata size and $PM_{2.5}$ deposition. Further investigation on a larger number of taxa may clarify the present results.

Trichomes, wax and stomata could be identified as common dust adhesion traits for the species investigated in the present study as similarly suggested in literature (Sæbø *et al*., 2012; Chen *et al*., 2017; Chiam *et al*., 2019; Castanheiro *et al*., 2020). In this regard, foliar uptake of dust particles via cuticle and stomata requires further attention as often reported for different leafy food crops (Schreck *et al*., 2012; Xiong *et al*., 2019). In addition, all species with the highest foliar Cr wt% and total dust counts showed dust adhesion enhancing effects of various species specific leaf surface roughness features.

C. papaya and *P. africanum* sampled close to mines and roads had the highest foliar Cr wt% but 'low' total dust numbers. On the other hand, *I. batatas* sampled farthest from a mining site, had Cr below the EDS detection limit but high total dust counts. Furthermore, Cr particles were detected on leaves of all species except *S. italica* sampled from areas < 5 km from the nearest mine. Pöykiö *et al.* (2005) noted the highest Cr concentrations in wild lingonberries (*Vaccinium vitis-idaea* L.) from areas within 3 km from an opencast Cr mine. Present results, therefore, suggest an influence of proximity to active Cr mines on dust contamination, rather than dust density to increase Cr on leaves. In literature, metal contamination is hence proximity dependent for traffic (Ottelé *et al*., 2010; Sternberg *et al*., 2010; Popek *et al*., 2015) and mine-smelter (Pöykiö *et al*., 2005) affected areas.

Unlike past studies stating significantly high dust amounts on the adaxial compared to the abaxial leaf surfaces in traffic and city emission polluted areas (Ottelé *et al.*, 2010; Mo *et al.*, 2015; Chen *et al.*, 2017), no such difference was observed in the present study. Not only mines and smelters are extensive emitters of heavy metal-enriched PM (Csavina *et al*., 2012; Entwistle *et al*., 2019) in Sekhukhuneland, but additional particle emission from the naturally metal-rich soil (Venter *et al*., 2015) and road dust (Tshehla & Djolov, 2018) may increase foliar dust exposure from below and both leaf sides could become equally vulnerable to dust deposition. Effects of pollution factors including proximity and number of Cr emitters, therefore, should be investigated further in Sekhukhuneland.

3.4.3 Study limitations

It should be mentioned here that there are other fixatives recommended for SEM analysis (Ensikat & Barthlott, 1993; Pathan *et al*., 2009) that could have improved the study results. Concerning foliar micromorphology, none of the investigated features increased foliar Cr contamination significantly. This could be explained by the conclusions drawn by Leonard *et al*. (2016) and Weerakkody *et al.* (2018), stating a collective influence of various species specific leaf morphological characteristics on dust deposition. A comprehensive analytical approach combining various statistical analysis techniques could be a better approach in this regard. Further inclusion of pollution factors in the mix could provide critical information regarding the interaction between plant morphology and Cr pollution.

Summary

Selected SEM-EDS analysis confirmed Cr particle deposition on most of the food and medicinal plant leaves sampled from home gardens and rangelands in Cr-Pt mining and ferrochrome smelting areas in Sekhukhuneland. A high percentage of Cr containing dust on the plant leaves points to considerable presence of dust borne Cr in the region. Furthermore, the presence of Cr in $PM_{2.5}$, PM_{10} and PM > 10 µm indicated potential hazard associated with all PM size fractions. Abundance of a similar group of elements on leaf surfaces and in deposited dust indicates alteration of leaf surface elemental composition due to dust deposition. Large leaf area increased Cr dust amount on the adaxial leaf surface and deposition of larger particles on both leaf surfaces. Plant tallness further increased the deposition possibility of larger Cr dust on the abaxial leaf surface. Plant groups could be identified based on leaf traits that enhance total dust accumulation by plant leaves. In this regard, presence of longer trichomes on the adaxial leaf surface may contribute significantly. Proximity to active mining sites increased foliar Cr particle deposition probability. Hence, plant leaves harvested in the vicinity of active Cr emitters should be washed thoroughly before use to limit ingestion of dust particles that may contain Cr. To assess the contribution of anthropogenic polluters on Cr dust contamination of plant leaves, possible Cr sources were identified based on EDS recorded foliar elemental composition and results are presented in the next chapter. In addition, a comprehensive analysis was conducted to link and report on the collective influence of plant morphology and pollution factors on leaf surface-Cr dust interaction in Sekhukhuneland.

References

Bamisaiye, O.A., Eriksson, P.G., van Rooy, J.L., Brynard, H.M., Foya, S., Nxumalo, V., Adeola, A.M. & Billay, A. 2014. Three dimensional geometry of the Rustenburg Layered Suite, South Africa. *Canadian Journal of Tropical Geography*, 2 (1):1–14.

Barthlott, W., Neinhuis, C., Cutler, D., Ditsch, F., Meusel, I., Theisen, I. & Wilhelmi, H. 1998. Classification and terminology of plant epicuticular waxes. *Botanical Journal of the Linnean Society*, 126:237–260.

Beckett, K.P., Freer-Smith, P.H. & Taylor, G. 2000. Particulate pollution capture by urban trees: effect of species and wind speed. *Global Change Biology,* 6:995–1003.

Castanheiro, A., Hofman, J., Nuyts, G., Joosen, S., Spassov, S., Blust, R., … Samson, R. 2020. Leaf accumulation of atmospheric dust: biomagnetic, morphological and elemental evaluation using SEM, ED-XRF and HR-ICP-MS. *Atmospheric Environment*, 221, art. 117082. https://doi.org/10.1016/j.atmosenv.2019.117082

Chen. X., Zhou, Z., Teng, M., Wang, P. & Zhou, L. 2015. Accumulation of three different sizes of particulate matter on plant leaf surfaces: effect on leaf traits. *Archives of Biological Sciences*, 67:1257–1267.

Chen, L., Liu, C., Zhang, L., Zou, R. & Zhang, Z. 2017. Variation in tree species ability to capture and retain airborne fine particulate matter ($PM_{2.5}$). *Scientific Report,* 7:1–11.

Chiam, Z., Song, X.P., Lai, H.R. & Tan, H.T.W. 2019. Particulate matter mitigation via plants: understanding complex relationships with leaf traits. *Science of the Total Environment,* 688:398–408.

Chieco, C., Rotondi, A., Morrone, L., Rapparini, F. & Baraldi, R. 2013. An ethanol-based fixation method for anatomical and micro-morphological characterization of leaves of various tree species. *Biotechnic & Histochemistry*, 88:109–119.

Coetzee, J.J., Bansal, N. & Chirwa, E.M.N. 2018. Chromium in environment, its toxic effect from chromite-mining and ferrochrome industries, and its possible bioremediation. *Exposure and Health*, 12:51–62.

Csavina, J., Field, J., Taylor, M.P., Gao, S., Landázuri, A., Betterton, E.A. & Eduardo Sáez, A. 2012. A review on the importance of metals and metalloids in atmospheric dust and aerosol from mining operations. *Science of the Total Environment*, 433:58–73.

Dreicer, M., Hakonson, T.E., White, G.C. & Whicker, F.W. 1984. Rainsplash as a mechanism for soil contamination of plant surfaces. *Health Physics*, 46:177–187.

Dudu, V.P., Mathuthu, M. & Manjoro, M. 2018. Assessment of heavy metals and radionuclides in dust fallout in the West Rand mining area of South Africa. *Clean Air Journal,* 28:42–52.

Dzierżanowski, K., Popek, R., Gawrońska, H., Sæbø, A. & Gawroński, S.W. 2011. Deposition of particulate matter of different size fractions on leaf surfaces and in waxes of urban forest species. *International Journal of Phytoremediation*, 13:1037–1046.

El-Khatib, A.A., Abdel-Rahman, A.M. & El-Sheikh, O.M. 2011. Leaf geometric design of urban trees: potentiality to capture airborne particle pollutants. *Journal of Environmental Studies*, 7:49–59.

Ensikat, H.J. & Barthlott, W. 1993. Liquid substitution: a versatile procedure for SEM specimen preparation of biological materials without drying or coating. *Journal of Microscopy*, 172(3):195–203.

Entwistle, J.A., Hursthouse, A.S., Marinho Reis, P.A. & Stewart, A.G. 2019. Metalliferous mine dust: human health impacts and the potential determinants of disease in mining communities. *Current Pollution Reports*, 5:67–83.

Goldstein, J., Newbury, D.E., Michael, J.R., Ritchie, N.W.M. & Joy, D.C. 2017. *Scanning electron microscopy and x-ray microanalysis*. 4th ed. New York: Springer.

Grange, G.H. 1973. The control of dust from mine dumps. International Conference - Air pollution, Pretoria, South Africa. *Journal of the Southern African Institute of Mining and Metallurgy,* 67–73.

Grantz, D.A, Garner, J.H.B. & Johnson, D.W. 2003. Ecological effects of particulate matter. *Environment International,* 29:213–239.

Janhäll, S. 2015. Review on urban vegetation and particle air pollution – deposition and dispersion. *Atmospheric Environment*, 105:130–137.

Jiménez, V.M., Mora-Newcomer, E. & Gutiérrez-Soto, M.V. 2014. Biology of the papaya plant. In: Ming, R. & Moore, P.H., eds. *Genetics and genomics of papaya, plant genetics and genomics: Crops and models* 10. New York: Springer. pp. 17–33.

Joshi, N. & Joshi, A. 2014. Urban tree canopy analysis. *Pollution Research*, 33:1–5.

Kimbrough, D.E., Cohen, Y., Winer, A.M., Creelman, L. & Mabuni, C. 1999. A critical assessment of chromium in the environment. *Critical Reviews in Environmental Sciences and Technology,* 29:1–46.

Leonard, R.J., McArthur, C. & Hochuli, D.F. 2016. Particulate matter deposition on roadside plants and the importance of leaf trait combinations. *Urban Forestry & Urban Greening,* 20:249–253.

Li, Z., Ji, C. & Liu, J. 2008. Leaf area calculating based on digital Image. In: Li, D., ed. *Computer and computing technologies in agriculture 2*. Boston: Springer. pp. 1427–1433.

Liang, D., Ma, C., Wang, Y., Wang, Y. & Chen-xi, Z. 2016. Quantifying $PM_{2.5}$ capture capability of greening trees based on leaf factors analyzing. *Environmental Science and Pollution Research*, 23:21176–21186.

Liu, L., Guan, D. & Peart, M.R. 2012. The morphological structure of leaves and the dust retaining capability of afforested plants in urban Guangzhou, south China. *Environmental Sciences and Pollution Research,* 19:3440–3449.

Liu, Y., Yang, Z., Zhu, M. & Yin, J. 2018. Size fractions of dust and amount of associated metals on leaf surface and inner wax of 15 plant species at Beijing roadside. *International Journal of Phytoremediation*, 21:334–351.

Lu, X., Wang, L., Li, L.Y., Lei, K., Huang, L. & Kang, D. 2010. Multivariate statistical analysis of heavy metals in street dust of Baoji, NW China. *Journal of Hazardous Materials*, 173:744–749.

Mo, L., Ma, Z., Xu, Y., Sun, F., Lun, X., Liu, X., Chen, J. & Yu, X. 2015. Assessing the capacity of plant species to accumulate particulate matter in Beijing, China. *Plos One,* 10(10), e0140664. https://doi.org/10.1371/journal.pone.0140664

Mogale, M.M.P., Raimondo, D.C. & Van Wyk, B.-E. 2019. The ethnobotany of central Sekhukhuneland, South Africa. *South African Journal of Botany,* 122:90–119.

Naidoo, G. & Naidoo, Y. 2005. Coal dust pollution effects on wetland tree species in Richards Bay, South Africa. *Wetlands Ecology and Management*, 13:509–515.

Naldrett, A.J., Wilson, A., Kinnaird, J., Yudovskaya, M. & Chunnett, G. 2012. The origin of chromitites and related PGE mineralization in the Bushveld Complex: new mineralogical and petrological constraints. *Mineralium Deposita,* 47:209–232.

Newbury, D.E. & Ritchie, N.W.M. 2013. Is Scanning Electron Microscopy/Energy Dispersive X-ray Spectrometry (SEM/EDS) quantitative? *Scanning*, 35:141–168.

Nguyen, T., Yu, X., Zhang, Z., Liu, M. & Liu, X. 2015. Relationship between types of urban forest and $PM_{2.5}$ capture at three growth stages of leaves. *Journal of Environmental Sciences*, 27:33–41.

Nowak, D.J., Crane, D.E. & Stevens, J.C. 2006. Air pollution removal by urban trees and shrubs in the United States. *Urban Forestry & Urban Greening*, 4:115–123.

Othman, N., Isa, M.N., Mohamed, N. & Hasan, R. 2015. Street planting compositions: the public and expert perspectives. *Procedia - Social and Behavioral Sciences,* 170:350–358.

Ottelé, M., van Bohemen, H.D. & Fraaij, A.L.A. 2010. Quantifying the deposition of particulate matter on climber vegetation on living walls. *Ecological Engineering*, 36:154–162.

Olowoyo, J.O., van Heerden, E., Fischer, J.L. & Baker, C. 2010. Trace metals in soil and leaves of *Jacaranda mimosifolia* in Tshwane area, South Africa. *Atmospheric Environment,* 44:1826–1830.

Pathan, A.K., Bond, J. & Gaskin, R.E. 2009. Sample preparation for SEM of plant surfaces: review. *Materials Today*, 12:32–43.

Perini, K., Ottelé, M., Giulini, S., Magliocco, A. & Roccotiello, E. 2017. Quantification of fine dust deposition on different plant species in a vertical greening system. *Ecological Engineering*, 100:268–276.

Popek, R., Gawrońska, H. & Gawroński, S.W. 2015. The level of particulate matter on foliage depends on the distance from the source of emission. *International Journal of Phytoremediation*, 17:1262–1268.

Pöykiö, R., Mäenpää, A., Perämäki, P., Niemelä, M. & Välimäki, I. 2005. Heavy metals (Cr, Zn, Ni, V, Pb, Cd) in lingonberries (*Vaccinium vitis-idaea* L.) and assessment of human exposure in two industrial areas in the Kemi-Tornio region, northern Finland. *Archives of Environmental Contamination and Toxicology*, 48:338–343.

Ram, S.S., Majumder, S., Chaudhuri, P., Chanda, S., Santra, S.C., Maiti, P.K., … Chakraborty, A. 2012. Plant canopies: bio-monitor and trap for re-suspended dust particulates contaminated with heavy metals. *Mitigation and Adaptation Strategies for Global Change*, 19:499–508.

Sæbø, A., Popek, R., Nawrot, B., Hanslin, H.M., Gawronska, H. & Gawronski, S.W. 2012. Plant species differences in particulate matter accumulation on leaf surfaces. *Science of the Total Environment*, 427–428:347–354.

Schreck, E., Foucault, Y., Sarret, G., Sobanska, S., Cécillon, L., Castrec-Rouelle, M., … Dumat, C. 2012. Metal and metalloid foliar uptake by various plant species exposed to atmospheric industrial fallout: mechanisms involved for lead. *Science of The Total Environment,* 427–428:253–262.

Scoon, R.N. & Viljoen, M.J. 2019. Geoheritage of the eastern limb of the Bushveld Igneous Complex, South Africa: a uniquely exposed layered igneous intrusion. *Geoheritage,* 11:1723–1748.

Semenya, S.S. & Potgieter, M.J. 2014. Medicinal plants cultivated in Bapedi traditional healers homegardens, Limpopo Province, South Africa. *African Journal of Traditional, Complementary and Alternative Medicines*, 11(5):126–132.

Sgrigna, G., Sæbø, A., Gawronski, S., Popek, R. & Calfapietra, C. 2015. Particulate matter deposition on *Quercus ilex* leaves in an industrial city of central Italy. *Environmental Pollution*, 197:187–194.

Shahid, M., Dumat, C., Khalid, S., Schreck, E., Xiong, T. & Niazi, N.K. 2016. Foliar heavy metal uptake, toxicity and detoxification in plants: a comparison of foliar and root metal uptake. *Journal of Hazardous Materials*, 325:36–58.

Shi, S., Wu, Z., Liu, F. & Fan, W. 2016. Retention of atmospheric particles by local plant leaves in the Mount Wutai scenic area, China. *Atmosphere*, 7(8), 104. https://doi.org/10.3390/atmos7080104

Siebert, S.J., Van Wyk, A.E. & Bredenkamp, G.J. 2002. The physical environment and major vegetation types of Sekhukhuneland, South Africa. *South African Journal of Botany*, 68:127–142.

Sokol, E.V., Nigmatulina, E.N. & Nokhrin, D.Y. 2010. Dust emission of chromium from chromite ore processing residue disposal areas in the vicinity of Krasnogorskii village in Chelyabinsk Oblast. *Contemporary Problems of Ecology*, 3:621–630.

Speak, A.F., Rothwell, J.J., Lindley, S.J. & Smith, C.L. 2012. Urban particulate pollution reduction by four species of green roof vegetation in a UK city. *Atmospheric Environment,* 61:283–293.

Sternberg, T., Viles, H., Cathersides, A. & Edwards, M. 2010. Dust particulate absorption by ivy (*Hedera helix* L) on historic walls in urban environments. *Science of The Total Environment*, 409:162–168.

Tallis, M., Taylor, G., Sinnett, D. & Freer-Smith, P. 2011. Estimating the removal of atmospheric particulate pollution by the urban tree canopy of London, under current and future environments. *Landscape and Urban Planning*, 103:129–138.

Tomašević, M., Vukmirović, Z., Rajšić, S., Tasić, M. & Stevanović, B. 2005. Characterization of trace metal particles deposited on some deciduous tree leaves in an urban area. *Chemosphere*, 61:753–760.

Tshehla, C. & Djolov, G. 2018. Source profiling, source apportionment and cluster transport analysis to identify the sources of PM and the origin of air masses to an industrialised rural area in Limpopo. *Clean Air Journal*, 28:54–66.

Tshehla, C. & Wright, C.Y. 2019. Spatial variability of PM_{10}, $PM_{2.5}$ and PM chemical components in an industrialised rural area within a mountainous terrain. *South African Journal of Science,* 115(9/10), art. 6174. https://doi.org/10.17159/ sajs.2019/6174

Utembe, W., Faustman, E.M., Matatiele, P. & Gulumian, M. 2015. Hazards identified and the need for health risk assessment in the South African mining industry. *Human and Experimental Toxicology*, 34:1212–1221.

Venter, A., Levanets, A., Siebert, S.J. & Rajakaruna, N. 2015. A preliminary survey of the diversity of soil algae and cyanoprokaryotes on mafic and ultramafic substrates in South Africa. *Australian Journal of Botany*, 63:341–352.

Venter, A.D., Beukes, J.P., van Zyl, P.G., Josipovic, M., Jaars, K. & Vakkari, V. 2016. Regional Cr(VI) pollution from the Bushveld Complex, South Africa. *Atmospheric Pollution Research,* 7:762–767.

Wang, L., Gong, H., Liaob, W. & Wang, Z. 2015. Accumulation of particles on the surface of leaves during leaf expansion. *Science of the Total Environment*, 532:420–434.

Watanabe, Y. 2015. Canopy, leaf surface structure and phenology: arboreal factors influencing aerosol deposition in forests. *Journal of Agricultural Meteorology,* 71:167–173.

Weber, F., Kowarik, I. & Säumel, I. 2014. Herbaceous plants as filters: immobilization of particulates along urban street corridors. *Environmental Pollution*, 186:234–240.

Weerakkody, U., Dover, J.W., Mitchell, P. & Reiling, K. 2018. Evaluating the impact of individual leaf traits on atmospheric particulate matter accumulation using natural and synthetic leaves. *Urban Forestry & Urban Greening*, 30:98–107.

Wu, Y., Ma, W., Liu, J., Zhu, L., Cong, L., Zhai, J., Wang, Y. & Zhang, Z. 2018. *Sabina chinensis* and *Liriodendron chinense* improve air quality in Beijing, China. *Plos One*, 13(1), e0189640. https://doi.org/10.1371/journal.pone.0189640

Xiong, T., Zhang, T., Dumat, C., Sobanska, S., Dappe, V., Shahid, M., … Li, S. 2019. Airborne foliar transfer of particular metals in *Lactuca sativa* L.: translocation, phytotoxicity, and bioaccessibility. *Environmental Science and Pollution Research*, 26:20064–20078.

Zha, Y., Shi, Y., Tang, J., Liu, X., Feng, C. & Zhang, Y. 2019. Spatial-temporal variability and dust-capture capability of 8 plants in urban China. *Polish Journal of Environmental Studies,* 28:453–462.

Chapter 4

Factors influencing foliar chromium dust deposition

4.1 Introduction

Particulate matter (PM) containing heavy metals (HMs) are generated by various natural processes, but anthropogenic activities significantly accelerate the influx and widespread distribution of these hazardous particles in the environment (Csavina *et al*., 2012; Entwistle *et al*., 2019). Amongst others, the mining industry is one of the main HM polluters that emit volumes of particles in the atmosphere at a comparatively continuous pace (Csavina *et al*., 2012; Gabarrón *et al*., 2018; Entwistle *et al*., 2019). HMs form persistent and non-biodegradable pollutants with high bioaccumulation and hazard potential at low concentrations (Shi *et al*., 2008; Masindi & Muedi, 2018). Different mining operations, such as excavation, extraction, and transportation of raw and waste materials, as well as dust particles blown from open mine pits and dumpsites, cause air pollution that could affect the quality of human life at nearby, or even distant localities (Balabanova *et al*., 2011; Nkosi *et al*., 2017; Entwistle *et al*., 2019; Tian *et al*., 2019).

PM distribution by air primarily depends on the aerodynamic diameters of the released particles and prevalent wind movement (Csavina *et al*., 2012). Dust particles have extensive spatial-temporal dispersion potential by wind leading to pollution in downwind areas (Balabanova *et al*., 2011; Csavina *et al*., 2012). Metal smelters and mines are two of the top ten global pollution challenges (Csavina *et al*., 2012), but the potential hazards of airborne dust generated by these industries have received less attention compared to water and soil pollution effects. Transportation in mining areas is also denoted as a major air polluter (Tshehla & Djolov, 2018; Tian *et al*., 2019).

Mines and smelters are major environmental pollution sources and generate large quantities of discarded rock residue, tailings, and slag, respectively, which could pollute farmlands and human settlements within the impact zone (Pöykiö *et al*., 2005; Balabanov *et al*., 2011; Ebenebe *et al*., 2017; Coetzee *et al*., 2018). The biological toxicity potential of mine released PM is affected mainly by two factors: (1) methods applied at various stages of mining, which determine the size of dispersed particles, and (2) type of mineral mined, which influences the chemical composition of PM (Csavina *et al*., 2012; Gabarrón *et al*., 2018).

Atmospheric particle removal by plants is a tested and applied HMs mitigation technique in many polluted urban areas (Nguyen *et al*., 2015; Grote *et al*., 2016; Chen *et al*., 2017). Local vegetation is often used as a cost-effective biological indicator of atmospheric pollution (Mingorance & Oliva, 2006; Oliva & Espinosa, 2007; Naderizadeh *et al*., 2016; Ebenebe *et al*., 2017). Plant leaves in

polluted areas have been reported to accumulate considerable amounts of HMs from the air and used as ecological and environmental assessment tools (Suzuki *et al*., 2009; Norouzi & Khademi, 2015; Perini *et al*., 2017). It is generally accepted that elements detected in the dust on foliar surfaces provide reliable indications of atmospheric chemical composition (Gajbhiye *et al*., 2016; Perini *et al*., 2017). Dust deposition in polluted areas therefore could alter the elemental composition of soil and plant leaves and for leaves of food and medicinal plants that may present health risks to users.

Soil around mines is generally polluted by larger dust particles due to near-source deposition because of gravity (Grantz *et al*., 2003; Popek *et al*., 2015). Rain and wind re-emit particles from leaves to settle on soil (Mingorance & Oliva, 2006), while grounded particles could also be re-suspended by air movement or precipitation induced soil splash can contaminate lower growing vegetation (Dreicer *et al*., 1984; Kimbrough *et al*., 1999). Weathering of local parent substrate (Siebert *et al*., 2002; Boneschans *et al*., 2015) and wind erosion, depending on soil parameters, climate, land use and vegetation cover, might change soil chemical composition further and contribute to HM enrichment (Csavina *et al*., 2012).

Air and soil both act as dust sources that may contaminate plant leaves (Mingorance & Oliva, 2006). Foliar particle deposition depends on species specific morphological features (Weerakkody *et al*., 2018). Plant height together with leaf macro- and micromorphological traits (leaf area or size, epicuticular wax, stomata and trichome density and size) has been considered noteworthy regarding foliar dust contamination (Mo *et al*., 2015; Chen *et al*., 2017, Zha *et al*., 2019). Recently, a more comprehensive approach has been suggested to consider a collective influence of plant morphological traits on leaf-dust interactions (Leonard *et al*., 2016; Weerakkody *et al*., 2018). Based on the positioning of the two sides of the leaf (adaxial, abaxial), dust exposure, particle deposition mechanisms (i.e. sedimentation, impaction, interception and diffusion) and consequent PM adhesion differ (Ottelé *et al.*, 2010; Ram *et al*., 2012; Mo *et al*., 2015). Leaves act as functional interfaces between plants and their surroundings by interacting with atmospheric PM which is influenced by meteorological parameters especially wind movement in the area (Neinhuis & Barthlott, 1998; Grantz *et al*., 2003; Csavina *et al*., 2012). Proximity to polluters is another important aspect to consider when evaluating dust deposition on aerial plant parts (Pöykiö *et al*., 2005; Popek *et al*., 2015; Sgrigna *et al*., 2015). Considering the variation in quantity and quality of the emitted dust by different pollution sources (Csavina *et al*., 2012; Tshehla & Djolov, 2018; Entwistle *et al*., 2019), the influence of various emitters and their number should be accounted for when investigating dust contamination of vegetation.

Mining of chromite, the economically viable ore of chromium (Cr), is reported as one of the main human activities that cause environmental Cr pollution (Kimbrough *et al*., 1999; Pöykiö *et al*., 2005). Cr mines and ferrochrome smelters pollute the air, water, and soil of the surrounding areas (Coetzee *et al*., 2018; Tshehla & Djolov, 2018). Ore transportation further contributes to Cr dust pollution (Tshehla & Djolov, 2018). Communities living around Cr mines are therefore directly exposed to airborne Cr through inhalation, dermal contact and ingestion of dust contaminated crops (Kimbrough *et al*., 1999; Pöykiö *et al*., 2005; Coetzee *et al*., 2018). In its highest oxidation state, hexavalent Cr (Cr(VI)), is carcinogenic to living organisms (Kimbrough *et al*., 1999; Beukes *et al*., 2010; Coetzee *et al*., 2018).

South Africa's economy is highly dependent on mining, but with such development comes considerable environmental degradation (Mhlongo & Amponsah-Dacosta, 2015; Ebenebe *et al*., 2017; Masindi & Muedi, 2018). South African Cr reserves are of the largest globally and the ferrochrome industry is a world leader, but in turn, it causes considerable air pollution (Venter *et al*., 2016; Tshehla & Djolov, 2018; Tshehla & Wright, 2019a, 2019b). Sekhukhuneland is a region in South Africa that presents considerable Cr and platinum (Pt) resources (Siebert *et al*., 2002; Scoon & Viljoen, 2019). Air pollution in Sekhukhuneland is a recognized concern, and regional Air Quality Management Plans are developed in line with The Municipal Systems Act No. 32 of 2000 (Tshehla & Wright, 2019b). Notwithstanding such efforts, the mining and smelting affected region in Sekhukhuneland is polluted with atmospheric Cr (Tshehla & Djolov, 2018, Tshehla & Wright, 2019a).

The present chapter investigates leaf surface-Cr dust interactions of locally useful plant species under the influence of multifaceted Cr emission in Sekhukhuneland. The two objectives were, firstly, to identify Cr sources in soil and on leaf surfaces, and secondly, to explore the leaf surface-Cr dust interaction. Regarding the first objective, it was postulated that various Cr polluting sectors in the region, namely mining and smelting industries and transportation, would affect the adjacent localities in terms of the elemental composition of the soil and vegetation. To test this hypothesis, the elemental composition of soil and plant leaf surfaces were analysed to identify possible Cr sources. With regards to the second objective, it was hypothesized that the two major sets of variables, namely, plant morphology (comprised of plant height, leaf area, epicuticular wax, and size and density of stomata and trichomes) and pollution source (proximity to and the number of Cr mines and roads) would collectively determine deposition of Cr particles (as Cr variables: Cr amount and particle size) on leaf surfaces. A comprehensive statistical analysis approach was designed by incorporating both these sets of variables to investigate leaf surface-Cr dust interaction per leaf surface as the two sides of a leaf interact differently with the exposed dust.

4.2 Materials and method

4.2.1 Study area

The study was conducted in Sekhukhune District in Limpopo Province, South Africa (Fig. 4.1), which hosts multiple Cr and Pt mines and ferrochrome smelters. Consequently, several mine dumps in the region lack sufficient management and rehabilitation planning and are left as overburdens that cover large areas and generate dust particles. Such a scenario is common in South African mining areas (Mhlongo & Amponsah-Dacosta, 2015; Nkosi *et al*., 2015; Coetzee *et al*., 2018). Opencast Cr mining in the region may further expose ore layers to expedite weathering of minerals and subsequent environmental pollution as reported globally (Pöykiö *et al*., 2005; Kien *et al.*, 2010). In addition, informal small scale ore excavation on abandoned mine sites in Sekhukhuneland produce large quantities of waste as reported nationwide (Mhlongo & Amponsah-Dacosta, 2015). National Pt units produce chromite concentrates as a by-product that is used in local ferrochrome smelters (Cramer *et al*., 2004; Beukes *et al*., 2010). Hence, alongside the mining industry, three operating ferrochrome smelters pollute the area (Tshehla & Djolov, 2018; Tshehla & Wright, 2019a). Other smelters in the north (Pt smelter in Polokwane, Limpopo) and south (ferrochrome smelter in Lydenburg, Mpumalanga), further away from the study location may also contribute to aerial dust pollution in the study region.

Mining and industrial growth expanded transportation routes. Roads connecting mines, industries and dumpsites produce and disperse volumes of hazardous dust in the region. Many informal dirt roads linking mines, industries and dumpsites frequently intersect adjacent human settlements where harmful particles could be dispersed along the way. Mining and associated socio-economic developments have led to the formation of human settlements close to the above-mentioned polluters. Pollution from mines and smelters may exacerbate already high regional concentrations of geogenic HMs including Cr in soil (Siebert *et al*., 2002).

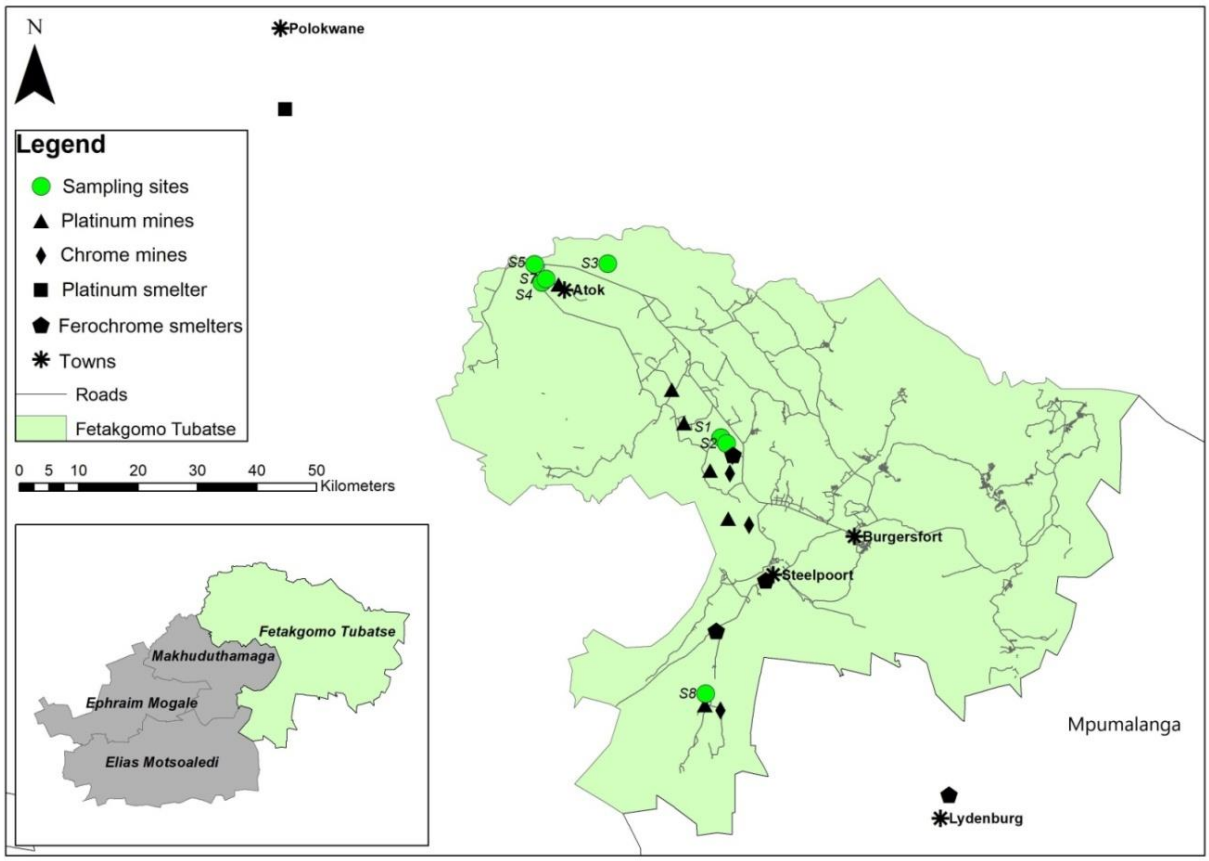

Figure 4.1. Location of sampling sites, Cr and Pt mines, ferrochrome and Pt smelters, and roads in the Fetakgomo-Tubatse municipal area in Sekhukhuneland, and surrounding areas in South Africa.

4.2.2 Air mass movement

To assess the influence of wind on foliar dust deposition, air mass movements were determined for this study by calculating back trajectories. Such back trajectories represent the movements of air parcels over space and time towards the sampling sites that contrast wind direction measured at a specific site providing local wind movement information. According to meteorological information received from Potlake Nature Reserve in Sekhukhuneland, the last significant rain, 20 mm in the rainy season of 2017/2018 was on 23 March 2018. The first spring rain during the 2018/19 rainy season was on 22 October 2018 (5.6 mm). These dates and rain volume are important since > 15 mm rain can wash the dust off the leaf surfaces (Liu *et al*., 2012). In addition, it was anticipated that there will not be significant differences in air mass movements for sites that were near one another. Therefore, to assess the possible transport of dust from sources to the sampling sites, they were grouped as Area 1 (site 3, 4, 5 and 7), Area 2 (site 1 and 2) and Area 3 (site 8), to reflect their proximity to one another. Consequently, 96-hour back trajectories arriving at a height of 100 m above ground level, for every hour during the period 1 April 2018 to 30 November 2018 for each of the three areas were modelled. The Hybrid Single-Particle Lagrangian Integrated Trajectory Model (HYSPLIT, version 4.8) was used for this purpose (Draxler & Hess,

2004). Meteorological data of the Global Data Assimilation System (GDAS) archive of the Natio nal Centre for Environmental Prediction of the United States National Weather Service was used (ftp://arlftp.arlhq.noaa.gov/pub/archives/gdas1, accessed on 12 Sept. 2020). Overlay back trajectory maps (introduced in Vakkari *et al*., 2011) were compiled for each area (1, 2 and 3) (Fig. 4.9a, b, c), to get an overview of air mass movement for the aforementioned period. Such maps give statistical representations of wind movement towards the sampling localities.

4.2.3 Sample collection

See Chapter 3, section 3.2.2 for detailed sampling strategy, leaf collection procedure and morphology of the twelve plant species investigated in this chapter.

4.2.4 Leaf SEM-EDS analysis

For detailed Scanning electron microscopy (SEM) and Energy dispersive x-ray spectroscopy (EDS) method used for plant leaves see Chapter 3, section 3.2.3.

4.2.5 Soil EDS analysis

To determine the major elements in soil samples, EDS elemental analysis was performed. This analysis was aimed to identify the possible sources of predominant soil elements including Cr. Soil samples were prepared by homogenizing the material with a porcelain pestle and mortar. Ground sample per site was then mounted on C-taped Al specimen stubs, coated with Au/Pd, and analysed at 15 kV and 10 mm working distance with an Oxford X-map 20 EDS detector and INCA software integrated into an FEI Quanta 250 FEG SEM. The most abundant elements were recorded (Cr wt% in Table 4.1). Figure 4.1 represents sample preparation and SEM-EDS analysis followed in this investigation.

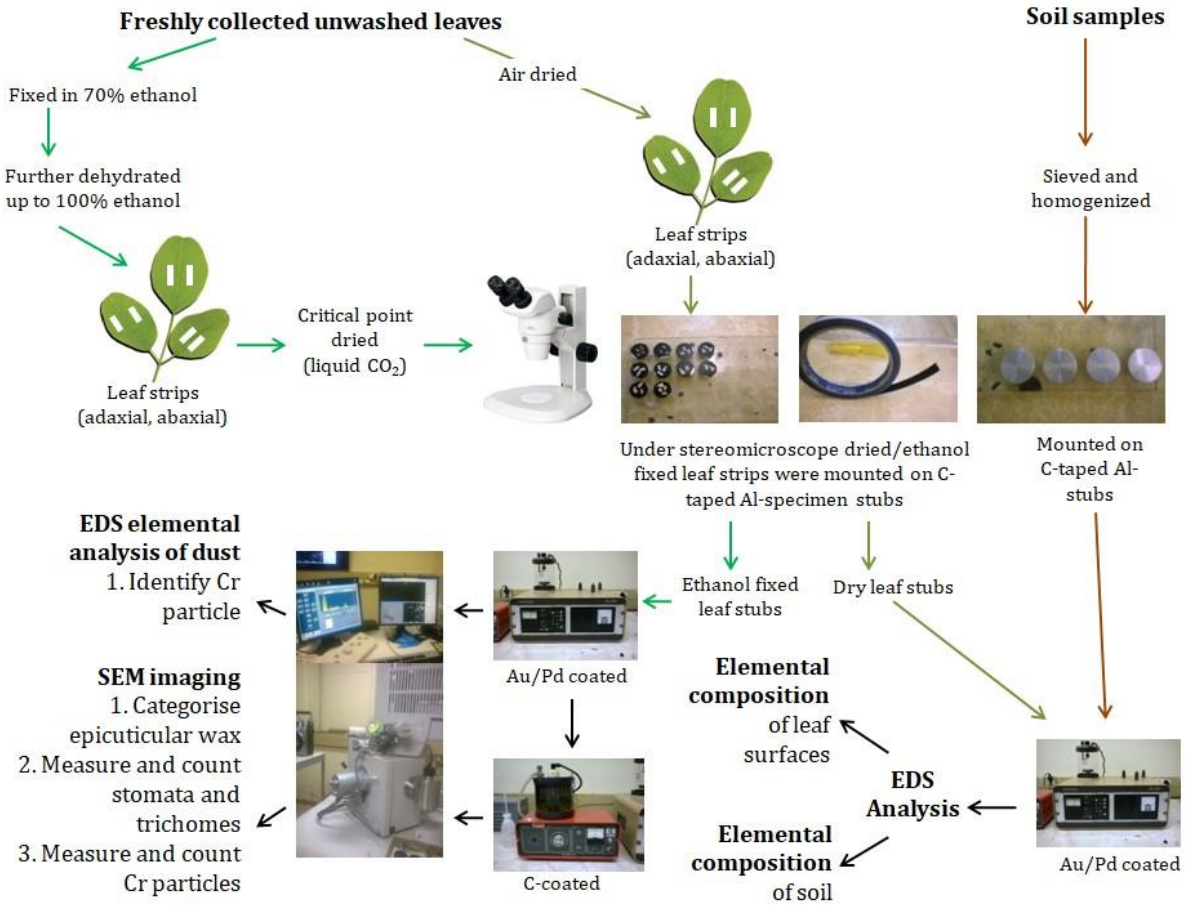

Figure 4.2. Outline of leaf and soil sample preparation and SEM-EDS analysis.

4.2.6 Plant morphology

For details see Chapter 3, sections 3.2.4.2 and 3.2.5.

4.2.7 Variables: Cr, plant and pollution

4.2.7.1 Cr

This set of variables comprised of EDS determined leaf surface Cr wt% (the highest Cr amounts detected on the adaxial and abaxial leaf surface per species) and Cr particle size (the largest among detected particles per leaf surface per species) (see Chapter 3, section 3.3.1 and 3.3.2). PM size fractions considered in the present study were fine ($PM_{2.5}$), coarse (PM_{10}) and large (PM > 10 µm).

4.2.7.2 Plant

Plant morphological traits, i.e. plant height, leaf area, leaf wax (epicuticular wax), and size (area) and density of stomata and trichomes (see Chapter 3, section 3.3.4 and 3.3.5) are selected as plant variables as these are critical features to consider in the process of determining dust adhesion and deposition on leaves. Studied plant species showed considerable variations with

respect to the above mentioned morphological features. All these traits were quantifiable, and values were treated as categorical data for statistical analyses (du Toit & Cilliers, 2010).

Epicuticular wax as a foliar surface feature was not quantified in terms of wax amount in this investigation. However, besides wax amount, higher dust holding ability is also associated with the wax structures (Dzierżanowski *et al*., 2011; Nguyen *et al*., 2015). Hence, the density of epicuticular wax crystalloid structures (wax films, plates, platelets, threads) was categorized in values ranging from 1 to 4 to represent wax structural aggregation density, where 4 represented very dense; 3, dense; 2, moderate; 1, low and 0, undetected (Table C1, Appendix C). SEM micrographs were used to identify epicuticular wax morphology and wax crystal aggregation patterns based on the classification by Barthlott *et al.* (1998) to analyse further.

4.2.7.3 Pollution

Pollution variables were incorporated to evaluate the effect of major Cr particle emitters (mines and roads), on contamination of plant leaf surfaces. As most of the study locations in the present investigation were close to more than one mine and road (Table 4.1), a combined approach based on distances and number of neighbouring Cr and Pt mines and roadways were considered and denoted as mine and road frequency, the two pollution variables. Mine and road frequency indices were constructed accordingly (Table C2, Appendix C). For the indices, five distance zones were created for mines (km): 0–3, 3–6, 6–9, 9–15, 15–20 and roads (m): 0–5, 5–15, 15–25, 45–15, 45–105. Values from 5 to 1 were assigned for nearest to most distant zone and sampling locations were scored according to the number of mines and roads within each distance zone in the site locality. In the present study, both tar and non-tar roads were considered as they all transport various mine associated materials in the study region.

Table 4.1. Sampling sites, soil Cr wt% and distance to Cr-Pt mines within 20 km radius and roadways within 110 m radius. Sites close to ferrochrome smelters are indicated as follows: ˣˣˣ< 3 km; ˣˣ< 5 km and ˣ< 13 km. LOD, below the limit of detection by EDS, 0.01 wt%.

Sites	Plant species sampled	Site description	Soil Cr (wt%)	Mine (km)	Road (m)
S1ˣˣ	Arg och, Gom fru	Tailing, Moretha	8.93	4.1, 7.4 (Cr); 10.1 (Pt)	24, 29.4
S2ˣˣˣ	Car pap, Cat ros, Psi gua, Sen ita	Home garden near S1, Moretha	4.02	2.8 (Cr); 9.8, 12.4, 16 (Pt)	13.6
S3	Cit lim, Ipo bat	Home garden, outside the Potlake Nature Reserve	0.4	17.9 (Pt)	104.1
S4	Pel afr	Near a Pt mine, Zeekoegat	<LOD	3.1 (Pt)	4.7, 44.2
S5	Tri ter	Abandoned informal Cr excavation site, Bogalatladi	18.45	7 (Pt)	4.1, 20.5
S7	Mor ole	Home garden near S4, Sefateng	<LOD	2.4 (Pt)	4.9, 23.1
S8ˣ	Ozo pan	Cr Heritage site, Dwars River Valley, Steelpoort	3.62	4.1 (Cr); 3.8 (Pt)	64.2

Arg och = *Argemone ochroleuca*; Car pap = *Carica papaya*; Cat ros = *Catharanthus roseus*; Cit lim = *Citrus limon*; Gom fru = *Gomphocarpus fruticosus*; Ipo bat = *Ipomoea batatas*; Mor ole = *Moringa oleifera*; Ozo pan = *Ozoroa paniculosa*; Pel afr = *Peltophorum africanum*; Psi gua = *Psidium guajava*; Sen ita = *Senna italica*; Tri ter = *Tribulus terrestris*.

Previous investigations noted positive influence of proximity to mines (Pöykiö *et al*., 2005) and roads (Popek *et al*., 2015; Sgrigna *et al*., 2015) on dust contamination of aerial plant parts. Hence, based on proximity, plants were categorised further in the present study. Two plant species groups were created for mine proximity, (1) leaves sampled within 3 km and (2) 3–5 km from the nearest mine (Table 4.2a). Regarding road proximity, group 1 and 2 included plant species sampled within 20 m and from 20 to 70 m, respectively, from the nearest road (Table 4.2b).

Table 4.2. Categorisation of plant species based on mine and road proximity. Plant species with detected leaf surface Cr (wt%) were considered.

a. Mine proximity (km)		**b.** Road proximity (m)	
Group 1 (0–3)	Group 2 (3–5)	Group 1 (0–20)	Group 2 (20–70)
Car pap	Arg och	Car pap	Arg och
Cat ros	Gom fru	Cat ros	Gom fru
Mor ole	Pel afr	Mor ole	Ozo pan
Psi gua	Ozo pan	Pel afr	
		Psi gua	

Arg och = *Argemone ochroleuca*; Car pap = *Carica papaya*; Cat ros = *Catharanthus roseus*; Gom fru = *Gomphocarpus fruticosus*; Mor ole = *Moringa oleifera*; Ozo pan = *Ozoroa paniculosa*; Pel afr = *Peltophorum africanum*; Psi gua = *Psidium guajava*.

4.2.8 Data analysis

EDS analysis generated data on Cr wt% on leaf surfaces and in particles, SEM micrograph observations based results on Cr particle size, PM size distribution and micromorphology (stomata and trichome), and plant morphology (plant height, leaf area) data was used for the following statistical analyses. Combinations of bi- and multivariate statistical analysis techniques were applied.

Major elements detected on plant surfaces and in soils were subjected to Pearson correlation coefficient (*r*) to determine significant correlations among elements. This analysis revealed the degree of similarity in terms of linear correlation between variables (Shi *et al*., 2008; Suzuki *et al*., 2009; Sungur, 2016). The data was further subjected to Principal Component Analysis (PCA) and Hierarchical Cluster Analysis to substantiate correlation coefficient results and identify the possible Cr sources in the above-stated matrices, i.e. leaf surfaces and soils. The combined use of correlation, PCA and cluster analysis is often applied as the data analysis process for elemental source identification (Norouzi & Khademi, 2015).

To study the interaction patterns between leaf surface and Cr pollution, correlation matrices were developed that pointed out significant relations between plant and pollution variables with Cr variables. Later, PCA and Factor Analysis (FA) were applied to determine the combined influence of variables. PCA detected key variables while retaining information of the input dataset (Shi *et al*., 2008; Gabarrón *et al*., 2018). PCA is a frequently used technique in environmental science to study metal-plant interactions (Mingorance & Olivia, 2006; Naderizadeh *et al*., 2016).

FA was selected as an extended dimension reduction process in addition to PCA as the first component in PCA after the rotation does not represent maximum variance (du Toit & Cilliers, 2010). Hence, though PCA and FA are often confused and used interchangeably, and both could be applied to recognize data subsets that are representative of the whole input data, PCA derived principal components present maximum variability of a smaller set of variables while FA explains the underlying or latent variables based on shared variance among variables and uses a correlation matrix to extract most correlated variables (du Toit & Cilliers, 2010). In the current project, FA was therefore included to complement PCA outcomes by identifying the most correlated variables concerning Cr variables, based on which leaf surface-Cr particle interaction was deduced.

Additional cluster analysis on selected leaf morphological features was used to group plant species based on dominant leaf morphological features for adaxial and abaxial leaf surface. A follow-up One-way Analysis of Variance (ANOVA) was chosen to determine any significant difference in mean values of plant variables for the plant species groups created after cluster analysis outcomes. The non-parametric Kruskal-Wallis test was selected to determine the existing significant difference between plant species categories on mine and road proximity regarding Cr wt%, Cr particle size and PM size distribution. These analyses were aimed to complement PCA and FA findings.

For PCA and FA, Correlation matrix, Varimax rotation, Kaiser normalisation and Principal Component Analysis and Principal Axis Factoring method were selected. Variables with loadings > 0.45 were considered for interpreting PCA and FA results. Hierarchical clusters were constructed using the Ward linkage method in conjunction with Euclidean distance. Dendrograms are used to represent hierarchical cluster analysis outcomes to visualize similarity-based association among variables within each cluster (Lu *et al*., 2010; Sungur, 2016). Formed clusters are presented with the letter ‘C’ with corresponding cluster number in the figures of this study. Data was standardised with z-score and tested for homogeneity. Statistical significance was considered at $p<0.05$. Statistica version 7 (FA, PCA and Pearson Correlation Coefficient) and IBM SPSS version 27 (ANOVA, Hierarchical Cluster Analysis, Kruskal-Wallis) were used to analyse the data.

4.3 Results

4.3.1 Cr source identification

4.3.1.1 Soil

For soil Cr source identification, correlation coefficient analysis determined a strong negative correlation between Cr and Ca, while Fe had a significant positive correlation with Mg and a negative association with Al and Ca. Mg had a significant negative correlation with Ca and Al (Table 4.3a). PCA showed high positive loadings for Mg and Fe with negative values for Al and Ca on PC1, confirming correlation results. PC2 gave negative values for Fe and Cr, but with a positive loading for Si. PC1 and PC2 represented 46% and 44% of the total variance, respectively, suggesting an almost equal contribution of the two components (Table 4.4a). Cluster analysis grouped Al and Ca in C1, Mg, Fe and Cr under C2, while Si formed the third cluster (Fig. 4.3). This supports the association between Mg, Fe and Cr.

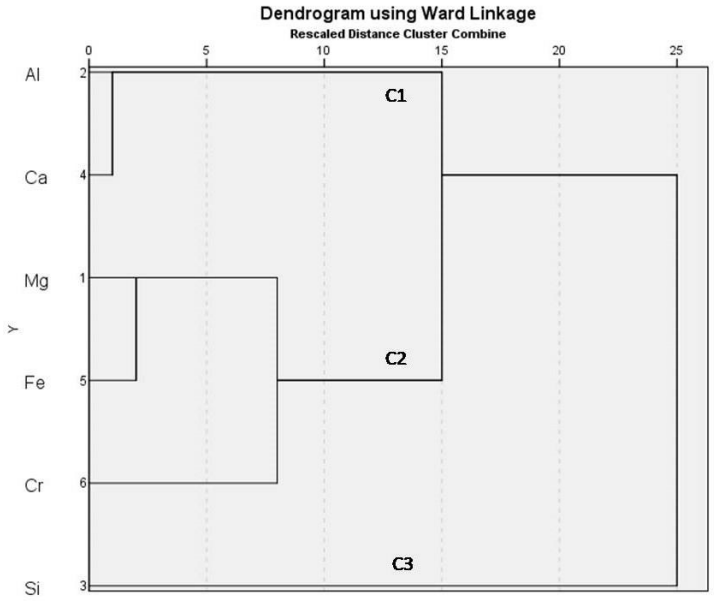

Figure 4.3. Cluster analysis dendrogram of common elements detected in soil samples by EDS elemental analysis.

Table 4.3. Pearson correlation coefficient matrices of selected elements in (a) soil and on (b) leaf surfaces. Significant correlations are in bold. Superscripts: Ad, adaxial; Ab, abaxial values. Significance,* = p<0.05; ** = p<0.01; *** = p<0.001.

a. Soil

	Cr	Fe	Mg	Al	Si
Fe	0.641				
Mg	0.5429	**0.9104****			
Al	–0.5888	**–0.7945***	**–0.9308****		
Si	–0.6768	0.0594	0.1617	0.0738	
Ca	**–0.7406***	**–0.9134****	**–0.7120***	0.6783	0.2486

b. Leaf surfaces

	Cr	Fe	Mg	Al	Si	Ca
Fe	**0.9847^{ad}*****					
	0.8527^{ab}**					
Mg	**0.8011^{ad}***	**0.8139^{ad}***				
	–0.0328^{ab}	0.0198^{ab}				
Al	**0.7881^{ad}****	**0.8573^{ad}****	0.6785^{ad}			
	0.8012^{ab}*	0.6864^{ab}	–0.0260^{ab}			
Si	**0.9867^{ad}*****	**0.9939^{ad}*****	**0.8405^{ad}****	**0.8677^{ad}****		
	0.8535^{ab}**	**0.7225^{ab}***	0.1112^{ab}	**0.8486^{ab}****		
Ca	0.1699^{ad}	–0.0923^{ad}	0.3205^{ad}	0.1057^{ad}	-0.07260^{ad}	
	0.0334^{ab}	–0.2952^{ab}	0.6999^{ab}	0.0794^{ab}	0.1478^{ab}	
K	0.4202^{ad}	0.4755^{ad}	0.4803^{ad}	0.4356^{ad}	0.4420^{ad}	0.5990^{ad}
	–0.3533^{ab}	–0.4097^{ab}	0.6010^{ab}	–0.6647^{ab}	–0.2976^{ab}	0.5254^{ab}

Table 4.4. Varimax rotated PCA results on elemental compositions of soil (a) and (b) leaf surfaces. Loadings > 0.45 are in bold. Ad, adaxial; Ab, abaxial. For soil samples, K was not detected as a common element in soil samples.

Elements	**a**. Soil		**b**. Leaf surface			
			Ad		Ab	
	PC1	PC2	PC1	PC2	PC1	PC2
Al	**–0.938**	0.103	**0.866**	0.180	**0.932**	–0.096
Cr	0.145	**–0.962**	**0.987**	–0.023	**0.940**	–0.017
Fe	**0.620**	**–0.723**	**0.994**	0.054	**0.860**	–0.172
Mg	**0.968**	0.201	**0.816**	0.376	0.066	**0.903**
Si	0.267	**0.901**	**0.998**	0.055	**0.933**	0.122
Ca	**–0.690**	**0.589**	–0.128	**0.963**	0.052	**0.895**
K	-	-	0.404	**0.789**	–0.471	**0.754**
Eigenvalue	2.768	2.657	4.554	1.729	3.591	2.239
Cumulative %	46.130	90.416	65.057	89.764	51.294	83.275

4.3.1.2 Leaf surfaces

Common elements with the highest wt% determined on the adaxial leaf surface indicated a strong correlation between Cr and Fe, while both were positively correlated with Mg, Al and Si (Table 4.3b). A follow-up PCA (Table 4.4b) substantiated correlation findings and recognised the same five elements (Cr, Fe, Mg, Al, Si) with high loadings on PC1 that represented 65% of the variance. Ca and K had greater loadings on PC2 that contributed only 25% of the total variance. Dendrograms corroborated PCA outcomes for adaxial leaf surface by constructing two clusters on the same set of elements (Fig. 4.4a). For the abaxial surface, correlations detected a significant positive relation between Cr and Fe, Al and Si, while a negative correlation was determined with Mg (Table 4.3b). Corresponding PCA had the highest loadings for Cr, Fe, Al and Si on PC1 which contributed 51% of the variance. PC2 had higher loadings for Mg, Ca and K that represented 32% of the total variance (Table 4.4b). Cluster analysis was in accord with PCA findings and formed two clusters with Cr, Fe, Al and Si under C1 while Mg, Ca and K in the other cluster (Fig. 4.4b).

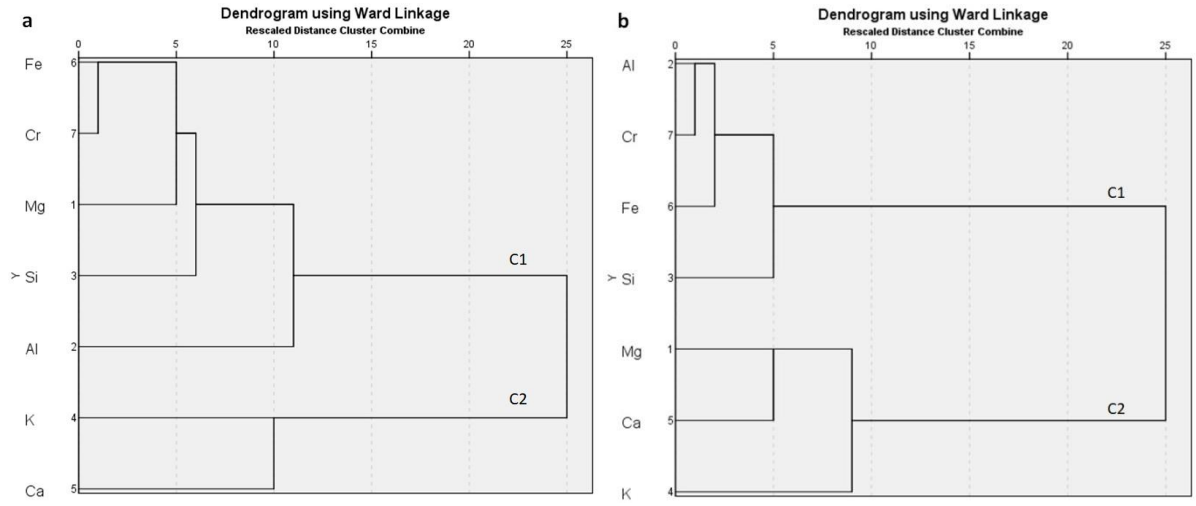

Figure 4.4. Cluster analysis dendrograms of selected elements detected on leaf surfaces. a. Adaxial; b. abaxial.

4.3.2 Leaf surface-Cr particle interaction

4.3.2.1 Pearson Correlation Coefficient Analysis

For the adaxial surface, the cross-correlation matrix showed a strong positive correlation between leaf area and both Cr wt% (r = 0.9870***) and Cr particle size (r = 0.8692***) (Table 4.5). On the contrary, for the abaxial leaf surface, no significant correlations were determined for Cr wt%, but Cr dust size was positively correlated with plant height (r = 0.6937*) and leaf area (r = 0.6837*) (Table 4.5). For the adaxial surface, a significant positive correlation was determined between leaf area and coarse (PM_{10}) fraction (r = 0.6204*), while stomata size and the fine fraction ($PM_{2.5}$) (r = –0.6696*) had a significant negative correlation on the abaxial surface (Table 4.5).

Table 4.5. Pearson correlation coefficient matrices of plant and pollution variables with Cr variables (Cr wt%, CrD) and PM size fractions. Significant values are in bold. Ad, adaxial; Ab, abaxial; Cr wt%, Cr amount; CrD, Cr particle size. Significance, * = p<0.05; ** = p<0.01; *** = p<0.001.

Variables	Cr wt%	CrD	PM size fractions		
			Fine ($PM_{2.5}$)	Coarse (PM_{10})	Large (> 10 µm)
Ad					
Mine frequency (MF)	0.2987	0.3590	0.0021	0.0366	–0.1447
Road frequency (RF)	–0.431	0.1036	–0.2318	0.1924	0.1468
Plant height (PH)	0.3103	0.3646	–0.0470	–0.0410	0.3291
Leaf area (LA)	**0.9870*** **	**0.8692*** **	–0.4662	**0.6204***	–0.1869
Epicuticular wax (EW)	0.3903	0.4084	–0.4521	0.5229	–0.2657
Stomata size (SS)	–0.2404	–0.4042	0.1386	–0.1394	0.0034
Stomata density (SD)	–0.2808	–0.4634	0.0001	–0.0288	0.1078
Trichome size (TS)	–0.2971	–0.1172	0.2283	–0.3438	0.4324
Trichome density (TD)	–0.3155	0.0595	–0.1358	0.0603	0.2824
Ab					
Mine frequency (MF)	0.2291	0.3195	–0.1667	0.3583	–0.2691
Road frequency (RF)	0.5459	0.1013	–0.3067	0.1591	0.2858
Plant height (PH)	0.2271	**0.6937***	0.4305	–0.4431	–0.0580
Leaf area (LA)	–0.2652	**0.6837***	–0.1746	0.3769	–0.2844
Epicuticular wax (EW)	0.5404	0.4184	–0.3407	0.5006	–0.1883
Stomata size (SS)	0.5373	–0.1471	**–0.6696***	0.5153	0.3617
Stomata density (SD)	0.1008	0.4075	0.0011	–0.0580	0.0886
Trichome size (TS)	0.0206	–0.1929	–0.1101	–0.1150	0.3716
Trichome density (TD)	–0.2390	0.1736	0.5295	–0.5055	–0.1330

PM, particulate matter is a mix of particles of heterogeneous origin, size and chemical composition and is primarily defined by size (Grantz *et al*., 2003).

Various significant positive correlations were detected for elements and PM size fractions (Table 4.6). Of specific importance for this study was that Cr wt% on the adaxial leaf surface was positively correlated with coarse PM fraction (PM_{10}) (r = 0.7191*).

Table 4.6. Pearson correlation coefficient matrices of selected leaf surface elements with PM size fractions. Significant values are in bold. Ad, adaxial; Ab abaxial. Significance, * = p<0.05; ** = p<0.01; *** = p<0.001.

Variables	Fine ($PM_{2.5}$)	Coarse (PM_{10})	Large (> 10 µm)
Ad			
Cr	–0.6506	**0.7191***	–0.5286
Fe	–0.6036	0.6887	–0.6014
Mg	**–0.8649****	**0.9153****	–0.4939
Al	–0.3166	0.4178	–0.6056
Si	–0.6294	0.**7081***	–0.5756
Ca	–0.2737	0.3268	–0.3471
K	–0.4263	0.5441	**–0.7210***
Ab			
Cr	–0.1171	–0.1185	0.3956
Fe	0.1964	–0.2836	0.0323
Mg	–0.3141	0.6144	–0.2839
Al	–0.3220	–0.0497	0.6895
Si	–0.3020	0.0579	0.4958
Ca	**–0.7578***	**0.8045***	0.2929
K	–0.1280	0.5377	–0.5304

Correlation matrices of common elements (i.e. Cr, Fe, Mg, Al, Si Ca) determined on the leaf surface (adaxial, abaxial) and soil did not produce any significant correlation (Table C3, Appendix C).

4.3.2.2 Principal Component Analysis

PCA on standardised data produced four principal components for both adaxial and abaxial leaf surface that had eigenvalues > 1 (Table 4.7a). For the adaxial surface, the first component (PC1) had the highest loadings for Cr wt% and leaf area (Fig. 4.5a). PC3 had the second-highest positive Cr wt%, epicuticular wax and mine frequency loadings with a negative loading for stomata density. PC 1 and PC3 contributed 22.6 and 19.3% of the total variance, respectively. Regarding Cr particles, PC2 had the highest positive loadings for Cr size and leaf area, and a negative stomata size loading (Fig. 4.5c). PC3 had the second-highest Cr particle size loading and the same group of variables as for Cr wt%. Around 21.9 and 19.3% of the total variance was contributed by PC2 and PC3, respectively. These variables with high loadings represented most of the variability of the input data on the corresponding component.

Table 4.7. Varimax rotated PCA results on selected variables. Loadings > 0.45 are in bold. Ad, adaxial; Ab, abaxial.

Variables	**a.** Ad				**b.** Ab			
	PC1	PC2	PC3	PC4	PC1	PC2	PC3	PC4
Cr weight % (CrWt)	**0.952**	0.140	0.231	–0.047	**0.618**	–0.022	**0.581**	–0.140
Mine frequency (MF)	0.114	–0.87	**0.739**	0.212	**0.713**	0.110	0.085	0.039
Road frequency (RF)	0.065	–0.158	–0.020	**0.937**	0.169	–0.118	**0.926**	–0.052
Plant height (PH)	0.166	**0.860**	0.046	0.136	0.145	**0.926**	0.127	0.132
Leaf area (LA)	**0.956**	0.163	0.175	–0.068	0.100	0.231	–0.037	**0.824**
Epicuticular wax (EW)	0.247	–0.049	**0.873**	–0.086	**0.891**	**–**0.091	0.142	0.257
Stomata size (SS)	–0.241	**–0.702**	0.075	0.176	**0.634**	**–0.558**	0.206	0.235
Stomata density (SD)	–0.021	**–0.614**	**–0.654**	0.324	–0.012	–0.238	–0.130	**0.699**
Trichome size (TS)	–0.357	**0.650**	–0.263	**0.453**	**–0.578**	0.045	**0.701**	–0.335
Trichome density (TD)	**–**0.387	0.386	0.192	**0.705**	–0.161	**0.860**	–0.303	–0.336
Eigenvalue	2.262	2.261	1.932	1.794	2.502	2.053	1.893	1.470
Cumulative %	22.617	45.225	64.547	82.484	25.022	45.558	64.485	79.189
Cr dust size (CrD)	0.215	**0.873**	0.329	0.112	0.264	0.364	**0.869**	0.070
Mine frequency (MF)	–0.050	0.044	**0.793**	0.173	**0.761**	0.134	0.097	–0.069
Road frequency (RF)	–0.126	0.089	–0.031	**0.954**	0.241	–0.162	0.029	**0.919**
Plant height (PH)	**0.843**	0.210	0.052	0.042	0.049	**0.834**	0.406	0.078
Leaf area (LA)	0.002	**0.946**	0.155	–0.101	0.141	0.078	**0.785**	–0.017
Epicuticular wax (EW)	–0.094	0.297	**0.830**	–0.085	**0.866**	–0.162	0.306	0.036
Stomata size (SS)	**–0.606**	**–0.472**	0.162	0.178	**0.667**	**–0.493**	–0.243	0.154

Stomata density (SD)	**–0.591**	–0.184	**–0.617**	0.349	–0.173	–0.424	**0.676**	–0.323
Trichome size (TS)	**0.740**	–0.316	–0.226	0.391	**–0.492**	0.043	–0.154	**0.787**
Trichome density (TD)	**0.472**	–0.201	0.160	**0.720**	–0.175	**0.933**	–0.145	–0.217
Eigenvalue	2.270	2.195	1.936	1.798	2.227	2.201	2.200	1.658
Cumulative %	22.699	44.651	64.014	81.995	22.272	44.278	66.273	82.849

Regarding the abaxial surface, PCA showed high positive loadings for Cr wt%, epicuticular wax, mine frequency, stomata size and a negative value for trichome size on PC1 (Fig. 4.5b). PC3 had the second highest positive loading for Cr wt% and high values for road frequency and trichome size. The variable contributions of the two components were around 25% and 20.5%, respectively (Table 4.7b). Regarding Cr particle size, the result was complex as PC3 had the highest loading for Cr particle size along with leaf area, stomata density and plant height (Fig. 4.5d) with almost equal (22%) variable contribution as PC2 (22.2%) and PC1 (22%) that had the second and third highest loading for Cr particle size, respectively (Table 4.7). Figure 7 illustrates the first three components for both the leaf surfaces in a three-dimensional space.

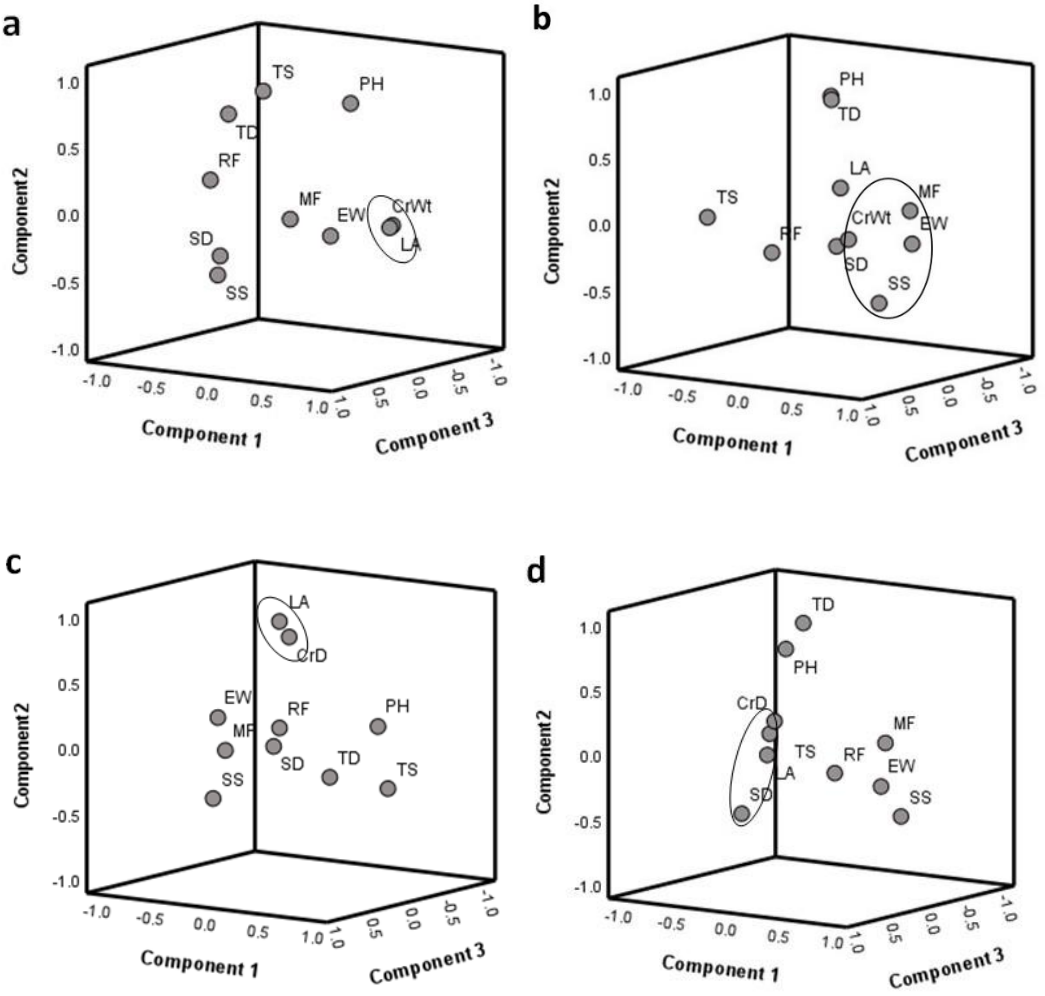

Figure 4.5. Rotated PCA component plots of plant and pollution variables. Cr wt% represented as CrWt, a. adaxial; b. abaxial; and Cr particle size, represented as CrD, c. adaxial; d. abaxial. Variables with maximum variability contributions are encircled. MF, mine frequency; RF, road frequency; PH, plant height; LA, leaf area; EW, epicuticular wax; SS, stomata size; SD, stomata density; TS, trichome size; TD, trichome density.

4.3.2.3 Factor Analysis

The same standardised data used for PCA was used in FA. Each factor summarised the most correlated variables concerning Cr wt% and Cr particle size. Factors highlighted a different set of correlated variables for adaxial and abaxial leaf surfaces (Table 4.8). FA results for adaxial leaf surfaces were consistent by providing the same set of variables with the highest loadings under both the factors for Cr wt% and Cr particle size. F1 had both Cr wt% and Cr particle size positively correlated with leaf area, epicuticular wax and plant height, but had a negative correlation with stomata density. In the second factor (F2), plant height and trichome features (size and density) were negatively correlated to both Cr variables (wt% and size). Trichome size had a loading > 0.9 for both Cr variables on F2 that indicated this variable to be considered as a pure measure of the factor (du Toit & Cilliers, 2010) (Table 4.8).

For the abaxial surface, FA extracted different sets of variables correlated with Cr wt% and Cr particle size (Table 4.8). On F1, Cr wt% was positively correlated with stomata size, road frequency, epicuticular wax and negatively with trichome density. F2 showed a negative correlation with trichome size and a positive relation with epicuticular wax and mine frequency. Regarding Cr particle size, F1 extracted epicuticular wax as the most correlated variable followed by leaf area, mine frequency and stomata size. Under F2, Cr particle size was negatively correlated with stomata size and epicuticular wax, but positively with trichome density and plant height. Epicuticular wax appeared in both factors for Cr wt% and particle size on this leaf surface. Similarly, stomata size had > 0.45 loading values on both factors for Cr particle size. Such a scenario is recognised as ‘factorially complex’ meaning the variable can be moderately predictable under each factor (du Toit & Cilliers, 2010). Based on the low loadings of Cr variables on the second factor, values of the above mentioned variables were considered and interpreted for the first factor only.

Table 4.8. Varimax rotated FA matrix on, a. Cr wt% and b. Cr particle size. Loadings > 0.45 are in bold. Ad, adaxial; Ab, abaxial.

a.	Ad		Ab		**b.**	Ad		Ab	
	Factor 1	Factor 2	Factor 1	Factor 2		Factor 1	Factor 2	Factor 1	Factor 2
Cr wt%	**0.874**	–0.215	**0.652**	0.071	Cr particle size (CrD)	**0.890**	0.004	**0.915**	–0.367
Mine frequency	0.298	–0.028	0.256	**0.458**	Mine frequency	0.333	0.056	**0.461**	0.184
Road frequency	–0.172	0.196	**0.705**	–0.372	Road frequency	–0.102	–0.235	0.055	0.311
Plant height	**0.485**	**0.696**	–0.243	0.120	Plant height	**0.477**	**–0.607**	0.433	**–0.687**
Leaf area	**0.848**	–0.208	–0.098	0.342	Leaf area	**0.751**	0.231	**0.571**	–0.136
Epicuticular wax	**0.515**	–0.196	**0.659**	**0.712**	Epicuticular wax	**0.556**	0.290	**0.757**	**0.507**
Stomata size	–0.382	–0.300	**0.738**	0.171	Stomata size	–0.429	0.253	**0.450**	**0.734**
Stomata density	**–0.584**	–0.238	–0.003	0.251	Stomata density	**–0.666**	0.131	0.277	0.034
Trichome size	–0.190	**0.916**	0.109	**–0.839**	Trichome size	–0.127	**–0.996**	–0.389	–0.084
Trichome density	–0.135	**0.598**	**–0.598**	–0.036	Trichome density	–0.021	**–0.575**	–0.056	**–0.802**
Eigenvalue	2.645	1.996	2.404	1.753	Eigenvalue	2.664	1.972	2.400	2.202
Cumulative %	26.449	46.405	24.040	41.571	Cumulative %	26.641	46.367	24.006	46.027

4.3.2.4 Additional analyses

Dendrograms of input variables on dominant leaf traits of the adaxial and abaxial leaf surfaces illustrated plant species grouping. The two clusters for the adaxial surface portrayed mostly the absence of trichomes (C1), except for the two species, *S. italica* and *T. terrestris* that had trichomes, and C2 that presented species with trichomes (Fig. 4.6a). Clusters for abaxial surfaces showed much heterogeneity regarding dominant surface features (Fig. 4.6b). C1 grouped species with moderate to very dense epicuticular wax, large stomata, and moderate stomata density; species under C2 primarily featured low to very dense epicuticular wax, medium-sized stomata, and high stomata density; while C3 grouped only two species, namely *T. terrestris* which had no distinct epicuticular wax structure and low frequency of small stomata and *O. paniculosa* which had low wax density with stomata not observed.

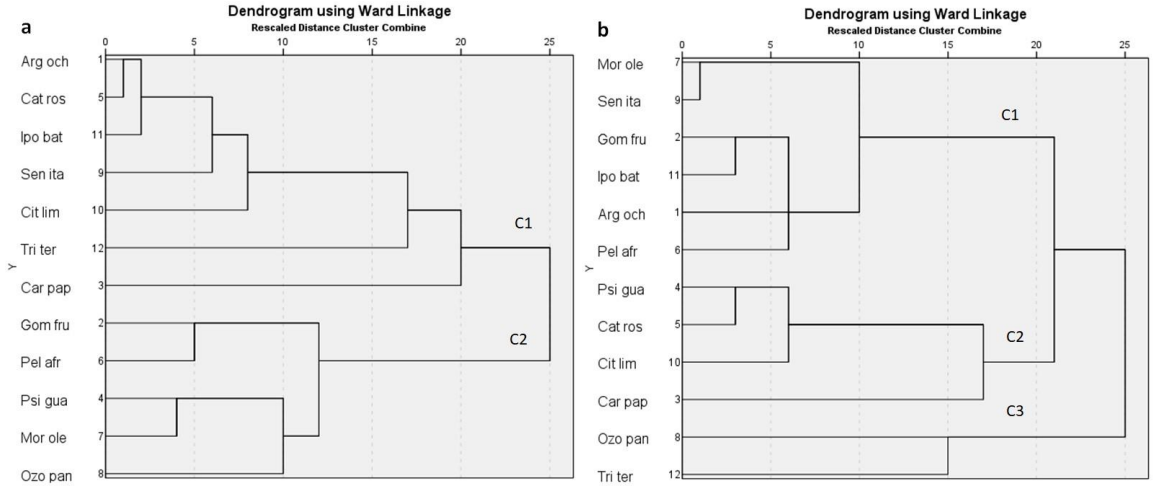

Figure 4.6. Dendrograms of plant species clusters based on leaf traits. a. Adaxial; b. abaxial. As leaf trait data included measurements on different scales it was standardized with z-score before the analysis.

ANOVA on species groups (Table 4.9a) formed after the cluster analysis results (Figure 4.6) indicated significant differences for certain variables. For the adaxial surface, a significant difference in the mean values was determined for both trichome size and density (p<0.001) (Table C4, Appendix C). For the abaxial leaf surface, results showed significant differences among the three plant species groups (Table 4.9b) for epicuticular wax (p<0.05), stomata size (p<0.05) and stomata density (p<0.01). Tukey's Unequal HSD (Honestly Significant Difference) tests yielded no further statistical significance for stomata size, but a difference was confirmed between group 1 and 3 for epicuticular wax (p<0.05) (Fig. 4.7a) (Table C5, Appendix C) and between group 1 and 2 (p<0.01) and 2 and 3 (p<0.01) for stomata density (Fig. 4.7b) (Table C5, Appendix C).

Table 4.9. Plant species groups based on dominant a. adaxial and b. abaxial leaf features. Ad, adaxial; Ab, abaxial.

a. Ad (presence/absence of trichomes)		**b**. Ab (stomata density, mm^{-2})		
Group 1 (mostly glabrous)	Group 1 (pubescent)	Group 1 (6–45)	Group 2 (68–146)	Group 3 (0–13)
Arg och, Car pap	Gom fru, Mor ole	Arg och, Gom fru	Car pap, Cat ros	Ozo pan
Cat ros, Cit lim	Ozo pan, Pel afr	Ipo bat, Mor ole	Cit lim, Psi gua	Tri ter
Ipo bat, Sen ita	Psi gua	Pel afr, Sen ita		
Tri ter				

Arg och = *Argemone ochroleuca*; Car pap = *Carica papaya*; Cat ros = *Catharanthus roseus*; Cit lim = *Citrus limon*; Gom fru = *Gomphocarpus fruticosus*; Ipo bat = *Ipomoea batatas*; Mor ole = *Moringa oleifera*; Ozo pan = *Ozoro apaniculosa*; Pel afr = *Peltophorum africanum*; Psi gua = *Psidium guajava*; Sen ita = *Senna italica*; Tri ter = *Tribulus terrestris*.

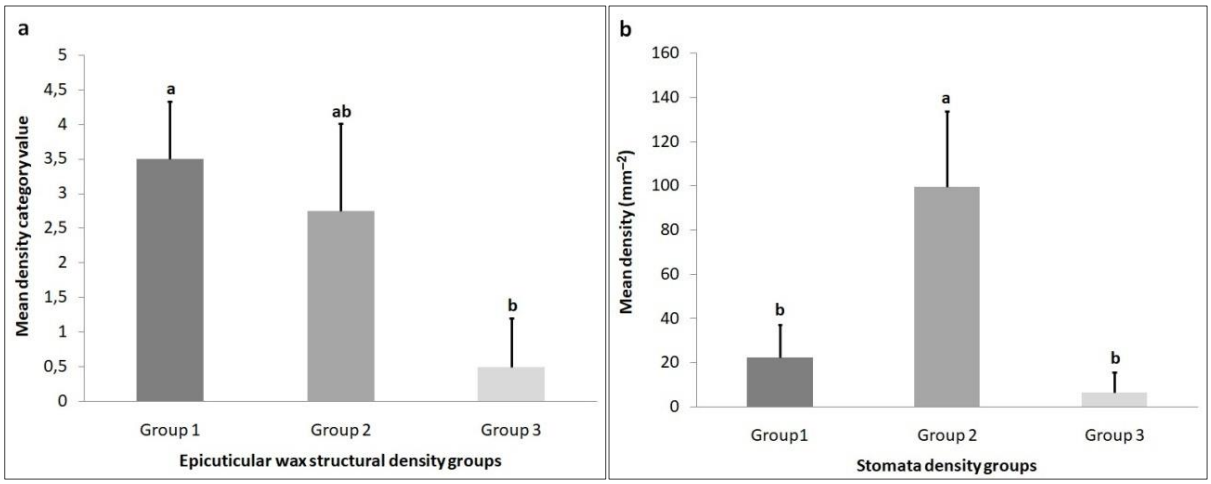

Figure 4.7. Significant difference in mean values for plant groups regarding abaxial leaf traits. a. Epicuticular wax density groups; b. stomata density groups; different letters indicate significant difference (p<0.05).

Kruskal-Wallis results showed no significant difference regarding plant groups on road proximity, but a significant difference was observed between the two plant groups on mine proximity regarding Cr particle size. Group 1 (species sampled < 3 km from the nearest mine) had significantly larger Cr particles on the adaxial surface than group 2 (species sampled 3–5 km from the nearest mine) (p<0.05) (Fig. 4.8) (Table C6, Appendix C).

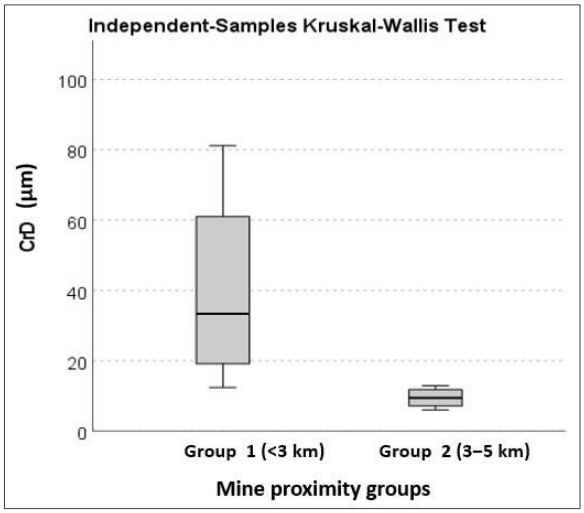

Figure 4.8. Significant difference between mine proximity groups regarding adaxial Cr particle size. Whiskers represent the largest and smallest values. Significant difference at p<0.05. CrD, Cr particle size (µm).

4.3.3 Air mass movement patterns

As is evident from the air mass history for Area 1, presented in Figure 4.9a, dust generated in relative proximity around 20–25 km (indicated by the darker red zone in Figure 4.9a), in all directions of the sampling area, likely contributed to dust deposited on the leaves. The R37 and a Pt mine lie within this specific air mass fetch region. In addition, dust generated in a larger zone between northeast and southeast, as well as a smaller zone between southwest and west (both indicated by the less intense red colour in Figure 4.9a) from the sampling area likely also contributed to dust. However, no mines, smelters and roads that are used to transport ore, occur in this fetch region. Therefore, the dust originating from there could be of natural, farming or grazing origin. Sources occurring in the fetch region over which lower air mass overpass frequencies occurred, i.e. indicated with yellow and green, are unlikely to have considerable contribution towards the dust deposited on the plant leaves at sampling sites of Area 1.

The air mass histories for Area 2 and 3 (Figs. 4.9b and 4.9c) indicated similar patterns to that observed for Area 1 (Fig. 4.9a), i.e. relatively local (approximately 20–25 km, indicated by the darker red areas in the figures) contributions to dust deposited on the leaves and regional contribution from the large fetch region between northeast and southeast of the sites. However, from north to south in the mapped area, the contribution of the most prominent fetch region (indicated by darker red) between northeast and southeast of the sites weaken. Therefore, four platinum mines, two chrome mines, one ferrochrome smelter and the R37 likely make local contributions to dust deposited on Area 2. Similarly, one Pt mine, one Cr mine, one ferrochrome smelter and the R555 contributed at Area 3. Other sources are located within the fetch regions

with lower overpass frequencies (i.e. indicated by the less intense red colour) that may contribute as well.

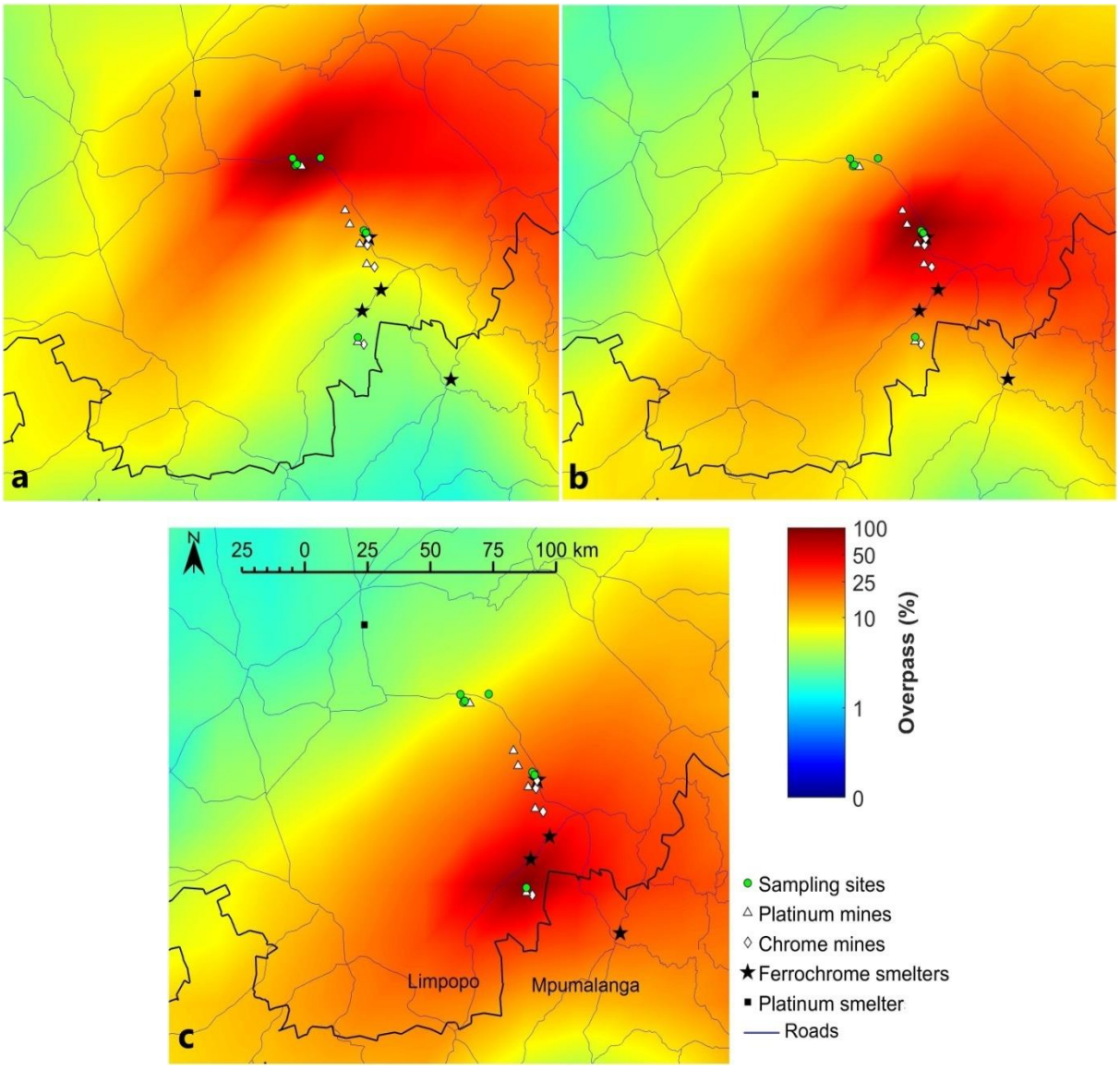

Figure 4.9. Overlay back trajectory maps calculated over the period 1 April 2018 to 30 November 2018 for sampling sites. a. Area 1 (sampling site 3, 4, 5 and 7); b Area 2 (sampling site 1 and 2); c. Area 3 (sampling site 8), according to the method developed by Vakkari *et al*. (2011). The colour code indicates the percentage of the trajectories passing over 0.2° x 0.2° grid cells that were superimposed on the map area of interest. The colours red and blue indicate the highest and lowest percentage overpasses, respectively.

4.4 Discussion

4.4.1 Pollution sources

4.4.1.1 Soil

Source identification analysis for soil highlighted shared contributions of Cr, Fe and Mg from the ultramafic soils of Sekhukhuneland that are a generous source of these elements (Siebert *et al*., 2002) and anthropogenic activities (e.g. chromite ore used in mining, smelting or its transport). Chromite ore contains Cr_2O_3, Fe_2O_3 and FeO as the primary components with a heterogeneous mix of SiO_2, Al_2O_3, CaO and MgO (Gu & Wills, 1988; Coetzee *et al*., 2018; Sweeten *et al*., 2018; Tshehla & Djolov, 2018). Slag and dust produced by the ferrochrome smelter might also be enriched with SiO_2, Al_2O_3 and MgO with a mixture of Cr and Fe oxides (Coetzee *et al*., 2018; Tshehla & Djolov, 2018). Al and Ca could have a lithological or geological origin, but not from chromite, based on the negative association between Cr, Fe and Mg with Al and Ca. Si could be sourced from the soil, crustal or road dust and silicone mine in the region close to sampling site 8 (Tshehla & Djolov, 2018; Tshehla & Wright, 2019a).

Disentangling pollution sources is challenging in urban and mine impacted soil systems (Oliva & Espinosa, 2007; Shi *et al*., 2008; Gabarrón *et al*., 2018). In densely settled areas around mines in Sekhuhuneland that is developing rapidly with increasing Cr pollution from multiple anthropogenic sources, such complexity in soil elemental composition can be expected. Furthermore, the possibility of substitution of Fe in chromite by Mg or Ca and Cr by Fe or Al to form intermediates (Gu & Wills, 1988) could add elemental complexity to geogenic dust. Heterogeneity in soil Cr results, therefore, urges detailed future investigations and continuous soil contamination monitoring at a local and regional scale.

4.4.1.2 Leaf surfaces

In the present study, regarding the major elements (i.e. Cr, Fe, Mg, Al, Si and Ca) detected on leaf surfaces, atmospheric particles could be the major contributor compared to soil dust. Hence, a common or shared origin may be predicted for these elements most probably from chromite sourced from mining, transport or smelting operations. The association of Cr with Si could be a result of dust generated from ferrochrome smelter slag that contains Si (Coetzee *et al*., 2018; Tshehla & Djolov, 2018) or chromite could have SiO_2 in the ore (Gu & Wills, 1988; Coetzee *et al*., 2018; Tshehla & Djolov, 2018). For other elements, Ca and K, geology could be concluded as the main source and specifically Mg on the abaxial side as a prominent component of the serpentine mineralogy of the region (Siebert *et al*., 2002). A study by Tang and Han (2015) reported higher elemental concentrations in atmospheric particles than topsoil dust from polluted urban localities. This may further suggest a greater possibility of elemental contamination of leaves by aerial PM

than soil dust in the study region. A similar SEM-based dust deposition analysis study by Gajbhiye *et al.* (2016) suggested airborne Pb and Cd as the major source on leaf surfaces sampled from industrial areas. Obtained results suggested heterogeneous anthropogenic origin for most of the detected elements on leaf surfaces due to the accumulation of particles from varied sources over time (Yang *et al*., 2016).

For both soils and plant leaf surfaces, a significant positive association of Cr-Fe, indicated chrome mines and ferrochrome smelters as prime sources of deposited Cr particles as both these elements are the major constituents of chromite ore (Gu & Wills, 1988; Tshehla & Djolov, 2018) and smelter dust (Beukes *et al*., 2010; Coetzee *et al.*, 2018). The generated air mass movement patterns further supported the findings by indicating Cr and Pt mines, ferrochrome smelters and roads within < 25 km periphery around the sampling sites as primary dust contributors. Determined complexity in the elemental composition of plant leaf surfaces and soil in the present study could be explained with the recent findings by Tshehla and Wright (2019a) that reported notable spatial variability regarding chemical composition and size distribution of Cr and Fe-Cr enriched PM in the regional air mass over Sekhukhuneland.

4.4.2 Dust pollution

4.4.2.1 Plant traits

The variable that showed maximum influence on Cr contamination of leaf surfaces was leaf area (as determined in Chapter 3). This trait had a significant positive influence on Cr contamination of leaf surfaces. Previous reports suggested plants with bigger leaves as better options for air pollution mitigation (Mo *et al.*, 2015; Nguyen *et al*., 2015; Shi *et al*., 2016). Larger leaves, therefore, present bigger available areas (Leonard *et al.*, 2016) for Cr dust deposition.

Among foliar micromorphological traits, dense wax structures enhanced Cr particle adhesion on leaf surfaces of investigated species in the present study. Nguyen *et al.* (2015) noted that wax structures on large leaves hold dust better compared to smooth ones. Dzierżanowski *et al.* (2011) suggested that particle size in leaf wax differ among species primarily depending on species specific details such as wax chemistry and structure that could have influenced Cr particle contamination in Sekhukhuneland.

Other traits such as trichomes and stomata features, and plant height showed different effects on Cr particle adhesion on either side of the leaf. For example, the presence of longer trichomes could have restricted Cr contamination on the adaxial surface that is consistent with results from past studies stating hairy leaves as inefficient dust collectors (Perini *et al*., 2017). For the adaxial surface, glabrous/pubescence was also observed as the most significant characters to

differentiate plant species. Longer trichomes could have a similar limiting effect on the abaxial surface that matched with findings by Ram *et al.* (2012) that implicated such foliar character for low traffic dust amounts on the abaxial leaf surfaces of *Polyalthia longifolia*. On the contrary, dense trichomes favoured holding of larger Cr particles on the abaxial leaf surfaces in the present study as similarly reported in literature (El-Khatib *et al*., 2011), probably because pubescence prevents re-emission of dust (Leonard *et al.*, 2016) that could be particularly important for the abaxial leaf surfaces facing down.

Densely distributed stomata on the adaxial surface could be unfavourable for Cr dust adhesion in terms of both Cr wt% and Cr particle size. This contradicted past findings that established a positive correlation between foliar dust accumulation and stomata density on abaxial leaf surface (Liang *et al*., 2016; Zha *et al.*, 2019). For the present study, absence of adaxial stomata in half of the investigated species that possess other dust adhesion favouring traits such as larger leaf area and dense wax structures might influence the overall Cr contamination process. Such effects have been reported previously, for example, Leonard *et al.* (2016) reported that leaves with wax increased surface hydrophobicity and consequently limited dust deposition on leaves with trichomes even though trichomes may hold more dust. Higher stomata density and larger stomata on the adaxial and abaxial surface, respectively, enhanced deposition of smaller Cr particles. Likewise, Mo *et al*. (2015) and Zha *et al.* (2019) suggested such stomata features to create a moisture enriched foliar environment that generally favours deposition of smaller particles especially the hygroscopic $PM_{2.5}$. For the studied species, besides epicuticular wax, stomata density was found as a major abaxial leaf surface trait to differentiate plant species.

Regarding plant height, taller species showed higher Cr dust contamination possibility in terms of Cr amount and adhesion of larger Cr particles on the adaxial leaf surfaces. The same was observed for the abaxial surface regarding the size of the Cr particles as indicated by Mo *et al.* (2015) stating a greater adhesion possibility of large PM on the abaxial leaf surface. Plant tallness is critical to create air turbulence leading to higher deposition of PM especially on tree leaves (Tallis *et al*., 2011; Ram *et al.*, 2012). In addition, plant height determines the dominance of airborne or soil dust exposure to plant leaves (Mo *et al.*, 2015). Tallness hence increased exposure possibility of airborne Cr dust to plant leaves in the present study which was expected considering high atmospheric Cr pollution in Sekhukhuneland (Tshehla & Djolov, 2018; Tshehla & Wright, 2019a).

4.4.2.2 Pollution

An enhancing effect of road frequency (combining road proximity and number) on the abaxial Cr wt% can be explained by the high probability of deposition of re-suspended road dust particularly

spilled Cr ore during transportation in the region (Tshehla & Djolov, 2018). Overlay back trajectory maps for the study region also indicated the two main roads as primary dust sources for the sampling sites. Pöykiö *et al.* (2005) and Tian *et al.* (2019) suggested transportation routes in mining regions as noteworthy pollution sources of Cr and Rare Earth Elements, respectively.

Mine frequency also increased foliar Cr wt% and particle size on the abaxial leaf surface. In other words, several mines in close vicinity to sampling sites presented a higher probability of vegetation being contaminated with Cr particles. Air mass movement patterns for the study sites indicated the same. Cr mine proximity effect on wild vegetation was reported (Pöykiö *et al*., 2005). The higher adhesion possibility of larger Cr particles on the adaxial leaf surfaces of plants sampled from areas close to mines further supported gravity caused near-source deposition of larger particles (Sgrigna *et al*., 2015).

In this context, as revealed in the present study, a higher probability of coarse particles (PM_{10}) to contain Cr was consistent with the fact that mining operations generally emit particles of this size fraction (Entwistle *et al*., 2019). Numerous mine dumps in the study region could be another potential source of PM_{10} carrying Cr as this PM size fraction is the most abundant one in typical mine dump affected areas in South Africa (Nkosi *et al*., 2017). Further research in this regard may substantiate such a possibility in Sekhukhuneland.

4.4.2.3 Leaf surface-Cr dust interaction

The above-discussed prominent traits were represented by the main factors that explained leaf surface-Cr particle interactions in Sekhukhuneland. An individualistic leaf surface-dust interaction system is recognized for the two leaf surfaces. For the adaxial surface, ‘plant morphology’ was the primary factor where leaf area, epicuticular wax and plant height increased Cr particle deposition possibility. The second factor, ‘leaf morphology’ was entirely represented by the negative influence of longer trichomes on Cr dust deposition.

On the abaxial surface, leaf morphological features such as stomata size, epicuticular wax and leaf area and pollution variables conjointly created the ‘leaf surface-dust interface’ which mainly controlled the interaction of leaf surface to environmental Cr particles in terms of Cr wt% and Cr particle size. The second factors, for Cr wt% also reflected a similar positive influence of plant traits (smaller trichomes and denser wax structures) and mine frequency in this regard. Concerning Cr particle size, ‘plant morphology’ represented the second factor that suggested smaller stomata and plant height to promote the deposition of larger Cr particles. For both adaxial and abaxial leaf surface, low loadings for Cr variables on the second factors could suggest that these factors contributed less to Cr dust contamination of the assessed species.

In this regard, trichomes, epicuticular wax and stomata in the present study reflected contradictory outcomes (enhancing and limiting) for the two leaf surfaces. Trichomes and leaf wax were identified to favour or restrict PM accumulation by plant leaves in literature (Leonard *et al.*, 2016; Chen *et al*., 2017; Perini *et al.*, 2017; Liu *et al*., 2018). For stomata, however, the present study results contradicted past reports that necessitate extensive future investigation.

Various leaf micromorphology, therefore, contributed to foliar contact surfaces (Neinhuis & Barthlott, 1998; Chen *et al*., 2017) by adding structural heterogeneity on which extraneous particle interaction was favoured or restricted. In the present study, therefore, plant morphological traits cohesively affected foliar Cr dust deposition rather than individual dominance as similarly suggested in previous investigations (Leonard *et al*., 2016; Weerakkody *et al*., 2018). Further investigation on a larger number of taxa may help conclude better in this regard. The adopted comprehensive analytical approach to explore the leaf surface-Cr particle interaction in the present study is suitable to address the influence of both plant and pollution variables and can be tested further in mine polluted areas in South Africa.

4.4.3 Study limitations

Dust pollution may alter plant morphology (Chen *et al*., 2015; Popek *et al*., 2015), hence, comparative analysis by integrating plant species from non-polluted habitat might provide insight regarding possible plasticity of plant morphological characters observed in Sekhukhuneland. Dust accumulation on leaves is a time-dependent phenomenon related to both leaf phenology, as well as fluctuations in emission rates and consequent dispersion and deposition by wind movements (Pöykiö *et al*., 2005; Mingorance & Oliva, 2006; Chen *et al*., 2015; Grote *et al*., 2016). Accounting for seasonal dust variability might be an important additional sampling approach (Sigrigna *et al*., 2015; Tang & Han, 2015; Chen *et al*., 2017; Zha *et al*., 2019). The influence of the number of Cr polluters proved to be critical in the present study and should be investigated further at a broader scale. Continuous monitoring and research are expected to add further information to understand the pollution factor better in Sekhukhuneland.

Summary

This study considered leaf surface-Cr particle interaction dynamics and possible Cr dust sources in soil and plant leaves under multifaceted Cr particle exposure in a mining-smelting region in Sekhukhuneland. Cr in soil probably had its origin from both ultramafic geology and anthropogenic sources. Cr dust contamination of the leaf surfaces was predominantly from environmental pollution ascribed to dust originating from varied mining associated activities. As evident from the overlay back trajectory maps dust sources within the 25 km zone around sampling locations could be important. Both matrices (i.e. soil and plant) showed heterogeneity regarding elemental composition probably due to the presence of a variety of polluters. The two leaf surfaces, i.e.

facing up or down, interacted differently with atmospheric pollution and soil dust depending on plant morphology. Plant morphology predominantly controlled leaf surface-Cr particle interaction on the adaxial surface where plant tallness increased Cr contamination probability of larger leaves with dense epicuticular wax. Cr dust adhesion on the abaxial leaf surface could be a more complex process between plant morphology and pollution sources and hence 'leaf surface-dust interface' could be identified as the main factor to control the dust deposition process. Proximity to several roads and mines enhanced the abaxial Cr particle contamination that could be further favoured on bigger leaves with dense epicuticular wax structures and larger stomata. These poorly understood drivers of foliar dust adhesion require extensive scientific attention. Future studies on the elemental composition of the soil, road and atmospheric dust, along with analysis of a wider variety of vegetation are essential to make more informed predictions regarding the risk associated with human use of dust polluted plant leaves in this part of South Africa. The following chapter provides some perspective on the contribution of Cr dust towards Cr accumulation by plant leaves and human health risk associated with their consumption.

References

Balabanova, B., Stafilov, T., Šajn, R. & Bačeva, K. 2011. Distribution of chemical elements in attic dust as reflection of their geogenic and anthropogenic sources in the vicinity of the copper mine and flotation plant. *Archives of Environmental Contamination and Toxicology,* 61(2):173–184.

Barthlott, W., Neinhuis, C., Cutler, D., Ditsch, F., Meusel, I., Theisen, I. & Wilhelmi, H. 1998. Classification and terminology of plant epicuticular waxes. *Botanical Journal of the Linnean Society*, 126:237–260.

Beukes, J.P., Dawson, N.F. & van Zyl, P.G. 2010. Theoretical and practical aspects of Cr(VI) in the South African ferrochrome industry. *The Journal of the Southern African Institute of Mining and* Metallurgy, 110:743–750.

Boneschans, R.B., Coetzee, M.S. & Siebert, S.J. 2015. A geobotanical investigation of the Koedoesfontein Complex, Vredefort Dome, South Africa. *Australian Journal of Botany*, 63(4):324–340.

Chen, X., Zhou, Z., Teng, M., Wang, P. & Zhou, L. 2015. Accumulation of three different sizes of particulate matter on plant leaf surfaces: effect on leaf traits. *Archives of Biological Sciences,* 67(4):1257–1267.

Chen, L., Liu, C., Zhang, L., Zou, R. & Zhang, Z. 2017. Variation in tree species ability to capture and retain airborne fine particulate matter ($PM_{2.5}$). *Scientific Report*, 7(1):1–11.

Coetzee, J.J., Bansal, N. & Chirwa, E.M.N. 2018. Chromium in environment, its toxic effect from chromite-mining and ferrochrome industries, and its possible bioremediation. *Exposure and Health,* 12:51–62.

Cramer, L.A., Basson, J. & Nelson, L.R. 2004. The impact of platinum production from UG2 ore on ferrochrome production in South African. *The Journal of the South African Institute of Mining and Metallurgy*, 104(9):517–527.

Csavina, J., Field, J., Taylor, M.P., Gao, S., Landázuri, A., Betterton, E.A. & Eduardo Sáez, A. 2012. A review on the importance of metals and metalloids in atmospheric dust and aerosol from mining operations. *Science of The Total Environment,* 433:58–73.

Dreicer, M., Hakonson, T.E., White, G.C. & Whicker, F.W. 1984. Rainsplash as a mechanism for soil contamination of plant surfaces. *Health Physics*, 46(1):177–187.

Draxler, R.R. & Hess, G.D. 2004. Description of the HYSPLIT 4 Modelling System. *National Oceanic and Atmospheric Administration (NOAA) Technical Memorandum ERL ARL*–224. Air Resources Laboratory Silver Spring, Maryland. https://www.arl.noaa.gov/data/web/models/hysplit4/win95/arl-224.pdf Date of access: 10 Aug. 2020.

Du Toit, M.J. & Cilliers, S.S. 2010. Aspects influencing the selection of representative urbanization measures to quantify urban - rural gradients. *Landscape Ecology,* 26(2):169–181.

Dzierżanowski, K., Popek, R., Gawrońska, H., Sæbø, A. & Gawroński, S.W. 2011. Deposition of particulate matter of different size fractions on leaf surfaces and in waxes of urban forest species. *International Journal of Phytoremediation,* 13(10):1037–1046.

Ebenebe, P.C., Shale, K., Sedibe, M., Tikilili, P. & Achilonu, M.C. 2017. South African mine effluents: heavy metal pollution and impact on the ecosystem. *International Journal of Chemical Sciences,* 15(4):1–12.

El-Khatib, A.A., Abdel-Rahman, A.M. & El-Sheikh, O.M. 2011. Leaf geometric design of urban trees: potentiality to capture airborne particle pollutants. *Journal of Environmental Studies*, 7:49–59.

Entwistle, J.A., Hursthouse, A.S., Marinho Reis, P.A. & Stewart, A.G. 2019. Metalliferous mine dust: human health impacts and the potential determinants of disease in mining communities. *Current Pollution Reports,* 5:67–83.

Gabarrón, M., Faz, A. & Acosta, J.A. 2018. Use of multivariable and redundancy analysis to assess the behavior of metals and arsenic in urban soil and road dust affected by metallic mining as a base for risk assessment. *Journal of Environmental Management*, 206:192–201.

Gajbhiye, T., Pandey, S.K., Kim, K.H., Szulejko, J.E. & Prasad, S. 2016. Airborne foliar transfer of PM bound heavy metals in *Cassia siamea*: a less common route of heavy metal accumulation. *Science of the Total Environment,* 573:123–130.

Grantz, D.A., Garner, J.H.B. & Johnson, D.W. 2003. Ecological effects of particulate matter. *Environment International,* 29:213–239.

Grote, R., Samson, R., Alonso, R., Amorim, J.H., Cariñanos, P., Churkina, G., … Calfapietra, C. 2016. Functional traits of urban trees: air pollution mitigation potential. *Frontiers in Ecology and the Environment,* 14(10):543–550.

Gu, F. & Wills, B.A. 1988. Chromite - mineralogy and processing. *Minerals Engineering,* 1(3):235–240.

Kien, C.N., Noi, N.V., Son, L.T., Ngoc, H., Tanaka, S., Nishina, T. & Iwasak, K. 2010. Heavy metal contamination of agricultural soils around a chromite mine in Vietnam. *Soil Science and Plant Nutrition*, 56:344–356.

Kimbrough, D.E., Cohen, Y., Winer, A.M., Creelman, L. & Mabuni, C. 1999. A critical assessment of chromium in the environment. *Critical Review in Environmental Sciences and Technology,* 29(1):1–46.

Leonard, R.J., McArthur, C. & Hochuli, D.F. 2016. Particulate matter deposition on roadside plants and the importance of leaf trait combinations. *Urban Forestry & Urban Greening,* 20:249–253.

Liang, D., Ma, C., Wang, Y., Wang, Y. & Chen-xi, Z. 2016. Quantifying $PM_{2.5}$ capture capability of greening trees based on leaf factors analyzing. *Environmental Science and Pollution Research,* 23:21176–21186.

Liu, L., Guan, D. & Peart, M.R. 2012. The morphological structure of leaves and the dust retaining capability of afforested plants in urban Guangzhou, south China. *Environmental Sciences and Pollution Research,* 19(8):3440–3449.

Liu, Y., Yang, Z., Zhu, M. & Yin, J. 2018. Size fractions of dust and amount of associated metals on leaf surface and inner wax of 15 plant species at Beijing roadside. *International Journal of Phytoremediation,* 21(6):1–18.

Lu, X., Wang, L., Li, L.Y., Lei, K., Huang, L. & Kang, D. 2010. Multivariate statistical analysis of heavy metals in street dust of Baoji, NW China. *Journal of Hazardous Materials*, 173:744–749.

Masindi, V. & Muedi, K.L. 2018. *Environmental contamination by heavy metals*. Available from Intech Open: https://www.intechopen.com/books/heavy-metals/environmental-contamination-by-heavy-metals Date of access: 01 Sep. 2020.

Mhlongo, S.E. & Amponsah-Dacosta, F. 2015. A review of problems and solutions of abandoned mines in South Africa. *International Journal of Mining, Reclamation and Environment*, 30(4). https://doi.org/10.1080/17480930.2015.1044046

Mingorance, M.D. & Oliva, S.R. 2006. Heavy metals content in *N. oleander* leaves as urban pollution assessment. *Environmental Monitoring and Assessment,* 119:57–68.

Mo, L., Ma, Z., Xu, Y., Sun, F., Lun, X., Liu, X., Chen, J. & Yu, X. 2015. Assessing the capacity of plant species to accumulate particulate matter in Beijing, China. *Plos One,* 10(10), e0140664. https://doi.org/10.1371/journal.pone.0140664

Naderizadeh, Z., Khademi, H. & Ayoubi, S. 2016. Biomonitoring of atmospheric heavy metals pollution using dust deposited on date palm leaves in southwestern Iran. *Atmósfera*, 29(2):141–155.

Neinhuis, C. & Barthlott, W. 1998. Seasonal changes of leaf surface contamination in beech, oak, and ginkgo in relation to leaf micromorphology and wettability. *New Phytologist*, 138:91–98.

Nguyen, T., Yu, X., Zhang, Z., Liu, M. & Liu, X. 2015. Relationship between types of urban forest and $PM_{2.5}$ capture at three growth stages of leaves. *Journal of Environmental Sciences*, 27:33–41.

Nkosi, V., Wichmann, J. & Voyi, K. 2015. Mine dumps, wheeze, asthma, and rhinoconjunctivitis among adolescents in South Africa: any association? *International Journal of Environmental Health Research*, 25(6):583–600.

Nkosi, V., Wichmann, J. & Voyi, K. 2017. Indoor and outdoor PM_{10} levels at schools located near mine dumps in Gauteng and North West Provinces, South Africa. *BMC Public Health*, 17, 42. https://doi.org/10.1186/s12889-016-3950-8

Norouzi, S. & Khademi, H. 2015. Source identification of heavy metals in atmospheric dust using *Platanus orientalis* L. leaves as bioindicator. *Eurasian Journal of Soil Science*, 4(3):144–152.

Oliva, S.R. & Espinosa, F.A.F. 2007. Monitoring of heavy metals in topsoils, atmospheric particles and plant leaves to identify possible contamination sources. *Microchemical Journal*, 86:131–139.

Ottelé, M., van Bohemen, H.D. & Fraaij, A.L.A. 2010. Quantifying the deposition of particulate matter on climber vegetation on living walls. *Ecological Engineering*, 36:154–162.

Perini, K., Ottelé, M., Giulini, S., Magliocco, A. & Roccotiello, E. 2017. Quantification of fine dust deposition on different plant species in a vertical greening system. *Ecological Engineering,* 100:268–276.

Popek, R., Gawrońska, H. & Gawroński, S.W. 2015. The level of particulate matter on foliage depends on the distance from the source of emission. *International Journal of Phytoremediation,* 17(12):1262–1268.

Pöykiö, R., Mäenpä, A., Perämäki, P., Niemelä, M. & Välimäki, I. 2005. Heavy metals (Cr, Zn, Ni, V, Pb, Cd) in Lingonberries (*Vaccinium vitis-idaea* L.) and assessment of human exposure in two industrial areas in the Kemi-Tornio region, northern Finland. *Archives of Environmental Contamination and Toxicology*, 48:338–343.

Ram, S.S., Majumder, S., Chaudhuri, P., Chanda, S., Santra, S.C., Maiti, P.K., … Chakraborty, A. 2012. Plant canopies: bio-monitor and trap for re-suspended dust particulates contaminated with heavy metals. *Mitigation and Adaptation Strategies for Global Change,* 19:499–508.

Scoon, R.N. & Viljoen, M.J. 2019. Geoheritage of the eastern limb of the Bushveld Igneous Complex, South Africa: a uniquely exposed layered igneous intrusion. *Geoheritage,* 11:1723–1748.

Sgrigna, G., Sæbø, A., Gawronski, S., Popek, R. & Calfapietra, C. 2015. Particulate matter deposition on *Quercus ilex* leaves in an industrial city of central Italy. *Environmental Pollution*, 197:187–194.

Shi, G., Chen, Z., Xu, S., Zhang, J., Wang, L., Bi, C. & Teng, J. 2008. Potentially toxic metal contamination of urban soils and roadside dust in Shanghai, China. *Environmental Pollution,* 156(2):251–260.

Shi, S., Wu, Z., Liu, F. & Fan, W. 2016. Retention of atmospheric particles by local plant leaves in the Mount Wutai scenic area, China. *Atmosphere*, 7(8), 104. https://doi.org/10.3390/atmos7080104

Siebert, S.J., Van Wyk, A.E. & Bredenkamp, G.J. 2002. The physical environment and major vegetation types of Sekhukhuneland, South Africa. *South African Journal of Botany,* 68(2):127–142.

Sungur, A. 2016. Heavy metals mobility, sources, and risk assessment in soils and uptake by apple (*Malus domestica* Borkh.) leaves in urban apple orchards. *Archives of Agronomy and Soil Science*, 62(8):1051–1065.

Suzuki, K., Yabuki, T. & Ono, Y. 2009. Roadside *Rhododendron pulchrum* leaves as bioindicators of heavy metal pollution in traffic areas of Okayama, Japan. *Environmental Monitoring and Assessment*, 149:133–141.

Sweeten, N.J., Verryn, S.M.C., Oberholzer, J. & Zietsman, J.H. 2018. Chrome ore mineralogy and the furnace mass and energy balance. *The Journal of South African Institute of Mining and Metallurgy*, 118:637–643.

Tallis, M., Taylor, G., Sinnett, D. & Freer-Smith, P. 2011. Estimating the removal of atmospheric particulate pollution by the urban tree canopy of London, under current and future environments. *Landscape and Urban Planning*, 103:129–138.

Tang, Y. & Han, G. 2015. Characteristics of major elements and heavy metals in atmospheric dust in Beijing, China. *Journal of Geochemical Exploration*, 176:114–119.

Tian, S., Liang, T. & Li, K. 2019. Fine road dust contamination in a mining area presents a likely air pollution hotspot and threat to human health. *Environment International*, 128:201–209.

Tshehla, C. & Djolov, G. 2018. Source profiling, source apportionment and cluster transport analysis to identify the sources of PM and the origin of air masses to an industrialised rural area in Limpopo. *Clean Air Journal*, 28(2):54–66.

Tshehla, C. & Wright, C.Y. 2019a. Spatial variability of PM_{10}, $PM_{2.5}$ and PM chemical components in an industrialised rural area within a mountainous terrain. *South African Journal of Science*, 115(9/10), art. 6174. https://doi.org/10.17159/sajs.2019/6174

Tshehla, C. & Wright, C.Y. 2019b. 15 Years after the National Environmental Management Air Quality Act: Is legislation failing to reduce air pollution in South Africa? *South African Journal of Science*, 115(9/10), art. 6100. https://doi.org/10.17159/sajs.2019/6100

Vakkari, V., Laakso, H., Kulmala, M., Laaksonen, A., Mabaso, D., Molefe, M., …Laakso, L. 2011. New particle formation events in semi-clean South African savannah. *Atmospheric Chemistry and Physics,* 11:3333–3346.

Venter, A.D., Beukes, J.P., van Zyl, G.P., Josipovic, M., Jaars, K. & Vakkari, V. 2016. Regional Cr(VI) pollution from the Bushveld Complex, South Africa. *Atmospheric Pollution Research,* 7(5):762–767.

Weerakkody, U., Dover, J.W., Mitchell, P. & Reiling, K. 2018. Evaluating the impact of individual leaf traits on atmospheric particulate matter accumulation using natural and synthetic leaves. *Urban Forestry & Urban Greening,* 30:98–107.

Yang, J., Teng, Y., Song, L. & Zuo, R. 2016. Tracing sources and contamination assessments of heavy metals in road and foliar dusts in a typical mining city, China. *Plos One*, 11(12), art. e0168528. https://doi.org/10.1371/journal.pone.0168528

Zha, Y., Shi, Y., Tang, J., Liu, X., Feng, C. & Zhang, Y. 2019. Spatial-temporal variability and dust-capture capability of 8 plants in urban China. *Polish Journal of Environmental Studies,* 28(1):453-462.

Chapter 5

Chromium accumulation by plant leaves (total Cr and Cr(VI))

5.1 Introduction

Mining of chromium (Cr), Cr processing industries and waste cause Cr-enrichment of soil and air (Kimbrough *et al*., 1999; Dhal *et al*., 2010b; Bolaños-Benítez *et al*., 2018; Coetzee *et al*., 2018). Cr accumulation in leaves because of increased root uptake in Cr mining, smelting and Cr-based industrial region is studied adequately (Economou-Eliopoulos *et al*., 2012; Mohanty *et al*., 2012; Reddy *et al*., 2012; Owolabi *et al*., 2016). In such localities, besides root uptake, Cr dust exposure to aerial plant parts might increase the contamination probability as suggested for other heavy metals (Bi *et al*., 2009; Liu *et al*., 2019; Wang *et al*., 2019).

Cr as a transition element may exist in multiple valence states, of which tri- (Cr(III)) and hexavalent chromium (Cr(VI)) are the least and most toxic form, respectively (Kimbrough *et al*., 1999; Economou-Eliopoulos *et al*., 2012; Oliveira, 2012). The biological toxicity of Cr, therefore, depends on the proportion of Cr(III) and Cr(VI) in the exposure environment (Kimbrough *et al*., 1999). Cr mine and smelter waste is rich in Cr(VI) (Cox *et al*., 1985; Ma & Garbers-Craig, 2006; Dhal *et al*., 2010a; Bolaños-Benítez *et al*., 2018; Coetzee *et al*., 2018). Waste from these industries also contains several other hazardous elements besides Cr (Pöykiö *et al*., 2005; Dhal *et al*., 2010a; Kien *et al*., 2010; Economou-Eliopoulos *et al*., 2012; Bolaños-Benítez *et al*., 2018). Among these elements, As (11), Cd (25) and Cr (28) ranked high as carcinogens listed by the International Agency for Cancer Research (IARC) (Cai *et al*., 2019). Exposure to multiple toxic elements, therefore, increases the health threat potential to users in mining-smelting impacted regions (Wang *et al*., 2019; Antisari *et al*., 2020). Safe limits of such elements in plants are therefore recommended by international regulatory bodies (Kohzadi *et al*., 2018) to ensure the safety of useful plants.

This chapter deals with two interlinked aims, first to present a comprehensive report on total Cr and Cr(VI) accumulation by the leaves of useful plant species from the mining-smelting region in Sekhukhuneland and second, to investigate leaf consumption associated health risk. The region has a long history of Cr and platinum (Pt) mining (both Cr and Pt mines extract elements from the same chromitite ore layers in the region to contribute to Cr pollution, Scoon & Viljoen, 2019), yet Cr contamination of local vegetation especially due to Cr dust exposure has never been investigated. The first objective was therefore to determine the contribution of deposited Cr particles to Cr accumulation in and on leaves of useful plants. It was hypothesized that the presence of various Cr dust emitters, e.g. mines, smelters, roads, and tailings in the region (Tshehla & Djolov, 2018; Tshehla & Wright, 2019) would result in considerable dust deposition

on plant leaves. To test this, leaf surface Cr concentration was determined as a difference in elemental concentrations between unwashed (UW) and washed (W) leaves of sixteen food and medicinal plants used by local inhabitants. The second objective was to assess Cr(VI) availability to plant leaves in the region. It was assumed that due to the presence of multiple Cr(VI) polluters, e.g. Cr mines, tailings and ferrochrome smelters in the region, local vegetation would be exposed to this hazardous Cr species. To test this, Cr(VI) amount in unwashed plant leaves were determined. The third objective was to evaluate the effect of plant growth form, Cr polluters and soil on Cr contamination of plant leaves. As indicated in past studies (Visoottiviseth *et al*., 2002; Pöykiö *et al*., 2005; Economou-Eliopoulos *et al*., 2012) it was hypothesised that such variables would affect Cr contamination of plant leaves in Sekhukhuneland. Plant species were hence categorised according to growth form and total number of Cr sources within a selected distance zone and analysed. Total Cr, Cr(VI) and soluble Cr concentrations in local soil samples were determined to investigate their possible influence on leaf Cr content. With regards to the second aim, it was postulated that consumption of mining-smelting sourced dust contaminated useful plant leaves would present substantial health risk to consumers as a result of exposure to multiple toxic elements. To test this, toxic elements in W and UW leaves were quantified and ingestion linked non-carcinogenic and carcinogenic health risk was estimated.

5.2 Materials and Method

5.2.1 Study area

Sampling was conducted in the mining-smelting region in the Fetakgomo-Tubatse municipal area in the Sekhukhune District, Limpopo. The geology of the study area comprises the eastern part of the world's largest layered igneous formation, the Rustenburg Layered Suite (RLS), part of the Bushveld Igneous Complex (BIC) (Naldrett *et al*., 2012; Scoon & Viljoen, 2019). The long crescent-shaped formation of the RLS is subdivided into five-rock zones (Fig. 5.1), of which the Critical Zone (CZ) predominantly features chromitite rock layers (stratiform Cr ore) with the largest global chromitite reserve and considerable proportions of Pt (Naldrett *et al*., 2012; Scoon & Viljoen, 2019).

The study was conducted following the CZ (Fig. 5.1) in the eastern part of the Sekhukhune district, starting at Atok (a Pt mine) in the north to Steelpoort (near a Cr and Pt mine) in the south. The middle section falls within the Motse River valley, known as the 'platinum valley' with multiple Pt mines (Scoon & Viljoen, 2019). Seven sampling sites (3 home gardens and 4 rangelands) were randomly selected following the chain of active Cr and Pt mines and the three operational ferrochrome smelters in the study region (Fig. 5.1). The area is further polluted by two main roads (R37 and R555) and numerous interconnecting non-tar roads. The metalliferous soils generated from the ultramafic-mafic formations of the RLS are primarily characterized by high concentrations

of Al, Co, Cr, Fe, Mg, Mn, Ni, Ti and V (Siebert *et al*., 2002). Sampling was therefore aimed to incorporate deposition of dust originating from the local geology and polluted areas on useful plant leaves.

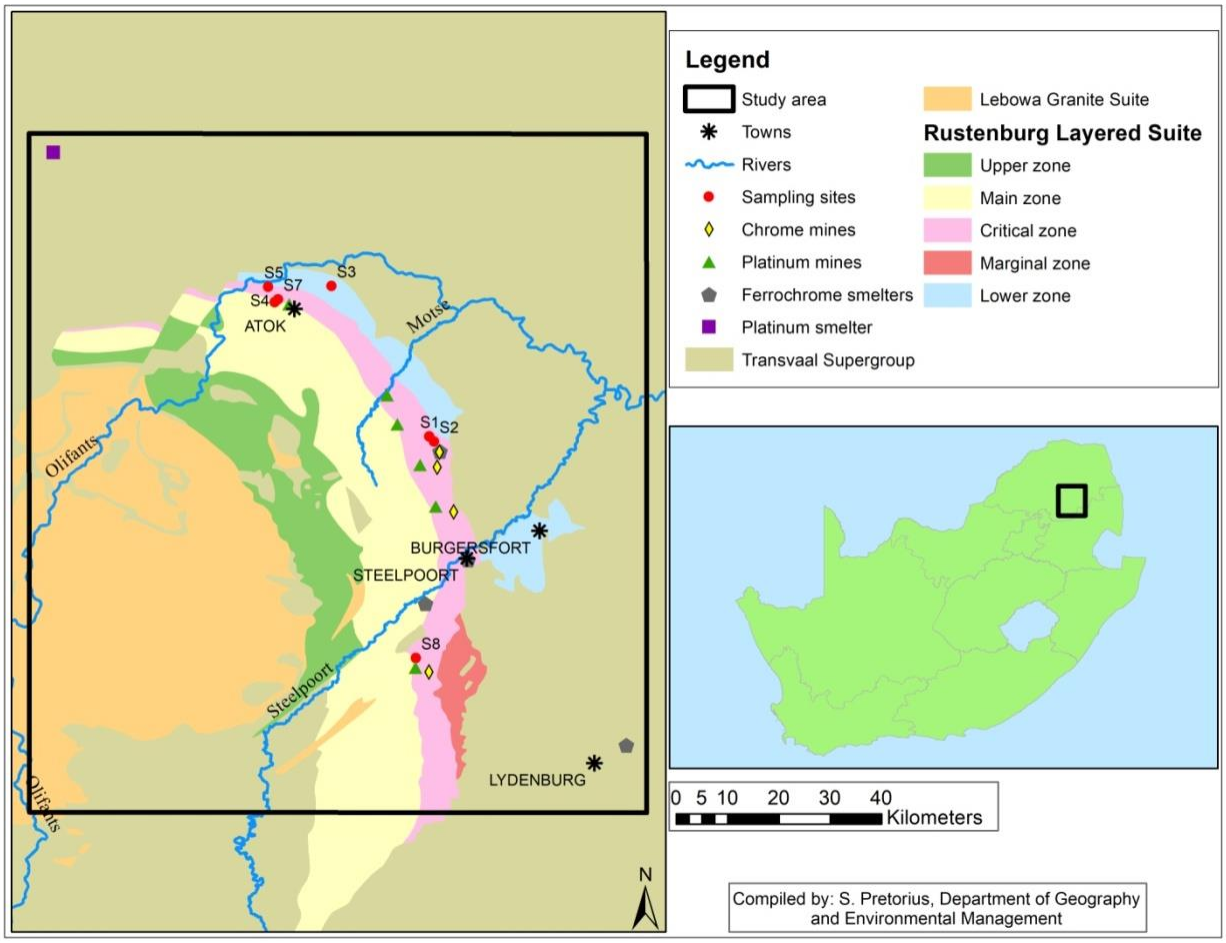

Figure 5.1. Geology of the eastern RLS accompanied by the sampling sites and major mines and smelters in Sekhukhuneland and neighbouring region.

5.2.2 Sample collection

For a detailed sampling procedure see Chapter 3, section 3.2.2. In the current study, Cr concentrations were determined in leaves of sixteen commonly used leafy vegetable and medicinal plant species in the region (Semeny & Potgieter, 2014; Mogale *et al*., 2019). Plant leaves were sampled randomly from home gardens (seven species) and rangelands (nine species). Detailed leaf-use of the twelve species is tabled in Chapter 3, under section 3.2.2 (Table 3.1) and the additional four species investigated here are described below (Table 5.1).

Table 5.1. Growth form and leaf use of the four plant species. *Exotic and [cv]cultivated species. Sampling site: HG, home garden; RL, rangeland; S4, sampling site 4; S5, sampling site 5; S7, sampling site 7.

Sampling site	Plant species	Family	Growth form	Leaf use
S5, RL	*Amaranthus spinosus* L.*	Amaranthaceae	Forb	Leafy vegetable
S7, HG	*Cleome gynandra* L.	Cleomaceae	Forb	Leafy vegetable
S7, HG	*Carpobrotus edulis* (L.) L.Bolus subsp. *edulis*	Aizoaceae	Succulent	Treat diabetes mellitus, goitre, toothache, sore throat, stomach pain
S4, RL	*Sansevieria trifasciata* Prain*	Ruscaceae	Succulent	Treat diarrhoea

Topsoil (< 10 cm depth) was collected from the base of each sampled plant, passed through a 2 mm sieve, and mixed to prepare composite samples per site (Fig. 5.2). Soil samples were dried and stored in sealed containers.

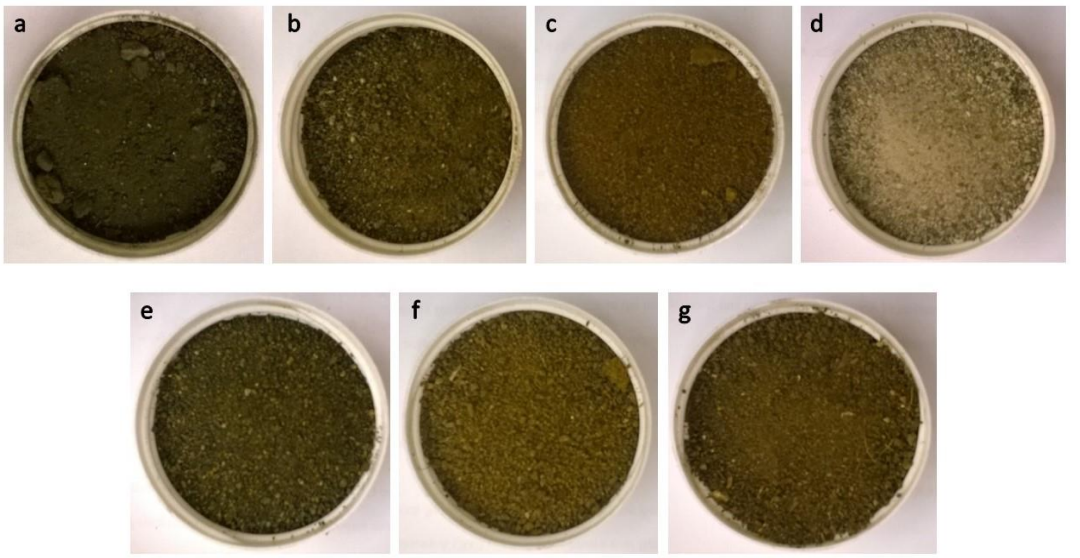

Figure 5.2. Soil composites of the seven sampling sites. a. Site 1, tailing facility; b. site 2, home garden near site 1; c. site 3, farthest home garden from a mining site; d. site 4, rangeland close to a Pt mine; e. site 5, abandoned informal Cr excavation location; f. site 7, home garden near site 4; g. site 8, rangeland in mountains, chromitite outcrop.

5.2.3 Soil and plant tissue analyses

Unwashed leaf composites per species were divided into two portions. One part of unwashed leaf material was air-dried and stored in brown paper bags to serve as the 'unwashed leaf material' (UW) and the rest was washed three times with distilled water after collection to get rid of surface dust, air-dried and stored in a brown paper bag as the 'washed leaf material' (W). Later, UW air-dried leaf material was dehydrated in an oven at 35 °C for 48 hours except succulents were dried at 60 °C for 48 hours. W leaves were further washed three times with 0.1 M HCl solution for about one minute and then rinsed with distilled water three times and oven-dried like UW leaves (Siebert *et al.*, 2018; Dobbins *et al.*, 2021). UW and W leaf materials and soil samples were ground in a tungsten carbide ring mill to a particle size less than 75 µm and stored in sealed vials at room temperature until analysis.

5.2.3.1 Determination of total elements in plant leaves

To determine the concentrations of Cr and other toxic elements, i.e. metals and metalloids (Al, As, Cd, Co, Cr, Cu, Hg, Mn, Mo, Ni, Pb, Sb, V and Zn) in plant leaves, UW and W leaves were analysed with the EPA 3051A microwave acid digestion method. This is a total recoverable method based on low sample requirement that ensures least sample loss; and is globally accepted and used in environmental studies, especially for the detection of heavy metals (Chen & Ma, 1998; Agazzi & Pirola, 2000).

Each 0.2 g of ground leaf sample was placed in a Teflon tube. Then 9 ml of 65% nitric acid (HNO_3) and 3 of ml 32% hydrochloric acid (HCl) (HNO_3–HCl, 3:1, v/v) was added to the tube, sealed, and placed in a high-performance microwave digestion system (Milestone, Ethos UP, Maxi 44) for 20 minutes until the system reaches 1800 MW at 200 °C. The state was maintained for 15 minutes. After cooling, the final volume was adjusted to 50 ml and analysed on an ICP-MS (Agilent 7500 series). For Cr concentrations of dust adhered to leaf surfaces, detected metal concentration in W leaves was subtracted from the UW leaf concentration. W leaf values of Cr were considered as concentrations in leaf tissue.

5.2.3.2 Quantifying Cr(VI) in leaves and soil

Due to lack of sufficient leaf material Cr(VI) was determined in UW leaves only and the values represented total Cr(VI) of leaf materials. To determine Cr(VI) in the UW leaves and soil, a method described by Ashley *et al.* (2003) was selected. The method uses an alkaline buffer to ensure maximum extraction of Cr(VI). Alkalinity stabilises Cr(VI) and prevent its reduction to Cr(III) but may increase the oxidation possibility of some Cr(III) to Cr(VI) at high temperature. Pure N_2 was supplied during the reaction to limit oxidation of Cr(III) (Ashley *et al.*, 2003).

Measured 2.5 g of ground sample (leaf or soil) was transferred into a 250 ml beaker and mixed with 50 ml of Na_2CO_3–NaOH buffer (3% sodium bicarbonate, 2% sodium hydroxide, m/v). The buffer was de-oxygenated before use by supplying N_2 gas for 45 min. The sample was then digested on a hot plate for 2 h with a constant supply of N_2. For plant samples, after the extraction, solutions were filtered through Whatman 540 filter paper to remove leaf residue. The beaker was then washed with 30 ml of freshly de-oxygenated buffer and filtered through a 0.45 µm filter paper. The extract was collected in a 100 ml volumetric flask, filled to volume with de-oxygenated buffer and analysed with an Agilent 7500 ICP-MS.

5.2.3.3 Determination of total elements in soil

Total concentrations of elements in collected soil samples from the seven study sites were determined with a handheld x-ray fluorescence (XRF) machine (Koch *et al*., 2017). The method is specifically recommended to analyse the contamination status of soils that are impacted by anthropogenic disturbances such as mining (Galuszka *et al*., 2015). The technique is reported to provide adequate quantitative and qualitative data for a range of elements within a minimum time frame and least sample preparation (Kalnicky & Singhvi, 2001; Jang, 2010).

The ground soil sample was taken in a sample cup, levelled and covered with a piece of XRF-film to obtain a flat surface for a consistent XRF contact (Fig. 5.3). The equipment, Thermo Scientific Niton XL3t GOLDD+ handheld XRF was calibrated before the analysis. "*Mining*" setting was selected with a scan time of 120 seconds to detect all possible elements and to optimise the identification of lighter elements with lower detection limits. The XRF was held onto the flat soil surface until the scan was completed. The method was repeated three times per soil sample while changing the physical contact point of the XRF for each reading to capture maximum elemental variability. Standard protocol for the equipment and recommended precautionary measures were followed to ensure the validity of the data.

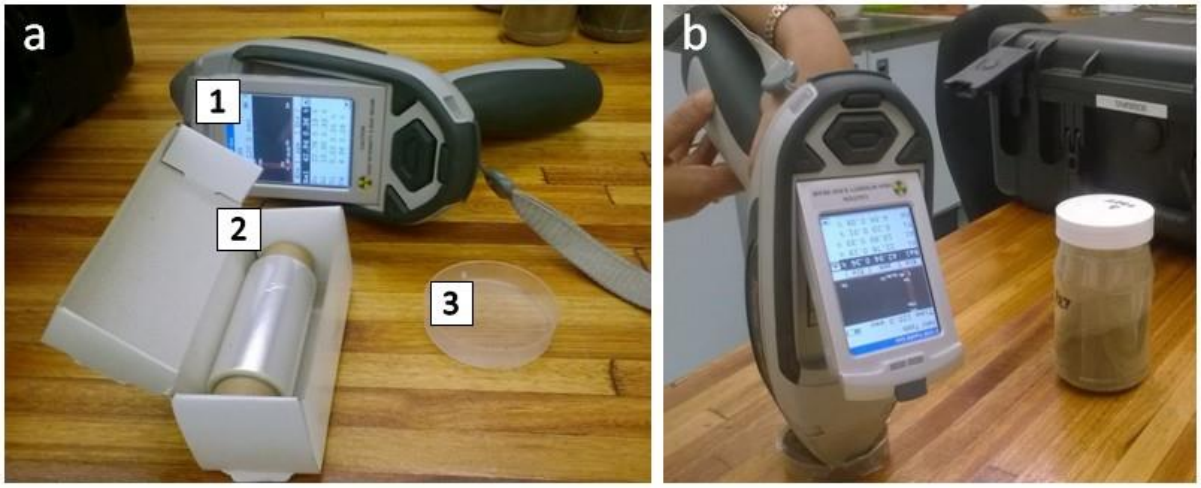

Figure 5.3. XRF analysis procedure. a. Components of handheld XRF analysis, 1. Thermo Scientific Niton XL3t GOLDD+ handheld XRF machine, 2. XRF-film, 3. sample cup; b. XRF analysis of soil samples.

5.2.3.4 Determination of soluble Cr in soil

To investigate the influence of soluble soil Cr on Cr accumulated in leaf tissue, collected soil samples were analysed with ammonium nitrate (NH_4NO_3) solution to extract soluble Cr (Siebert *et al*., 2018). NH_4NO_3 is chosen as it is comparatively less reactive, has a lower detection limit and minimum tendency to interfere with analytical measurements (Schöning & Brümmer, 2008). However, other reagents were reported to extract higher quantities of exchangeable heavy metals (Gryschko *et al*., 2005) compared to NH_4NO_3.

A volume of 50 ml of 1 M NH_4NO_3 solution was added to 20 g of soil in a 150 ml shaking flask. The solution was shaken at 20 rpm for 2 h at 25 °C and then left undisturbed for 15 min for particles to precipitate. The supernatant was filtered through a 0.45 µm Whatman filter paper. The filtrate was collected in a 50 ml vial and analyzed on an Agilent 7500 CE ICP-MS.

5.2.3.5 Soil pH determination

For each sampling site, soil pH (KCl) was determined using a 1:2.5 extraction solution (Siebert *et al.*, 2018). In a beaker, 50 ml of deionised water was added to a 20 gm of soil sample and stirred with a glass rod for five seconds. The solution was left undisturbed for 4 h. After which the solution was stirred thoroughly and left undisturbed for another 10 min. A Radiometer Copenhagen PHM 80 pH meter was used to measure the pH after the electrode was stabilised in the solution for 3 min.

5.2.4 Variables

5.2.4.1 Growth form

Plant growth form was selected as a variable to test if Cr concentration in plant leaves varies significantly among different growth forms. Sixteen plant species investigated in this study were categorized according to growth forms, i.e. trees, forbs and succulents (Table 5.2).

Table 5.2. Plant species groups based on growth form.

Group 1 Trees	Group 2 Forbs	Group 3 Succulents
Car pap, Cit lim, Mor ole, Ozo pan, Pel afr, Psi gua	Ama spi, Arg och, Cat ros, Cle gyn, Gom fru, Ipo bat, Sen ita, Tri ter	Car edu, San tri

Ama spi = *Amaranthus spinosus*; Arg och = *Argemone ochroleuca*; Car edu = *Carpobrotus edulis*; Car pap = *Carica papaya*; Cat ros = *Catharanthus roseus*; Cit lim = *Citrus limon*; Cleo gya = *Cleome gynandra*; Gom fru = *Gomphocarpus fruticosus*; Ipo bat = *Ipomoea batatas*; Mor ole = *Moringa oleifera*; Ozo pan = *Ozoroa paniculosa*; Pel afr = *Peltophorum africanum*; Psi gua = *Psidium guajava*; San tri = *Sansevieria trifasciata*; Sen ita = *Senna italica*; Tri ter = *Tribulus terrestris*.

5.2.4.2 Polluters

Of the seven localities sampled, only three sites, 1, 2 (< 4.5 km) and 8 (around 12 km) were in close vicinity to ferrochrome smelters. Considering the influence of such industry towards Cr and specifically Cr(VI) pollution (Cox *et al*., 1985; Ma & Garbers-Craig, 2006; Coetzee *et al*., 2018), an integrative approach was adopted to incorporate the effect of all major Cr sources. For each sampling site, a 10 km distance zone was determined within which all active mines (Cr and Pt), tar and non-tar roads and ferrochrome smelters were accounted. Hence, proximity, type and number of pollution sources were considered at the same time. The effect of the number of polluters has not investigated often however the presence of several Cr emitters in the vicinity of all sampling sites (see Chapter 4, section 4.2.7.3) necessitated this approach in the present study. Plant species were categorised accordingly into two groups (Table 5.3).

Table 5.3. Plant species groups based on the total number of various pollution sources within the 10 km periphery.

Group 1 (≤ 3)	Group 2 (4–6)
Ama spi, Car edu, Cit lim, Cle gyn, Ipo bat,	Arg och, Car pap, Cat ros
Mor ole, Ozo pan, Pel afr, San tri, Tri ter	Gom fru, Psi gua, Sen ita

Ama spi = *Amaranthus spinosus*; Arg och = *Argemone ochroleuca*; Car edu = *Carpobrotus edulis*; Car pap = *Carica papaya*; Cat ros = *Catharanthus roseus*; Cit lim = *Citrus limon*; Cleo gya = *Cleome gynandra*; Gom fru = *Gomphocarpus fruticosus*; Ipo bat = *Ipomoea batatas*; Mor ole = *Moringa oleifera*; Ozo pan = *Ozoroa paniculosa*; Pel afr = *Peltophorum africanum*; Psi gua = *Psidium guajava*; San tri = *Sansevieria trifasciata*; Sen ita = *Senna italica*; Tri ter = *Tribulus terrestris*.

5.2.4.3 Soil

Concentrations of soluble Cr was considered as a soil variable that could influence Cr concentrations in plant leaf tissue in the present study. Total Cr and Cr(VI) levels in soil samples were considered as additional variables to compare sampling sites regarding Cr pollution.

5.2.5 Data analysis

For data analysis purposes, detected foliar Cr concentrations were assessed (Table 5.4) as 'total Cr of leaf' (total Cr concentration of UW leaf), 'Cr in leaf tissue' (total Cr concentration in W leaves), 'Cr on leaf surface' (the difference between Cr amounts in UW and W leaf) and 'total Cr(VI) of leaf' (total Cr(VI) concentration of UW leaf). Note that if Cr(VI) is not specified, then total Cr is referred to.

Table 5.4. Summary of Cr concentrations determined for leaves.

Total measured	Material analysed	Content (Cr concentration categories)
Cr	Unwashed (UW)	Total Cr of leaf
Cr	Washed (W)	Cr in leaf tissue
Cr	UW – W	Cr on leaf surface
Cr(VI)	UW	Total Cr(VI) of leaf

To find out if there are significant differences in mean (1) Cr values in UW and W leaves of all sampled species, (2) UW and W leaf Cr contents of home garden and rangeland, and (3) UW and W leaf Cr contents in food and medicinal plants, non-parametric Kruskal-Wallis tests were conducted. In addition, linear regression analysis (R^2) was chosen to determine the relation between Cr on leaf surface to total Cr of leaf and Cr in leaf tissue to find out if Cr dust contribute significantly towards total Cr and tissue Cr.

To indicate if plant species groups on growth forms (Table 5.2) and total polluters (Table 5.3) differ significantly in terms of the four leaf Cr concentration categories (Table 5.4), Kruskal-Wallis test was performed. Sampling sites were grouped based on leaf Cr concentration categories with hierarchical cluster analysis using the Ward linkage method in conjunction with Euclidean distance. The letter 'C' with the corresponding cluster number is used to denote generated clusters in the figures.

Likewise, to determine similarity among sampling sites in terms of total soil Cr, hierarchical cluster analysis was performed. A follow-up Kruskal-Wallis test was conducted on the groups created after cluster analysis to assess if total soil Cr concentrations differ significantly between the groups. Furthermore, to determine the relationship between soluble soil Cr and Cr in leaf tissue, a linear regression was performed. Data was standardised with z-score and tested for homogeneity. Throughout the result interpretation, statistical significance was considered at $p<0.05$. IBM SPSS version 26 was used for data analysis.

5.2.6 Human health risk

Health Risk Assessment (HRA) was performed to evaluate ingestion linked health hazard potential of fourteen elements (Al, As, Cd, Co, Cr, Cu, Hg, Mn, Mo, Ni, Pb, Sb, V and Zn) detected in plant leaves (Table 5.5, 5.6). Assessments were conducted for the leaves of five food plant species commonly used as leafy vegetables (*A. spinosus*, *C. gynandra*, *G. fruticosus*, *I. batatas* and *T. terrestris*) in Sekhukhuneland (Mogale *et al*., 2019). Medicinal plant species were excluded from the analysis due to the unavailability of data on daily dose amounts for the selected species. HRA included non-carcinogenic and carcinogenic risk assessments. UW and W leaf materials were used to evaluate health risks and compare the risk between properly cleaned materials (Guerra *et al*., 2012) to unwashed materials.

5.2.6.1 Non-carcinogenic risk

Hazard Quotient (HQ), a ratio of the potential exposure to a substance (i.e. Estimated daily index, EDI) and the level at which no adverse effects can be expected (i.e. the Reference dose, RfD, US EPA, IRIS 2006, Integrated Risk Information System, IRIS, in the present study it is the oral RfD) (Guerra *et al*., 2012). Mean concentrations for each element recorded in the five leafy vegetables was used to calculate HQ per element using the following formula by US EPA, 1999 (Can *et al*., 2020),

$$\mathrm{HQ} = \frac{\mathrm{EDI}}{\mathrm{RfD}}$$

Where EDI was calculated using the below-stated formula,

$$\mathrm{EDI} = \frac{\mathrm{C} \times \mathrm{Cf} \times \mathrm{DC}}{\mathrm{BW}}$$

EDI (mg kg^{-1} body weight day^{-1}); C is mean metal concentration (mg kg^{-1} or µg g^{-1}) in UW and W leafy vegetables (Table 5.6, 5.7); Cf is the conversion factor, 0.085 (fresh to dry weight conversion, Rattan *et al*., 2005); DC presents daily consumption in kg day^{-1} (0.1862 kg day^{-1}, Rose *et al*., 2002); BW, body weight in kg, considering 70 kg as the average body weight of an adult (World Health Organisation, WHO, 2011; Antisari *et al*., 2020; Yaman, 2020); RfD (mg kg^{-1} body weight day^{-1}) (Table 5.10). RfD for each element was obtained from the Chemical Assessment Summary records by US EPA, IRIS.

From the HQs, the Hazard Index (HI) was calculated. HI represents the sum of all HQs. It is assumed that potential hazard to be magnified as a result of ingestion of several toxic elements (Guerra *et al*., 2012). For the present study, HI was calculated by adding HQs of the fourteen elements using the below-given formula by US EPA (1986) (Guerra *et al*., 2012).

$$HI = \sum HQ = HQ_{Al} + HQ_{As} + HQ_{Cd} + HQ_{Co} + HQ_{Cr} + HQ_{Cu} + HQ_{Hg} + HQ_{Mn} + HQ_{Mo} + HQ_{Ni} + HQ_{Pb} + HQ_{Sb} + HQ_{V} + HQ_{Zn}$$

For both, HQ and HI, values > 1 indicate a probability of non-carcinogenic health risk due to lifelong exposure of an individual element and all, respectively (US EPA, 2005) (Guerra *et al*., 2012; Can *et al*., 2020; Yaman, 2020).

5.2.6.2 Carcinogenic risk

Carcinogenic Risk (CR) was calculated for the elements recognized as human carcinogens (As, Cd, Cr and Ni) by the IARC (Monographs, 2020) and US EPA (IRIS, 1986), or regarded as probable carcinogens (Pb, Cd and Ni) by the US EPA (IRIS, 1986) and IARC (1990) (Kim *et al*., 2016). In addition to elemental concentrations in UW and W leaves, CR was calculated for leaf surface (S, concentration difference between UW and W) for As, total Cr and Pb. Ni and Cd that had W amounts > UW amounts, surface CR could not be estimated. The following formula was used to calculate the CR based on US EPA guidelines on carcinogenic risk assessment (Can *et al*., 2020).

$$\mathrm{CR} = \mathrm{EDI} \times \mathrm{SF}$$

EDI is the estimated daily intake (see section 5.2.5.1), and SF is the oral cancer slope factor in mg kg^{-1} body weight day^{-1}. According to US EPA (Background document 2, 1992, US EPA, IRIS, 2007, Yaman, 2020), SF is the 'upper bound estimation of possible cancer risk by a substance over a lifetime'. SF, therefore, is an estimate of the increased cancer risk from oral exposure to a dose of 1 mg kg^{-1} day^{-1} for a lifetime. SF for As, Cd, Cr, Ni and Pb is 1.5, 0.38, 0.5, 1.7 and 0.0085, respectively (Can *et al*., 2020).

The US EPA (2010) recognised CR values ≤ 1×10^{-6} (1 chance in 1,000,000 to develop cancer over lifelong exposure) to present a negligible cancer risk. Considerable CR could be linked to values greater than 1×10^{-4} (1 chance in 10,000) that serves as the upper safe limit. A value > 1×10^{-3} (1 chance in 1000) considered to indicate probable lifelong cancer risk to consumers (Can *et al*., 2020).

5.3 Results

5.3.1 Cr in leaf

Mean total Cr concentrations in UW leaves was significantly higher compared to W leaves (p<0.05, Kruskal-Wallis test). Cr values in UW and W leafy vegetables were 13- and 8-fold higher than the Maximum Permissible Concentrations (2.3 µg g^{-1}) set by WHO and Food and Agriculture Organisation, FAO (Pajević *et al*., 2018). Around 22- and 9-fold, higher mean total Cr concentrations in UW and W leaves of medicinal plants than the Maximum Residual Level (2 µg g^{-1}) set for raw medicinal plants by WHO (2005) (Kumar *et al*., 2018) was observed.

Leafy vegetables had higher mean values for Cr concentrations for home gardens under both leaf treatments (i.e. UW and W). For medicinal plant species, an opposite scenario was observed (Fig. 5.4). However, Kruskal-Wallis tests produced no significant differences between home gardens and rangelands or the two useful plant categories, i.e. medicinal and food, regarding the mean total Cr concentrations in UW and W leaves.

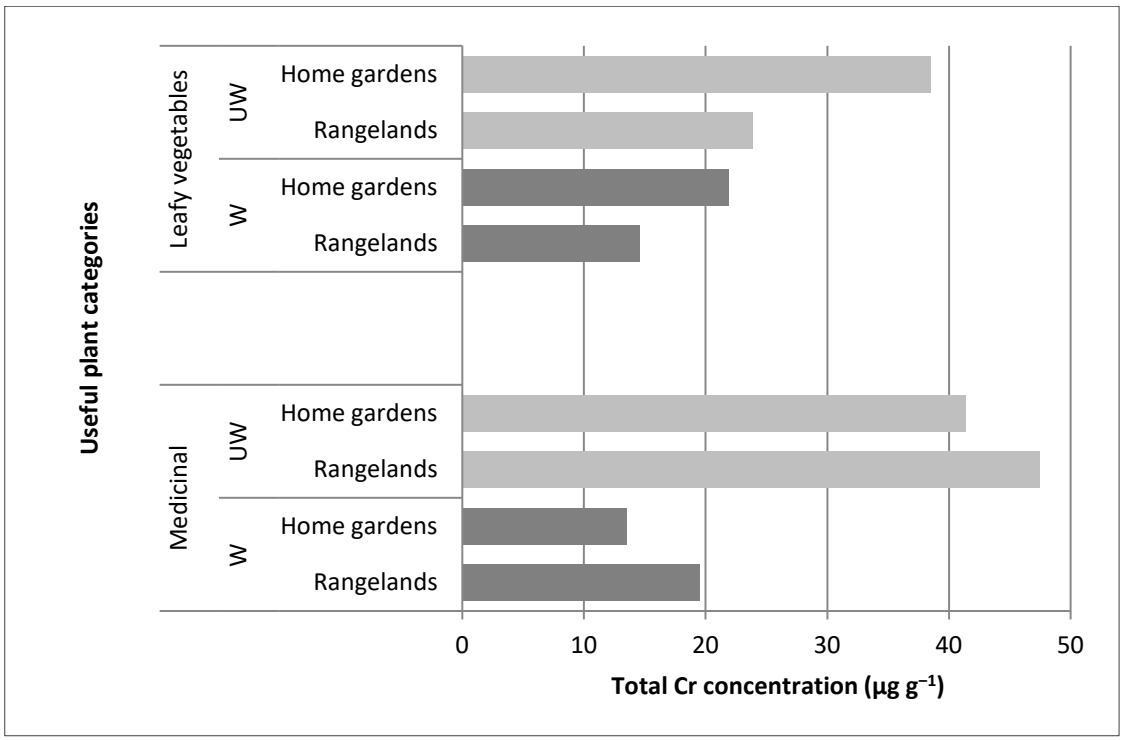

Figure 5.4. Mean values of total Cr concentrations in UW and W leaves of leafy vegetables and medicinal plant species sampled from home gardens and rangelands.

Table 5.5. Concentrations of hazardous elements in UW leaves (µg g^{-1} dry weight). Trees first followed by forbs and succulents. $^{\$}$*Gomphocarpus fruticosus* was noted for both food and medicinal use (Mogale *et al*., 2019). The highest and lowest means are in bold.

Medicinal plants

	Al	As	Cd	Co	Cr	Cu	Hg	Mn	Mo	Ni	Pb	Sb	V	Zn
Car pap	742.4	0.38	0.04	15.9	142.6	4.66	2.88	49.78	0.7	9.46	0.57	0.06	2.60	17.95
Cit lim	236.1	0.17	0.06	12.13	8.54	6.83	1.01	94.53	0.45	6.33	0.31	0.59	0.86	23.05
Mor ole	305.5	0.28	0.04	57.45	27.32	4.59	4.13	63.61	0.53	2.68	0.36	0.73	0.98	15.84
Ozo pan	242.8	0.14	0.02	2.81	37.21	7.51	0.78	16.05	0.17	1.9	0.34	0.03	1.09	16.21
Pel afr	258.2	0.18	0.05	5.28	13.73	3.88	1.22	55.25	0.16	4.26	0.49	0.03	0.67	17.82
Psi gua	234.8	0.14	0.03	6.82	24.65	5.25	1.15	26.27	0.39	4.43	0.28	0.03	1.03	17.46
Arg och	623.5	0.16	0.46	16.64	180.3	7.34	2.57	109.5	127.9	501.2	0.31	1.49	1.37	35.84
Car edu	100	0.28	0.04	25.57	3.96	1.89	2.19	15.38	0.26	1.25	0.13	0.01	0.55	13.35
Cat ros	156.1	0.41	0.04	13.52	28.78	3.53	2.09	29.3	0.27	4.21	0.38	0.03	0.65	11.29
$^{\$}$Gom fru	322	0.15	0.05	9.23	32.47	10.45	1.61	99.64	0.50	5.07	0.27	0.02	0.91	19.31
San tri	524.2	0.2	0.04	33.72	11.3	9.59	4.38	12.6	0.19	6.55	0.42	0.02	0.72	15.43
Sen ita	199.7	0.21	0.02	5.831	19.64	7.292	1.158	49.1	0.75	3.28	0.23	0.02	0.78	16.53
Mean	**328.78**	0.23	**0.08**	17.08	44.2	6.07	2.1	51.75	11.03	45.89	0.34	0.26	1.02	18.34
SD	196.6	0.1	0.12	15.5	56.2	2.5	1.2	34.3	36.8	143.4	0.1	0.5	0.5	6.2

Leafy vegetable

	Al	As	Cd	Co	Cr	Cu	Hg	Mn	Mo	Ni	Pb	Sb	V	Zn
Ama spi	520	0.3	0.22	44.78	19.24	6.35	7.2	52.42	0.8	2.5	0.28	0.03	0.98	63.67

Cle gyn	4536	0.34	0.63	113.4	53.65	9.54	16.2	99.21	1.32	14.42	0.96	0.08	3.49	51.32
$Gom fru	322	0.15	0.05	9.23	32.47	10.45	1.61	99.64	0.5	5.077	0.27	0.02	0.91	19.31
Ipo bat	271.2	0.2	0.06	19.68	23.46	7.13	3.98	102.3	0.65	6.24	0.3	0.02	0.98	23.54
Tri ter	239.3	0.22	0.24	31	19.9	8.61	5.68	35.15	0.38	3.97	0.26	0.04	0.64	53.94
Mean	**1177.7**	**0.25**	**0.25**	43.62	29.74	8.42	6.94	77.74	0.74	6.44	0.42	0.04	1.4	42.36
SD	1880.5	0.08	0.2	41.2	14.4	1.7	5.6	31.6	0.4	4.7	0.3	0.02	1.2	19.7
Mean (all species)	**578.46**	0.23	**0.13**	24.89	39.95	6.76	3.52	59.39	8	34.29	0.37	0.19	1.14	25.4
SD	1034.2	0.09	0.2	27.3	47.7	2.5	3.7	34.7	30.9	120.4	0.19	0.4	0.8	15.8

Ama spi = *Amaranthus spinosus*; Arg och = *Argemone ochroleuca*; Car edu = *Carpobrotus edulis*; Car pap = *Carica papaya*; Cat ros = *Catharanthus roseus*; Cit lim = *Citrus limon*; Cleo gya = *Cleome gynandra*; Gom fru = *Gomphocarpus fruticosus*; Ipo bat = *Ipomoea batatas*; Mor ole = *Moringa oleifera*; Ozo pan = *Ozoroa paniculosa*; Pel afr = *Peltophorum africanum*; Psi gua = *Psidium guajava*; San tri = *Sansevieria trifasciata*; Sen ita = *Senna italica*; Tri ter = *Tribulus terrestris*.

Table 5.6. Concentrations of hazardous elements in W leaves (µg g^{-1} dry weight). Trees first followed by forbs and succulents. $*Gomphocarpus fruticosus* was noted for both food and medicinal use (Mogale *et al*., 2019). The highest and lowest means are in bold.

Medicinal

	Al	As	Cd	Co	Cr	Cu	Hg	Mn	Mo	Ni	Pb	Sb	V	Zn
Car pap	166.6	0.21	0.12	62.39	28.41	4.63	9.13	36.24	2.41	9.10	0.21	0.22	0.83	14.99
Cit lim	91.65	0.18	0.05	18.41	7.99	5.88	0.99	87.6	0.46	4.46	0.21	0.65	0.63	24.04
Mor ole	109.1	0.20	0.07	174.5	14.81	4.46	15.39	33.55	0.56	1.57	0.65	0.05	0.59	9.74
Ozo pan	94.24	0.13	0.03	5.78	20.33	7.58	1.55	14.24	0.23	1.18	0.26	0.02	0.75	17.5
Pel afr	144.3	0.07	0.15	16.17	12.27	3.66	3.21	44.6	0.14	3.13	0.26	0.03	0.41	17.08
Psi gua	100.5	0.11	0.08	13.83	13.93	5.21	2.83	20.2	0.64	3.26	0.23	0.67	0.71	21.34
Arg och	164.5	0.31	0.25	51.47	51.47	6.88	5.62	112.7	20.24	81.66	0.23	0.56	1.27	37.13
Car edu	32.5	0.24	0.07	69.45	2.70	1.74	4.56	14.63	0.266	0.96	0.10	0.01	0.46	13.96
Cat ros	60.77	0.26	0.15	54.98	12.44	3.38	4.96	23.57	0.28	2.94	0.20	0.03	0.55	11.94
$Gom fru	91.79	0.15	0.11	13.83	21.44	9.64	2.54	94.41	11.62	44.75	0.21	1.26	0.57	18.53
San tri	349.9	0.20	0.07	16.14	7.06	10.51	2.54	12.87	0.14	6.11	0.31	0.03	0.64	15.54
Sen ita	99.63	0.17	0.07	17.89	11.72	6.83	1.84	40.86	0.70	1.92	0.15	0.03	0.62	16.67
Mean	**125.46**	0.19	**0.11**	42.14	17.05	5.87	4.6	44.62	3.14	13.42	0.26	0.29	0.68	18.2
SD	80.7	0.07	0.06	46.9	12.9	2.6	4.1	34.4	6.3	24.7	0.1	0.4	0.2	7

Leafy vegetable

	Al	As	Cd	Co	Cr	Cu	Hg	Mn	Mo	Ni	Pb	Sb	V	Zn
Ama spi	250.7	0.24	0.24	51.76	8.76	6.21	7.06	43.35	0,75	1.7	0.17	0.03	0.65	66.14

Cle gyn	255.5	0.18	0.39	270.1	25.79	8.41	31	45.73	2,07	5.08	0.32	0.031	0.84	30.07
$Gom fru	91.79	0.15	0.11	13.83	21.44	9.64	2.54	94.41	11,62	44.75	0.21	1.26	0.57	18.53
Ipo bat	118.1	0.15	0.11	24.38	18.07	5.642	5.43	109.8	0,52	3.67	0.16	0.02	0.65	21.78
Tri ter	113.3	0.23	0.42	47.05	13.47	7.83	8.84	29.03	0,35	3.26	0.21	0.03	0.58	46.07
Mean	165.**88**	**0.19**	0.26	81.42	17.51	7.55	10.99	64.46	3.07	11.69	0.22	0.28	0.67	36.52
SD	80.3	0.1	0.2	106.6	6.5	1.6	11.5	35.4	4.8	18.5	0.1	0.6	0.1	19.7
Mean (all species)	**137.35**	0.19	**0.15**	53.69	17.18	6.36	6.48	50.46	3.12	12.92	0.25	0.29	0.67	23.59
SD	80.3	0.1	0.1	68.6	11.2	2.4	7.3	34.8	5.7	22.5	0.1	0.4	0.2	14.3

Ama spi = *Amaranthus spinosus*; Arg och = *Argemone ochroleuca*; Car edu = *Carpobrotus edulis*; Car pap = *Carica papaya*; Cat ros = *Catharanthus roseus*; Cit lim = *Citrus limon*; Cleo gya = *Cleome gynandra*; Gom fru = *Gomphocarpus fruticosus*; Ipo bat = *Ipomoea batatas*; Mor ole = *Moringa oleifera*; Ozo pan = *Ozoroa paniculosa*; Pel afr = *Peltophorum africanum*; Psi gua = *Psidium guajava*; San tri = *Sansevieria trifasciata*; Sen ita = *Senna italica*; Tri ter = *Tribulus terrestris*.

Regression analysis produced a significant positive relation between Cr on leaf surface to total Cr of leaf (R^2 = 0.986, p<0.001) (Fig. 5.5a) and Cr in leaf tissue (R^2 = 0.740, p<0.001) (Fig. 5.5b).

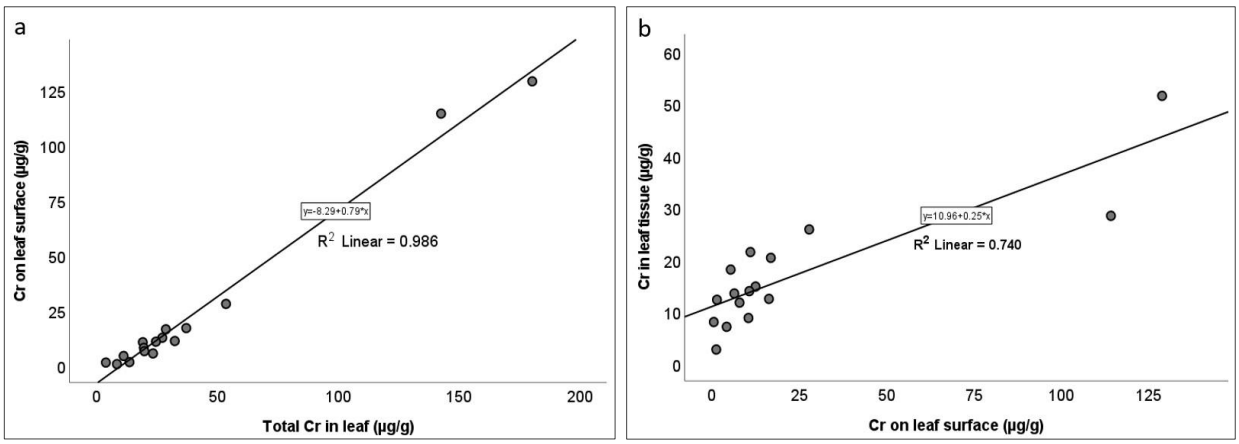

Figure 5.5. Relation between Cr on leaf surface to, a. total Cr of leaf; b. Cr in leaf tissue.

Based on the four Cr concentration categories, hierarchical cluster analysis clustered sampling sites into two groups (Fig. 5.6a). Cluster 1 (C1) incorporated all sites but S1 (the tailings facility) that represented cluster 2 (C2). S1 had higher mean Cr values for all categories. Cluster analysis on mean values for Cr concentration on leaf surface (Fig. 5.6b), created two clusters, where C1 included all sites except site 1 and 2 that were included under C2. S1 and S2 again had higher Cr values than other sites. The home garden, S2, was the closest locality to the tailing facility, S1.

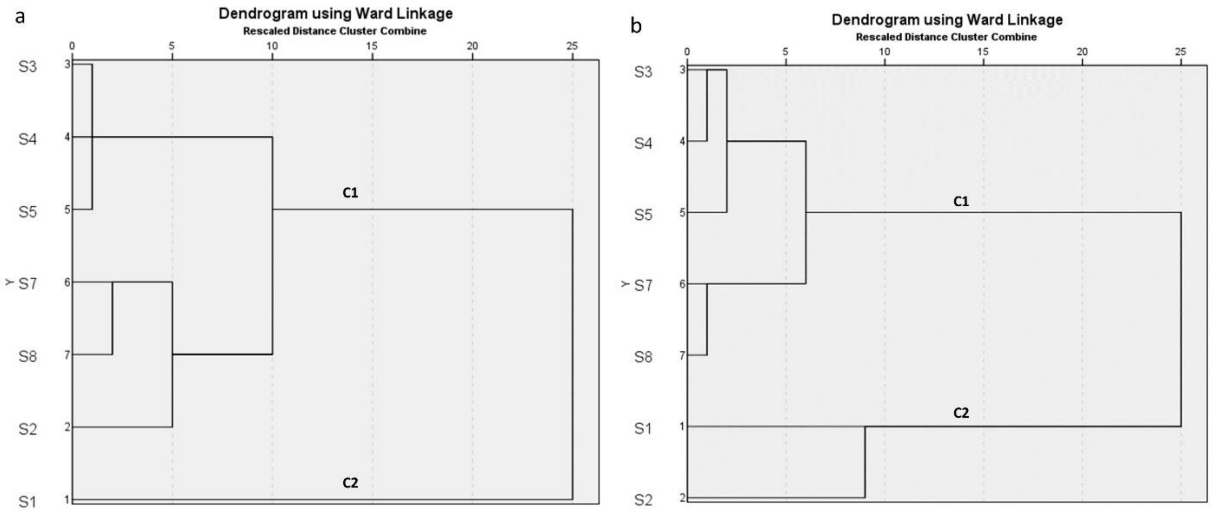

Figure 5.6. Cluster dendrograms featuring the two sampling site groups based on the mean values for, a. the four leaf Cr concentration categories; b. Cr concentration on leaf surface. The four leaf Cr concentration categories are total Cr of leaf, Cr in leaf tissue, Cr on leaf surface and total Cr(VI) of leaf.

5.3.2 Influence of variables

5.3.2.1 Growth form

The highest means for total, tissue and surface Cr concentration categories were recorded from forbs (Fig. 5.7). Succulents had the lowest values for all Cr concentration categories but Cr(VI) (Table 5.7, Fig. 5.7). Other than the five species including one tree and four forbs, the rest (~ 69%) had higher Cr concentrations in leaf tissue than on leaf surface (Table 5.7). Among forbs, 50% had higher Cr on leaf surface, while 83% of trees and all succulents had leaf tissue Cr amounts higher than surface Cr amounts (Table 5.7). Around 4- and 2.5-fold higher Cr concentrations on leaf surface was determined in *C. papaya* and *A. ochroleuca*, respectively. The two trees, *C. limon* and *P. africanum*, on the other hand, had nearly 14.5- and 8-times higher Cr in leaf tissue than on leaf surface. Two deciduous tree species had the highest (*P. africanum*) and lowest (*M. oleifera*) total Cr(VI) concentrations. The outcome of a Kruskal-Wallis test showed no significant difference among growth forms regarding any of the Cr concentration categories (Table D1, Appendix D).

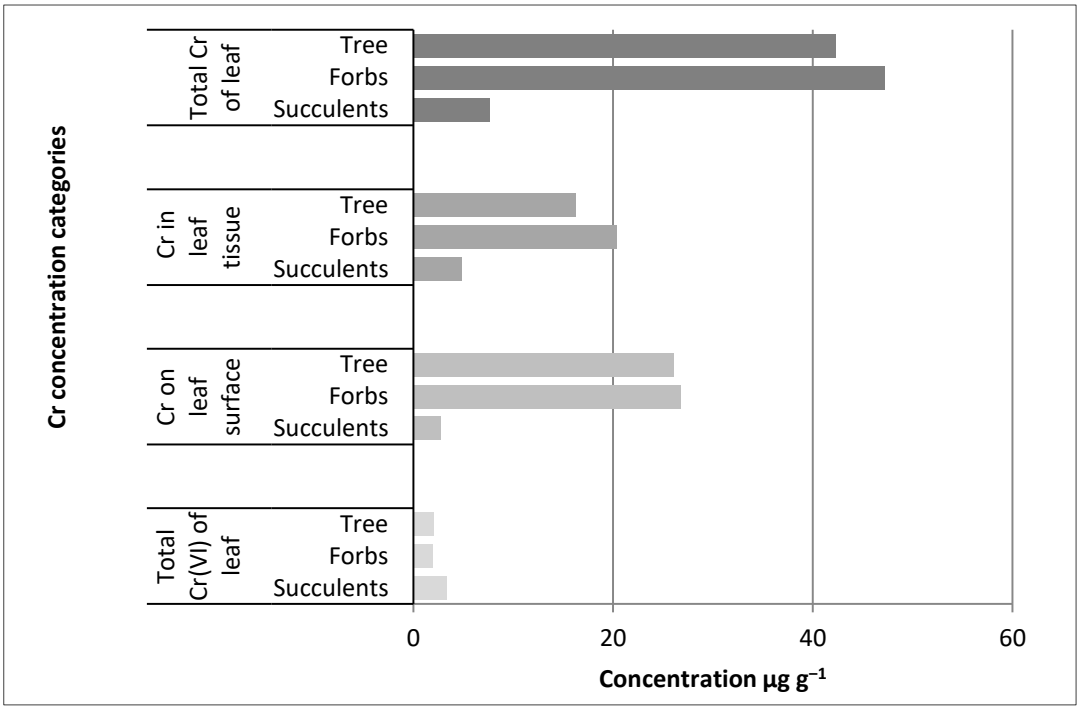

Figure 5.7. Cr concentration means per growth form.

Table 5.7 Foliar Cr concentrations (μg g^{-1} dry weight) according to growth forms. Highest values are in bold.

Plant species	Total Cr of leaf	Cr in leaf tissue	Cr on leaf surface	Total Cr(VI) of leaf
Trees				
ˣCar pap	142.6	28.41	114.19	1.83
Cit lim	8.55	7.99	0.55	1.18
Mor ole	27.32	14.81	12.51	0.87
Ozo pan	37.21	20.33	16.88	1.98
Pel afr	13.73	12.27	1.46	**3.83**
Psi gua	24.65	13.93	10.72	1.78
Forbs				
ˣAma spi	19.24	8.77	10.47	3.21
ˣArg och	**180.3**	**51.47**	**128.83**	1.99
ˣCat ros	28.78	12.44	16.34	1.63
ˣCle gyn	53.65	25.79	27.86	1.58
Gom fru	32.47	21.44	11.03	2.01
Ipo bat	23.46	18.07	5.39	3.68
Sen ita	19.64	11.72	7.92	1.94
Tri ter	19.9	13.47	6.43	2.94
Succulents				
Car edu	3.96	2.7	1.26	2.85
San tri	11.3	7.07	4.2	1.37

ˣPlant species with Cr on leaf surface > Cr in leaf tissue. Ama spi = *Amaranthus spinosus*; Arg och = *Argemone ochroleuca*; Car edu = *Carpobrotus edulis*; Car pap = *Carica papaya*; Cat ros = *Catharanthus roseus*; Cit lim = *Citrus limon*; Cleo gya = *Cleome gynandra*; Gom fru = *Gomphocarpus fruticosus*; Ipo bat = *Ipomoea batatas*; Mor ole = *Moringa oleifera*; Ozo pan = *Ozoroa paniculosa*; Pel afr = *Peltophorum africanum*; Psi gua = *Psidium guajava*; San tri = *Sansevieria trifasciata*; Sen ita = *Senna italica*; Tri ter = *Tribulus terrestris*.

5.3.2.2 Polluters

Kruskal-Wallis test revealed plant leaves sampled from localities with four to six different types of polluters within the 10 km periphery had significantly higher (p<0.05) concentrations of total Cr of leaf and Cr on leaf surface compared to that collected from localities impacted by less than four polluters within that periphery (Table D2, Appendix D).

5.3.2.3 Soil

Soils were mostly alkaline, and pH ranged between 6.24–7.95 (Table 5.8). Handheld XRF detected eleven major elements, i.e. Al, Ca, Cr, Fe, Mg, Mn, Ni, Si, Sr, Ti and V in all soil samples (Table 5.8). Site 1 (tailing facility) had the highest concentrations of total Cr, Cr(VI) and soluble Cr (Table 5.8). The lowest concentrations of total Cr, Cr(VI) and soluble Cr were detected for sites 7 (home garden), 4 (rangeland near mine) and 8 (rangeland, natural chromitite outcrop), respectively. Regression analysis determined non-significant positive relation between soluble soil Cr and Cr in leaf tissue.

Based on mean values of total Cr in sampled soils, hierarchical cluster analysis formed two clusters. The first cluster (C1) included soil with the lowest total Cr concentrations, namely the two home gardens S3 and S7 and rangeland, S4, near S7. Other rangelands (i.e. S1, S5 and S8) and the home garden S2 were grouped under cluster two (C2) (Fig. 5.8). These sites in C2 had heightened Cr exposure from anthropogenic activities such as tailing disposal (site 1 and 2) and extensive ore excavation (site 5) or natural chromitite outcrops (site 8). Kruskal-Wallis test determined a significant difference (p<0.05) in total soil Cr concentrations between the two sampling site groups formed after cluster analysis outcome.

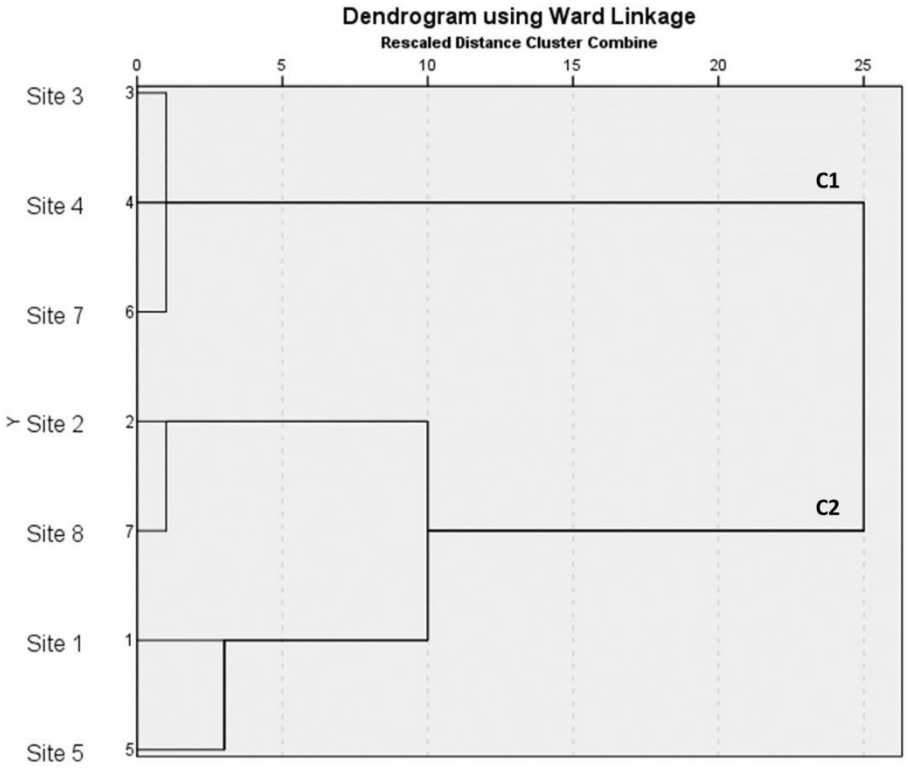

Figure 5.8. Cluster dendrogram featuring two groups based on mean values of total Cr in soil per sampling site.

Table 5.8. Soil pH and concentrations of major elements (µg g^{-1}) detected. The highest values for soluble Cr, Cr(VI) and total Cr are in bold.

Sites	pH (KCl)	Soluble Cr	Cr(VI)	Total Cr	Al	Ca	Fe	Mg	Mn	Ni	Si	Sr	Ti	V
Site 1	7.89	**0.01119**	**4.64**	**174389.4**	58902.5	20313.01	123936	73462.91	1988.86	662	133723.4	25.88	3514.36	1357.08
Site 2	7.52	0.004116	2.969	89474.9	61491.12	29356.81	107093.5	52454.24	2523.24	606.34	197249.1	56.58	2793.8	780.97
Site 3	6.24	0.007838	3.815	3210.98	33555.12	18268.76	77567.29	25014.07	1836.26	802.6	219273.5	19	1414.62	145.05
Site 4	7.95	0.00249	2.124	3000.5	69244.74	74943.72	50435.37	32071.37	1142.84	499.06	225417.5	198.26	811.23	158.95
Site 5	7.85	0.005325	2.746	144215.2	58502.74	22767.7	130396.8	53647.54	2902.68	695.63	175984.5	50.63	3393.16	1147.92
Site 7	7.70	0.01032	2.412	2326.39	59526.14	69436.93	42082.78	16693.16	924.37	237.79	219004.1	194.28	1226.84	120.98
Site 8	6.70	0.002146	2.167	84079.6	156096.4	48071.62	91224.2	15991.94	2863.81	407.17	232162.1	166.31	4113.21	1163.6

5.3.3 Health risk assessments

Several toxic elements were detected in UW and W leaves of the sampled food and medicinal plants (Table 5.5, 5.6). Other than Cr, Al, Hg and Zn (in both UW and W) and Co (W) concentrations exceeded the WHO/FAO (2010) recommended safe limits, i.e. Al, 10–50; Hg, 0.001; Zn, 9.4 and Co, 50 µg g^{-1} in plants (Chary *et al*., 2008; Okem *et al*., 2014). Al had the highest mean values in UW and W leaves of both types of useful plants. Concentrations of Al, Cr and Ni in UW leaves were 4, 3 and 2 times higher, respectively than that of W leaves.

5.3.3.1 Non-carcinogenic risk

Among the 14 elements, the estimated EDI indicated a far higher daily intake of Al than the recommended oral RfD via UW (1430-fold) and W (234-fold) leaves. For Co, EDI was 1.3 times higher for W leaves than the recommended oral RfD (Table 5.9). Except for Al, HQ values for all elements were within the safe limit for both leaf treatments, i.e. UW and W. Cr had the lowest HQ values for UW and W leaves. All corresponding HI values (UW and W) exceeded the safe limit by several folds (Table 5.9).

Table 5.9. Summary of non-carcinogenic risk assessments for the five leafy vegetables. Oral RfD and EDI in mg kg^{-1} body weight day^{-1}. EDI > RfD (oral), and HQ and HI values > 1 are in bold. UW, unwashed leaves; W, washed leaves.

Elements	Oral RfD	EDI		HQ	
		UW	W	UW	W
Al	0.0004	**0.5720**	**0.0805**	**665.6949**	**93.7625**
As	0.0003	0.0001	0.00009	0.1850	0.1476
Cd	0.001	0.0001	0.0001	0.0555	0.0583
Co	0.03	0.0211	**0.0395**	0.3287	0.6136
Cr	1.5	0.0144	0.0085	0.0044	0.0026
Cu	0.04	0.004	0.0036	0.0475	0.0426
Hg	0.1	0.0033	0.0053	0.0156	0.0248
Mn	0.14	0.0377	0.0313	0.1255	0.1041
Mo	0.005	0.0003	0.0014	0.0333	0.1386
Ni	0.02	0.0031	0.0056	0.0728	0.1322
Pb	0.004	0.0002	0.0001	0.0237	0.0124
Sb	0.0004	0.00002	0.0001	0.0245	0.1560
V	0.009	0.0006	0.0003	0.0352	0.0167
Zn	0.3	0.0205	0.0177	0.0319	0.0275
HI	**–**	**–**	**–**	**666.679**	**95.24**

5.3.3.2 Carcinogenic risk

CR values showed different elemental trend for UW (total Cr > Ni > total Cr(VI) > As > Cd > Pb), W (Ni > total Cr > As > Cd > Pb) and S (Total Cr > As > Pb) (Table 5.10). Except for Pb, elements exceeded the recommended safe limit (> 1×10^{-6}) for all concentration categories, i.e. UW, W and S (Fig. 5.9, 5.10). Cd values were between 1×10^{-6} and 1×10^{-4} for UW and W. Total Cr(VI) had values between 1×10^{-4} and 1×10^{-3} for UW. For total Cr, CR values exceed 1×10^{-3} for UW, W and S category. Greater than 1×10^{-3} CR values were observed for Ni in UW and W leaves. Based on such values, total Cr, total Cr(VI) and Ni were grouped as elements with high CR (Fig. 5.9) while As, Cd and Pb were grouped as elements with low possible CR (Fig. 5.10).

Table 5.10. Carcinogenic risk values for total, leaf tissue and leaf surface elemental concentration categories for the leafy vegetables. Highest values are in bold. ND, not determined; NE, not estimated due to higher elemental concentration in W than UW; NT, not tested; S, the surface of leaves; UW, unwashed leaves; W, washed leaves.

Elements	UW	W	S
As	8.33E–05	6,65E–05	1.68E–05
Cd	2.11E–05	2,22E–05	NE
Total Cr	**3.36E–03**	**1.98E–03**	**1.38E–03**
Cr(VI)	3.67E–04	NT	ND
Ni	**2.48E–03**	**4.49E–03**	NE
Pb	8.07E–07	1.73E–06	4.23E–07

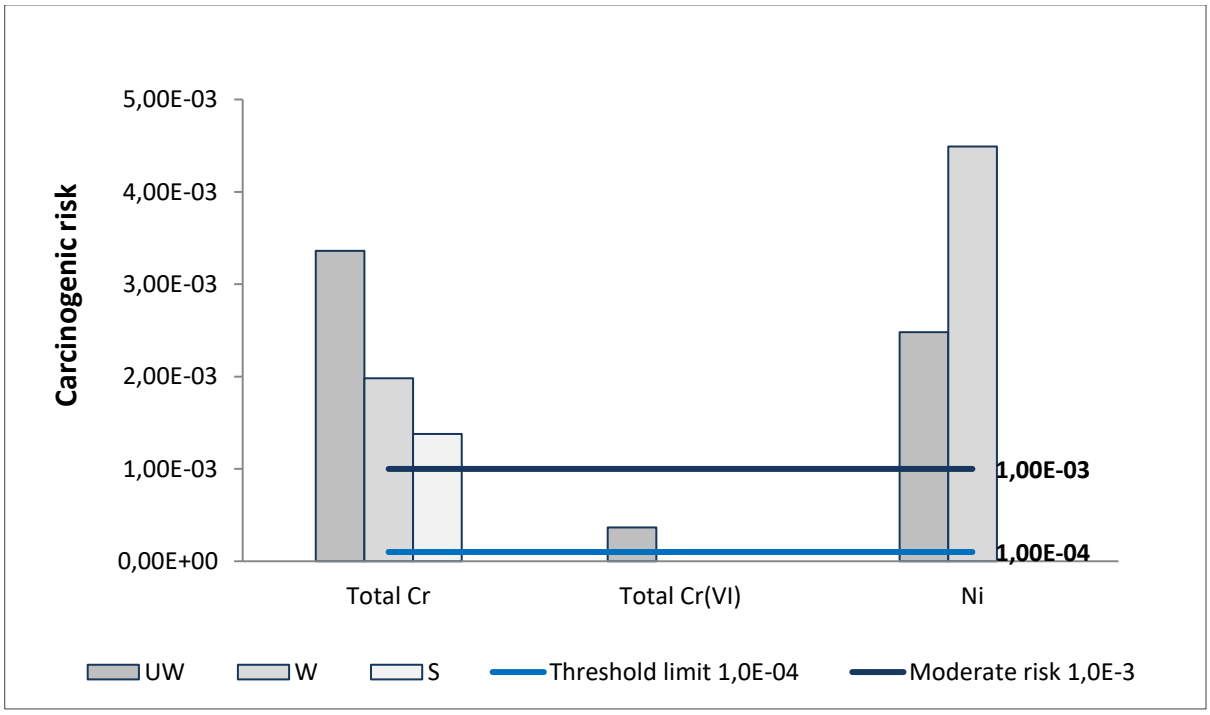

Figure 5.9. Estimated carcinogenic risk for Ni, total Cr and total Cr(VI)).

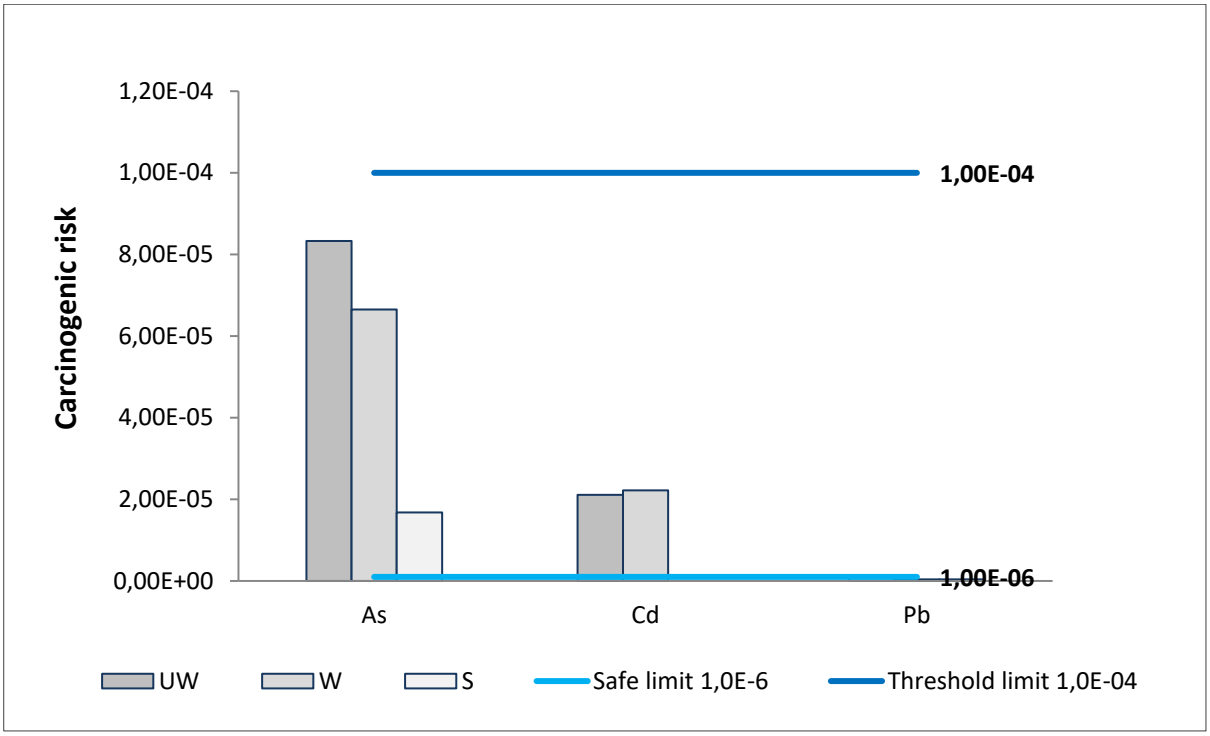

Figure 5.10. Estimated carcinogenic risk for As, Cd and Pb.

5.4 Discussion

5.4.1 Cr contamination of useful plant leaves

Mean total Cr concentrations in UW and W leaves of food and medicinal plant leaves exceeded the recommended international permissible limits (Kumar *et al*., 2018; Pajević *et al*., 2018) by multiple folds that confirmed foliar Cr contamination in these mining-smelting areas in Sekhukhuneland. Elevated Cr levels in leaves of local vegetation are common in Cr mining localities (Mohanty *et al*., 2012; Reddy *et al*., 2012).

Comparable total Cr in sampled leaves from rangelands and home gardens indicated Cr contamination of both of these common plant sources in the study area. Nationally, such sources are considered as easily accessible and affordable especially in rural areas (Drimie *et al*., 2009; Faber *et al*., 2010; Semenya & Potgieter, 2014; Mogale *et al*., 2019), yet are poorly investigated for metal pollution in mining-smelting regions. Present findings, therefore, calls for future attention in this regard.

For polluted areas around chromite (economically viable Cr ore) mines, accumulation in plant leaves is primarily reported as a result of waste-water irrigation (Mohanty *et al*., 2012) and polluted soil (Reddy *et al*., 2012), but is scarcely linked to dust particles dispersed from mines. Significantly high Cr concentrations in UW than W leaves in the present study provide evidence of Cr containing dust as a major contamination source in the region. Majority of the species (around

69%) in the present study had higher Cr amounts in leaf tissue than on the surface suggesting efficient accumulation. However, in this regard indicated significant contribution of dust borne Cr to tissue Cr may highlight possible foliar uptake of Cr. This is also probable considering the generally accepted low translocation rate of Cr from root to leaf (Oliveira, 2012). Similarly, past studies have suggested foliar uptake of heavy metals in metal mining and smelting areas (Bi *et al*., 2009; Liu *et al*., 2019; Wang *et al*., 2019). Foliar uptake of Cr should be investigated further to substantiate present findings.

Total Cr levels in UW leaves were much higher in the present study compared to that of UW lingonberries (*Vaccinium vitis-idaea* L.) reported by Pöykiö *et al.* (2005) from an open cast chromium mine and ferrochrome smelter impacted region. This could be attributed to multifaceted environmental Cr exposure in Sekhukhuneland. A report by Sokol *et al.* (2010), indicated hazardous dust as a probable contamination source of vegetation in areas polluted by the Cr metallurgical industry generated waste. The authors noted a wide range for Cr concentrations in analysed plant leaves, with some far exceeding the Cr levels determined in this Sekhukhuneland study.

Presence of Cr(VI) in UW leaves confirmed the environmental availability of this hazardous Cr species in the investigated region. Cr(VI) availability and accumulation in various plant parts from Cr based industrial and geogenic Cr enriched areas (Economou-Eliopoulos *et al*., 2012), natural Cr outcrops in South Africa (chromitite substrate) and Russia (ultrabasic massif substrate) (Panichev *et al*., 2005) and ferrochrome smelter impacted areas in South Africa (Owolabi *et al*., 2016) has been reported. Outcomes from the present study indicated sites within 20 km (which was the maximum sampling distance in the present study) from the nearest mine were under the influence of hazardous Cr(VI) pollution. As environmental Cr(VI) is mainly sourced from anthropogenic activities rather than the rare occurrence of natural oxidation of geogenic Cr(III) (Kimbrough *et al.*, 1999; Oze *et al*., 2004), the same can be suggested for Sekhukhuneland. This is an important outcome considering the far greater biological toxicity potential of Cr(VI) than that of Cr(III) (Kimbrough *et al.*, 1999; Dhal *et al.*, 2010a; Oliveira, 2012). A comparative study on UW and W leaves may indicate the contribution of dust in this regard. Future investigators may determine the maximum Cr(VI) impact zone around mines and smelters in Sekhukhuneland.

5.4.2 Influence of variables

Comparable mean total Cr levels observed in studied growth forms suggested susceptibility of all types to Cr contamination in the region. Trees and forbs are the most cultivated species (trees > forbs) in home gardens of traditional healers in Limpopo (Semenya & Potgieter, 2014). This indicates awareness to be initiated regarding the safety of useful plants in the region especially

as Cr is noted as one of the most found heavy metals in traditional herbal remedies to cause mortalities in South Africa (Steenkamp *et al.*, 2002). Forbs could be more susceptible to Cr dust pollution than trees due to a higher deposition possibility of dust generated during ore transportation in the area (Tshehla & Djolov, 2018) or polluted soil dust in general (Dreicer *et al*., 1984). Trees could be studied further for Cr accumulation in leaf tissue. Cr(VI) accumulation in succulent leaves requires further attention as various species from this growth form were often noted to accumulate elevated concentrations of metals from ultramafic outcrops (Siebert *et al*., 2018) and tailing soils (Dobbins *et al*., 2021) in South Africa. Small sample size could have influenced the outcome of the present study indicating a need for elaborate future investigation.

In the present study, plant leaves sampled from localities that had four to six different types of Cr polluters within the 10 km periphery had significantly higher Cr amounts compared to the species exposed to three or fewer pollution sources within that zone. A far greater influence of proximity to several major polluters (i.e. mines, roads, and ferrochrome smelters) on metal accumulation by plant leaves is indicated. Similarly, variation in Cr accumulation by vegetation was often related to proximity to Cr mines, smelters and waste sites (Pöykiö *et al*., 2005; Sokol *et al*., 2010). However, no literature was obtained determining the influence of the number of polluters in this regard, with this Sekhukhuneland study the first to report on this issue.

Concentrations of total Cr in investigated localities in Sekhukhuneland were higher than the permissible Cr concentration (80 µg g^{-1}) reported for South African agricultural soils (Herselman *et al*., 2005). However, except the tailing and abandoned Cr excavation site, total soil Cr (that is primarily Cr(III)) and Cr(VI) concentrations were within South African limits suggested for industrial and commercial locations and informal/formal residential areas (Department of Environmental Affairs, 2010). Nevertheless, like plant leaves, the presence of Cr(VI) in all sampling soils indicates probable anthropogenic soured Cr(VI) pollution.

The lowest soluble Cr concentration in natural Cr outcrop in the present study showed low solubility of geogenic Cr as reported previously (Oze *et al*., 2004; Oliveira, 2012). This may explain a positive but non-significant relation between soil soluble Cr and Cr in leaf tissue in this study. Furthermore, though high soil Cr was observed in localities characterized by both Cr-outcrops and anthropogenic pollution, distinctly high Cr concentrations in leaves sampled from tailings than the rest of the study localities imply elevated phytoavailability of Cr in these sites (Dhal *et al*., 2010b; Oliveira, 2012; Bolaños-Benítez *et al*., 2018). This can be explained by the conclusion drawn by Sokol *et al*. (2010), which stated anthropogenic activity discarded Cr may leach rapidly from waste localities and hence its bioavailability to local vegetation is increased.

Higher foliar dust content was linked to the tailing site and its surroundings. Mine tailings are known as major dust polluters due to wind erosion of discarded hazardous materials (Stovern *et al*., 2016). Such erosion effect could become excessive in semi-arid regions like Sekhukhunealnd (Siebert *et al*., 2002) where low moisture in air and soil and scarce plant cover on tailings enhance the process further (Stovern *et al*., 2016). The mountainous topography of the region may influence wind movement and consequent dust dispersion from highly polluted tailing facilities to nearby localities in Sekhukhuneland (Stovern *et al*., 2016; Tshehla & Wright, 2019).

5.4.3 Health risk associated with toxic elements

Besides Cr, presence of fourteen other hazardous elements (metals and metalloids) in both W and UW leaves of investigated food and medicinal plants in Sekhukhuneland is of concern based on their potency to induce various health ailments in humans (Oliveira, 2012; Kim *et al*., 2016; Carver & Gallicchio, 2018). In addition to Cr, Al, Co, Hg and Zn concentrations in leaves were above the recommended safe limits in plants (Chary *et al*., 2008; Malan *et al*., 2015; Kohzadi *et al*., 2018) suggesting substantial availability of several toxic elements to plant leaves in these localities. Multiple times higher concentration of Al, Cr and Ni in UW leaves than W ones suggested dust as a major contributor of these elements in Sekhukhuneland.

5.4.3.1 Non-carcinogenic risk

Among the elements, Al had extremely high EDI and HQ values for both UW and W leaves than the recommended safe limits which was indicative of considerable health threat to consumers. Therefore, Al should be investigated further across a larger number of taxa and in more localities to explore its pollution extent in Sekhukhuneland. Comparable concentrations of Al in medicinal plant species have been reported in South Africa (Okem *et al*., 2014). Al accumulation by various food (Antoine *et al*., 2017; Ghasemidehkordi *et al*., 2018) and medicinal plants (Kohzadi *et al*., 2018) was reported globally.

For Sekhukhuneland, greater than 1 HI values for UW and W leaves indicated considerable health threat to consumers due to lifelong ingestion of multiple toxic elements. About 7-fold higher HI value for UW leaves than that of W ones confirmed greater health threat associated with hazardous dust contaminated plant leaves.

5.4.3.2 Carcinogenic risk

Other than Pb, carcinogenic risk (CR) estimated for elements (Ni and Total Cr > Total Cr(VI) > As and Cd) revealed probable lifelong ingestion linked risk to consumers. While As and Cd could present negligible risk, total Cr(VI) in UW leaves will possibly pose a higher carcinogenic risk and total Cr and Ni in both UW and W leaves showed the highest CR values that require immediate

attention. In addition, when surface total Cr was considered, the risk was concerning that again was suggestive of considerable carcinogenic threat associated with dust borne Cr in the region. In this regard, it should be mentioned here, ingestion associated carcinogenicity of Cr species is yet to be proved and accepted by US EPA and WHO/IARC as both these regulatory bodies concluded consumption linked Cr exposure pathway as 'likely to be carcinogenic to human' (Yaman, 2020).

Varying degree of health hazards was frequently noted for vegetables harvested from mining and smelting areas (Liu *et al*., 2019; Wang *et al*., 2019; Antisari *et al*., 2020). For Sekhukhuneland, UW leafy vegetables presented a higher non-carcinogenic and carcinogenic health risk than W ones. However, for both categories of human health risk (i.e. non-carcinogenic and carcinogenic), high values estimated for even well-washed leaf materials is concerning.

Nationally, sufficient reports are available regarding heavy metal and metalloid contamination of food (Malan *et al*., 2015; Mbangi *et al*., 2018) and medicinal plants (Mtunzi *et al*., 2012; Street, 2012; Okem *et al*., 2014), yet such data is scarce specifically for Cr mining areas and especially regarding dust contamination and associated health risk estimations, of which this Sekhukhuneland study makes a considerable contribution.

5.4.4 Study limitations

Considering the constrains of handheld XRF such as lower limits of element detection compared to other methods (e.g. Atomic Absorption Spectroscopy and Inductively Coupled Plasma Atomic Emission Spectroscopy), less accuracy for detecting lighter elements, interelemental interference and possible variation in data quality and accuracy with soil composition, particle size and its distribution in soil and sample preparation (Galuzska *et al*., 2015; Weindorf & Chakraborty, 2016; Koch *et al*., 2017), results of XRF and other methods can be compared to ensure data reliability further. With the reported dependency of locals on home garden-grown crops in Sekhukhune District (Drimie *et al*., 2009) and comparatively high intake quantity and consumption frequency of wild-harvested leafy vegetables in rural areas in Limpopo (Faber *et al*., 2010), the health risk estimated in the present study may escalate further. Furthermore, when one considers the use of contaminated medicinal plant leaves the lifelong health risk is expected to be higher. Awareness towards health risk associated with dust polluted leaves must be initiated and sufficient washing of aerial plant parts should be promoted among local inhabitants. A shift in regional rainfall regime (Drimie *et al*., 2009; Quinn *et al*., 2011) due to climate change could further complicate the situation in terms of adequate water availability in these rural areas. This becomes important considering the estimated health threat associated with metalliferous dust contaminated useful plant leaves in Sekhukhuneland.

Summary

Leaves of food and medicinal plants from Sekhukhuneland mining regions accumulated Cr at concentrations far higher than international safe limits that confirmed Cr contamination. In addition, Cr(VI) accumulation by plant leaves was indicative of the availability of the most toxic Cr species in these mining and smelting areas. The possibility of foliar Cr uptake was indicated that should be investigated further. More useful trees and forbs should be targeted to study their Cr accumulation potential in leaf tissue and on the leaf surfaces, respectively. Special attention should be allocated to explore Cr(VI) accumulation potential of the succulents. It seems that the collective influence of polluter proximity, and the number and types of Cr emitters, could be critical regarding Cr contamination of plant leaves in the study region. Besides Cr, dust borne Al and Ni contributed significantly towards higher elemental amounts in plant leaves. Other than Cr, Al, Co, Hg and Zn, exceeded recommended international safe limits in plants. As a consequence, high cumulative lifelong non-carcinogenic risk was estimated as a result of exposure to multiple hazardous elements via ingestion of both W and UW leaf materials to which Al contributed the most. Total Cr, total Cr(VI) and Ni might pose substantial lifelong carcinogenic risk (CR) to consumers of leafy vegetables. Future studies may focus on Al and Ni toxicity impact further. High metal accumulation in plant leaves as observed in the present chapter motivated to investigate metal accumulation further by a larger group of dominant species (47 species in total including indigenous, endemic and exotic species) observed in Sekhukhuneland catena. Results are presented in the next chapter that further reports on the phytoremediation prospect of such species.

References

Agazzi, A. & Pirola, C. 2000. Fundamentals, methods and future trends of environmental microwave sample preparation. *Microchemical Journal*, 67:337–341.

Antisari, L.V., Bini, C., Ferronato, C., Gherardi, M. & Vianello, G. 2020. Translocation of potential toxic elements from soil to black cabbage (*Brassica oleracea* L.) growing in an abandoned mining district area of the Apuan Alps (Tuscany, Italy). *Environmental Geochemistry and Health*, 42:2413–2423.

Antoine, J.M.R., Fung Hu, L.A. & Grant, C.N. 2017. Assessment of the potential health risks associated with the aluminium, arsenic, cadmium and lead content in selected fruits and vegetables grown in Jamaica. *Toxicology Reports*, 4:181–187.

Ashley, K., Howe, A.M., Demange, M. & Nygren, O. 2003. Sampling and analysis considerations for the determination of hexavalent chromium in workplace air. *Journal of Environmental Monitoring*, 5:707–716.

Bi, X., Feng, X., Yang, Y., Li, X., Shin, G.P.Y., Li, F., … Fu, Z. 2009. Allocation and source attribution of lead and cadmium in maize (*Zea mays* L.) impacted by smelting emissions. *Environmental Pollution,* 157(3):834–839.

Bolaños-Benítez, V., van Hullebusch, E., Lens, P., Quantin, C., van de Vossenberg, J., Subramanian, S. & Sivry, Y. 2018. (Bio)leaching behavior of chromite tailings. *Minerals,* 8(6), 261. https://doi.org/10.3390/min8060261

Cai, K., Li, C., Song, Z., Gao, X. & Wu, X. 2019. Pollution and health risk assessment of carcinogenic elements As, Cd, and Cr in multiple media - a case of a sustainable farming area in China. *Sustainability*, 11(19):1–22.

Can, H., Ozyigit, I.I., Can, M., Hocaoglu-Ozyigit, A. & Yalcin, I.E. 2020. Environment-based impairment in mineral nutrient status and heavy metal contents of commonly consumed leafy vegetables marketed in Kyrgyzstan: a case study for health risk assessment. *Biological Trace Element Research*, 199:1123–1144.

Carver, A. & Gallicchio, V.S. 2018. Heavy metals and cancer. In: Atroshi, F., ed. *Cancer causing substances*. Available from Intech Open eBook Collection. www.intechopen.com/books/cancer-causing-substances/heavy-metals-and-cancer Date of access: 11 Sep. 2020.

Chary, N.S., Kamala, C.T. & Raj, D.S.S. 2008. Assessing risk of heavy metals from consuming food grown on sewage irrigated soils and food chain transfer. *Ecotoxicology and Environmental Safety*, 69:513–524.

Chen, M. & Ma, L.Q. 1998. Comparison of four US EPA digestion methods for trace metal analysis using certified and Florida soils. *Journal of Environmental Quality*, 27(6):1294–1300.

Coetzee, J.J., Bansal, N. & Chirwa, E.M.N. 2018. Chromium in environment, its toxic effect from chromite-mining and ferrochrome industries, and its possible bioremediation. *Exposure and Health*, 12:51–62.

Cox, X.B., Linton, R.W. & Butler, F.E. 1985. Determination of chromium speciation in environmental particles. Multitechnique study of ferrochrome smelter dust. *Environmental Science & Technology,* 19(4):345–352.

Department of Environmental Affairs (South Africa). 2010. The Framework for the Management of Contaminated Land. Available online: http://sawic.environment.gov.za/documents/562.pdf Accessed: 15 Sep. 2020.

Dhal, B., Thatoi, H.N., Das, N.N. & Pandey, B.D. 2010a. Reduction of hexavalent chromium by *Bacillus* sp. isolated from chromite mine soils and characterization of reduced product. *Journal of Chemical Technology & Biotechnology,* 85(11):1471–1479.

Dhal, B., Das, N.N., Pandey, B.D. & Thatoi, H.N. 2010b. Environmental quality of the Boula-Nuasahi chromite mine area in India. *Mine Water and the Environment,* 30(3):191–196.

Dobbins, D.C., Marcelo-Silva, J. & Siebert, S.J. 2021. Screening the phytoextractability of trace metals by *Aloe cryptopoda* Baker and *Aloe vera* (L.) Burm.f. cultivated on mine tailings. *South African Journal of Botany*, 140:110–113.

Dreicer, M., Hakonson, T.E., White, G.C. & Whicker, F.W. 1984. Rainsplash as a mechanism for soil contamination of plant surfaces. *Health Physics*, 46(1):177–187.

Drimie, S., Germishuyse, T, Rademeyer, L. & Schwabe, C. 2009. Agricultural production in Greater Sekhukhune: the future for food security in a poverty node of South Africa? *Agrekon*, 48(3):245–275.

Economou-Eliopoulos, M., Vasilatos, D.A.C. & Megremi, I. 2012. Evaluation of the Cr(VI) and other toxic element contamination and their potential sources: the case of the Thiva basin (Greece). *Geoscience Frontiers*, 3(4):523–539.

Faber, M., Oelofse, A., Van Jaarsveld, P.J., Wenhold, F.A.M. & Jansen van Rensburg, W.S. 2010. African leafy vegetables consumed by households in the Limpopo and KwaZulu-Natal provinces in South Africa. *South African Journal of Clinical Nutrition*, 23(1):30–38.

Gałuszka, A., Migaszewski, Z.M. & Namieśnik, J. 2015. Moving your laboratories to the field - advantages and limitations of the use of field portable instruments in environmental sample analysis. *Environmental Research,* 140:593–603.

Ghasemidehkordi, B., Malekirad, A.A., Nazema, H., Fazilatia, M., Salavatic, H., Shariatifard, N., … Khaneghah, A.M. 2018. Concentration of lead and mercury in collected vegetables and herbs from Markazi province, Iran: a non-carcinogenic risk assessment. *Food and Chemical Toxicology*, 113:204–210.

Gryschko, R., Kuhnle, R., Terytze, K., Breuer, J. & Stahr, K. 2005. Soil extraction of readily soluble heavy metals and As with 1 M NH_4NO_3 solution evaluation of DIN 19730. *Journal of Soils and Sediments*, 5:101–106.

Guerra, F., Trevizam, A.R., Muraoka,T., Marcante, N.C. & Canniatti-Brazaca, S.G. 2012. Heavy metals in vegetables and potential risk for human health. *Scientia Agricola,* 69 (1):54–60.

Herselman, J.E., Steyn, C.E. & Fey, M.V. 2005. Baseline concentration of Cd, Co, Cr, Cu, Pb, Ni and Zn in surface soils of South Africa. *South African Journal of Science*, 101(11–12):509–512.

Jang, M. 2010. Application of portable X-ray fluorescence (pXRF) for heavy metal analysis of soils in crop fields near abandoned mine sites. *Environmental Geochemistry and Health,* 32(3):207–216.

Kalnicky, D.J. & Singhvi, R. 2001. Field portable XRF analysis of environmental samples. *Journal of Hazardous Materials,* 83(1-2):93–122*.*

Kien, C.N., Noi, N.V., Son, L.T., Ngoc, H., Tanaka, S., Nishina, T. & Iwasak, K. 2010. Heavy metal contamination of agricultural soils around a chromite mine in Vietnam. *Soil Science and Plant Nutrition*, 56:344–356.

Kim, H.S., Kim, Y.J. & Seo, Y.R. 2016. An overview of carcinogenic heavy metal: molecular toxicity mechanism and prevention. *Journal of cancer prevention*, 20(4):232–240.

Kimbrough, D.E., Cohen, Y., Winer, A.M., Creelman, L. & Mabuni, C. 1999. A critical assessment of chromium in the environment. *Critical Reviews in Environmental Science and Technology*, 29(1):1–46.

Koch, J., Chakraborty, S., Li, B., Kucera, J.M., Van Deventer, P., Daniell, A., … Weindorf, D.C. 2017. Proximal sensor analysis of mine tailings in South Africa: an exploratory study. *Journal of Geochemical Exploration,* 181:45–57.

Kohzadi, S., Shahmoradi, B., Ghaderi, E., Loqmani, H. & Maleki, A. 2018. Concentration, source, and potential human health risk of heavy metals in the commonly consumed medicinal plants. *Biological Trace Element Research*, 187(1):41–50.

Kumar, N., Kulsoom, M., Shukla, V., Kumar, D., Priyanka, Kumar, S., … Dwivedi, N. 2018. Profiling of heavy metal and pesticide residues in medicinal plants. *Environmental Science and Pollution Research*, 25:29505–29510.

Liu, H-L., Zhou, J., Li, M., Hu, Y., Liu, X. & Zhou, J. 2019. Study of the bioavailability of heavy metals from atmospheric deposition on the soil-pakchoi (*Brassica chinensis* L.) system. *Journal of Hazardous Materials*, 362:9–16.

Ma, G. & Garbers-Craig, A.M. 2006. Cr(VI) containing electric furnace dusts and filter cake from a stainless steel waste treatment plant: Part 2 – formation mechanisms and leachability. *Ironmaking & Steelmaking,* 33(3):238–244.

Malan, M., Müller, F., Cyster, L., Raitt, L. & Aalbers, J. 2015. Heavy metals in the irrigation water, soils and vegetables in the Philippi horticultural area in the Western Cape Province of South Africa. *Environmental Monitoring and Assessment,* 187, art. 4085. https://doi.org/10.1007/s10661-014-4085-y.

Mbangi, A., Muchaonyerwa, P. & Zengeni, R. 2018. Accumulation of multiple heavy metals in plants grown on soil treated with sewage sludge for more than 50 years presents health risks and an opportunity for phyto-remediation. *Water SA*, 44(4):569–576.

Mohanty, M., Pattnaik, M.M., Mishra, A.K. & Patra, H.K. 2012. Bio-concentration of chromium – an in situ phytoremediation study at South Kaliapani chromite mining area of Orissa, India. *Environmental Monitoring and Assessment*, 184(2):1015–1024.

Mogale, M.M.P., Raimondo, D.C. & Van Wyk, B-E. 2019. The ethnobotany of central Sekhukhuneland, South Africa. *South African Journal of Botany,* 122:90–119.

Mtunzi, F., Muleyal, E., Modise, J, Sipamla, A. & Dikiol, E. 2012. Heavy metals content of some medicinal plants from Kwazulu-Natal, South Africa. *Pakistan Journal of Nutrition,* 11 (9):757–761.

Naldrett, A.J., Wilson, A., Kinnaird, J., Yudovskaya, M. & Chunnett, G. 2012. The origin of chromitites and related PGE mineralization in the Bushveld Complex: new mineralogical and petrological constraints. *Mineralium Deposita,* 47:209–232.

Okem, A., Southway, C., Stirk, W.A., Street, R.A., Finnie, J.F. & Van Staden, J. 2014. Heavy metal contamination in South African medicinal plants: a cause for concern. *South African Journal of Botany*, 93:125–130.

Oliveira, H. 2012. Chromium as an environmental pollutant: insights on induced plant toxicity. *Journal of Botany,* 1–8, art. 375843. https://doi.org/10.1155/2012/375843

Owolabi, I.A., Mandiwana, K.L. & Panichev, N. 2016. Speciation of chromium and vanadium in medicinal plants. *South African Journal of Chemistry*, 69:67–71.

Oze, C., Fendorf, S., Bird, D.K. & Coleman, R.G. 2004. Chromium geochemistry of serpentine soils. *International Geology Review*, 46(2):97–126.

Pajević, S., Arsenov, D., Nikolić, N., Borišev, M., Orčić, D., Župunski, M. & Mimica-Dukić, N. 2018. Heavy metal accumulation in vegetable species and health risk assessment in Serbia. *Environmental Monitoring and Assessment*, 190(8), 459. https://doi.org/10.1007/s10661-018-6743-y

Panichev, N., Mandiwana, K.L., Kataeva, M. & Siebert, S.J. 2005. Determination of Cr(VI) in plants by electrothermal atomic absorption spectrometry after leaching with sodium carbonate. *Spectrochimica Acta Part B: Atomic Spectroscopy*, 60(5):699–703.

Pöykiö, R., Mäenpä, A., Perämäki, P., Niemelä, M. & Välimäki, I. 2005. Heavy metals (Cr, Zn, Ni, V, Pb, Cd) in lingonberries (*Vaccinium vitis-idaea* L.) and assessment of human esxposure in two industrial areas in the Kemi-Tornio region, northern Finland. *Archives of Environmental Contamination and Toxicology*, 48:338–343.

Quinn, C.H., Ziervogel, G., Taylor, A., Takama, T. & Thomalla, F. 2011. Coping with multiple stresses in rural South Africa. *Ecology and Society*, 16(3), 2. http://dx.doi.org/10.5751/ES-04216-160302

Rattan, R.K., Datta, S.P., Chhonkar, P.K., Suribabu, K. & Singh, A.K. 2005. Long-term impact of irrigation with sewage effluents on heavy metal content in soils, crops and groundwater – a case study. *Agriculture, Ecosystems and Environment*, 109:310–322.

Reddy, L.C.S., Reddy, K.V.R, Humane, S.K. & Damodaram, B. 2012. Accumulation of chromium in certain plant species growing on mine dump from Byrapur, Karnataka, India. *Research Journal of Chemical Sciences*, 2(12):17–20.

Rose, D., Bourne, L. & Bradshaw, D. 2002. Food and nutrient availability in South African households. Development of a nationally representative database. Medical Research Council, Parow. https://www.samrc.ac.za/sites/default/files/files/2017-07-03/foodnutrientavail.pdf Date of access: 10 Aug. 2020.

Schöning, A. & Brümmer, G.W. 2008. Extraction of mobile element fractions in forest soils using ammonium nitrate and ammonium chloride. *Journal of Plant Nutrition and Soil Science*, 171:392–398.

Scoon, R.N. & Viljoen, M.J. 2019. Geoheritage of the eastern limb of the Bushveld Igneous Complex, South Africa: a uniquely exposed layered igneous intrusion. *Geoheritage*, 11:1723–1748.

Semenya, S.S. & Potgieter, M.J. 2014. Medicinal plants cultivated in Bapedi traditional healers homegardens, Limpopo Province, South Africa. *African Journal of Traditional, Complementary and Alternative Medicines*, 11(5):126–132.

Siebert, S.J., Van Wyk, A.E. & Bredenkamp, G.J. 2002. The physical environment and major vegetation types of Sekhukhuneland, South Africa. *South African Journal of Botany*, 68(2):127–142.

Siebert, S.J., Steytler, J., Boneschans, R.B, Siebert, F. & Coetzee, M.S. 2018. Manganese tolerance of *Aloe greatheadii* Schönland var. *davyana* (Schönland) Glen & D.S.Hardy (Asphodelaceae: Alooideae) on ultramafic-peralkaline outcrops, South Africa. *Haseltonia,* 25:1–9.

Sokol, E.V., Nigmatulina, E.N. & Nokhrin, D.Y. 2010. Dust emission of chromium from chromite ore processing residue disposal areas in the vicinity of Krasnogorskii village in Chelyabinsk Oblast. *Contemporary Problems of Ecology*, 3(6):621–630.

Steenkamp, V., Stewart, M.J., Curowska, E. & Zuckerman, M. 2002. A severe case of multiple metal poisoning on a child treated with traditional medicine. *Forensic Science International*, 128:123–126.

Stovern, M., Guzmán, H., Rine, K., Felix, O., King, M., Ela, W., … Eduardo Sáez, A. 2016. Windblown dust deposition forecasting and spread of contamination around mine tailings. *Atmosphere,* 7(2), 16. https://doi.org/10.3390/atmos7020016

Street, R.A. 2012. Heavy metals in medicinal plant products – an African perspective. *South African Journal of Botany*, 82:67–74.

Tshehla, C. & Djolov, G. 2018. Source profiling, source apportionment and cluster transport analysis to identify the sources of PM and the origin of air masses to an industrialised rural area in Limpopo. *Clean Air Journal,* 28(2):54–66.

Tshehla, C. & Wright, C.Y. 2019. Spatial variability of PM_{10}, $PM_{2.5}$ and PM chemical components in an industrialised rural area within a mountainous terrain. *South African Journal of Science*, 115(9/10), art. 6174. https://doi.org/10.17159/sajs.2019/6174

Visoottiviseth, P., Francesconi, K. & Sridokchan, W. 2002. The potential of Thai indigenous plant species for the phytoremediation of arsenic contaminated land. *Environmental Pollution,* 118(3):453–461.

Wang, J., Su, J., Li, Z., Liu, B., Cheng, G., Jiang, Y., ... Yuan, W. 2019. Source apportionment of heavy metals and their health risks in soil-dustfall-plant system nearby a typical non-ferrous metal mining area of Tongling, eastern China. *Environmental Pollution,* 254, art. 113089. https://doi.org/10.1016/j.envpol.2019.113089

WHO (World Health Organization). 2011. Evaluation of certain food additives and contaminants. (Seventy-third report of the Joint FAO/WHO Expert Committee on Food Additives). WHO Technical Report Series, No 960, Geneva, Switzerland. https://apps.who.int/iris/handle/10665/44515 Date of access: 06 Nov. 2020.

Weindorf, D.C. & Chakraborty, S. 2016. Portable x-ray fluorescence spectrometry analysis of soils. *Methods of Soil Analysis,* 1(1). https://doi.org/10.1002/saj2.20151

Yaman, B. 2020. Health effects of chromium and its concentrations in cereal food together with sulfur. *Exposure and Health*, 12:153–161.

Chapter 6

Metal distribution patterns in soil and plant leaves (metallophytes)

6.1 Introduction

Local topography is the major determinant of the spatial distribution of metals in soils of a given area (Duan *et al*., 2015; Ding *et al*., 2017; Gaspar *et al*., 2020). In a general soil profile, the geochemistry of the parent material dominates the subsoil layers, whereas the topsoil continues to evolve under the influence of weathering, erosion and sedimentation processes resultant from topographic and climatic factors (Eze *et al*., 2010; Duan *et al*., 2015). Typically, soils generated from serpentine, basaltic or ultramafic outcrops are metalliferous with unusually high concentrations of metals (e.g. Mg, Fe, Cr, Mn, Ni and Co), low essential plant nutrients (e.g. N, P, Ca, B, Mo) and a high Mg to Ca ratio (Proctor, 2003; Brady *et al*., 2005; Williamson & Balkwill, 2006; Rajakaruna & Boyd, 2014).

Anthropogenic factors such as land use also alter the quantity and types of heavy metals found within an edaphic system (Qiao *et al*., 2019). Mining activities for instance, intensively modify existing soil homeostasis by adding volumes of multiple heavy metals (Wang *et al*., 2019; Zhang *et al*., 2019). Soil, in this case, acts as a sink and a source of heavy metals, from both natural geomorphologic and anthropogenic activities (Wuana & Okieimen, 2011; Gaspar *et al*., 2020). In addition to mineral mining, soil erosion caused by vegetation clearing and overgrazing, or due to weak soil structure (Mirzabaev *et al*., 2015), can also overtake the slow-paced pedogenesis process (Morgan, 2005; White, 2005).

Indigenous flora of serpentine habitats with anomalous soils have evolved through adaptations which are collectively referred to as the ‘serpentine syndrome’, a soil condition containing high concentrations of heavy metals, low soil nutrient levels and Mg:Ca of > 1 (Brady *et al*., 2005; Harrison & Rajakaruna, 2011). Metallophytes, species tolerant of metal-rich edaphic environments, comprises a considerable proportion of the local vegetation, including the endemic taxa on metalliferous soil (Baker *et al*., 2010; Reeves *et al.*, 2017).

Plant species from metalliferous sites require special attention since they can accumulate or even hyperaccumulate abundant metals from soil (van der Ent *et al.*, 2013; Siebert *et al*., 2018a, 2018b). Such species are valuable for technologies applied in rehabilitation (i.e. re-vegetation to reclaim metal contaminated environments), restoration (i.e. re-establish the original vegetation in degraded ecosystems), phytoremediation (i.e. decontamination of polluted environments using plants) and phytomining (i.e. economically viable recovery of elements via hyperaccumulator plants) (Rajakaruna *et al*., 2006; Baker *et al*., 2010; O’Dell, 2014; van der Ent *et al.*, 2015).

Spatial distribution patterns of heavy metals in soil offers valuable information about heavy metal pollution of an area that fluctuates over time largely due to type and level of anthropogenic disturbance (Eze *et al*., 2010; Gaspar *et al*., 2020). Further heavy metal assessments of environmental matrices, along with their biota, may render essential information regarding suitable environmental management of areas prone to metal contamination of soil (Gall *et al.*, 2015; Marcelo-Silva & Christofoletti, 2019).

Serpentine habitats with their unique flora are threatened by human interference and climate change (Baker *et al*., 2010; Rajakaruna & Boyd, 2014; Mizuno & Kirihata, 2015), and especially by mining as noted in South Africa (Siebert *et al*., 2002; Williamson & Balkwill, 2006). Sekhukhuneland, in South Africa, is least explored in terms of metallophytes, although it is a well-known region for its chromitite reserves enriched with chromium (Cr) and platinum (Pt), and an endemic flora, for which it was recognised as a Centre of Plant Endemism (Van Wyk & Van Wyk, 1997).

The north-south ranging Leolo Mountain in the study area provides a suitable catena with prominent natural (ultramafic soils) and anthropogenic sources of heavy metals, especially from mining activities (Siebert *et al*., 2002; Quinn *et al*., 2011; Scoon & Viljoen, 2019). On a catena, the upper slope is characterized by a constant outflux of matter, followed by a transition slope which mainly determines mobilization and localized deposition, while the bottomland areas, valleys and lowlands, primarily serve as landscapes for final deposition (Malinowska & Szumacher, 2013). At the valley bottoms, sheet and gully erosion result in accelerated loss of topsoil layers especially under the influence of anthropogenic interferences (Dlamini *et al*., 2011; Amare *et al*., 2019), which alters heavy metal content in the soil. Sekhukhuneland, therefore, presents an ideal serpentine site to assess the influence of topography and land use on heavy metal distribution and plant-soil associations and to explore the bioaccumulation potential of local vegetation.

Therefore, a catena approach was followed to assess the soil and dominant plant species from sites with diverse land uses, to evaluate the concentrations of metals in soil and plants in Sekhukhuneland. It was hypothesized that topography (i.e. natural factor) and land use (i.e. anthropogenic factor) would affect metal concentrations in soil and above-ground plant parts. To test this, total concentrations of major metals were determined for soil and plant leaves collected along an altitudinal gradient and across land use sites. Plant growth form was considered as an additional factor for the elucidation of metal concentrations in plant leaves as noted in literature (Visoottiviseth *et al.*, 2002). It was expected that, due to the elevated soil metal concentrations in Sekhukhuneland, the common species of the region could be classified as metallophytes. Foliar

metal bioaccumulation by locally collected dominant species was, therefore, determined to study the metal tolerance strategy (i.e. indicators, excluders, accumulators or hyperaccumulators, Baker, 1981) in response to high soil metal concentrations. Findings from the present study may stimulate future investigations to draw up similar comprehensive assessments to determine the baseline flow of heavy metals within and between environmental matrices and to predict soil pollution trends in mining areas.

6.2 Materials and method

6.2.1 Study area

The study area in Sekhukhuneland is located in the eastern part of the Limpopo Province in South Africa. The hilly physiography of the region was formed by the erosion of the eastern part of the Rustenburg Layered Suite (RLS) of the Bushveld Igneous Complex (BIC) that is characterized by substantial quantities of Fe, Cr and Pt in its rocky habitat of pyroxenite, norite, anorthosite, harzburgite and dunite (Siebert *et al*., 2002, 2003).

This ultramafic-mafic formation of the RLS is up to 10 km thick and around 30 km wide and was formed by multiple magma surges (Naldrett *et al*., 2012; Scoon & Viljoen, 2019). The RLS is subdivided into five lithostratigraphic zones (rock layers; Fig. 6.1) with variation in mineral composition (Scoon & Viljoen, 2019). The Critical Zone predominantly features chromitite rock layers (Naldrett *et al*., 2012; Scoon & Viljoen, 2019). The primary chromitite layers are around 0.15 mm to > 2 m thick and represent the largest global chromite (the economically viable Cr ore) reserve (Scoon & Viljoen, 2019). The chromitite rock layers in the Critical Zone further contain various proportions of Platinum Group Metals (Naldrett *et al*., 2012; Scoon & Viljoen, 2019) and both Cr and Pt are exploited heavily in the study region.

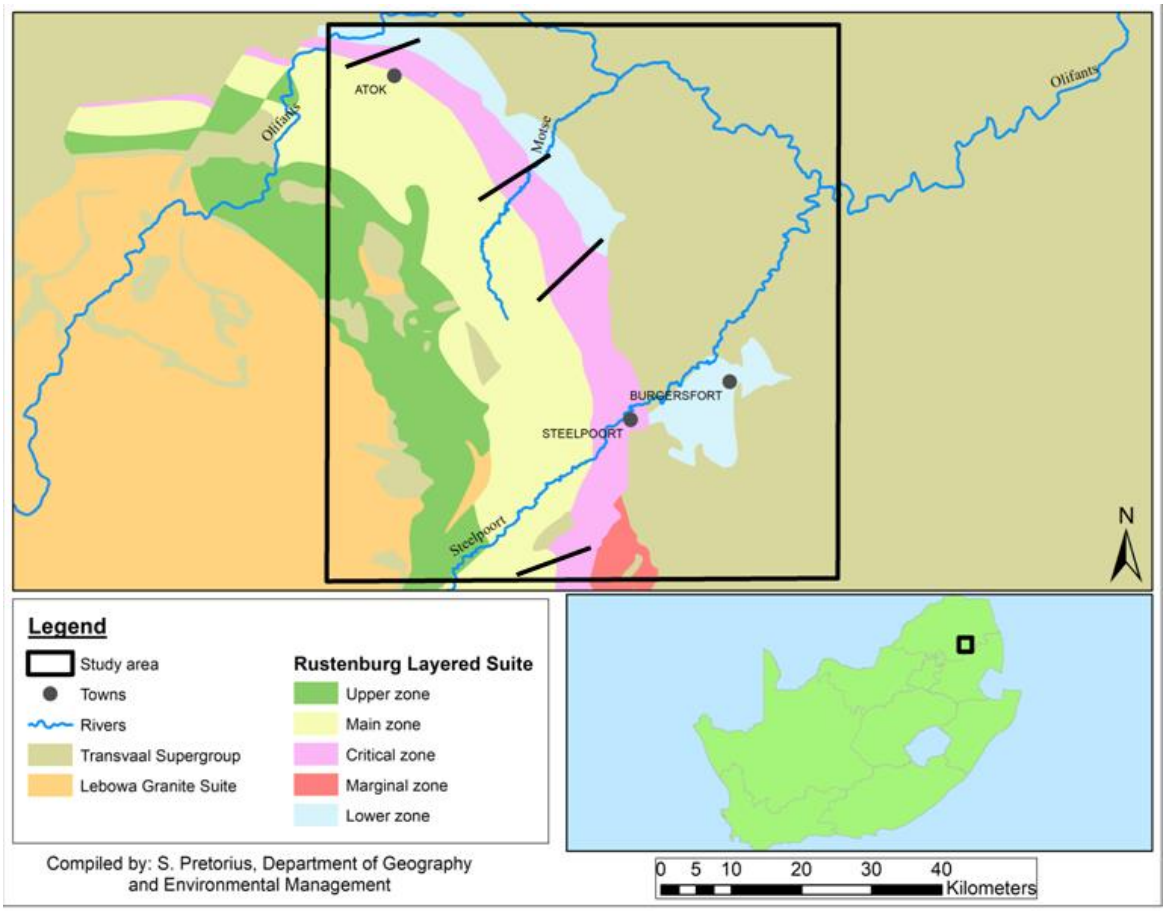

Figure 6.1. Rustenburg Layered Suite featuring the five lithostratigraphic zones (upper zone, main zone, critical zone, marginal zone and lower zone; Scoon & Viljoen, 2019). Four black lines represent the sampling transects along the same catena, decreasing in altitude from west to east.

The ultramafic soils derived from chromitite outcrops of the region are metal-rich and host vegetation categorized as mountain bushveld dominated by grasses and forbs (Siebert *et al*., 2002). The complex interactions of topography, geology, ultramafic soils and climate are proposed to drive the evolution in this centre of plant endemism and its high floristic diversity of around fifty endemics and seventy sub-endemic taxa (Siebert *et al*., 2002). The plant resources are well-integrated into human traditional uses as grazing, food, medicinal and cultural components in Sekhukhuneland (Siebert *et al*., 2003; Mogale *et al*., 2019). Nonetheless, loss of communal lands with its wild flora is pronounced in the region due to poor land management, overgrazing, and expansion of mining and related developments (Quinn *et al*., 2011; Du Plessis *et al*., 2020; Shackleton, 2020).

Semi-arid climatic conditions in the study area contribute to the edaphic profile of the catena with shallow soil layers on the mountain slopes and deep alluvium in the valleys (Siebert *et al*., 2002). Rainfall on hills may cause rapid soil erosion on the mountain slopes, while water eroded gullies, locally known as 'dongas', and sheet erosion are known to cause severe soil displacement and

degradation (Dlamini *et al*., 2011; van Zijl *et al*., 2014), especially in valley bottoms. Wind erosion could accelerate topsoil removal during dry winter months when soil lacks moisture. Changes in rainfall regime in these mountainous areas (Quinn *et al*., 2011) could further promote erosion especially on bare ground lacking plant cover in overgrazed areas, tailings, and open cast mining sites during seasonal droughts. Sampling sites were therefore chosen randomly at various catena positions starting from the upper slope to the valley bottom targeting both less disturbed habitats as well as mining activities and settlements to compare the influence of human interference together with topography on the metal distribution in local soil and plant leaves.

6.2.2 Sample collection

Soil and plant leaves were sampled during early summer (November) along a catena in Sekhukhuneland. Seventeen sites were investigated along four transects of the catena. These sites were chosen according to topographic position and land use type: mountain slope (sectioned in 'upper slope' and 'footslope'), valley (sectioned in three land uses: 'rangelands', 'gardens' and 'tailings') and valley bottom (sectioned in 'sheet erosion' and 'gully erosion' area) (Fig. 6.2). Fifty mature leaves of five individuals (i.e. composite sample), from each of the six or seven most abundant species in each site (Siebert *et al*., 2002) were sampled according to their different growth forms: grasses, forbs (prostrate or erect), dwarf shrubs, shrubs and trees. At each site, mature leaf samples were targeted as they were expected to have accumulated more metals (Siebert *et al*., 2018b). Leaf preparation procedure is detailed in Chapter 5, section 5.2.3.

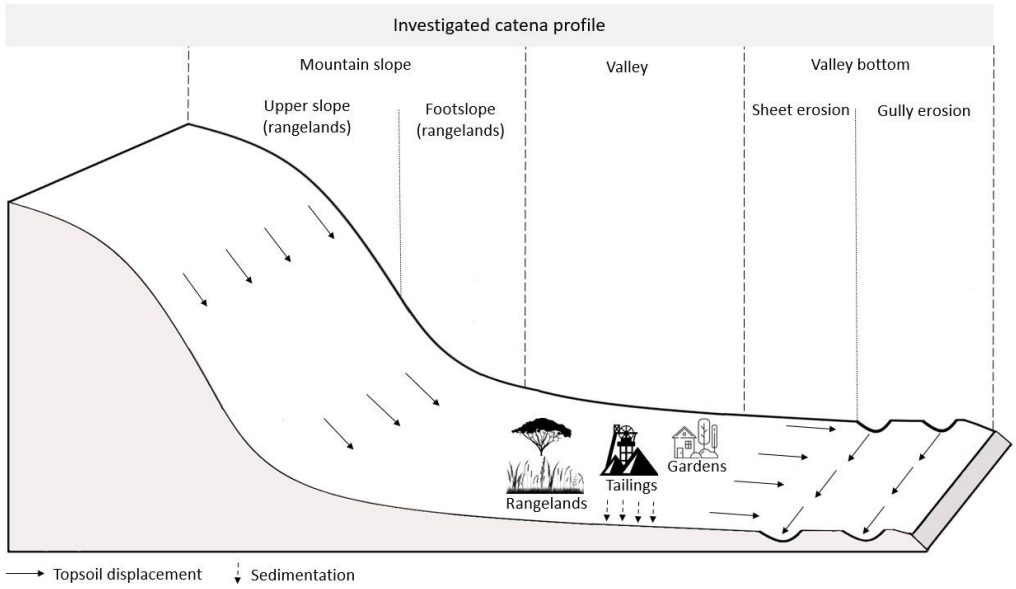

Figure 6.2. Catena profile investigated in Sekhukhuneland.

Topsoil (50 g) from a depth of 10–15 cm was randomly sampled four times in each sampling site, from the base of sampled plants. The soil per site was mixed into a composite, passed through a 2 mm sieve, air-dried and stored in sealed vials at room temperature. Leaf and soil samples were

ground in a tungsten carbide ring mill to a particle size < 75 µm. Powdered samples were stored in labelled vials at room temperature until analysis.

6.2.3 Determination of total metals in soil and plant leaf tissue

An EPA 3051A microwave acid digestion method was used to determine the total concentrations of metals in soil and plant leaf material (for detailed method see Chapter 5, section 5.2.3.1). The metals evaluated were Co, Cr, Cu, Fe, Mg, Mn, Mo, Ni, Sr and Zn. Mg is generally not considered a 'heavy metal' – which as it happens, is an imprecise categorization by the International Union of Pure and Applied Chemistry (IUPAC, Duffus, 2002), but was selected given its reported richness in serpentine soils (Brady *et al*., 2005) and contribution to the soil erosion potential that affects plant distribution (Keren, 1991; Siebert *et al*., 2002). The remaining heavy metals are common in both ultramafic soils (e.g. Cr, Co and Ni) (Siebert *et al*., 2002; Proctor, 2003) and soils surrounding metal ore mines (Qiao *et al*., 2019; Wang *et al*., 2019). Except for Cr and Sr, all the above-mentioned elements are also micronutrients for plants (Hänsch & Mendel, 2009; Anjum *et al*., 2015), and therefore, are important to consider in this investigation.

6.2.4 Bioaccumulation factor (BAF)

To evaluate the foliar metal accumulation of the plant species, the Bioaccumulation Factors (BAFs) for metals was calculated based on the following formula by US EPA, 2000 (Infante *et al*., 2021),

$$\mathrm{BAF} = \frac{\text{Metal concentration in plant leaf tissue}}{\text{Metal concentration in soil}}$$

Plant species with BAF value(s) above 1 are considered accumulators whereas species with values equal to or less than 1 are indicators or excluders, respectively (Baker, 1981).

6.2.5 Data analysis

Data on metal concentrations of soil and plant samples were analyzed through permutational analysis of variance (PERMANOVA), after a log (x + 1) transformation and under Euclidean resemblance matrices. Three factors, one natural (i.e. topography) and one anthropogenic (land-use) – tested on soil and plant samples; and a morphological one (i.e. growth form) – tested only on plant samples, were evaluated separately (i.e. one way analysis) for their influence on the metal concentrations.

Growth form factor was categorized as grass, prostrate forb, short erect forb (150– 500 mm), tall erect forb (> 600 mm), dwarf shrub, shrub, succulent and tree (i.e. 1 factor, 7 levels). The topography factor was tested in samples from the Upper slope (n = 4 for soil; n = 7 for plants), Footslope (n = 3 for soil; n = 7 for plants), Valley rangelands (from here on referred only as Valley; n = 4 for soil; n = 7 for plants) and Valley bottom (as a composite of the Sheet erosion and the Gully erosion samples; n = 8 for soil; n = 14 for plants) (i.e. 1 factor, 4 levels). The land use factor was tested in samples from the Rangelands (composed by the Upper slope, the Footslope and the Valley samples; n = 11 for soil; n = 21 for plants), Gardens (n = 4 for soil; n = 7 for plants), Tailings (n = 4 for soil; n = 7 for plants), Sheet erosion (n = 4 for soil; n = 6 for plants)and Gully erosion (n = 4 for soil; n = 7 for plants) (i.e. 1 factors, 5 levels).

Differences were considered significant for a *p*-value < 0.05. The identification of the significant differences between sites was made through post hoc tests using the pairwise method. Cluster dendrograms of the centroids from each site were used as an ordination method for the samples under all factors. The main variables (metals) were identified by distance-based linear models and tested individually for differences when the main factor was of significant influence. Statistical packages used were Primer 6 and Permanova+ (PRIMER-E).

6.3 Results

6.3.1 Metal concentrations in soil and plant leaf tissue

Sekhukhuneland catena soils were characterized in terms of contamination by heavy metals. It was also possible to identify the bioaccumulating metallophytes along with their bioaccumulation factors and their distribution among exotic, indigenous and endemic species. Patterns in terms of distribution of heavy metals in soils and plant species were only evident under anthropogenic influences (i.e. land use). Accumulating trends in plant growth forms were also identified.

6.3.1.1 Soil

The soils from all the sampling sites of the catena generally had mean metal concentrations above the permissible levels in South African agricultural soils (Herselman *et al*., 2005) (Table 6.1). The footslope and the rangelands within the valley had Co concentrations below the level, while gardens and tailings were the only land uses with Zn levels above such limit. Metal concentrations in sites were generally within the range of the metal levels reported in serpentine soils in South Africa (Venter *et al*., 2018) except tailings that had higher Co, Cr, Fe and Mn values. Likewise, Cr values for a couple of tailing localities and Co values in all tailing sites were above the reported world serpentine levels (Adriano, 1986). Tailings had the highest metal concentrations of all metals, except for Sr. Only Mo concentrations were consistent throughout the catena positions.

Table 6.1. Total metal concentrations (µg g^{-1}) of soils from each of the sites along the Sekhukhuneland catena and comparative literature. [a]Herselman *et al*., 2005; [b]Venter *et al*., 2018; [c]Adriano, 1986. NR, not reported in reviewed literature.

			pH	Mg	Cr	Mn	Fe	Co	Ni	Cu	Zn	Sr	Mo
Topography	Land use	Samples											
Upper slope	Rangelands	1	7.4	2377.00	205.70	308.90	14590.00	14.50	156.90	14.80	12.70	104.20	21.20
		2	7.6	5184.00	981.50	566.80	30280.00	39.10	265.40	16.80	28.60	12.30	0.50
		3	7.9	7339.00	248.70	297.00	14590.00	16.20	61.90	26.20	23.40	112.70	0.20
		4	6.4	2825.50	896.30	695.40	36045.00	37.00	330.70	7.30	28.80	4.70	0.20
Footslope		1	8.3	16270.00	360.30	499.10	19040.00	22.10	108.80	9.50	17.00	129.10	0.10
		2	8.4	4503.00	79.30	255.00	16350.00	11.00	50.70	12.10	13.40	122.30	0.10
		3	8.1	18750.00	43.30	493.50	9704.00	11.20	37.10	7.20	8.90	278.60	0.10
Valley		1	8.5	60895.40	2277.90	1583.10	70223.60	18.00	522.40	15.00	67.00	15.10	1.10
		2	8.9	10470.00	213.90	445.00	25380.00	20.90	104.30	20.60	23.40	94.60	3.20
		3	8.4	5036.00	67.70	425.00	24160.00	21.50	77.90	15.60	18.50	82.90	0.10
		4	8.4	17210.00	83.00	264.70	15570.00	11.60	48.80	10.00	15.40	231.40	0.10
Valley bottom	Sheet erosion	1	7.8	5136.00	165.80	346.00	15880.00	17.10	78.20	12.10	10.30	93.10	0.10
		2	7.7	6053.00	488.20	880.30	25990.00	34.70	138.80	17.30	25.10	133.70	0.30
		3	8.7	6202.00	64.50	670.00	22360.00	24.50	84.00	14.60	16.60	89.40	0.20
		4	7.1	6821.00	304.60	304.50	21080.00	28.10	93.70	21.40	19.40	85.70	0.20
	Gulley erosion	1	8.4	10991.00	422.30	1084.00	32420.00	42.70	177.00	20.00	30.30	103.70	0.20
		2	8.5	15490.00	326.70	520.20	16250.00	20.70	104.90	10.20	15.40	128.40	0.20
		3	8.2	11480.00	213.90	264.90	16370.00	16.50	66.70	9.70	24.10	134.90	0.20
		4	7,0	6004.00	205.70	858.60	14870.00	16.90	58.90	15.50	15.30	25.10	0.10
	Gardens	1	6.7	33670.00	2165.10	1771.80	74835.10	51.00	576.10	39.60	74.50	20.90	0.20
		2	8.3	29867.80	1484.60	1086.90	49702.20	233.20	336.00	81.80	53.80	219.30	0.20
		3	8,0	21528.70	819.50	898.70	41343.30	21.00	201.50	28.10	89.90	218.30	0.20
		4	8.7	23980.00	277.20	666.90	31750.00	29.70	123.70	18.10	28.40	133.80	0.20
	Tailings	1	8.5	78793.20	158245.60	2385.10	118149.50	372.20	651.40	59.90	298.50	27.50	0.20
		2	8.3	52552.20	64089.40	2310.70	108239.20	124.10	556.00	42.10	166.60	37.30	0.20
		3	8.5	46433.00	142412.40	3117.40	135115.30	261.00	714.40	97.00	359.70	40.70	0.20
		4	7.2	4909.00	29024.00	2131.00	92979.00	285.40	507.10	188.50	170.10	90.90	0.20
SA permissible limits[a]				NR	80.00	NR	NR	20.00	50.00	6.60	46.50	NR	NR
SA serpentine range[b]				11000–50000	229–3500	910–2100	38700–86000	43–185	198–2530	NR	NR	NR	NR
World serpentine range[c]				NR	634–125000	NR	NR	≥100	24–5500	NR	NR	NR	NR

6.3.1.2 Plants

Out of the 47 evaluated species, 35 (74%) bioaccumulated (i.e. BAF > 1) at least one of the metals assessed (Table 6.2, Fig. 6.3). These species included 3 of the 5 observed endemics (i.e. *Lydenburgia cassinoides*, *Euclea sekhukhuniensis* and *Polygala sekhukhuniensis*) and 6 of the 10 observed exotics (i.e. *Amaranthus spinosus*, *Argemone ochroleuca, Carica papaya*, *Ipomoea batatas*, *Moringa oleifera* and *Psidium guajava*). No endemic species were observed in the valley, while no exotics were observed outside this site. Bioaccumulation was frequent in species from the rangelands, especially in the upper slope and the footslope, and less frequent at the gardens and tailings which had higher soil metal concentrations.

None of the species had BAF values > 1 for Cr, Fe, Mn and Ni. Zn and Mo were, respectively, accumulated by 46 and 44% of the total species sampled followed by Co in 25% of plants (Zn > Mo > Co > Mg > Sr > Cu). High BAF's were observed for Co, Mo and Zn and the highest scores were all for Mo. Most of the accumulators were grass species although there were no collected species from the valley, gardens or tailings, while succulents had the lowest occurrences (Fig. 6.4). All the grass species accumulated Zn which was also accumulated by at least one species within each of the other growth forms. Dwarf shrubs were the only growth form to accumulate all the metals.

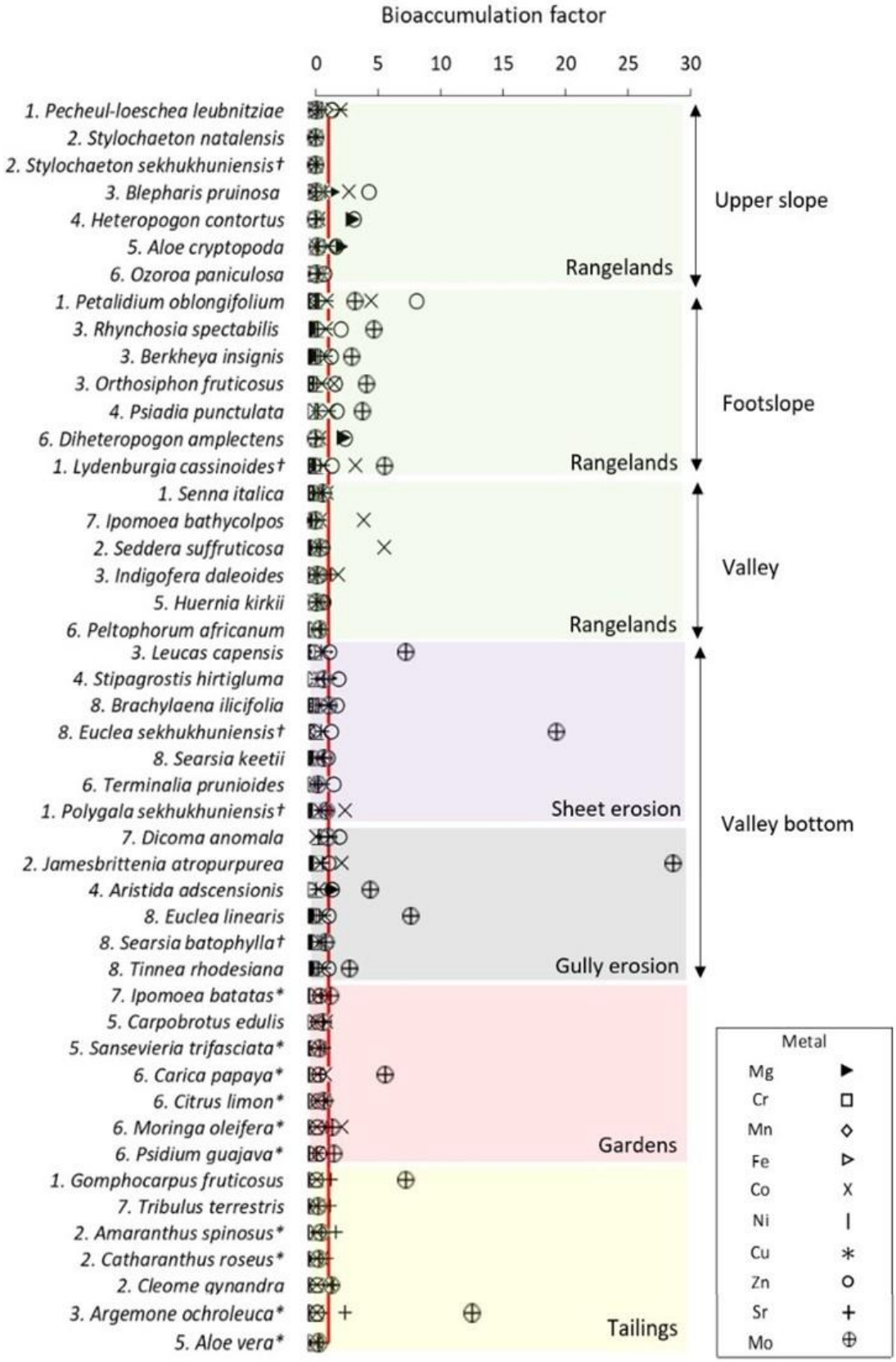

Figure 6.3. BAF for metals in leaves of the 47 plant species evaluated in Sekhukhuneland under topography and land use factors. 1. Dwarf shrub; 2. short erect forb; 3. tall erect forb; 4. grass; 5. succulent; 6. tree; 7. prostrate forb; 8. shrub. †Endemic and *exotic species. Red line indicates bioaccumulation threshold (BAF = 1).

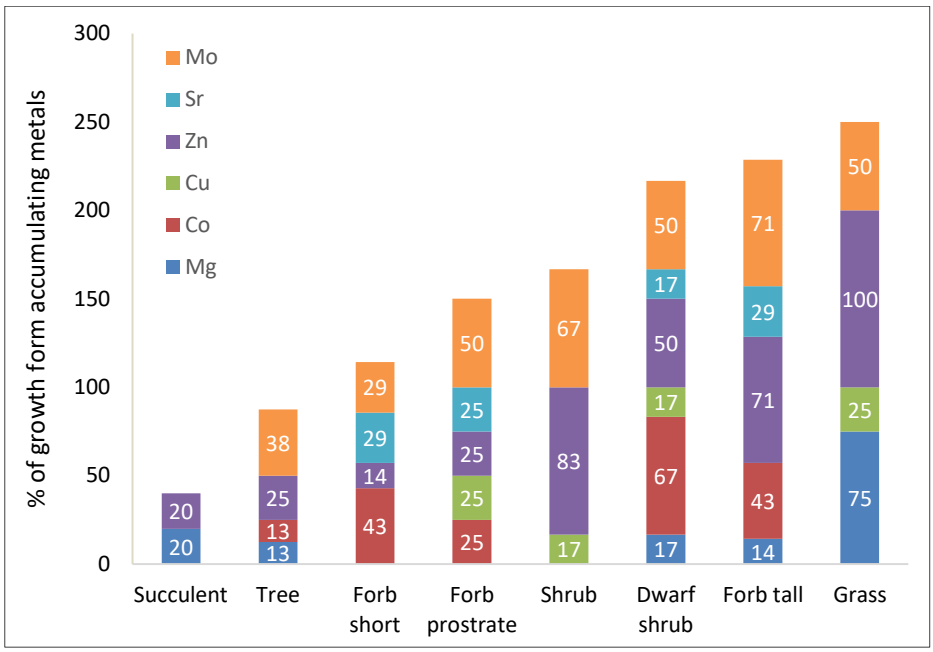

Figure 6.4. Occurrence of accumulators among the plant growth forms, according to the accumulated metals.

6.3.1.3 Metal distribution patterns in growth forms

Grasses and shrubs formed the two extreme clusters in terms of foliar metal concentrations, with the remaining growth forms in the between. All the species in this intermediary group differed significantly from each other, with short forbs being similar to all of them (Table E1c,d, Appendix E; Fig. 6.5a). Co was the only element to differ significantly when evaluated individually. It was significantly low in grasses (Fig. 6.5b).

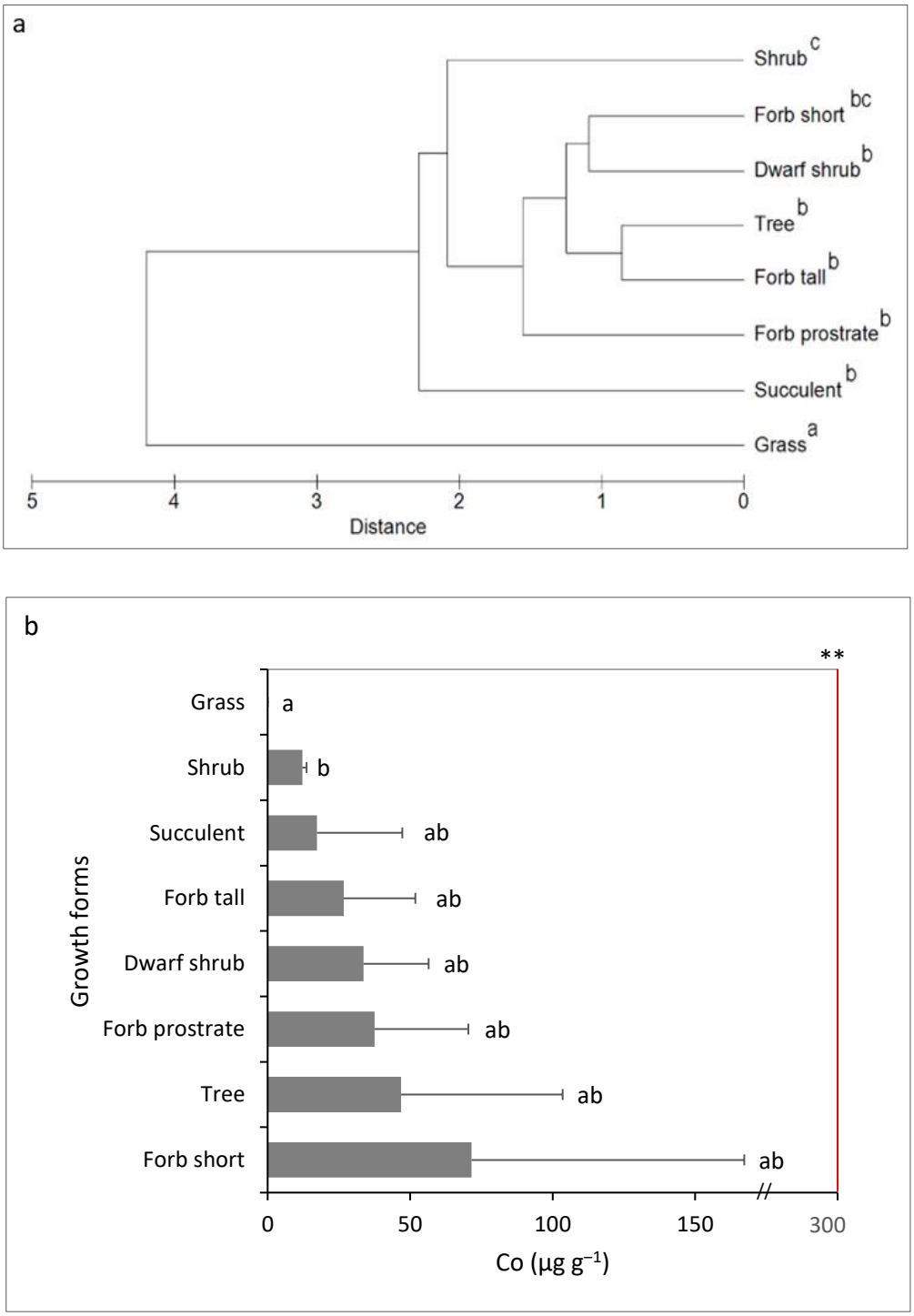

Figure 6.5. Metal distribution in different growth forms. a. Dendrogram of metal distribution ordination of plant growth forms based on group averages of metal concentrations; b. concentration of Co among growth forms. **Hyperaccumulation threshold (van der Ent et *al*., 2013). Different letters represent significant difference in the pairwise post hoc comparison (*p*<0.05).

Table 6.2. Total metal concentrations in plant leaves (µg g^{-1}, mean) and soil samples (µg g^{-1}, mean ± SD), and the bioaccumulation factors (BAF) of plant species in the study sites of the Sekhukhuneland catena. †Endemic and *exotic species.

				Mg		Cr		Mn		Fe		Co		Ni		Cu		Zn		Sr		Mo	
Topography	Land use	Growth form	Species	µg g^{-1}	BAF	µg g^{-1}	BAF	µg g^{-1}	BAF	µg g^{-1}	BAF	µg g^{-1}	BAF	µg g^{-1}	BAF	µg g^{-1}	BAF	µg g^{-1}	BAF	µg g^{-1}	BAF	µg g^{-1}	BAF
Upper slope	Rangelands	Dwarf shrub	*Pecheul-loeschea leubnitziae*	6556.00	1.50	12.10	0.00	30.10	0.06	416.40	0.02	35.70	1.34	59.60	0.29	32.30	1.98	30.60	1.31	23.60	0.40	0.60	0.11
		Forb short	*Stylochaeton natalensis*	527.40	0.10	0.70	0.00	6.90	0.01	20.90	0.00	0.00	0.00	0.40	0.00	0.40	0.03	2.00	0.09	2.40	0.40	0.00	0.00
		Forb short	*Stylochaeton sekhukhuniensis* †	437.80	0.10	0.50	0.00	10.70	0.02	19.50	0.00	0.00	0.00	0.40	0.00	0.50	0.03	1.90	0.08	4.10	0.07	0.00	0.00
		Forb tall	*Blepharis pruinosa*	6090.00	1.40	16.40	0.00	18.60	0.04	536.20	0.02	71.20	2.66	5.60	0.03	10.30	0.63	100.40	4.30	44.10	0.75	0.40	0.06
		Grass	*Heteropogon contortus*	12954.00	2.90	19.80	0.00	39.30	0.08	811.20	0.03	0.00	0.00	47.80	0.23	3.50	0.21	72.00	3.08	5.20	0.09	0.10	0.00
		Succulent	*Aloe cryptopoda*	8879.80	2.00	46.60	0.10	80.20	0.17	213.50	0.01	0.60	0.02	15.30	0.08	16.00	0.98	38.20	1.63	38.70	0.66	1.10	0.12
		Tree	*Ozoroa paniculosa*	1537.00	0.30	20.30	0.00	14.20	0.03	126.40	0,01	5.80	0.22	1.20	0.01	7.60	0.47	17.50	0.75	10.80	0.18	0.20	0.06
			Soil	4431 ± 2296		583 ± 413		467 ± 197		23876 ± 10978		26.70 ± 13		204 ± 119		16.30 ± 8		23.40 ± 8		58.50 ± 58		5.50 ± 10	
Footslope		Dwarf shrub	*Petalidium oblongifolium*	6110.00	0.50	2.30	0.00	10.30	0.03	61.40	0.00	65.60	4.44	7.50	0.11	8.50	0.88	105.90	8.10	38.50	0.22	0.40	3.19
		Dwarf shrub	*Rhynchosia spectabilis*	1246.00	0.10	11.70	0.10	44.20	0.11	115.60	0.01	12.70	0.86	1.70	0.03	7.90	0.82	26.80	2.05	21.60	0.12	0.50	4.70
		Forb tall	*Berkheya insignis*	473.00	0.00	5.40	0.00	33.50	0.08	470.70	0.03	7.60	0.52	2.90	0.04	7.50	0.78	16.80	1.28	59.70	0.34	0.30	2.89
		Forb tall	*Orthosiphon fruticosus*	3248.00	0.20	6.80	0.00	23.20	0.06	162.30	0.01	22.00	1.49	1.80	0.03	4.70	0.49	20.60	1.58	18.80	0.11	0.50	4.08
		Forb tall	*Psiadia punctulata*	2727.50	0.20	3.80	0.00	60.20	0.15	99.80	0.01	0.10	0.01	1.10	0.02	10.10	1.05	22.40	1,71	23.10	0.13	0.40	3.80
		Grass	*Diheteropogon amplectens*	28857.00	2.20	13.20	0.10	73.30	0.18	1686.80	0.11	0.00	0.00	20.70	0.32	2.90	0.30	31.20	2.39	4.30	0.02	0.00	0.00
		Tree	*Lydenburgia cassinoides* †	2610.00	0.20	3.20	0.00	8.90	0.02	54.80	0.00	46.80	3.17	3.50	0.05	5.60	0.58	17.00	1.30	58.60	0.33	0.60	5.56
			Soil	13174 ± 7611		161 ± 174		399 ± 126		15031 ± 4806		14.80 ± 6		65.52 ± 38		9.60 ± 3		13.10 ± 4		177 ± 88		0.1 ± 0	
Valley		Dwarf shrub	*Senna italica*	5404.00	0.20	11.70	0.00	40.90	0.08	212.30	0.01	17.90	0.88	1.90	0.01	6.80	0.48	16.70	0.71	51.70	0.48	0.70	0.63
		Forb prostrate	*Ipomoea bathycolpos*	1408.00	0.10	5.90	0.00	8.60	0.02	152.80	0.01	77.90	3.84	6.70	0.04	4.70	0.33	18.10	0.00	48.50	0.00	0.50	0.00
		Forb short	*Seddera suffruticosa*	2877.00	0.10	15.70	0.00	30.40	0.06	455.50	0.02	111.50	5.50	6.20	0.04	3.80	0.27	14.40	0.62	38.40	0.36	0.40	0.32
		Forb tall	*Indigofera daleoides*	5349.00	0.20	4.80	0.00	31.10	0.06	153.90	0.01	36.60	1.80	4.30	0.03	1.90	0.14	10.00	0.43	127.30	1.18	0.20	0.15
		Succulent	*Huernia kirkii*	6890.00	0.30	7.10	0.00	328.80	0.63	142.50	0.01	0.30	0.02	7.90	0.05	2.10	0.15	15.10	0.65	43.20	0.40	0.10	0.08
		Tree	*Peltophorum africanum*	3387.00	0.10	12.30	0.00	44.60	0.04	176.00	0.00	16.20	0.19	3.10	0.01	3.70	0.09	17.10	0.28	70.30	0.47	0.10	0.32
			Soil	23403 ± 25486		661 ± 1080		680 ± 607.80		33833 ± 24650		18 ± 5		188 ± 224		15.30 ± 4		31.10 ± 24		106 ± 91		1.10 ± 1	
Valley bottom	Sheet erosion	Forb tall	*Leucas capensis*	5094.00	0.80	2.70	0.00	26.90	0.05	108.30	0.01	7.00	1.27	0.50	0.01	8.80	0.54	20.60	1.15	40.80	0.41	2.30	7.18
		Grass	*Stipagrostis hirtigluma*	7023.00	1.20	5.20	0.00	22.40	0.04	411.20	0.02	0.00	0.00	11.40	0.12	5.40	0.33	33.00	1.85	5.70	0.06	0.20	0.65
		Shrub	*Brachylaena ilicifolia*	1544.00	0.30	7.00	0.00	6.80	0.01	88.00	0.00	11.30	0.43	9.60	0.10	16.90	1.03	31.30	1.75	39.00	0.39	0.30	1.06
		Shrub	*Euclea sekhukhuniensis* †	2804.00	0.50	17.40	0.10	12.70	0.02	47.50	0.00	13.30	0.51	26.80	0.27	8.80	0.54	22.60	1.27	39.60	0.39	6.10	19.17
		Shrub	*Searsia keetii*	847.00	0.10	6.50	0.00	10.70	0.02	117.40	0.01	10.00	0.38	2.60	0.03	6.20	0.38	18.40	1.03	13.60	0.13	0.20	0.66
		Tree	*Terminalia prunioides*	2230.00	0.40	5.20	0.00	21.60	0.04	107.80	0.01	0.10	0.00	2.70	0.03	10.40	0.63	26.60	1.49	15.70	0.16	0.10	0.24
			Soil	6053 ± 696		256 ± 184		550 ± 274		21328 ± 4185		26.10 ± 7		98.70 ± 28		16.40 ± 4		17.90 ± 6		101 ± 22		0.30 ± 0	
	Gulley erosion	Dwarf shrub	*Polygala sekhukhuniensis* †	1479.00	0.10	4.70	0.00	8.40	0.01	81.40	0.00	56.10	2.32	3.30	0.03	5.10	0.37	15.70	0.74	39.00	0.40	0.20	0.84
		Forb prostrate	*Dicoma anomala*	799.00	0.10	74.20	0.20	27.80	0.04	3154.60	0.16	0.70	0.03	29.40	0.29	17.00	1.22	41.50	1.95	42.70	0.44	0.20	1.01
		Forb short	*Jamesbrittenia atropurpurea*	948.00	0.10	24.10	0.10	32.70	0.05	1413.70	0.07	49.00	2.03	16.90	0.17	5.90	0.42	22.70	1.07	55.70	0.57	6.40	28.47
		Grass	*Aristida adscensionis*	13879.00	1.30	6.30	0.00	9.40	0.01	153.30	0.01	0.00	0.00	7.50	0.07	2.90	0.21	27.70	1.30	4.00	0.04	1.00	4.34
		Shrub	*Euclea linearis*	551.00	0.10	6.30	0.00	17.50	0.03	114.40	0.01	12.20	0.05	13.90	0.14	9.20	0.66	22.90	1.08	26.60	0.27	1.70	7.57
		Shrub	*Searsia batophylla* †	621.00	0.10	6.80	0.00	5.80	0.01	126.40	0.01	14.30	0.59	4.70	0.05	4.80	0.35	19.20	0.90	14.40	0.15	0.20	0.80
		Shrub	*Tinnea rhodesiana*	1006.00	0.10	19.60	0.10	11.40	0.02	199.10	0.01	12.00	0.49	16.50	0.16	9.30	0.67	23.00	1.08	23.40	0.24	0.60	2.70
			Soil	10991 ± 3888		297 ± 111		682 ± 362		19978 ± 8323		24.20 ± 13		102 ± 54		13.90 ± 5		21.30 ± 7		98 ± 50		0.20 ± 0	
	Gardens	Forb prostrate	*Ipomoea batatas* *	10880.00	0.40	18.10	0.00	109.80	0.10	313.20	0.01	24.40	0.29	3.70	0.01	5.60	0.13	21.80	0.35	58.60	0.40	0.50	1.21
		Succulent	*Carpobrotus edulis*	17010.00	0.60	2.70	0.00	14.60	0.01	47.30	0.00	69.50	0.83	1.00	0.00	1.70	0.04	14.00	0.23	83.30	0.56	0.30	0.61
		Succulent	*Sansevieria trifasciata* *	18170.00	0.70	7.10	0.00	12.90	0.01	175.60	0.00	16.10	0.19	6.10	0.02	10.50	0.25	15.50	0.25	103.90	0.70	0.10	0.33
		Tree	*Carica papaya* *	12180.00	0.40	28.40	0.00	36.20	0.03	351.80	0.01	62.40	0.75	9.10	0.03	4.60	0.11	15.00	0.24	45.80	0.31	2.40	5.54
		Tree	*Citrus limon* *	5322.00	0.20	8.00	0.00	23.60	0.02	162.10	0.00	55.00	0.66	2.90	0.01	3.40	0.08	11.90	0.19	140.30	0.95	0.30	0.65
		Tree	*Moringa oleifera* *	4716.00	0.20	14.80	0.00	33.60	0.03	223.80	0.00	175.40	2.08	1.60	0.01	4.50	0.11	9.70	0.16	114.80	0.78	0.60	1.30
		Tree	*Psidium guajava* *	3050.00	0.10	13.90	0.00	20.20	0.02	204.40	0.00	13.80	0.17	3.30	0.01	5.20	0.12	21.30	0.35	12.50	0.08	0.60	1.47
			Soil	27262 ± 5523		1174 ± 837		1106 ± 476		49408 ± 18471		83.70 ± 101		309 ± 198		41.90 ± 28		61.70 ± 27		148 ± 94		0.40 ± 0.30	
	Tailings	Dwarf shrub	*Gomphocarpus fruticosus*	7810.00	0.20	21.40	0.00	94.40	0.04	170.10	0.00	13.80	0.05	44.80	0.07	9.60	0.10	18.50	0.07	57.50	1.17	11.60	7.17
		Forb prostrate	*Tribulus terrestris*	6090.00	0.10	13.50	0.00	29.00	0.01	231.00	0.00	47.10	0.18	3.30	0.01	7.80	0.08	46.10	0.19	54.20	1.10	0.40	0.22
		Forb short	*Amaranthus spinosus* *	9992.00	0.20	8.80	0.00	43.40	0.02	279.50	0.00	51.80	0.20	1.70	0.00	6.20	0.06	66.10	0.27	78.60	1.60	0.80	0.46
		Forb short	*Catharanthus roseus* *	9209.00	0.20	12.40	0.00	87.60	0.04	197.20	0.00	18.40	0.07	4.50	0.01	5.90	0.06	24.00	0.10	43.70	0.89	0.50	0.28
		Forb short	*Cleome gynandra*	8438.00	0.20	25.80	0.00	45.70	0.02	505.70	0.00	270.10	1.04	5.10	0.01	8.40	0.09	30.10	0.12	67.50	1.37	2.10	1.28
		Forb tall	*Argemone ochroleuca* *	18300.00	0.40	51.50	0.00	112.70	0.05	255.20	0.00	42.30	0.16	81.70	0.13	6.90	0.07	37.10	0.15	112.80	2.30	20.20	12.48
		Succulent	*Aloe vera* *	5856.80	0.10	15.50	0.00	13.40	0.01	73.80	0.00	0.20	0.00	7.70	0.01	4.70	0.05	12.30	0.05	8.00	0.16	0.40	0.25
			Soil	45672 ± 30586		98442 ± 61938		2486 ± 434		113621 ± 17678		2601 ± 103		607 ± 93		96.90 ± 65		249 ± 96		49.10 ± 28		1.60 ± 0.70	

6.3.2 Patterns of metal distribution in soil and plant leaf tissue

The concentrations of the assessed metals in soil samples and plant species followed similar patterns of metal distribution for topography and land use factors.

6.3.2.1 Natural factor- Topography

Both the soil samples and the plant species had no significantly distinct metal concentrations along the topographic profile (Table E1a, Appendix E). However, a somewhat similar grouping pattern could be observed in the dendrograms (Fig. 6.6). The upper slope and the Valley samples were distinctly different from the rest of the topographic position for soils and plants, respectively. Footslope and Valley bottom were intermediate for both soill and plants. The main metals driving the dispersion of the soil and plants data under this factor were Ni (51% of contribution), Mg (17%) and Mo (13%); and Co (33%), Fe (26%) and Mg (13%), respectively.

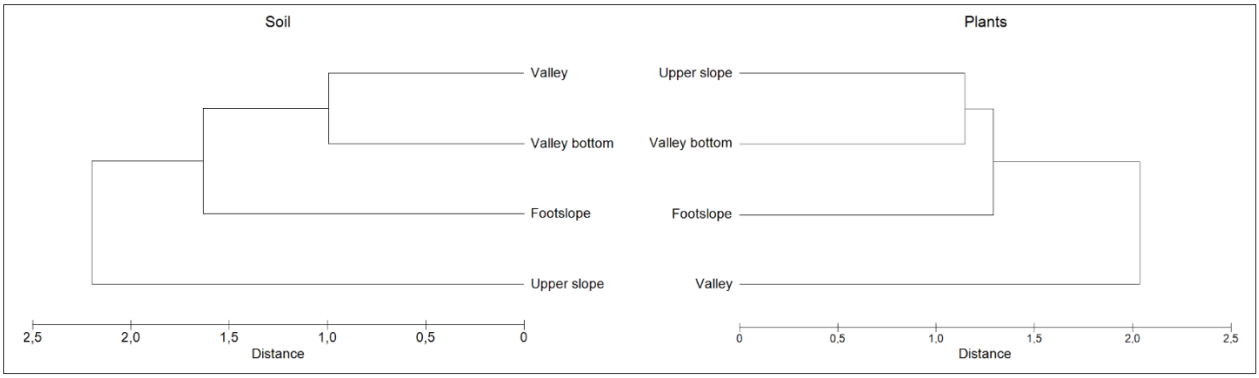

Figure 6.6. Dendrograms of metal concentration ordinations of the soil and the plant samples based on group averages of metal concentrations under the topography factor.

6.3.2.2 Anthropogenic factor - Land use

Sites were significantly different regarding both the soil and plant samples (Table E1a,b, Appendix E). Tailings was the outer group in soils, while in plants, it was grouped with Gardens. In both soil and plant analysis, Tailings and Gardens were different from all the remaining sites, which formed a similar group (Fig. 6.7). The main metals driving the distribution of data of soil and plant samples, respectively, in this case were Cr (77% of contribution), Sr (8%) and Mg (6%); and Co (35%), Cr (22%) and Mg (14%). Cr was the only heavy metal that differed significantly among soil samples (Fig. 6.8) being highest for tailings and lowest for sheet erosion, while no element was particularly different in the plants.

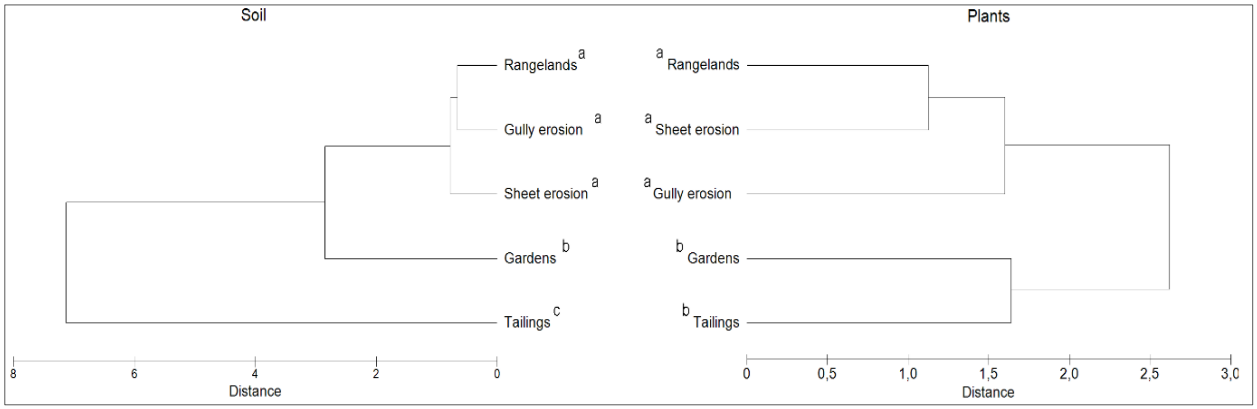

Figure 6.7. Dendrograms of metal concentration ordinations of the soil and the plant samples based on group averages of heavy metal concentrations under the land use factor. Different letters indicate significant differences in the pairwise post hoc comparisons among sites (*p*<0.05).

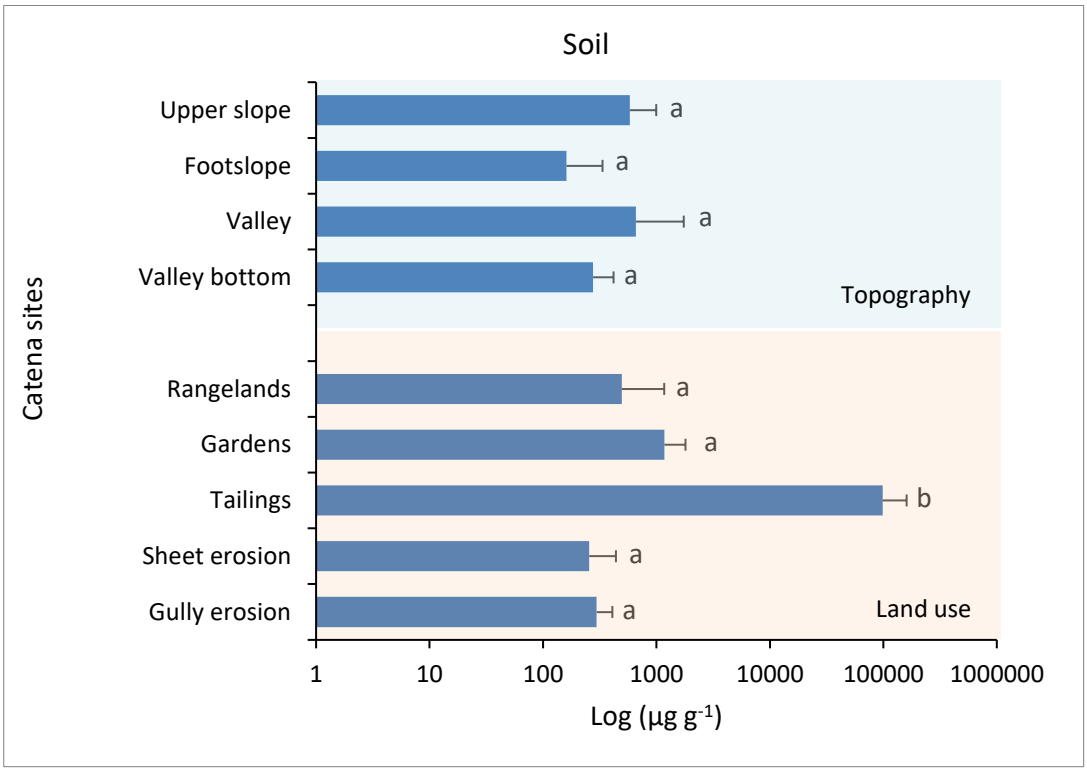

Figure 6.8. Cr concentration in soil under topography and land use factor. Different letters represent significant difference in the pairwise post hoc comparison (*p*<0.05).

6.4 Discussion

6.4.1 Metal levels in soil and plant leaves

As predicted, soils in Sekhukhuneland are enriched with multiple metals as most metals exceeded permissible limits reported for South African agricultural soils (Herselman *et al*., 2005). Except for the tailings, metal concentrations of the study area were within the range reported for serpentine regions worldwide (Rajakaruna & Bohm, 2002; Mizuno & Kirihata, 2015; Williamson & Balkwill, 2015; Hseu *et al*., 2018). Findings pointed out high metal concentrations along the catena soils in Sekhukhuneland, which confirms their ultramafic classification. In this regard, again, except for tailings in Sekhukhuneland, metal concentrations were comparable to reported levels for 'natural' serpentine soil in South Africa (Venter *et al*., 2018) and the world (Adriano, 1986).

Foliar metal accumulation in 74% of the plant species points to local adaptation via accumulation of several metals (Baker, 1981). Though hyperaccumulation is common in serpentine floras (Rajakaruna & Bohm, 2002; van der Ent *et al*., 2013; Siebert *et al*., 2018a), none of the species from the present investigation could be classified as hyperaccumulators according to the criteria outlined by van der Ent *et al.* (2013). Vegetation with high metal tolerance, but lacking hyperaccumulators as observed in the present study, is usually the norm, and has been reported for ultramafic areas in South Africa (Siebert *et al*., 2018b) and globally (Oze *et al*., 2008; van der Ent & Reeves, 2015), as well as for mine tailings (Mansfield *et al.*, 2014; Paul *et al*., 2018) and mining affected areas (Tang *et al*., 2020).

Three of the five Sekhukhuneland endemics were detected as bioaccumulators of multiple metals (i.e. Co, Mo and Zn) in their leaves. This is noteworthy as restricted range species often form a major component of metallophytes of an area due to their evolutionary selection to tolerate metal-rich soils (Baker *et al*., 2010). Overall, the indigenous species accumulated a variety of metals from natural habitats such as rangelands and eroded areas. Exotics from tailings and gardens (disturbed habitats) accumulated mostly Mo from both and Sr from tailings. This indicates a greater bioaccumulation trait for indigenous species in metalliferous sites in Sekhukhuneland and their suitability for phytoremediation as is often suggested in literature (Midhat *et al*., 2019). Indigenous plants with BAF values > 1 for more than one metal could be investigated for their potential to decontaminate soil. Such species could present better options for phytoremediation than hyperaccumulators that mostly remove single elements (Rajakaruna *et al*., 2006; Ferrero *et al.*, 2020).

Besides Mg, metals with the highest soil concentrations, i.e. Cr, Fe, Mn and Ni were effectively excluded (BAF < 1) by all plant species. Such a survival mechanism by plants is often suggested

in case of serpentine species (Baker, 1981; Rajakaruna & Baker, 2004; Oze *et al*., 2008; van der Ent & Reeves, 2015) and metallophytes from mines (Paul *et al*., 2018; Tang *et al*., 2020).

Common plants from Sekhukhuneland, therefore, differ in their response strategy to metalliferous soils along a catena, as some metals are accumulated efficiently in leaves while others are excluded. This could be primarily related to differential uptake, translocation and accumulation mechanisms for individual metal (Baker, 1981). Nonetheless, plants withstand elevated levels of metals of both geogenic and anthropogenic origins, which makes them eligible as metallophytes (Baker *et al*., 2010; Boyd & Rajakaruna, 2013; Pollard *et al.*, 2014; Paul *et al*., 2018).

Among the growth forms, the overall distinct concentration levels among grasses, shrubs and the remaining forms reflected how plant structure can also be a predictor of bioaccumulation. Grasses are relatively better adapted to the metal enriched soils of Sekhukhuneland (Siebert *et al*., 2002, 2003). This was even more evident in relation to Co which can be more available in serpentine soils (Echevarria, 2018), but accumulated in low amounts in grasses of this study. Oze *et al.* (2008) reported grasses being excluders of Co from serpentine outcrops. With the exception of Co, the present study did not point out particular elements to be accumulated more or less effectively by different growth forms. However, accumulation of multiple elements altogether could be differentiated among growth forms. Future investigations may focus on grasses, shrubs and short, erect forbs that had distinctly different metal accumulation to identify the best-fit species to be considered for phytoremediation in Sekhukhuneland. Species from such growth forms are often recommended for phytoremediation in mining areas (Visoottiviseth *et al*., 2002; Paul *et al.*, 2018).

6.4.2 Influence of topography and land use

Under the topography factor, although without significant differences, soil samples from the upper slope could be ordinated as an outer group in comparison to all the other sites. Soils in these sites are shallow (Duan *et al*., 2015; Ding *et al*., 2017; Qiao *et al*., 2019), which closely resemble parent material mineralogy (Gaspar *et al*., 2020). Such soils can be metal-rich but eroded easily by gravity, wind, raindrop splash effect and high velocity of run-off water resulting in loss of heavy metals (Duan *et al*., 2015; Zhang *et al*., 2019). The erosion effect is more prominent in sloping serpentine outcrops with stony soil structure lacking clay and moisture to bind the soil (Brady *et al*., 2005), as observed in Sekhukhuneland. On the other hand, for plants, valley formed a separate cluster than the rest of the land uses. Valleys with higher soil clay content as reported for the study region (Siebert *et al*., 2002) may contain more metals in clay (Alloway, 2013) to act as sinks for sediment borne metals sourced from mountains and rivers (Jarsjö *et al*., 2017; Zhang *et al*., 2019) unlike the upper slope and valley bottom that are mainly characterised by topsoil

displacement (Duan *et al*., 2015; Amare *et al*., 2019). In valleys, therefore, an increase in metal quantity over time could increase the bioavailability of metals to plants in Sekhukhuneland.

Regarding the land-use factor, the significant differences found among both soils and plant samples can be attributed to the presence of mining activities in Sekhukhuneland, especially observing high concentrations of metals near tailings facilities. Metal enrichment of local soils around mine tailings is reported globally (Mansfield *et al.*, 2014; Paul *et al*., 2018; Wang *et al*., 2019; Tang *et al*., 2020). Cr mine tailings contain considerable proportions of Cr_2O_3 and other metals mainly Fe, Mg, Mn and Ni (Dhal *et al*., 2010; Özgen, 2012) which explains the high overall metal quantities in tailing soils in Sekhukuneland. More evidence for the outstanding influence of mining activity is Cr being highlighted as the main metal driving the differences among the soil samples. Oze *et al.* (2004) suggested that the presence of chromite even at a very low amount in soil may increase overall Cr content enormously. Consequently, metal availability in soils around tailings could be increased due to fast leaching of metals especially Cr that can be in highly reactive and mobile forms even at an alkaline pH (7–9) (Dhal *et al*., 2010), which is the common pH range observed in tailings in Sekhukhuneland. Elevated foliar uptake of metals from mine areas has been reported globally (Paul *et al*., 2018; van der Ent *et al*., 2020). Gardens, on the other hand, differ from tailings regarding soils samples, but not regarding plant samples, which might point to a limit of uptake to be reached by the plant species in the tailings in spite of the higher soil metal concentrations that match with past reports (Dudka & Miller, 1999). Metal enrichment in garden soils and crops around metal mines is reported extensively (Felix-Henningsen *et al*., 2011; Alloway, 2013; Antisari *et al*., 2020) and can be concluded for Sekhukhuneland as most sampled gardens were in proximity to multiple tailings and mines. Considering the high human health hazard potential of metals, especially Cr and Ni (Infante *et al*., 2021), garden crops should be evaluated for potential health risk (Adhikari *et al*., 2021).

Other land uses (rangelands and wastelands comprising sheet and gully erosion), forming a separate group for soils and plants regarding metal distribution, was anticipated as in these natural habitats most geogenic sourced metals are released slowly from minerals (Wuana & Okieimen, 2011). In this regard, pH could be an important determinant as the availability of individual metal may vary with this soil parameter (Echevarria, 2018; Siebert *et al*., 2018b). Particularly for Cr, weather resistance of chromite would produce Cr at a slow pace and formed Cr will quickly produce stable mineral or organic complexes of low solubility at pH > 4 (Oze *et al*., 2004). Alkaline soils of rangelands, therefore, in spite of having Cr quantities mostly higher than 200 µg g^{-1} that is common for serpentine soils (Oze *et al*., 2004), may present comparatively less Cr availability to plants. Overgrazing could be an important agent to induce and aggravate soil

erosion in wastelands especially in sloping regions (Dlamini *et al*., 2011; Amare *et al*., 2019) such as the study area that may further decrease metal quantity in the topsoil.

The similarity in the distribution of metals in both soil and plant samples, under the natural and anthropogenic factors evaluated in this study, suggested that both factors are actively influencing metal concentrations in the Sekhukhuneland catena. As indicated previously, the adverse effects of excess metals on ecosystems are a complex outcome governed by geological and anthropogenic sources (Gaspar *et al*., 2020). In this regard, Sekhukhuneland can be identified as a 'secondary metalliferous site' (Baker *et al*., 2010) where outcrops are exploited heavily by mining and considering the long mining history of Sekhukhuneland (Scoon & Viljoen, 2019), a greater influence of land use factor on metal distribution in soils and plant leaves is reasonable.

Summary

The study attempted to unravel the influence of topography and land use on the metal distribution along a catena in Sekhukhuneland and evaluate the foliar metal bioaccumulation potential of common species from the region. A greater influence of land use on metal distribution in soils and plant leaves indicated human interference as a principal driver in this regard. Significantly higher Cr concentration in soils around tailings could be indicative of mines as a soil polluter in the study region. Plants, including indigenous, endemic and exotic species, could be classified as metallophytes that successfully inhabited metal-rich soils by selectively accumulating and excluding metals. Metal concentrations differed among growth forms, with grasses, shrubs and short, erect forbs showing the most potential for phytoremediation properties. Continuous monitoring of the spatial distribution of metals in soil is urgent, as rapidly changing land use patterns in Sekhukhuneland could lead to further evolution of the soil-plant dynamics. Future research on metallophytes of the region should be prioritized to conserve them and explore their pollution mitigation potential.

References

Adhikari, S., Siebert, S.J. & Jordaan, A. 2021. Chromium dust deposition on *Moringa oleifera* leaves harvested by local communities in Sekhukhuneland, South Africa. *Acta Horticulturae,* 1306:99–106.

Adriano, D.C. 1986. *Trace elements in the environment.* New York: Springer.

Alloway, B.J. 2013. Sources of heavy metals and metalloids in soils. *Heavy metals in soils: Trace metals and metalloids in soils and their bioavailability*. Dordrecht: Springer. pp. 11–50. (Environmental Pollution, Vol. 22).

Amare, S., Keesstra, S., van der Ploeg, M., Langendoen, E., Steenhuis, T. & Tilahun, S. 2019. Causes and controlling factors of valley bottom gullies. *Land,* 8(9), art. 141. https://doi.org/10.3390/land8090141

Anjum, N.A., Singh, H.P., Khan, M.I.R., Masood, A., Per, T.S., Negi, A., … Pereira, E. 2015. Too much is bad - an appraisal of phytotoxicity of elevated plant-beneficial heavy metal ions. *Environmental Science and Pollution Research,* 22(5):3361–3382.

Antisari, L.V., Bini, C., Ferronato, C., Gherardi, M. & Vianello, G. 2020. Translocation of potential toxic elements from soil to black cabbage (*Brassica oleracea* L.) growing in an abandoned mining district area of the Apuan Alps (Tuscany, Italy). *Environmental Geochemistry and Health*, 42:2413–2423.

Baker, A.J.M. 1981. Accumulators and excluders - strategies in the response of plants to heavy metals. *Journal of Plant Nutrition*, 3:643–654.

Baker, A.J.M., Ernst, W.H.O., van der Ent, A., Malaisse, F. & Ginocchio, R. 2010. Metallophytes: the unique biological resource, its ecology and conservational status in Europe, central Africa and Latin America. Batty, L.C. & Hallberg, K.B., eds. *Ecology of industrial pollution*. Cambridge: Cambridge University Press. pp. 7–40.

Boyd, R.S. & Rajakaruna, N. 2013. Heavy metal tolerance. In: Gibson, D., ed. *Oxford bibliographies in ecology*. New York: Oxford University Press. pp. 1–24.

Brady, K.U., Kruckeberg, A.R. & Bradshaw Jr., H.D. 2005. Evolutionary ecology of plant adaptation to serpentine soils. *Annual Review of Ecology, Evolution, and Systematics*, 36(1):243–266.

Dhal, B., Das, N.N., Pandey, B.D. & Thatoi, H.N. 2010. Environmental quality of the Boula-Nuasahi chromite mine area in India. *Mine Water and the Environment,* 30(3):191–196.

Dlamini, P., Orchard, C., Jewitt, G., Lorentz, S., Titshall, L. & Chaplot, V. 2011. Controlling factors of sheet erosion under degraded grasslands in the sloping lands of KwaZulu-Natal, South Africa. *Agricultural Water Management*, 98(11):1711–1718.

Ding, Q., Cheng, G., Wang, Y. & Zhuang, D. 2017. Effects of natural factors on the spatial distribution of heavy metals in soils surrounding mining regions. *Science of the Total Environment*, 578:577–585.

Duan, X., Zhang, G., Rong, L., Fang, H., He, D. & Feng, D. 2015. Spatial distribution and environmental factors of catchment-scale soil heavy metal contamination in the dry-hot valley of upper Red River in southwestern China. *Catena*, 135:59–69.

Dudka, S. & Miller, W.P. 1999. Accumulation of potentially toxic elements in plants and their transfer to human food chain. *Journal of Environmental Science and Health*, 34(4):681–708.

Duffus, J.H. 2002. “Heavy Metals” - a meaningless term? *Pure and Applied Chemistry*, 74(5):793–807.

Du Plessis, C., van Zijl, G., Van Tol, J. & Manyevere, A. 2020. Machine learning digital soil mapping to inform gully erosion mitigation measures in the Eastern Cape, South Africa. *Geoderma*, 368, art. 114287. https://doi.org/10.1016/j.geoderma.2020.114287

Echevarria, G. 2018. Genesis and behaviour of ultramafic soils and consequences for nickel biogeochemistry. In: Van der Ent, A., Echevarria, G., Baker, A.J.M. & Morel, J., eds. *Agromining: farming for metals. Mineral resource reviews*. Cham: Springer. pp. 135–156.

Eze, P.N., Udeigwe, T.K. & Stietiya, M.H. 2010. Distribution and potential source evaluation of heavy metals in prominent soils of Accra Plains, Ghana. *Geoderma*, 156:357–362.

Felix-Henningsen, P., Sayed, M.A.H.A., Narimanidze-King, E., Steffens, D. & Urushadze, T. 2011. Bound forms and plant availability of heavy metals in irrigated, highly polluted kastanozems in the Mashavera valley, Se Georgia. *Annals of Agrarian Science*, 9(1):111–119.

Ferrero, A., Walsh, P. & Rajakaruna, N. 2020. The physiology, genetics, adaptive significance and biotechnology of Ni-hyperaccumulating plants. In: Salwan, R. & Sharma, V., eds. *Physiological and biotechnological aspects of extremophiles*. S.I.: Elsevier. pp. 327–347.

Gall, J.E., Boyd, R.S. & Rajakaruna, N. 2015. Transfer of heavy metals through terrestrial food web: a review. *Environmental Monitoring and Assessment*, 187, 201. https://doi.org/10.1007/s10661-015-4436-3

Gaspar, L., Lizaga, I. & Navas, A. 2020. Elemental mobilisation by sheet erosion affected by soil organic carbon and water fluxes along a radiotraced soil catena with two contrasting parent materials. *Geomorphology,* 370(1), art. 107387. https://doi.org/10.1016/j.geomorph.2020.107387

Hänsch, R. & Mendel, R.R. 2009. Physiological functions of mineral micronutrients (Cu, Zn, Mn, Fe, Ni, Mo, B, Cl). *Current Opinion in Plant Biology*, 12(3):259–266.

Harrison, S.P. & Rajakaruna, N. 2011. *Serpentine: evolution and ecology in a model system*. Berkeley: University of California Press. pp. 1–373.

Herselman, J.E., Steyn, C.E. & Fey, M.V. 2005. Baseline concentration of Cd, Co, Cr, Cu, Pb, Ni and Zn in surface soils of South Africa. *South African Journal of Science*, 101(11–12):509–512.

Hseu, Z-Y., Zehetner, F., Fujii, K., Watanabe, T. & Nakao, A. 2018. Geochemical fractionation of chromium and nickel in serpentine soil profiles along a temperate to tropical climate gradient. *Geoderma*, 327:97–106.

Infante, E.F., Dulfo, C.P., Dicen, G.P., Hseu, Z.Y. & Navarrete, I.A. 2021. Bioaccumulation and human health risk assessment of chromium and nickel in paddy rice grown in serpentine soils. *Environmental Science and Pollution Research*, 28:17146–17157.

Jarsjö, J., Chalov, S.R., Pietroń, J., Alekseenko, A.V. & Thorslund, J. 2017. Patterns of soil contamination, erosion and river loading of metals in a gold mining region of northern Mongolia. *Regional Environmental Change*, 17:1991–2005.

Keren, R. 1991. Specific effect of magnesium on soil erosion and water infiltration. *Soil Science Society of America Journal*, 55:783–787.

Malinowska, E. & Szumacher, I. 2013. Application of the catena concept in studies of landscape system dynamics. *Miscellanea Geographica - Regional Studies on Development*, 17(4):42–49.

Mansfield, M., Pope, N. & Rajakaruna, N. 2014. Diversity and soil-tissue elemental relations of vascular plants of Callahan Mine, Brooksville, Maine, USA. *Rhodora*, 116:283–322.

Marcelo-Silva, J. & Christofoletti, R.A. 2019. Assessments of metals in coastal environments: state of art. *Archives of Environmental Contamination and Toxicology,* 77:162–170.

Midhat, L., Ouazzani, N., Hejjaj, A., Ouhammou, A. & Mandi, L. 2019. Accumulation of heavy metals in metallophytes from three mining sites (southern centre Morocco) and evaluation of their phytoremediation potential. *Ecotoxicology and Environmental Safety*, 169:150–160.

Mirzabaev, A., Nkonya, E., Goedecke, J., Johnson, T. & Anderson, W. 2015. Global drivers of land degradation and improvement. *Current Opinion in Environmental Sustainability,* 15:9–19.

Mizuno, T. & Kirihata, Y. 2015. Elemental composition of plants from the serpentine soil of Sugashima Island, Japan. *Australian Journal of Botany,* 63(4):252–260.

Mogale, M.M.P., Raimondo, D.C & Van Wyk, B.-E. 2019. The ethnobotany of central Sekhukhuneland, South Africa. *South African Journal of Botany,* 122:90–119.

Morgan, R.P.C. 2005. *Soil erosion and conservation*. 3rd ed. Oxford: Blackwell.

Naldrett, A.J., Wilson, A., Kinnaird, J., Yudovskaya, M. & Chunnett, G. 2012. The origin of chromitites and related PGE mineralization in the Bushveld Complex: new mineralogical and petrological constraints. *Mineralium Deposita*, 47:209–232.

O'Dell, R.E. 2014. Conservation and restoration of chemically extreme edaphic endemic flora in the western US. In: Rajakaruna, N., Boyd, S.R. & Harris, T.B., eds. *Plant ecology and evolution in harsh environments*. New York: Nova. pp. 313–364.

Oze, C., Fendorf, S., Bird, D.K. & Coleman, R.G. 2004. Chromium geochemistry of serpentine soils. *International Geology Review*, 46(2):97–126.

Oze, C., Skinner, C., Schroth, A.W. & Coleman, R.G. 2008. Growing up green on serpentine soils: biogeochemistry of serpentine vegetation in the Central Coast Range of California. *Applied Geochemistry*, 23(12):3391–3403.

Özgen, S. 2012. Modelling and optimization of clean chromite production from fine chromite tailings by a combination of multi gravity separator and hydro cyclone. *Journal of the Southern African Institute of Mining and Metallurgy,* 112(5):387–394

Paul, A.L.D., Erskine, P.D. & van der Ent, A. 2018. Metallophytes on Zn-Pb mineralised soils and mining wastes in Broken Hill, NSW, Australia. *Australian Journal of Botany*, 66(2):124–133.

Pollard, A.J., Reeves, R.D. & Baker, A.J.M. 2014. Facultative hyperaccumulation of heavy metals and metalloids. *Plant Science*, 217– 218:8–17.

Proctor, J. 2003. Vegetation and soil and plant chemistry on ultramafic rocks in the tropical far East. *Perspectives in Plant Ecology, Evolution and Systematics,* 6(1,2):105–124.

Qiao, P., Yang, S., Lei, M., Chen, T. & Dong, N. 2019. Quantitative analysis of the factors influencing spatial distribution of soil heavy metals based on geographical detector. *Science of the Total Environment*, 664:392–413.

Quinn, C.H., Ziervogel, G., Taylor, A., Takama, T. & Thomalla, F. 2011. Coping with multiple stresses in rural South Africa. *Ecology and Society,* 16(3), 2. https://doi.org/10.5751/ES-04216-160302

Rajakaruna, N. & Bohm, B.M. 2002. Serpentine and its vegetation: a preliminary study from Sri Lanka. *Journal of Applied Botany*, 76:20–28.

Rajakaruna, N. & Baker, A.J.M. 2004. Serpentine: a model habitat for botanical research in Sri Lanka. *Ceylon Journal of Science (Biological Sciences),* 32:1–19.

Rajakaruna, N., Tompkins, K.M. & Pavicevic, P.G. 2006. Phytoremediation: an affordable green technology for the clean-up of metal-contaminated sites in Sri Lanka. *Ceylon Journal of Science (Biological Sciences)*, 35:25–39.

Rajakaruna, N. & Boyd, R.S. 2014. Serpentine soils. In: Gibson, D., ed. *Oxford bibliographies in ecology*. New York: Oxford University Press. pp. 33–66.

Reeves, R.D., Baker, A.J.M., Jaffré, T., Erskine, P.D., Echevarria, G. & van der Ent, A. 2017. A global database for plants that hyperaccumulate metal and metalloid trace elements. *New Phytologist*, 218(2):407–411.

Scoon, R.N. & Viljoen, M.J. 2019. Geoheritage of the eastern limb of the Bushveld Igneous Complex, South Africa: a uniquely exposed layered igneous intrusion. *Geoheritage*, 11:1723–1748.

Shackleton, R.T. 2020. Loss of land and livelihoods from mining operations: a case in the Limpopo Province, South Africa. *Land Use Policy,* 99, art. 104825. https://doi.org/10.1016/j.landusepol.2020.104825

Siebert, S.J., Van Wyk, A.E. & Bredenkamp, G.J. 2002. The physical environment and major vegetation types of Sekhukhuneland, South Africa. *South African Journal of Botany,* 68(2):127–142.

Siebert, S.J., Matthee, M. & Van Wyk, A.E. 2003. Semi-arid savanna of the Potlake Nature Reserve and surrounding areas in Sekhukhuneland, South Africa. *Koedoe,* 46(1):29–52.

Siebert, S.J, Schutte, N.C, Bester, S.P., Komape, D.M. & Rajakaruna, N. 2018a. *Senecio conrathii* N.E.Br. (Asteraceae), a new hyperaccumulator of nickel from serpentinite outcrops of the Barberton Greenstone Belt, South Africa. *Ecological Research*, 33(3):651–658.

Siebert, S.J., Steytler, J., Boneschans, R.B., Siebert, F. & Coetzee, M.S. 2018b. Manganese tolerance of *Aloe greatheadii* Schönland var. *davyana* (Schönland) Glen & D.S.Hardy (Asphodelaceae: Alooideae) on ultramafic-peralkaline outcrops, South Africa. *Haseltonia*, 25:1–9.

Tang, R.H., Erskine, P.D., Lilly, R. & van der Ent, A. 2020. The biogeochemistry of copper metallophytes in the Roseby Corridor (North-West Queensland, Australia). *Chemoecology*, 31:19–30.

Van der Ent, A., Baker, A.J.M., Reeves, R.D., Pollard, A.J. & Schat, H. 2013. Hyperaccumulators of metal and metalloid trace elements: facts and fiction. *Plant and Soil*, 362(1-2):319–334.

Van der Ent, A. & Reeves, R.D. 2015. Foliar metal accumulation in plants from copper-rich ultramafic outcrops: case studies from Malaysia and Brazil. *Plant and Soil*, 389(1–2):401–418.

Van der Ent, A., Baker, A.J.M., Reeves, R.D., Chaney, R.L., Anderson, C.W.N., Meech, J.A., … Mulligan, D.R. 2015. Agromining: Farming for Metals in the Future? *Environmental Science and Technology,* 49(8):4773–4780.

Van der Ent, A., Vinya, R., Erskine, P.D., Malaisse, F., Przybyłowicz, W.J., Barnabas, A.D., … Mesjasz-Przybyłowicz, J. 2020. Elemental distribution and chemical speciation of copper and cobalt in three metallophytes from the copper–cobalt belt in northern Zambia. *Metallomics,* 12:682–701.

Van Zijl, G.M., Ellis, F. & Rozanov, A. 2014. Understanding the combined effect of soil properties on gully erosion using quantile regression. *South African Journal of Plant and Soil*, 31(3):163–172.

Van Wyk, B. & Van Wyk, P. 1997. *Field Guide to Trees of Southern Africa*. Cape Town: Struik.

Venter, A., Siebert, S.J., Rajakaruna, N., Barnard, S., Levanets, A., Ismail, A., … Sanko, T. 2018. Biological crusts of serpentine and non-serpentine soils from the Barberton Greenstone Belt of South Africa. *Ecological Research,* 33(3):629–640.

Visoottiviseth, P., Francesconi, K. & Sridokchan, W. 2002. The potential of Thai indigenous plant species for the phytoremediation of arsenic contaminated land. *Environmental Pollution,* 118(3):453–461.

Wang, P., Sun, Z., Hu, Y. & Cheng, H. 2019. Leaching of heavy metals from abandoned mine tailings brought by precipitation and the associated environmental impact. *Science of the Total Environment,* 695, art. 133893. https://doi.org/10.1016/j.scitotenv.2019.133893

White, R.E. 2005. *Principles and practice of soil science: The soil as a natural resource*. 4th ed. Oxford: Blackwell.

Williamson, S.D. & Balkwill, K. 2006. Factors determining levels of threat to serpentine endemics. *South African Journal of Botany,* 72(4):619–626.

Williamson. S.D. & Balkwill, K. 2015. Plant census and floristic analysis of selected serpentine outcrops of the Barberton Greenstone Belt, Mpumalanga, South Africa. *South African Journal of Botany*, 97:133–142.

Wuana, R.A. & Okieimen, F.E. 2011. Heavy metals in contaminated soils: a review of sources, chemistry, risks and best available strategies for remediation. *International Scholarly Research Network Ecology*, art. 402647. https://doi.org/10.5402/2011/402647

Zhang, J., Xu, Y., Wu, Y., Hu, S. & Zhang, Y. 2019. Dynamic characteristics of heavy metal accumulation in the farmland soil over Xiaoqinling gold-mining region, Shaanxi, China. *Environmental Earth Sciences,* 78, 25. https/doi.org/10.1007/s12665-018-8013-2

Chapter 7

Conclusions

A comprehensive summary of major findings of this study related to Cr adsorption and accumulation by plant leaves from the mining-smelting region in Sekhukhuneland is presented here. The chapter further reflects on study limitations and knowledge gaps that require future attention in this regard. Study objectives were reminded followed by findings to highlight alignment.

7.1 Study objectives and major findings

Objective 1: To assess Cr chemistry, toxicity and describe known chemical reaction mechanisms in the environment.

The two Cr oxidation states tri- (Cr(III)) and hexavalent (Cr(VI)) oxidation states differ in their origin, chemical property, bioavailability and toxicity. Cr(III) is the predominant formed as a result of weathering of the parent material and is rapidly immobilised as organic or inorganically bound complexes that are mainly soluble at acidic pH and have low reactivity and toxicity, therefore. On the contrary, the formation of Cr(VI) in nature due to oxidation of Cr(III) is an intermittent phenomenon. On the other hand, anthropogenic waste add generous amounts of Cr(VI) in the environment that can be extremely reactive, soluble at all pH and remain as persistent pollutants in the environment. Cr(VI) compounds hence present far greater biological hazard potential than Cr(III). The two Cr oxidation states (i.e. Cr(III) and Cr(VI)) may interconvert depending on ambient reaction parameters (e.g. temperature, pH, Eh, presence of oxidiser/reducer, organic matter and microbial community) making species specific concentration determination challenging in any matrix.

Objective 2: To evaluate phytotoxicity in useful plants and describe known plant-Cr interactions.

Cr induces phytotoxic effects at varying degree and type in different species. Results revealed the global occurrence of Cr accumulation by food and medicinal plants above the recommended safe limits. For most cases, exposure to human released Cr including Cr containing dust and, in few instances, geogenic Cr from outcrop or natural disasters were implicated for such high concentrations. Cr was associated with non-carcinogenic and carcinogenic health risks via consumption of useful crops primarily due to pollution from mines and industries. Plant-Cr interaction process has been recognised as a complex outcome of several variables namely plant species, concentration and availability of Cr oxidation states (i.e. Cr(III) and Cr(VI)), cultivation and preservation practices and the environment (e.g. geology, climate, proximity and type of

polluters and emission rate). In this regard, urban crops could be particularly susceptible to multifaceted Cr exposure. Prominent knowledge gaps identified during the review, i.e. lack of sufficient scientific report on Cr(VI) determination in plants, the contribution of dust towards Cr contamination especially in mining-smelting areas and contamination status of useful plants from home gardens and wild, are addressed in the present study.

Objective 3: To attest to the presence of Cr dust on plant leaf surfaces.

Energy Dispersive X-ray Spectroscopy determined Cr on the leaf surfaces of studied food and medicinal plant species sampled from the Cr mining-smelting region in Sekhukhuneland. Later the same analysis on randomly selected dust particles identified Cr containing particles on leaf surfaces. Cr dust deposition on leaf surfaces was therefore confirmed. Furthermore, considerable availability of dust borne Cr to local vegetation was indicated by the high percentage of Cr containing dust on leaf surfaces. High wt% of a similar group of elements on leaf surfaces and deposited dust suggested an alteration in leaf surface elemental composition due to dust deposition. Such elemental alterations may be concerning as both the nutritional and remedial properties of plant species depend on their typical elemental composition.

Objective 4: To assess the size distribution and shape of Cr dust to understand the morphology of the particles.

The three detected PM size fractions ($PM_{2.5}$, PM_{10} and PM > 10 µm) had varying concentrations of Cr. Detection of the highest Cr values in the three above-mentioned size fractions indicated possible Cr hazard linked to all PM sizes in the region.

Objective 5: To describe the plant morphological traits that are related to the deposition of Cr dust on leaf surfaces.

Two morphological traits, i.e. leaf area (leaf macromorphology) and plant height (plant morphology) showed a significant positive effect on Cr particle deposition on plant leaves. Comparatively taller plant species with larger leaves may be susceptible to atmospheric Cr dust pollution in the study region. Scanning Electron Microscopy (SEM) imaged Cr particles on various leaf surface micromorphological features, but none of these features influenced Cr amount or Cr particle size on leaf surfaces significantly. Results further revealed that proximity to active mining sites was the main determinant of Cr dust deposition on leaves rather than the high quantity of total dust. In terms of total dust accumulation potential by plant leaves, long trichomes may favour the process while larger leaves could accumulate more PM_{10} on the adaxial leaf surfaces.

Objective 6: To identify possible sources of Cr in soils and plant leaves based on their elemental composition.

EDS analysis recorded soil and leaf surface elemental composition data were used to identify possible Cr sources in the two matrices (soils and plant leaves). Cr in the soil could be contributed by natural (ultramafic geology) and anthropogenic (polluters) sources as most localities were characterised by the presence of both of these Cr sources. Leaf surface Cr was primarily associated with environmental pollution from chromite ore associated activities namely mining, smelting and ore transportation. Soil dust could be of less importance in this regard. The presence of anthropogenic Cr dust on leaf surfaces is concerning as such particles generally contain Cr in a more reactive and hazardous form (i.e. Cr(VI)) than geogenic Cr dust that is enriched with Cr(III) of low toxicity potential.

Objective 7: To determine the leaf surface-Cr dust interaction by assessing the contribution of plant morphology (e.g. plant height, leaf area, epicuticular wax, stomata and trichome size and density) and pollution source (proximity to and the number of mines, road) variables on this interaction process.

A statistical analytical approach was designed whereby the combined influence of plant morphological traits and pollution variables was assessed to deduce leaf surface-Cr dust interaction under multifaceted environmental Cr exposure in the region. The analysis was performed individually for adaxial and abaxial leaf surface as they varied in morphological features and were exposed differently (facing up or down) to environmental Cr dust. For the adaxial surface, the main factor was 'plant morphology' that summed up primarily the positive influence of leaf area, epicuticular wax and plant height. For the abaxial surface, 'leaf surface-dust interface' was the dominant factor that incorporated plant morphology (leaf area, epicuticular wax and stomata size) and pollution source (proximity to and the number of mines and roads) variables. It was revealed that a set of variables collectively promoted or restricted Cr particle deposition and adhesion on leaf surfaces rather than individual dominance.

Objective 8: To determine the contribution of deposited Cr particles to Cr accumulation in and on leaves of useful plants.

From a comparative analysis on Cr concentrations in W and UW leaf material, it was evident that Cr containing dust contributed significantly towards total Cr accumulation by useful plant leaves. In addition, foliar uptake of Cr dust was predicted that emphasised the importance of airborne dust as a viable contamination pathway to aerial plant parts besides the conventional root uptake in these mining-smelting polluted localities in Sekhukhuneland. Hence, Cr contamination of plant

leaves in Sekhukhuneland is a combined result of dust deposition on leaf surfaces and accumulation in leaf tissue. Since Cr concentrations in both W and UW leaves of useful plants sampled from home gardens and rangelands exceeded international permissible limits thus substantial Cr contamination of these common plant sources was confirmed.

Objective 9: To quantify the Cr(VI) content in plant leaves.

The presence of Cr(VI) in UW leaves of all investigated plant species suggested the environmental availability of the most hazardous Cr species in every locality investigated in Sekhukhuneland. Outcomes may indicate possible anthropogenic contribution towards plant-available Cr(VI) in the region as this oxidation state occurs in negligible concentrations in natural (unpolluted) environments. This is an important finding considering the multiple-fold higher biological toxicity potential of Cr(VI) than Cr(III).

Objective 10: To assess the effect of variables (plant growth form, soil and Cr polluters) on Cr concentration in and on leaves.

Different growth forms (trees, forbs and succulents) did not show a significant difference in foliar Cr levels suggesting all were capable of accumulating Cr in leaves. Proximity, number and types of Cr sources had a collective influence on leaf Cr content. Despite high soil Cr values in natural chromitite outcrops, leaf Cr levels were mostly influenced by the higher availability of anthropogenic Cr in soil (primarily in tailing facility). Presence of Cr(VI) in soils of all localities further suggested a higher possibility of human activity linked Cr pollution in the region. Tailings served as prime Cr dust sources to plant leaves in the surrounding areas.

Objective 11: To estimate the human health risk associated with the consumption of dust contaminated plant leaves.

Besides Cr, Al and Ni contamination of leaves were linked with dust. Concentrations of multiple elements (Cr, Al, Co, Hg and Zn) exceeded recommended safe limits in plants that may question the quality of locally harvested food and medicinal plant species in the region. Al presented exceptionally high estimated daily intake and non-carcinogenic risk. Cumulative non-carcinogenic risk associated with multiple toxic elements was far above the safe limit. Estimated carcinogenic risk was considerable for total Cr(VI) through UW, and total Cr via W and UW leafy vegetables. In addition, carcinogenic risk of Ni was substantial for both UW and W leaves. The local human population could therefore be at risk due to exposure to several hazardous elements including Cr through the ingestion of leafy vegetables. Any aerial plant parts need to be washed thoroughly

before use. Both non-carcinogenic and carcinogenic health risk possibility was higher for UW leaves than W ones.

Objective 12: To evaluate the influence of topography, land use (for soils and plants) and growth forms (plants only) on metal accumulation in soils and plant leaves.

Compared to less disturbed natural habitats, high metal values in soil and plant leaves from localities with human interference (i.e. tailings and gardens) indicated anthropogenic factor, i.e. land use (mining) as a primary driver to influence metal distribution in the two matrices in Sekhukhuneland catena. Results further revealed exceptionally high Cr content in tailings. Rehabilitation of tailings is therefore urgent to limit dispersion of hazardous substances further especially as human settlements often surround these facilities in Sekhukhuneland.

Objective 13: To determine the foliar metal bioaccumulation factors for the dominant plant species.

Dominant plant species (indigenous, endemic and exotic species) sampled from the catena in Sekhukhuneland were classified as metallophytes that were adapted to geogenic (chromitite outcrops) and anthropogenic (mines) sourced metal-rich soils. Indigenous species and endemics were the better accumulators of multiple elements and may present better phytoremediation potential to be explored further. Among growth forms grasses, shrubs and short, erect forbs could be investigated further for their phytoremediation prospect. Findings, therefore, provided valuable information regarding the possible use of metallophytes for soil pollution mitigation in Sekhukhuneland.

7.2 Study limitations

This study could be regarded as a pilot project that looked into foliar Cr contamination and associated human health impacts in a typical mining-smelting region in Sekhukhuneland, South Africa. Consequently, some study limitations need to be considered that could have restricted complete understanding of the plant leaf-Cr relation in the study area.

(1) No reliable wind speed and wind direction data were obtained for the study region. Such meteorological parameters are critical as they influence dust dispersion and deposition at a local, regional and national level. An alternative method was therefore selected to determine the air mass movements by calculating back trajectories that provided comprehensive information on air movements.

(2) There are scant scientific reports available on atmospheric Cr pollution in Sekhukhuneland that made it challenging to compare Cr particle morphology results of the present study with local data.
(3) Again, at a regional and national level, there is little or no available scientific data on Cr or Cr(VI) accumulation by local vegetation or Cr dust pollution of plants. This is a prominent knowledge gap that needs to be addressed.
(4) Similarly, only a few studies have explored the association between plant morphology and dust pollution in South Africa.
(5) The unavailability of any record on local reference dose for medicinal plants hindered health risk estimation for medicinal plants in the present study.
(6) In general, nationally, mining-smelting affected areas inhabited by underprivileged population are least studied in terms of health impacts associated with the use of polluted local food crops and medicinal plants. Hence, no local reference was obtained to compare the health risk assessment estimates of the present study.

7.3 Future directions

The current study presents some perspective on the current status of Cr enrichment of soils and local vegetation in Sekhukhuneland (Fig. 7.1). Extended research is envisioned on multiple interlinked research fields to comprehend the flow of Cr and other toxic metals within the air-soil-plant-human system (Fig. 7.1). Among others, the research areas that may require immediate extensive scientific attention are as follows:

(1) Health risk assessments – the region is inhabited by people who has a long history of use of numerous plant species (indigenous and exotic species) as food and medicinal components. Such species should be investigated to determine their metal accumulation capacity in useful part(s). Corresponding health risks should be estimated for different population groups (i.e. male/female and adult/child) to comprehend the lifelong health risk.
(2) Foliar uptake mechanism – investigation on the uptake mechanism of Cr, Cr(VI) and other toxic elements by aerial plant parts especially leaves and their subsequent translocation within the plant system may provide critical information regarding the safety of crop production under dust polluted environments in the region.
(3) Tailings – these are prominent Cr pollution sources in the region that should be investigated further to draw up a proper mitigation plan, if necessary. Continuous pollution monitoring is suggested.
(4) Metallophytes – should be explored for phytoremediation potential.

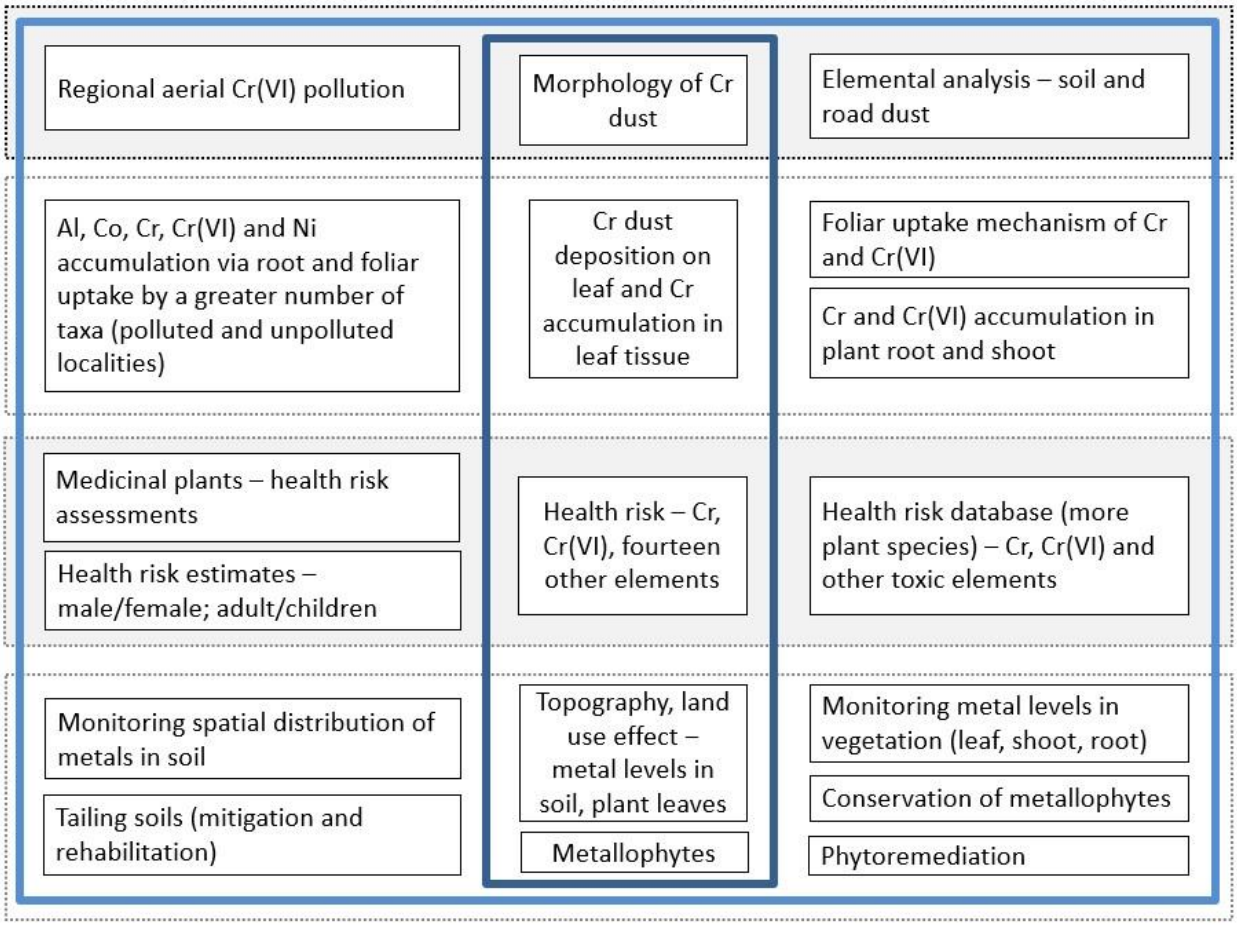

Figure 7.1. The current investigation (dark blue box in the centre) within a broader research field (light blue box) related to the plant-metal interactions in Sekhukhuneland. BAF, bioaccumulation factor.

Results point to a required re-evaluation of current pollution control measures by the respective managements in the study region. The outcomes of this study may also inform concerning authorities about the probable human health hazards especially the carcinogenic risk associated with the ingestion of metal contaminated useful plant leaves in the region to plan and implement necessary actions in this regard. Lastly, initiating social awareness among the locals regarding metal contamination of vegetation may limit exposure of Cr and other hazardous elements via ingestion of useful plants in these mining-smelting areas of Sekhukhuneland.

Appendix A: Chapter 2

Supplementary tables and figures

Table A1. Scopus search strings.

Search criteria	Search string per search criteria	Total number of articles by search	Number of articles selected
i.	**Cr toxicity in food plants** (TITLE-ABS KEY (*"Chromium"* AND *food* AND *plants*)) AND (((*pollution* OR *toxicity* AND *plants*)) AND (*crop* AND *vegetable* OR *herb* AND *plants*)) AND (*accum** OR *depos** AND NOT *waste* AND *water* OR *sewage* OR *sludge*) AND (LIMIT-TO (SUBJAREA , *"ENVI"*) OR LIMIT- TO (SUBJAREA ,*"AGRI"*) OR LIMITTO (SUBJAREA , *"EART"*)) AND (LIMIT-TO (LANGUAGE , *"English"*))	70	14
ii.	**Cr toxicity in medicinal plants** (TITLE-ABS- KEY (*"Chromium"* AND *medicinal* AND *plant*)) AND (*pollut** AND *contam** ANDNOT *nanoparticle*) AND (LIMITTO (SUBJAREA , *"PHAR"*) ORLIMITTO (SUBJAREA , *"ENVI"*) OR LIMITTO (SUBJAREA, *"AGRI"*)) AND(LIMITTO (LANGUAGE , *"English"*)) AND (EXCLUDE (SUBJAREA , *"MEDI"*) OR EXCLUDE (SUBJAREA , *"BIOC"*) OR EXCLUDE (SUBJAREA , *"CHEM"*) OREXCLUDE (SUBJAREA , *"CENG"*) OR EXCLUDE (SUBJAREA , *"CENG"*) OR EXCLUDE (SUBJAREA , *"IMMU"*) OR EXCLUDE (SUBJAREA , *"ENER"*))	49	15
iii.	**Most cited (Cr pollution/toxicity and food/medicinal plants)** (TITLE-ABS-KEY (*chrom** AND *pollut** AND *toxic**)) AND ((((*plant** ANDNOT *fish* OR *chicken* OR *mice*)) AND (*food** OR *veg** OR *medic** AND *plants*)) AND (*heavy* AND *met** AND *avail**)) AND (*chromium* AND *plant*) AND (LIMIT-TO (LANGUAGE , *"English"*)) AND (LIMITTO (SUBJAREA , *"ENVI"*) OR LIMITTO (SUBJAREA , *"AGRI"*) OR LIMITTO (SUBJAREA , *"PHAR"*) OR LIMITTO (SUBJAREA ,*"EART"*)) AND (EXCLUDE (SUBJAREA , *" MEDI"*) OR EXCLUDE (SUBJAREA , *"BIOC"*) OR EXCLUDE (SUBJAREA , *"CENG"*) OR EXCLUDE (SUBJAREA , *" ENGI"*) OR EXCLUDE (SUBJAREA , *"IMMU"*)) AND (EXCLUDE (LANGUAGE , *"Portuguese"*) OR EXCLUDE (LANGUAGE, *"Spanish"*) OR EXCLUDE (LANGUAGE , *"Turkish"*)) AND (EXCLUDE (EXACTKEYWORD , *"Lead"*) OR EXCLUDE (EXACTKEYWORD , *"Cadmium"*) OR EXCLUDE (EXACTKEYWORD , *"Zinc"*))	121	11
Total articles			39*

*1 article appeared in both i. and ii.

Table A2. Articles (63) sourced for systematic review

Year	First author	Journal	Title	Source
1992	Larsen, E.H.	*The Science of the Total Environment*	Atmospheric deposition of trace elements around point sources and human health risk assessment. II. Uptake of arsenic and chromium by vegetables grown near a wood preservation factory.	SCOPUS
1996	Voutsa, D.	*Environmental Pollution*	Trace elements in vegetables grown in an industrial area in relation to soil and air particulate matter	SCOPUS
1998	Zayed, A.	*Planta*	Chromium accumulation, translocation and chemical speciation in vegetable crops	SCOPUS
1999	Kimbrough, D.E.	*Critical Reviews in Environmental Science and Technology*	A critical assessment of chromium in the environment	Own database
2001	Cervantes, C.	*FEMS Microbiology Reviews*	Interactions of chromium with microorganisms and plants	Own database
2003	Pandey, N.	*Environmental and Experimental Botany*	Chromium interference in iron nutrition and water relations of cabbage	SCOPUS

2004	Dube, B.K.	*Journal of Vegetable Crop Production*	Chromium phytotoxicity alters metabolism in radish	SCOPUS
2004	Oze, C.	*International Geology Review*	Chromium geochemistry of serpentine soils	Own database
2004	Rai, V.	*Plant Science*	Effect of chromium accumulation on photosynthetic pigments, oxidative stress defense system, nitrate reduction, proline level and eugenol content of *Ocimum tenuiflorum* L.	Own database
2005	Panichev, N.	*Spectrochimica Acta*	Determination of Cr(VI) in plants by electrothermal atomic absorption spectrometry after leaching with sodium carbonate	Own database
2005	Rai, V.	*Bulletin of Environmental Contamination and Toxicology*	Chromium in some herbal drugs	SCOPUS

2005	Shanker, A.K.	*Environment International*	Chromium toxicity in plants	SCOPUS
2007	Mandiwana, K.L.	*Journal of Hazardous Materials*	The solubility of Cr(III) and Cr(VI) compounds in soil and their availability to plants	Own database
2007	Yang, Q.	*Environmental Monitoring and Assessment*	Heavy metals of vegetables and soils of vegetable bases in Chongqing, southwest China	SCOPUS
2008	Babula, P.	*Environmental Chemistry Letters*	Uncommon heavy metals, metalloids and their plant toxicity: a review	SCOPUS
2009	Tiwari, K.	*Journal of Environmental Biology*	Chromium (VI) induced phytotoxicity and oxidative stress in pea (*Pisum sativum* L.): biochemical changes and translocation of essential nutrients	SCOPUS
2010	Maharia, R.S.	*Journal of Environmental Science and Health*	Heavy metal bioaccumulation in selected medicinal plants collected from Khetri copper mines and comparison with those collected from fertile soil in Haridwar, India	SCOPUS

2010	Meena, A.K.	*Environmental Monitoring and Assessment*	Estimation of heavy metals in commonly used medicinal plants: a market basket survey	SCOPUS
2010	Nagajyoti, P.C.	*Environmental Chemistry Letters*	Heavy metals, occurrence and toxicity for plants: a review	SCOPUS
2011	Feng, J.	*Journal of Environmental Sciences*	Source attributions of heavy metals in rice plant along highway in eastern China	SCOPUS
2012	Säumel, I.	*Journal of Geochemical Exploration*	How healthy is urban horticulture in high traffic areas? Trace metal concentrations in vegetable crops from plantings within inner city neighbourhoods in Berlin, Germany	SCOPUS
2013	Abbasi, A.M.	*Ecotoxicology and Environmental Safety*	Health risk assessment and multivariate apportionment of trace metals in wild leafy vegetables from Lesser Himalayas, Pakistan	Own database
2013	Awodele, O.	*Journal of Ethnopharmacology*	Traditional medicinal plants in Nigeria-remedies or risks	SCOPUS

2013	Dhal, B.	*Journal of Hazardous Materials*	Chemical and microbial remediation of hexavalent chromium from contaminated soil and mining/metallurgical solid waste: a review	SCOPUS
2013	Ishaq, M.	*International Journal of Pharmaceutical Sciences Review and. Research*	Comparative study of heavy metals in *Albizia lebbeck,* collected from different environmental sites	SCOPUS
2013	Luginina, E.A.	*Annals of Warsaw University of Life Sciences*	The peculiarities of heavy metals accumulation by wild medicinal and fruit plants	Own database
2013	Mahmood, A.	*Journal of Ethnopharmacology*	Determination of toxic heavy metals in indigenous medicinal plants used in Rawalpindi and Islamabad cities, Pakistan	SCOPUS
2013	Sungur, S.	*International Journal of Food Properties*	Determination of Chromium Species in various medicinal plants consumed in Hatay region in Turkey	SCOPUS
2013	Tiwari, K.K.	*Bulletin of Environmental Contamination and Toxicology*	Chromium phytotoxicity in radish (*Raphanus sativus*): effects on metabolism and nutrient uptake	SCOPUS

2014	Barouchas, P.	*Australian Journal of Crop Science*	Effect of trivalent and hexavalent chromium (Cr) on the total Cr concentration in the vegetative plant parts of spearmint (*Mentha spicata* L.), lemon verbena (*Lippia citriodora* L.) and peppermint (*Mentha piperita* L.)	SCOPUS
2014	Ding, C.	*Ecotoxicology and Environmental Safety*	Phytotoxicity and accumulation of chromium in carrot plants and the derivation of soil thresholds for Chinese soils	SCOPUS
2014	Li, B.	*American Society of Agricultural and Biological Engineers (ASABE), Annual meeting paper*	Study on the migration of heavy metals pollution from soil to lettuce	SCOPUS
2014	Wahsha, M.	*Journal of Geochemical Exploration*	Potentially toxic elements in foodcrops (*Triticum aestivum* L., *Zea mays* L.) grown on contaminated soils	SCOPUS
2015	Kim, H.S.	*Soil Science and Plant Nutrition*	Influence of airborne dust on the metal concentrations in crop plants cultivated in a rooftop garden in Seoul	Own database

2015	Kozak, L.	*Environmental Toxicology and Chemistry*	Bioaccumulation of metals and metalloids in medicinal plant *Ipomoes pes-caprae* from areas impacted by Tsunami	SCOPUS
2015	Li, N.	*Science of the Total Environment*	Concentration and transportation of heavy metals in vegetables and risk assessment of human exposure to bioaccessible heavy metals in soil near a waste-incinerator site, south China	Own database
2015	Unver, M.C.	*Ekoloji*	Heavy metal contents of *Malva sylvestris* sold as edible greens in the local markets of Izmir	SCOPUS
2015	Ye, X.	*Environmental Monitoring and Assessment*	Assessment of heavy metal pollution in vegetables and relationships with soil heavy metal distribution in Zhejiang province, China	SCOPUS
2016	Arsenov, D.D.	*Matica Srpska Journal of Natural Sciences Archives*	Heavy metal contamination of vegetables from green markets in Novi Sad	Own database
2016	Aziz, M.A.	*Journal of Ethnopharmacology*	A review on the elemental contents of Pakistani medicinal plants: implications for folk medicines	SCOPUS

2016	Boechat, C.L.	*Water Air Soil Pollution*	Heavy metals and nutrients uptake by medicinal plants cultivated on multi-metal contaminated soil samples from an abandoned gold ore processing site	SCOPUS
2016	Kamunda, C.	*International Journal of Environmental Research and Public Health*	Health risk assessment of heavy metals in soils from Witwatersrand gold mining basin, South Africa	Own database
2016	Owolabi, I.A.	*South African Journal of Chemistry*	Speciation of chromium and vanadium in medicinal plants	Own database
2016	Shah, W.A.	*Pakistan Journal of Pharmaceutical Sciences*	Comparison of toxic heavy metals concentration in medicinal plants and their respective branded herbal formulations commonly available in Khyber Pakhtunkhwa	SCOPUS
2016	Shahid, M.	*Journal of Hazardous Materials*	Foliar heavy metal uptake, toxicity and detoxification in plants: a comparison of foliar and root metal uptake	Own database
2016	Venter, A.D.	*Atmospheric Pollution Research*	Regional atmospheric Cr(VI) pollution from the Bushveld Complex, South Africa	Own database

2017	Anjum, S.A.	*Pedosphere*	Phyto-toxicity of chromium in maize: oxidative damage, osmolyte accumulation, anti-oxidative defense and chromium uptake	SCOPUS
2017	Cheng, J.	*Environmental Toxicology and Pharmacology*	Concentrations and human health implications of heavy metals in market foods from a Chinese coal-mining city	Own database
2017	Dong, X-L.	*International Journal Of Food Properties*	Multivariate analyses of major and trace elements in 19 species of herbs consumed in Yunnan, China	Own database
2017	Ertani, A.	*Water Air Soil Pollution*	Chromium in agricultural soils and crops: a review	SCOPUS
2017	Gomes, M.A.D.C.	*Ecotoxicology and Environmental Safety*	Plant chromium uptake and transport, physiological effects and recent advances in molecular investigations	Own database
2017	Kim, H.S.	*Archives of Environmental Contamination and Toxicology*	Influence of road proximity on the concentrations of heavy metals in Korean urban agricultural soils and crops	Own database

2017	Pennisi, G.	*Acta Horticulturae*	Soilless cultivation in urban gardens for reduced potentially toxic elements (PTEs) contamination risk	SCOPUS
2017	Shahid, M.	*Journal of Environmental Biology*	Chromium speciation, bioavailability, uptake, toxicity and detoxification in soil-plant system: a review	SCOPUS
2017	Vaikosen, E.N.	*Journal of Pharmacy & Pharmacognosy Research*	Determination of heavy metals in medicinal plants from the wild and cultivated garden in Wilberforce Island, Niger Delta region, Nigeria	SCOPUS
2017	Zlatić, N.M.	*Environmental Monitoring and Assessment*	Secondary metabolites and metal content dynamics in *Teucrium montanum* L. and *Teucrium chamaedrys* L. from habitats with serpentine and calcareous substrate	Own database
2018	Kazakis, N.	*Environmental Pollution*	Environmentally available hexavalent chromium in soils and sediments impacted by dispersed fly ash in Sarigkiol basin (northern Greece)	SCOPUS
2018	Kumar, N.	*Environmental Science and Pollution Research*	Profiling of heavy metal and pesticide residues in medicinal plants	SCOPUS

2018	Milićević, T.	*Science of the Total Environment*	Bioavailability of potentially toxic elements in soil–grapevine (leaf, skin, pulp and seed) system and environmental and health risk assessment	SCOPUS
2018	Pajević, S.	*Environmental Monitoring and Assessment*	Heavy metal accumulation in vegetable species and health risk assessment in Serbia	Own database
2018	Sun, H.	*Ecotoxicology and Environmental Safety*	Bioaccumulation and sources of metal(loid)s in lilies and their potential health risks	Own database
2019	Zhang, T.	*Science of the Total Environment*	Assessment of heavy metals pollution of soybean grains in north Anhui of China	Own database
2021	Dobbins, D.	*South African Journal of Botany*	Screening the phytoextractability of trace metals by *Aloe cryptopoda* Baker and *Aloe vera* (L.) Burm.f. cultivated on mine tailings	Own database

Table A3. Inclusion of sourced articles under the seven research themes.

Article	Toxicity	Environmental sources of chromium	Accumulation pathways by plants	Phytotoxicity	Accumulation by food plants	Accumulation by medicinal plants	Toxicity impact on human health
Larsen *et al.*, 1992			X		X		
Voutsa *et al.*, 1996			X		X		X
Zayed *et al.*, 1998	X						X
Kimbrough *et al.*, 1999	X	X	X			X	X
Cervantes *et al.*, 2001	X	X		X			X
Pandey and Sharma, 2003	X			X	X		
Dube *et al.*, 2004		X		X	X		
Oze *et al.*, 2004	X	X					
Rai *et al.*, 2004						X	
Panichev *et al.*, 2005	X		X	X		X	X
Rai *et al.*, 2005		X		X		X	X
Shanker *et al.*, 2005	X	X		X			
Mandiwana *et al.*, 2007			X	X			X
Yang *et al.*, 2007		X			X		
Babula *et al.*, 2008		X		X			X
Tiwari *et al.*, 2009	X	X		X	X		X
Maharia *et al.*, 2010		X				X	

Meena *et al.*, 2010						X	
Nagajyoti *et al.*, 2010		X		X			
Feng *et al.*, 2011					X		
Säumel *et al.*, 2012			X		X		X
Abbasi *et al.*, 2013		X	X		X		X
Awodele *et al.*, 2013		X				X	X
Dhal *et al.*, 2013	X	X					X
Ishaq *et al.*, 2013						X	X
Luginina *et al.*, 2013					X	X	
Mahmood *et al.*, 2013						X	X
Sungur *et al.*, 2013	X					X	X
Tiwari *et al.*, 2013				X	X		
Ding *et al.*, 2014	X			X	X		X
Li *et al.*, 2014		X		X	X		
Barouchas *et al.*, 2014	X					X	X
Wahsha *et al.*, 2014			X	X	X		X
Kim *et al.*, 2015		X	X		X		
Kozak *et al.*, 2015		X				X	X
Li *et al.*, 2015			X		X		X
Unver *et al.*, 2015		X			X	X	X
Ye *et al.*, 2015					X		X
Arsenov *et al.*, 2016			X		X		X

Aziz *et al.*, 2016							
Boechat *et al.*, 2016				X		X	
Kamunda *et al.*, 2016		X			X		X
Owolabi *et al.*, 2016			X			X	
Shah *et al.*, 2016		X	X	X		X	X
Shahid *et al.*, 2016			X				X
Venter *et al.*, 2016		X					
Anjum *et al.*, 2017			X	X	X		
Cheng *et al.*, 2017					X		X
Dong *et al.*, 2017						X	X
Ertani *et al.*, 2017	X	X	X	X			X
Gomes *et al.*, 2017	X		X		Xs		
Kim *et al.*, 2017		X	X		X		
Pennisi *et al.*, 2017			X		X		
Shahid *et al.*, 2017	X	X	X	X	X		X
Vaikosen and Alade, 2017		X	X			X	X
Zlatić *et al.*, 2017		X				X	X
Kazakis *et al.*, 2018	X	X		X			X
Kumar *et al.*, 2018			X			X	X
Milićević *et al.*, 2018		X			X		X
Pajević *et al.*, 2018			X		X		X
Sun *et al.*, 2018			X		X		X

Zhang *et al.*, 2019			X		X		X
Dobbins *et al*., 2021		X			X		

Table A4. Highest Cr concentrations reported in food plants (μg g^{-1}, accumulating part(s); Cr(III)/Cr(VI) form, if specified). Collection site: P, polluted site; OS, other site specifications. Plant origin: WC, wild collected; F, farm produce; M, market product; L, laboratory set-up; OC, other conditions. NA, not applicable; NAV, not available; NS, not specified; UW, unwashed leaves; W, washed leaves.

Family	Plant species (common name)	Plant origin	Collection site	Cr level in plant (μg g^{-1})	Cr level in soil (μg g^{-1})	Reference
Amaranthaceae	*Spinacia oleracea* (spinach)[1,2]	F[1] M[2]	P[1] (possible dust pollution) NS[2]	7.13 (leaves)[1] 3.67 (2011),1.76 (2010), 1.67 (2009)[2]	NS[1] NAV[2]	Pajević *et al*., 2018[1] Arsenov *et al*., 2016[2]
Apiaceae	*Apium graveolens* (celery)	F	P (steel factory, mining, highway traffic)	0.17	16.4–195	Ye *et al*., 2015
	Daucus carota (carrot)	L (pot experiment; farmland soil, $CrCl_3$ solution)	NA	0.09–6.54 (high conc.) 0.06–2.21 (low conc.)	4.6–68.9	Ding *et al*., 2014
Asteraceae	*Lactuca sativa* (lettuce)[1,2,3]	F[1] L[2] (pot experiment; $CrCl_3$ solution), F[3]	P[1] (< 0.5 km from a domestic waste incinerator, NA[2]	125.52 (aerial parts)[1] 750 (root)[2] 9.72 (leaves)[3]	215–358[1] 43.9[2] 98.7[3]	Li *et al*., 2015[1] Li *et al*., 2014[2] Voutsa *et al*., 1996[3]

			P[3] (varied industrial emissions)			
	Cichorium endivia (bitter lettuce)	F	P (~ 20 km from domestic waste incinerator)	71.2 (aerial parts)	1–41.5	Li *et al*., 2015
Brassicaceae	*Brassica oleracea* var. *capitata* (cabbage)	L (sand culture; $CrCl_3$, $6H_2O$)	NA	1954 (root), 144 (leaves), 46.3 (shoot)	NA	Pandey & Sharma, 2003
	Brassica oleracea var. *acephala* (kale)	OC (Experimental plot)	P (~ 2.3 km from wood preservation factory)	0.3 (UW)	10–75	Larsen *et al*., 1992
	Brassica rapa (Chinese cabbage)[1,2]	F[1] (plot) F[2] (rooftop gardens)	P[1] (~5 m from traffic source), OS[2] (Asian dust wind)	8.86 (UW), 5.82 (W)[1] 22.17 (2012), 9.50 (2013) (UW); 20.48 (2012), 8.29 (2013) (W)[2]	70–71[1] 165.1 (2012), 132.6 (2013)[2]	Kim *et al*., 2017[1] Kim *et al*., 2015[2]
	Brassica oleracea var. *botrytis* (caulifower);	L (19.2 µM potassium chromate,	NA	> 350 (root) > 2 (shoot) (detected as Cr(III) only)	NA	Zayed *et al*., 1998

	Brassica oleracea L. var. *capitata* (cabbage); *B. oleracea* var. *acephala* (kale)	chromium chloride)				
	Raphanus sativus (radish)[1,2,3]	L[1] (garden soil (G), soilless, peat (P) media), L[2] ($K_2Cr_2O_7$), L[3] (dichromate solution)	P[1] (G-urban emissions) NA[2,3]	227 (G), 39.5 (P) (root)[1] 321.6 (root), 186.8 (shoot), 116.7 (leaves)[2] 280 (root), 253 (shoot)[3]	NS[1] NA[2,3]	Pennisi *et al*., 2017[1] Tiwari *et al*., 2013[2] Dube *et al*., 2004[3]
Convolvulaceae	*Ipomoea aquatic* (water convolvulus)	M	P (coal mine)	0.321 (leaves)	NAV	Cheng *et al*., 2017
Fabaceae	*Glycine max* (soybean)	F	P (multiple metal mining)	3.98	NS	Zhang *et al*., 2019
	Pisum sativum (pea)	L ($K_2Cr_2O_7$ solution)	NA	217.3 (root), 173.13 (shoot), 74.43 (leaves), 8.64 (seeds)	NA	Tiwari *et al*., 2009
Lamiaceae	*Mentha spicata* (mint)	F	P (urban traffic emissions)	5.06	NS	Säumel *et al*., 2012

Liliaceae	*Lilium davidii* var. *unicolor*	F	NS	0.99 (bulb)	NS	Sun *et al*., 2018
Malvaceae	*Malva sylvestris* (common mallow)	M	NS (city emissions)	1.133 (UW), 0.462 (W)	NAV	Unver *et al*., 2015
Poaceae	*Triticum aestivum* (wheat)	F[1,2]	OS[1] (geogenic, various anthropogenic emissions)	47.73 (root), 14.828 (shoot), 1.1401 (seeds)	95.5–572.7	Wahsha *et al*., 2014
	Zea mays (maize)[1,2]	L[1] ($CrCl_3$ solution conc.) F[2]	NA[1] OS[2] (geogenic, various anthropogenic emissions)	Roots > leaves > shoot > seeds[1] 84.69 (root), 12.327 (leaves), 4.1037 (shoot), 1.1917 (seed)[2]	NA[1] 95.5–572.7[2]	Anjum *et al*., 2017[1] Wahsha *et al*., 2014[2]
Solanaceae	*Solanum tuberosum* (potato)[1,2,3]	M[1] W[2] F[3]	NS[1] P[2] (Industrial) P[3] (urban traffic emissions)	1.67 (tuber) (2009)[1] 14.75 (leaf)[2] 4.69 (tuber)[3]	NAV[1] NS[2,3]	Arsenov *et al*., 2016[1] Abbasi *et al*., 2013[2] Säumel *et al*., 2012[3]
	Lycopersicon esculentum (tomato)	F	P (urban traffic emissions)	0.63	NS	Säumel*et al*., 2012
Vitaceae	*Vitis vinifera* (grape)	F	OS (parent substrate,	2.83 (leaves), 2.46 (pulp), 0.33 (seeds), 0.08 (skin)	221	Milićević *et al*., 2018

	anthropogenic sources)

Table A5. Highest Cr concentrations reported in medicinal plants (µg g^{-1}, accumulating tissue; Cr(III)/Cr(VI) forms, if specified). Collection site: P, polluted site; UP, unpolluted site; OS, other site specifications. Plant origin: WC, wild collected; F, farm produce; M, market product; L, laboratory set-up; OC, other conditions applied. DAM, Dry ash method; MADM, Microwave acid digestion method. NA, not applicable; NAV, not available; NS, not specified; UW, unwashed leaves; W, washed leaves.

Family	Plant species (common name and medicinal part, if mentioned)	Plant origin	Collection site	Cr conc. (µg g^{-1}, plant part, if specified)	Cr level in soil (µg g^{-1})	Reference
Amaranthaceae	*Amaranthus brasiliensis*	W	P (100 m from a paint factory), UP	0.048 (leaves)	0.155 (P) 0.13 (UP)	Awodele *et al*., 2013
Apocynaceae	*Rauvolfia serpentine*	M	NS	58.63 (leaves)	NAV	Kumar *et al*., 2018
Asteraceae	*Ageratum conyzoides*	W	P (100 m from a paint factory), and UP	0.058 (root)	0.155 (P), 0.13 (UP)	Awodele *et al*., 2013
Asteraceae	*Matricaria chamomilla* (chamomile)	M	NS	4.21, 3.12, 1.09 as total Cr, Cr(III) and Cr(VI)	NAV	Sungur *et al*., 2014

Asteraceae	*Parthenium hysterophorus* (flower)	W	P (city emissions)	43.6 (leaves, Islamabad)	NS	Mahmood *et al*., 2013
Asteraceae	*Taraxacu mmongolicum* (whole plant)	NS	NS	13.3 (whole plant)	NS	Dong *et al*., 2017
	Taraxacum officinale (leaves)	W	P (city emissions)	66.6 (leaves, Rawalpindi), 36.8 (root, Islamabad)	NAV	Mahmood *et al*., 2013
Berberidaceae	*Berberis aristata* (rhizome)	M	NS	0.00725 (rhizome)	NAV	Meena *et al*., 2010
Cannabaceae	*Cannabis sativa* (leaves)	W	P (City pollution, Rawalpindi)	66 (root), 52.2 (leaves)	NAV	Mahmood *et al*., 2013
Convolvulaceae	*Ipomoea pes-caprae*	W	OS (Tsunami)	15 (whole plant, 2007), 177 (flower), 18 (leaves) and 12 (shoot) (2008)	6.7 (2007), 3.6 (2008)	Kozak *et al*., 2015

Ericaceae	*Arctostaphylos uva-ursi*	W	P (~ 5 m from road)	3.87 (shoot)	NS	Luginina *et al*., 2013
Euphorbiaceae	*Euphorbia prostate* (whole plant)	NS	NS	27 (whole plant)	NS	Rai et al 2005
Fabaceae	*Albizia lebbeck*	NS	OS (Industrial area, IA, Heavy traffic, HT, Residential, R, Non-residential, NR)	1.10, 0.99, 0.79, 0.40 root, IA; shoot, IA; leaves, HT; seeds, HT	2.95 (IA), 2.45 (HT), 1.84 (R) 1.91 (NR)	Ishaq *et al*., 2013
Lamiaceae	*Mentha arvensis* (leaves)	M	NS	74.2	NAV	Shah *et al*., 2016
	Mentha piperita (peppermint)	L (Pot experiment, both Cr (III), Cr(VI))	NA	11.16, total Cr [Cr(VI), MADM]; 4.61, 2.91 of total Cr [Cr(VI) and Cr(III), DAM] (above-ground parts)	NA	Barouchas *et al*., 2014
	Mentha spicata (spearmint)	L (Pot experiment,Cr(III), Cr(VI))	NA	10.12 total Cr (above-ground parts) [Cr(III), MADM],	NA	Barouchas *et al*., 2014

	Nepeta cataria (leaves)	F	P (~8 km from FeCr, V smelter)	9.4 Cr(VI) (total Cr, 73)	1723 and 10 total Cr, Cr(VI)	Owolabi *et al*., 2016
	Ocimum tenuiflorum (leaves, seeds)	L (Cr(VI))	NA	419.5 (root), 198.8 (leaves)	NA	Rai *et al*., 2004
	Ocimum basilicum (basil)	L (pot experiment, soil from polluted sites)	P (abandoned gold ore processing unit)	3.2 (shoot)	NS	Boechat *et al*., 2016
	Rosmarinus officinalis (rosemary)	L (Pot experiment, soils from P sites)	P (abandoned gold ore processing area)	47.8 (root)	NS	Boechat *et al*., 2016
	Teucrium montanum	W	UP (Serpentine, SP; calcareous, CL outcrop)	45.3 and 12.45 (above-ground parts in SP, CL)	177.4 and 158.7 (SP and CL)	Zlatić *et al*., 2017
Malvaceae	*Malva sylvestris* (common mallow, whole plant)	M	NS	1.33, 0.46 in UW and W (whole plant)	NAV	Unver *et al*., 2015
Meliaceae	*Azadirachta indica*	NS	P (0.5–1 km, copper mining area)	5.92 (leaves)	102.8	Maharia *et al*., 2010

Plantaginaceae	*Plantago major*	W	P (1–20 m from road traffic)	3.53 (leaves)	NS	Luginina *et al*., 2013
Solanaceae	*Capsicum annuum* (seeds)	F	P (~ 3 km from FeCr, V smelter)	Total Cr: 368	1723,1 total Cr	Owolabi *et al*., 2016
Solanaceae	*Withania somnifera*	NS	NS	3.63 (leaves) (Haridwar)	33.4	Maharia *et al*., 2010
Valeriaceae	*Valeriana officinalis*	W	P (100–400 m from road traffic)	10.12 (root)	NS	Luginina *et al*., 2013

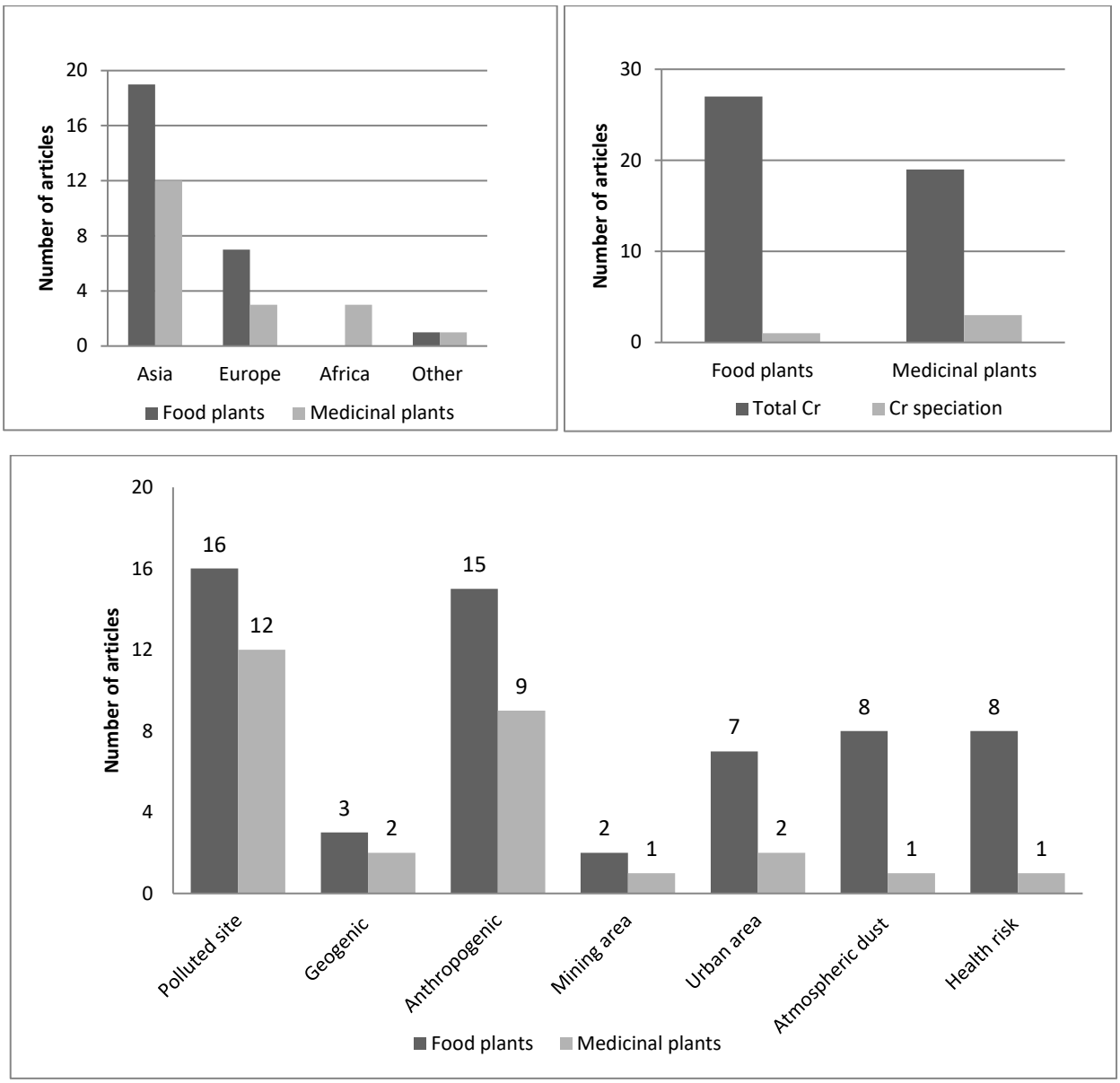

Figure A1. Identified knowledge gaps. a. global distribution of articles; b studies determined total Cr vs. Cr species; c. reviewed articles on various research areas.

Appendix B: Chapter 3

Supplementary tables

Table B1. Meteorological data (2018) received from Potlake Nature Reserve, Sekhukhuneland.

Month	Temperature (ºC)		Humidity (%)		Rainfall (mm)
	Max.	Min.	Max.	Min.	
January	13	38	19	25	68.5
February	11	33	20	25	22.3
March	12	37	20	27	22
April	10	36	18	25	4.2
May	10	46	10	27	4
June	12	34	11	19	0
July	12	35	9	18	0.3
August	10	39	15.5	21.5	0
September	11.5	47	14	30	14
October	6	35	15	28	14.4
November	7	39	11	31	39.5
December	21	35	18	26.5	21
Total	-	-	-	-	210.2

Table B2. Analysis of variance (ANOVA) post-hoc test results on total dust density groups. Significant results are highlighted. Significant at p<0.05.

Multiple Comparisons

(I) Group	(J) Group	Mean Difference (I-J)	Std. Error	Sig.	95% Confidence Interval Lower Bound	95% Confidence Interval Upper Bound
1	2	2276.000*	303.623	0.000	1428.28	3123.72
	3	3130.500*	303.623	0.000	2282.78	3978.22
2	1	-2276.000*	303.623	0.000	-3123.72	-1428.28
	3	854.500*	303.623	0.048	6.78	1702.22
3	1	-3130.500*	303.623	0.000	-3978.22	-2282.78
	2	-854.500*	303.623	0.048	-1702.22	-6.78

Table B3. Kruskal-Wallis results on growth forms (trees and forbs) for dust deposition (Cr particles, $PM_{2.5}$, PM_{10}, PM > 10 µm and total dust) on the abaxial leaf surface. Significant result is highlighted. CrD, largest Cr particle size; Cr wt%, highest Cr wt%.

Hypothesis Test Summary				
	Null Hypothesis	**Test**	**Sig.[a,b]**	**Decision**
1	The distribution of Cr wt% is the same across categories of Group.	Independent-Samples Kruskal-Wallis Test	0.880	Retain the null hypothesis.
2	The distribution of CrD is the same across categories of Group.	Independent-Samples Kruskal-Wallis Test	0.025	Reject the null hypothesis.
3	The distribution of PM2,5 is the same across categories of Group.	Independent-Samples Kruskal-Wallis Test/complex	0.764	Retain the null hypothesis.
4	The distribution of PM10 is the same across categories of Group.	Independent-Samples Kruskal-Wallis Test	0.131	Retain the null hypothesis.
5	The distribution of PM > 10 µm is the same across categories of Group.	Independent-Samples Kruskal-Wallis Test	0.764	Retain the null hypothesis.
6	The distribution of total dust is the same across categories of Group.	Independent-Samples Kruskal-Wallis Test	0.456	Retain the null hypothesis.

[a]Significant at $p<0.05$.

[b]Asymptotic significance is displayed.

Table B4. Kruskal-Wallis results on the simple and compound leaved species for adaxial and abaxial leaf surface dust values (Cr particles, $PM_{2.5}$, PM_{10}, PM > 10 µm and total dust). CrD, largest Cr particle size; Cr wt%, highest Cr wt% values.

	Hypothesis Test Summary				
	Null Hypothesis	**Test**	**Sig.[a,b] (Ad)**	**Sig.[a,b] (Ab)**	**Decision**
1	The distribution of Cr wt% is the same across categories of Group.	Independent-Samples Kruskal-Wallis Test	0.094	0.586	Retain the null hypothesis.
2	The distribution of CrD is the same across categories of Group.	Independent-Samples Kruskal-Wallis Test	0.387	0.604	Retain the null hypothesis.
3	The distribution of $PM_{2.5}$ is the same across categories of Group.	Independent-Samples Kruskal-Wallis Test	0.349	0.551	Retain the null hypothesis.
4	The distribution of PM_{10} is the same across categories of Group.	Independent-Samples Kruskal-Wallis Test	0.173	0.932	Retain the null hypothesis.
5	The distribution of PM > 10 µm is the same across categories of Group.	Independent-Samples Kruskal-Wallis Test	0.863	0.609	Retain the null hypothesis.
6	The distribution of Total is the same across categories of Group.	Independent-Samples Kruskal-Wallis Test	0.174	0.174	Retain the null hypothesis.

[a]Significant at $p<0.05$.
[b]Asymptotic significance is displayed.

Table B5. Kruskal-Wallis results on adaxial and abaxial leaf surface dust values (Cr particles, $PM_{2.5}$, PM_{10}, PM > 10 µm and total dust). CrD, largest Cr particle size; Cr wt%, highest Cr wt% values.

Hypothesis Test Summary				
	Null Hypothesis	**Test**	**Sig.[a,b]**	**Decision**
1	The distribution of Cr wt% is the same across categories of Group.	Independent-Samples Kruskal-Wallis Test	0.837	Retain the null hypothesis.
2	The distribution of CrD is the same across categories of Group.	Independent-Samples Kruskal-Wallis Test	0.769	Retain the null hypothesis.
3	The distribution of Total dust is the same across categories of Group.	Independent-Samples Kruskal-Wallis Test	0.204	Retain the null hypothesis.
4	The distribution of $PM_{2.5}$ is the same across categories of Group.	Independent-Samples Kruskal-Wallis Test	0.452	Retain the null hypothesis.
5	The distribution of PM_{10} is the same across categories of Group.	Independent-Samples Kruskal-Wallis Test	0.977	Retain the null hypothesis.
6	The distribution of PM > 10 µm is the same across categories of Group.	Independent-Samples Kruskal-Wallis Test	0.283	Retain the null hypothesis.

[a]Significant at $p<0.05$.
[b]Asymptotic significance is displayed.

Appendix C: Chapter 4

Supplementary tables

Table C1. Categorisation of epicuticular wax structural density. 4, very dense; 3, dense; 2, moderate; 1, low; 0, undetected; Ad, adaxial; Ab, abaxial.

Plant Species	Wax structural density rating	
	Ad	Ab
Trees		
C. papaya	4	4
C. limon	2	1
M. oleifera	4	4
O. paniculosa	2	1
P. africanum	2	4
P. guajava	2	3
Forbs		
A. ochroleuca	4	4
G. fruticosus	2	3
C. roseus	3	3
I. batatas	2	2
S. italica	4	4
T. terrestris	0	0

Table C2. a. Mine (distance, km) and b. road frequency (distance, m) indices. Total scores per site is given in bold.

a. Mine frequency index								
Distance range	Score	Site 1	Site 2	Site 3	Site 4	Site 5	Site 7	Site 8
0—3	5	0	1x5	0			1x5	
3—6	4	1x4	0	0	1x4			2x4
6—9	3	1x3	0	0		1x3		
9—15	2	2x2	2x2	0				
15—20	1	2x1	1x1	1x1				
Total score	**15**	**13**	**10**	**1**	**4**	**3**	**5**	**8**

b. Road frequency index								
Distance range	Score	Site 1	Site 2	Site 3	Site 4	Site 5	Site 7	Site 8
0—5	5				1x5	1x5	1x5	
5—15	4		1x4					
15—25	3	1x3				1x3	1x3	
25—45	2	2x2			1x2			
45—105	1			1x1				1x1
Total score	**15**	**5**	**4**	**1**	**7**	**8**	**8**	**1**

Table C3. Pearson correlation matrix of major elements detected in soil and on (a) adaxial and (b) abaxial leaf surface. Significant at *p*<0.05.

a	Mg	Al	Si	Ca	Fe	Cr
Mg	0.3052	-0.3823	0.2014	-0.0193	0.1280	-0.1033
	p=0.462	p=0.350	p=0.633	p=0.964	p=0.763	p=0.808
Al	00.6029	-0.4599	0.2608	-0.2649	0.5017	0.2755
	p=0.114	p=0.252	p=0.533	p=0.526	p=0.205	p=0.509
Si	0.4461	-0.3496	0.3004	-0.2888	0.4232	0.0764
	p=0.268	p=0.396	p=0.470	p=0.488	p=0.296	p=0.857
Ca	0.0214	-0.2767	-0.4849	0.2838	-0.2715	0.2422
	p=0.960	p=0.507	p=0.223	p=0.496	p=0.515	p=0.563
Fe	0.4921	-0.3881	0.3104	-0.3294	0.4715	0.1035
	p=0.215	p=0.342	p=0.454	p=0.426	p=0.238	p=0.807
Cr	0.3790	-0.2838	0.2772	-0.3187	0.4075	0.0547
	p=0.354	p=0.496	p=0.506	p=0.442	p=0.316	p=0.898
a	Mg	Al	Si	Ca	Fe	Cr
Mg	0.3867	-0.4061	0.4430	0.0677	0.1472	-0.2374
	p=0.344	p=0.318	p=0.272	p=0.873	p=0.728	p=0.571
Al	-0.1208	0.2053	0.5143	0.6405	-0.3735	-0.5094
	p=0.776	p=0.626	p=0.192	p=0.087	p=0.362	p=0.197
Si	0.1054	0.0050	0.4508	0.5009	-0.1781	-0.2678
	p=0.804	p=0.991	p=0.262	p=0.206	p=0.673	p=0.521
Ca	0.2482	-0.3533	-0.0418	0.1225	0.0019	0.0892
	p=0.553	p=0.391	p=0.922	p=0.773	p=0.996	p=0.834
Fe	0.0298	0.0550	0.4967	0.4700	-0.2055	-0.3964
	p=0.944	p=0.897	p=0.211	p=0.240	p=0.625	p=0.331
Cr	-0.0719	0.0683	0.1930	0.6221	-0.3853	-0.2384

	p=0.866	p=0.872	p=0.647	p=0.100	p=0.346	p=0.570

Table C4. Analysis of variance (ANOVA) results for plant species groups based on adaxial leaf surface traits. Significant results are highlighted. Significant at p<0.05.

Variable	T-tests; Grouping: Cluster number (Adaxial Clusters ANOVA) Group 1: 1 Group 2: 2							
	Mean 1	Mean 2	t-value	df	p	Valid N 1	Valid N 2	Std. Dev. 1
PM2,5	356.0000	362.8571	-0.11297	10	0.912291	5	7	136.1249
PM10	360.0000	341.4286	0.30707	10	0.765090	5	7	127.2792
PM >10	34.0000	45.7143	-0.74089	10	0.475798	5	7	27.0185
LS	9.6380	3.2157	1.47940	10	0.169832	5	7	11.2255
EW	3.0000	2.2857	0.98209	10	0.349217	5	7	1.0000
SS	7.5590	6.3088	0.28951	10	0.778104	5	7	7.2900
SF	10.2000	11.0000	-0.09408	10	0.926901	5	7	9.8082
TS	0.0000	125.2827	-4.74514	10	0.000786	5	7	0.0000
TF	0.0000	7.3714	-4.77896	10	0.000747	5	7	0.0000

Table C5. Analysis of variance (ANOVA) results for plant species groups rbased on abaxial leaf surface traits. Significant results are highlighted. Significant at p<0.05.

Variable	Analysis of Variance (Abaxial Cluster ANOVA in NEW Cluster ANOVA) Marked effects are significant at p < .05000							
	SS Effect	df Effect	MS Effect	SS Error	df Error	MS Error	F	p
PM2,5	5083.3	2	2541.7	45808.3	9	5089.81	0.49936	0.622788
PM10	7083.3	2	3541.7	33808.3	9	3756.48	0.94281	0.424864
PM >10	333.3	2	166.7	16433.3	9	1825.93	0.09128	0.913598
LS	181.2	2	90.6	488.7	9	54.30	1.66866	0.241878
EW	13.5	2	6.8	8.8	9	0.97	6.94286	0.014999
SS	195.7	2	97.8	200.8	9	22.31	4.38605	0.046802
SF	17880.0	2	8940.0	4663.0	9	518.11	17.25499	0.000833
TS	204681.0	2	102340.5	277455.4	9	30828.38	3.31968	0.083196
TF	97075.1	2	48537.5	112483.8	9	12498.20	3.88356	0.060817

Table C6. ANOVA post-hoc (Tukey's Honestly Significant Difference) results for abaxial leaf surface traits. a. Epicuticular wax; b. stomata density. Significant results are highlighted. Significant at p<0.05. Cr wt%, highest Cr wt% values; CrD, largest particle size.

a. Cluster number	Unequal N HSD; Variable: EW (Abaxial Cluster ANOVA) Marked differences are significant at p < .05000		
	1 M=3.5000	2 M=2.7500	3 M=.50000
1		0.551557	0.033953
2	0.551557		0.110163
3	0.033953	0.110163	

b. Cluster number	Unequal N HSD; Variable: SD (Abaxial Cluster) Marked differences are significant at p < .05000		
	1 M=22.500	2 M=99.500	3 M=6.5000
1		0.002694	0.767940
2	0.002694		0.007057
3	0.767940	0.007057	

Table C7. Kruskal-Wallis results for plant species groups based on mine proximity based on adaxial dust values (Cr particles, $PM_{2.5}$, PM_{10}, PM > 10 µm and total dust). Significant result is highlighted.

Hypothesis Test Summary				
	Null Hypothesis	**Test**	**Sig.[a,b]**	**Decision**
1	The distribution of Cr wt% is the same across categories of Group.	Independent-Samples Kruskal-Wallis Test	0.772	Retain the null hypothesis.
2	The distribution of CrD is the same across categories of Group.	Independent-Samples Kruskal-Wallis Test	0.043	Reject the null hypothesis.
3	The distribution of PM2,5 is the same across categories of Group.	Independent-Samples Kruskal-Wallis Test	0.561	Retain the null hypothesis.
4	The distribution of PM10 is the same across categories of Group.	Independent-Samples Kruskal-Wallis Test	1.000	Retain the null hypothesis.
5	The distribution of PM >10 is the same across categories of Group.	Independent-Samples Kruskal-Wallis Test	0.769	Retain the null hypothesis.

[a]Significant at $p<0.05$.

[b]Asymptotic significance is displayed.

Appendix D: Chapter 5

Supplementary tables

Table D1. Kruskal-Wallis results on growth forms (trees and forbs) for adaxial dust values (Cr particles, $PM_{2.5}$, PM_{10}, PM > 10 µm and total dust).

Hypothesis Test Summary				
	Null Hypothesis	**Test**	**Sig.[a,b]**	**Decision**
1	The distribution of Total Cr is the same across categories of Group.	Independent-Samples Kruskal-Wallis Test	0.109	Retain the null hypothesis.
2	The distribution of Tissue Cr is the same across categories of Group.	Independent-Samples Kruskal-Wallis Test	0.082	Retain the null hypothesis.
3	The distribution of Surface Cr is the same across categories of Group.	Independent-Samples Kruskal-Wallis Test	0.199	Retain the null hypothesis.
4	The distribution of Cr(VI) is the same across categories of Group.	Independent-Samples Kruskal-Wallis Test	0.162	Retain the null hypothesis.

[a]Significant at $p<0.05$.

[b]Asymptotic significance is displayed.

Table D2. Kruskal-Wallis results on plant species groups based on total polluters for leaf Cr concentration categories (total Cr of leaf, Cr in leaf tissue, Cr on leaf surface, total Cr(VI) of leaf). Significant results are highlighted.

Hypothesis Test Summary				
	Null Hypothesis	Test	Sig.[a,b]	Decision
1	The distribution of ATotal Cr is the same across categories of Group.	Independent-Samples Kruskal-Wallis Test	0.017	Retain the null hypothesis.
2	The distribution of Tissue Cr is the same across categories of Group.	Independent-Samples Kruskal-Wallis Test	0.064	Retain the null hypothesis.
3	The distribution of Surface Cr is the same across categories of Group.	Independent-Samples Kruskal-Wallis Test	0.017	Reject the null hypothesis.
4	The distribution of Cr(VI) is the same across categories of Group.	Independent-Samples Kruskal-Wallis Test	0.874	Retain the null hypothesis.

[a]Significant at $p<0.05$.

[b]Asymptotic significance is displayed.

Appendix E: Chapter 6

Supplementary tables

Table E1. Permutational multivariate analysis of variances (Permanovas) between sites under selected factors. a. Topograpgy and land use; b. pairwise comparisons among land uses; c. permanova for growth form factor; d. pairwise comparisons among growth forms. Significant results are highlighted. Significant at *p*<0.05.

a	Soil				Plant leaves			
Factor	df	MS	Pseudo-F	*p*	df	MS	Pseudo-F	*p*
Topography	3	6.70	1.63	0.116	3	10.64	1.14	0.316
Error	15	4.10			29	9.30		
Factor	df	MS	Pseudo-F	*p*	df	MS	Pseudo-F	*p*
Land use	4	52.36	11.19	0.001	4	18.75	2.22	0.005
Error	22	4.68			42	8.45		

b	Soil		Plant leaves	
Pairwise - Landuse	t	*p*	t	*p*
Gully erosion x Sheet erosion	0.81	0.680	1.07	0.341
Gully erosion x Rangelands	0.47	0.940	1.13	0.265
Gully erosion x Gardens	2.04	0.044	2.18	0.003
Gully erosion x Tailings	6.48	0.002	1.74	0.021
Sheet erosion x Rangelands	0.57	0.864	0.78	0.691
Sheet erosion x Gardens	2.43	0.015	2.43	0.003
Sheet erosion x Tailings	7.19	0.001	1.97	0.017
Rangelands x Gardens	1.95	0.019	1.59	0.043
Rangelands x Tailings	5.38	0.001	1.58	0.047
Gardens x Tailings	3.76	0.031	1.25	0.203

c	Plant leaves			
Factor	df	MS	Pseudo-F	*p*
Growth forms	7	16.94	2.12	0.002
Error	39	8.00		

d	Plant leaves	
Pairwise – Growth forms	t	*p*
Dwarf shrub x Forb short	0.80	0.522
Dwarf shrub x Forb tall	0.70	0.779
Dwarf shrub x Grass	2.97	0.005
Dwarf shrub x Succulents	1.31	1.38
Dwarf shrub x Tree	0.96	0.473
Dwarf shrub x Forb prostate	0.83	0.707
Dwarf shrub x Shrub	1.58	0.037
Forb short x Forb tall	0.63	0.765
Forb short x Grass	1.99	0.031
Forb short x Succulents	1.06	0.349
Forb tall x Tree	0.72	0.773
Forb tall x Forb prostate	0.71	0.846
Forb tall x Shrub	1.61	0.024
Grass x Succulents	1.87	0.025
Grass x Tree	3.35	0.003
Grass x Forb prostate	0.71	0.846
Grass x Shrub	4.21	0.011
Succulents x Tree	1.34	0.122
Succulents x Forb prostate	1.19	0.246
Succulents x Shrub	2.05	0.003
Tree x Forb prostate	0.98	0.441
Tree x Shrub	1.86	0.020
Forb prostate x Shrub	1.60	0.025

Appendix F

Letter from the proofreader

To whom it may concern,

I would like to confirm that the thesis, *Chromium dust deposition on plant leaves in Sekhukhuneland, South Africa, and the importance of leaf traits*, submitted in fulfilment of the requirements for the degree *Doctor of Philosophy in Science with Botany* at the North-West University, Potchefstroom Campus by Ms Sutapa Adhikari, has been thoroughly reviewed and proof-read. The language and grammar have been edited where necessary.

Yours faithfully,

Department of Mathematics and Applied Mathematics
University of Johannesburg
Kingsway campus
P.O. Box 524
Auckland Park
2006
South Africa

Phone (W): +27-(0)11 559 2869

Appendix G

Research output

Journal article:

Adhikari, S., Siebert, S.J. & Jordaan, A. 2021. Chromium dust deposition on *Moringa oleifera* leaves harvested by local communities in Sekhukhuneland, South Africa. *Acta Horticulturae*, 1306:99–106. https://doi.org/10.17660/ActaHortic.2021.1306.12

Conference presentations:

Oral presentation

Adhikari, S., Siebert, S.J. & Jordaan, A. 2019. Chromium dust deposition on *Moringa oleifera* leaves harvested by local communities in Sekhukhuneland, South Africa. 2nd International Moringa Symposium, Pretoria, South Africa, 10–13 Nov. 2019.

Poster presentation

Adhikari, S., Siebert, S.J. & Jordaan, A. 2020. Chromium dust detection on foliar surfaces of food and medicinal plant species used by local communities in Sekhukhuneland, South Africa. 46th SAAB Annual Conference, University of the Free State, Qwa Qwa, South Africa, 7–10 Jan. 2020.